UNCLASSIFIED

AD NUMBER

AD380190

CLASSIFICATION CHANGES

TO: unclassified

FROM: confidential

LIMITATION CHANGES

TO:

Approved for public release, distribution unlimited

FROM:

Distribution authorized to U.S. Gov't. agencies and their contractors; Administrative/Operational Use; Mar 1967. Other requests shall be referred to AFRPL [RPPR/STINFO], Edwards AFB, CA 93523.

AUTHORITY

31 Mar 1979 per Group-4 document marking; AFRPL ltr dtd 5 Feb 1986

THIS PAGE IS UNCLASSIFIED

AFRPL-TR-67-91

38078

(Unclassified Title)

FOURTH QUARTERLY PROGRESS REPORT

ADVANCED CRYOGENIC ROCKET ENGINE PROGRAM

AEROSPIKE NOZZLE CONCEPT

F. B. Lary
Rocketdyne, A Division of
North American Aviation, Inc.
6633 Canoga Ave.
Canoga Park, California

Technical Report AFRPL-TR-67-91

March 1967

APR 11 1967

Group 4
Downgraded at 3-Year Intervals
Declassified After 12 Years

THIS MATERIAL CONTAINS INFORMATION AFFECTING THE NATIONAL DEFENSE OF THE UNITED STATES WITHIN THE MEANING OF THE ESPIONAGE LAWS, TITLE 18 U.S.C., SECTIONS 793 AND 794, THE TRANSMISSION OR REVELATION OF WHICH IN ANY MANNER TO AN UNAUTHORIZED PERSON IS PROHIBITED BY LAW.

"In addition to security requirements which must be met, this document is subject to special export controls and each transmittal to foreign governments or foreign nationals may be made only with prior approval of AFRPL (RPPR/STINFO), Edwards, California, 93523."

Air Force Rocket Propulsion Laboratory
Research and Technology Division
Edwards Air Force Base, California
Air Force Systems Command
United States Air Force

CONFIDENTIAL

AFRPL-TR-67-91

(Unclassified Title)

Fourth Quarterly Progress Report

Advanced Cryogenic Rocket Engine Program, Aerospike Nozzle Concept

F. B. Lary
Rocketdyne, A Division of
North American Aviation, Inc.
6633 Canoga Ave.
Canoga Park, California

March 1967

Group 4
Downgraded at 3-Year Intervals
Declassified After 12 Years

THIS MATERIAL CONTAINS INFORMATION AFFECTING THE NATIONAL DEFENSE OF THE UNITED STATES WITHIN THE MEANING OF THE ESPIONAGE LAWS, TITLE 18 U.S.C. SECTIONS 793 AND 794, THE TRANSMISSION OR REVELATION OF WHICH IN ANY MANNER TO AN UNAUTHORIZED PERSON IS PROHIBITED BY LAW.

"In addition to security requirements which must be met, this document is subject to special export controls and each transmittal to foreign governments or foreign nationals may be made only with prior approval of AFRPL (RPPR/STINFO), Edwards, California, 93523."

Air Force Rocket Propulsion Laboratory
Research and Technology Division
Edwards Air Force Base, California
Air Force Systems Command
United States Air Force

PAGES NOT FILMED ARE BLANK

FOREWORD

(U) This report presents the work accomplished during the fourth report period of the Aerospike Advanced Development Program under Air Force Contract AF04(611)-11399. The report covers the period 1 December 1966 through 28 February 1967. A portion of the design and tooling effort in Task II represents a joint effort with the Advanced Engineering Program, Systems and Dynamics Investigation (aerospike) Contract NAS 8-19. This report has been assigned Rocketdyne report No. R-6537-4.

(U) Publication of this report does not constitute Air Force approval of the reports' findings or conclusions. It is published only for the exchange and stimulation of new ideas.

Vernon L. Mahugh
1/Lt, USAF
Project Engineer

ABSTRACT

(U) Program status and technical results obtained at the end of the report period are described for the Advanced Development Program, Aerospike. This program includes analysis and preliminary design of an advanced rocket engine using an Aerospike nozzle and experimental evaluation of critical technology related to the Aerospike concept. Component and system features, physical arrangements, and design parameters and details have been established for an optimum demonstrator engine. Studies of application of a flight engine to certain vehicles are completed. Experimental injector performance investigations on a segment chamber and experimental cooling investigations on segment chambers and material studies are completed. Fabrication of full-scale, cooled thrust chambers for performance demonstrations is under way. Fabrication of segments for structural and cooling evaluations is also in progress.

CONTENTS

ILLUSTRATIONS

TABLES

I. INTRODUCTION

(C) The Advanced Development Program (ADP), Aerospike Nozzle Concept started 1 March 1966 with a 17-month duration. The objectives are to evaluate critical technology associated with the Aerospike concept and produce the preliminary design of an advanced hydrogen-oxygen engine of the following characteristics:

1. 250,000-pound thrust (nominal rated) with throttling to 20 percent of rated thrust
2. 6:1 mixture ratio (nominal) with a range of 5 to 7:1
3. 96 percent (minimum) of theoretical shifting specific impulse at rated thrust; 95 percent (minimum) during throttling
4. 100-inch maximum overall diameter
5. 10-hours life between overhauls with 100 reuses
6. Restartable at altitude

The total effort is comprised of two major tasks:

Task 1, Analysis and Design

- A. Module Design
- B. Application Study

Task 2, Fabrication and Test

- A. Injector Performance Investigations
- B. Thrust Chamber Nozzle Investigations
- C. Thrust Chamber Cooling Investigations
- D. Segment Structural Evaluation

(C) The previous three quarterly reports covered the following major areas of work:

1. Design, fabrication, and testing of 2.5K solid-wall segments and an array of injector concepts and patterns
2. Design, fabrication, and initiation of testing of tube-wall segments for thrust chamber cooling investigations of nickel and copper tubes
3. Materials analysis and testing for determination of fatigue characteristics as a function of processing

4. Design and fabrication of 250K full-scale solid-wall and tube-wall thrust chambers and injectors for performance demonstrations

5. Design of a 20K structural evaluation segment

6. Design tradeoff studies, functional analyses, and preliminary design of a complete demonstrator engine and its components

7. Studies of installation arrangements and weights for a 250K flight module and the vehicle relative performance resulting

(U) This fourth quarterly report presents the program status, technical progress, and problem areas and solutions at the end of the fourth quarter of the Aerospike ADP, and a brief summary of planned effort.

II, SUMMARY

(U) The module design subtask of Task I was very nearly completed in this quarter. The engine system layout was refined including the valve selections made in the previous quarter, revised turbopump configuration, the selected thrust mount, and other subsystem design study results. Design studies of the turbine hot-gas discharge and base closure were conducted and one arrangement was tentatively selected. Start transient and throttling dynamic computer model studies were concluded with satisfactory tank-head start defined.

(U) All turbopump design features were selected including rear bearing support, preinducer drive, pump seal details, and turbine disc size and shape. The final layout of both pumps (prior to detailing) was nearly completed. The design of the hot-gas throttling valve and main propellant valves was completed. Final design reviews were conducted on these valves and on the two turbopumps. Demonstrator module thrust chamber design was concluded after study of an alternative, lightweight injector attachment, selection of tapoff manifold design, refinement of baffle seat, manifold, structural details for fabrication ease, and detailed tube design. The final thrust chamber layout was brought up to date.

(U) In the Application Study subtask, parametric installation weight data for the 350K thrust levels was completed and performance index values were calculated for all vehicles. The 250K data, previously completed, were modified for a new thrust cone angle limit. An individual optimum configuration was established for each of the 12 vehicle-thrust level cases, and various common optima were studied. Preparation of the applications study special report was initiated.

(C) In Task 2, there was no activity on the Injector Performance Investigations, this subtask having been completed in the previous quarter. In the Thrust Chamber Cooling Investigation subtask, the copper-tube-wall 2.5K segment was tested from 300 to 1500 psi and up to a mixture ratio of 5, demonstrating regenerative cooling. Overall heat flux and performance agreed with results obtained on the solid-wall 2.5K segments. Two additional nickel tube specimens were tested on the fatigue-life tube tester at the design wall temperature, indicating a capability of 300 stop-start cycles for nickel 200. The Thrust Chamber Cooling Investigation was completed except for analysis of results from related programs.

(U) Under the Thrust Chamber Nozzle Demonstration subtask, the first 250K injector and all components of the solid-wall chamber assembly were completed. The solid-wall experimental assembly was completed and mounted on the test stand, and prete t blowdowns were initiated. The tube-wall thrust chamber fabrication proceeded on schedule with the first outer body completing both furnace braze cycles and the inner ready for its second and final cycle. Inner and outer bodies for the second chamber were brought to the preparation for braze stage. The second injector completed welding and pressure test and entered electrical discharge machining of the face slots.

(U) In the 20K Segment Structural Evaluation subtask, fabrication of the first segment and injector was brought to the subassembly stage. Furnace brazing of tube-wall subassemblies was started and the injector welding and machining for braze completed, injector strips were drilled and flow tested. Details for the second chamber were completed.

(U) Of the program milestones (Fig. 1) scheduled for this quarter period, all except three were met in this period. Final Design Review Completed was deferred until the completion of Phase I. Vehicle Layouts Complete was rescheduled to 30 March 1967. The 250K Solid-Wall Tests Completed was rescheduled to 30 April 1967. It is expected that this reschedule will not affect the completing of other program objectives.

AIR FORCE
ADP AEROSPIKE ENGINE
SCHEDULE AND REVIEW PROCEDURE (SARP) CHART
TASK I -DESIGN AND ANALYSIS

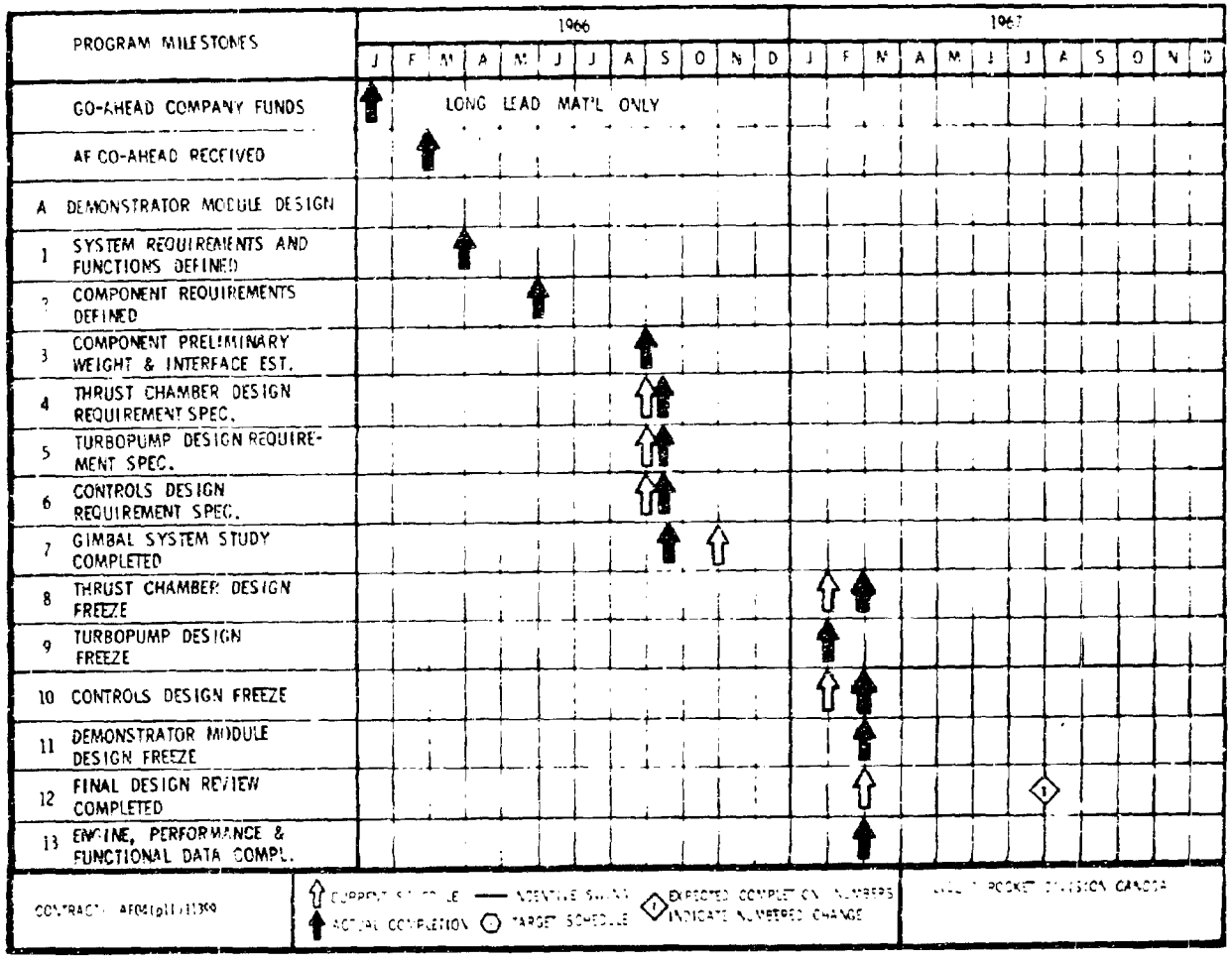

Figure 1. Program Milestones

CONFIDENTIAL

CONFIDENTIAL

CONFIDENTIAL

195 785
2 OF 2
12 66

AIR FORCE
ADP AEROSPIKE ENGINE
SCHEDULE AND REVIEW PROCEDURE (SARP) CHART
TASK I - DESIGN AND ANALYSIS

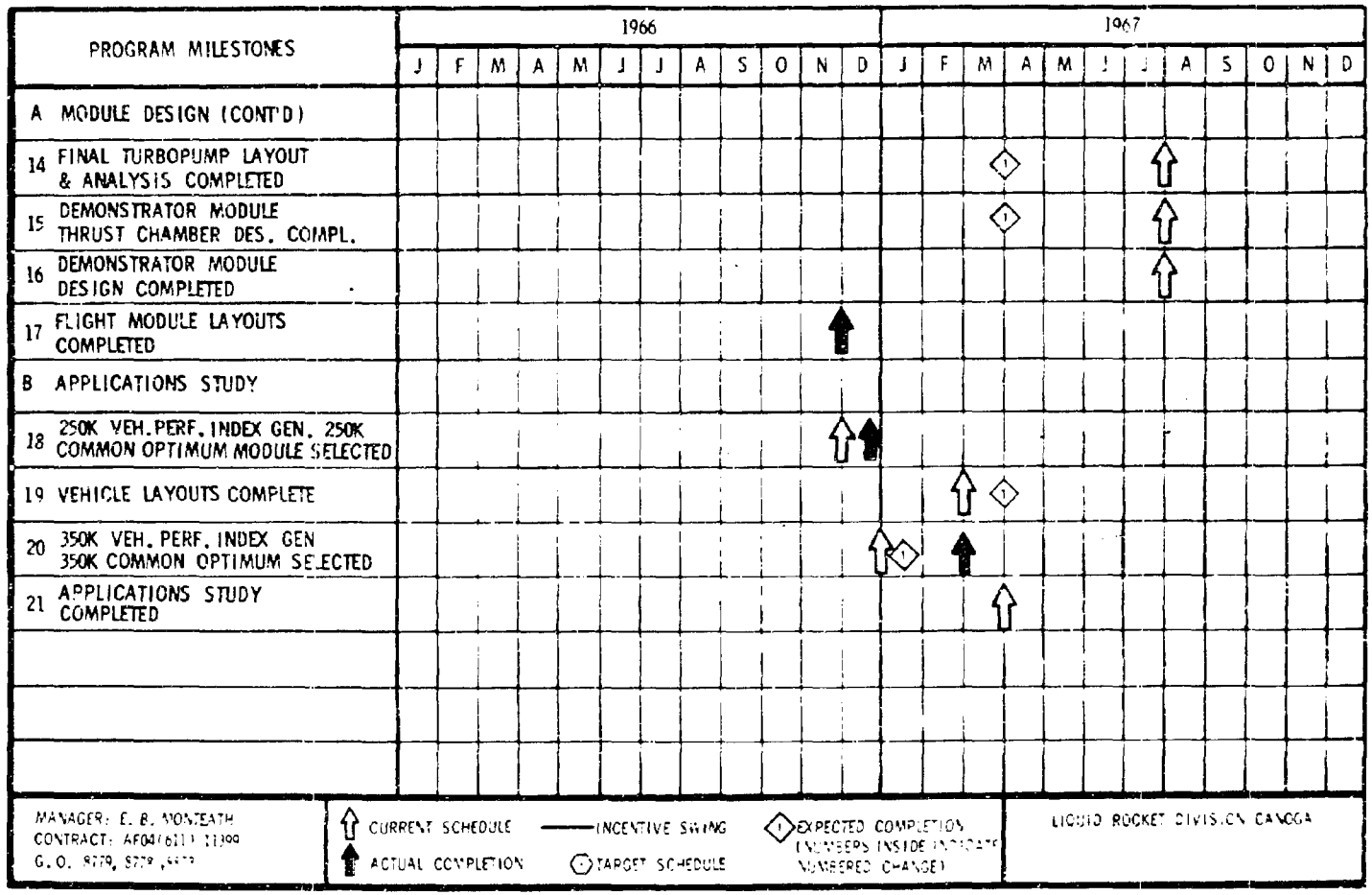

Figure 1. (Continued)

CONFIDENTIAL

AIR FORCE
ADP AEROSPIKE ENGINE
SCHEDULE AND REVIEW PROCEDURE (SARP) CHART
TASK II FABRICATION AND TEST

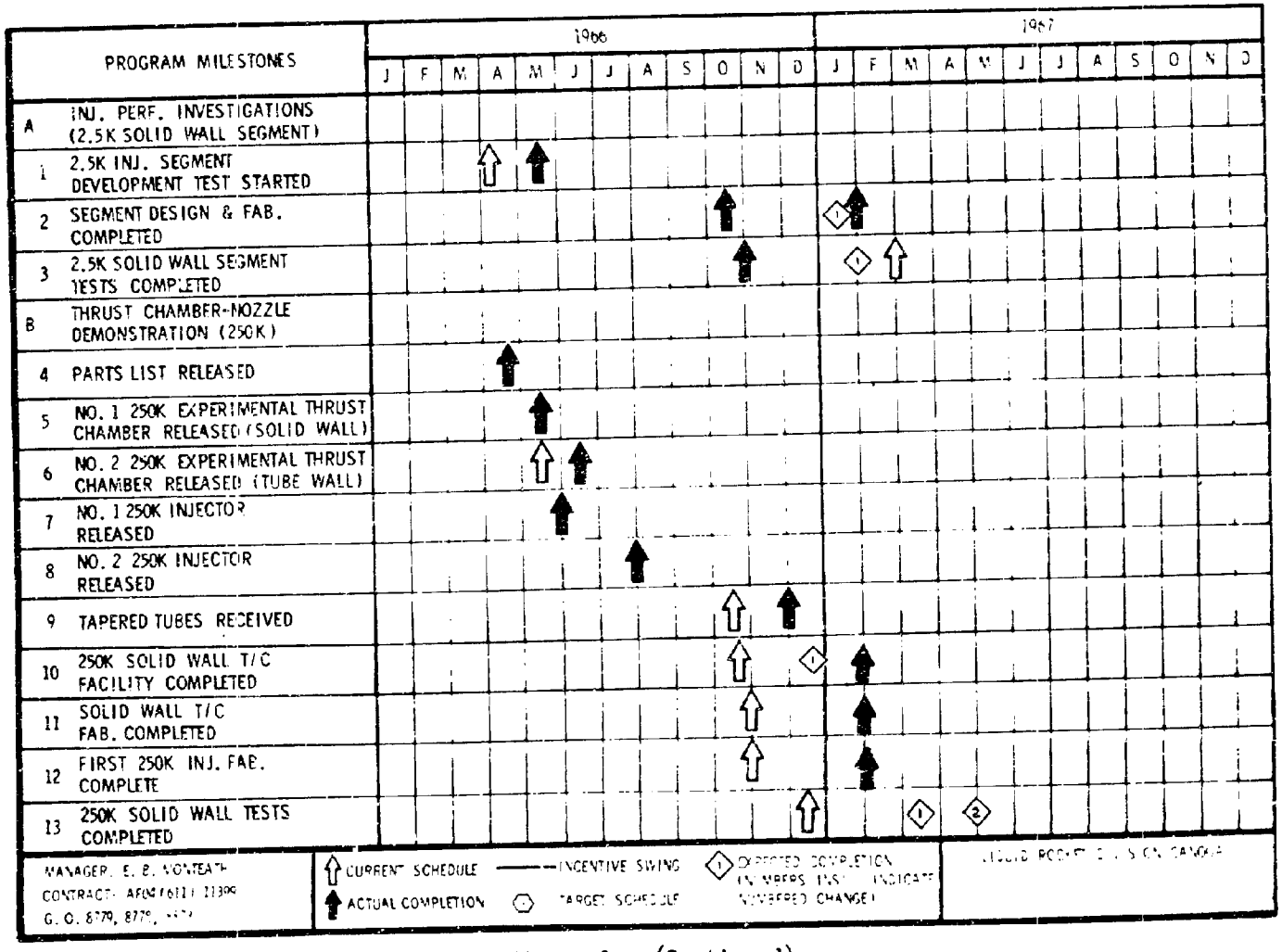

Figure 1. (Continued)

CONFIDENTIAL

CONFIDENTIAL

AIR FORCE

ADP AEROSPIKE ENGINE

SCHEDULE AND REVIEW PROCEDURE (SARP) CHART

TASK II FABRICATION AND TEST

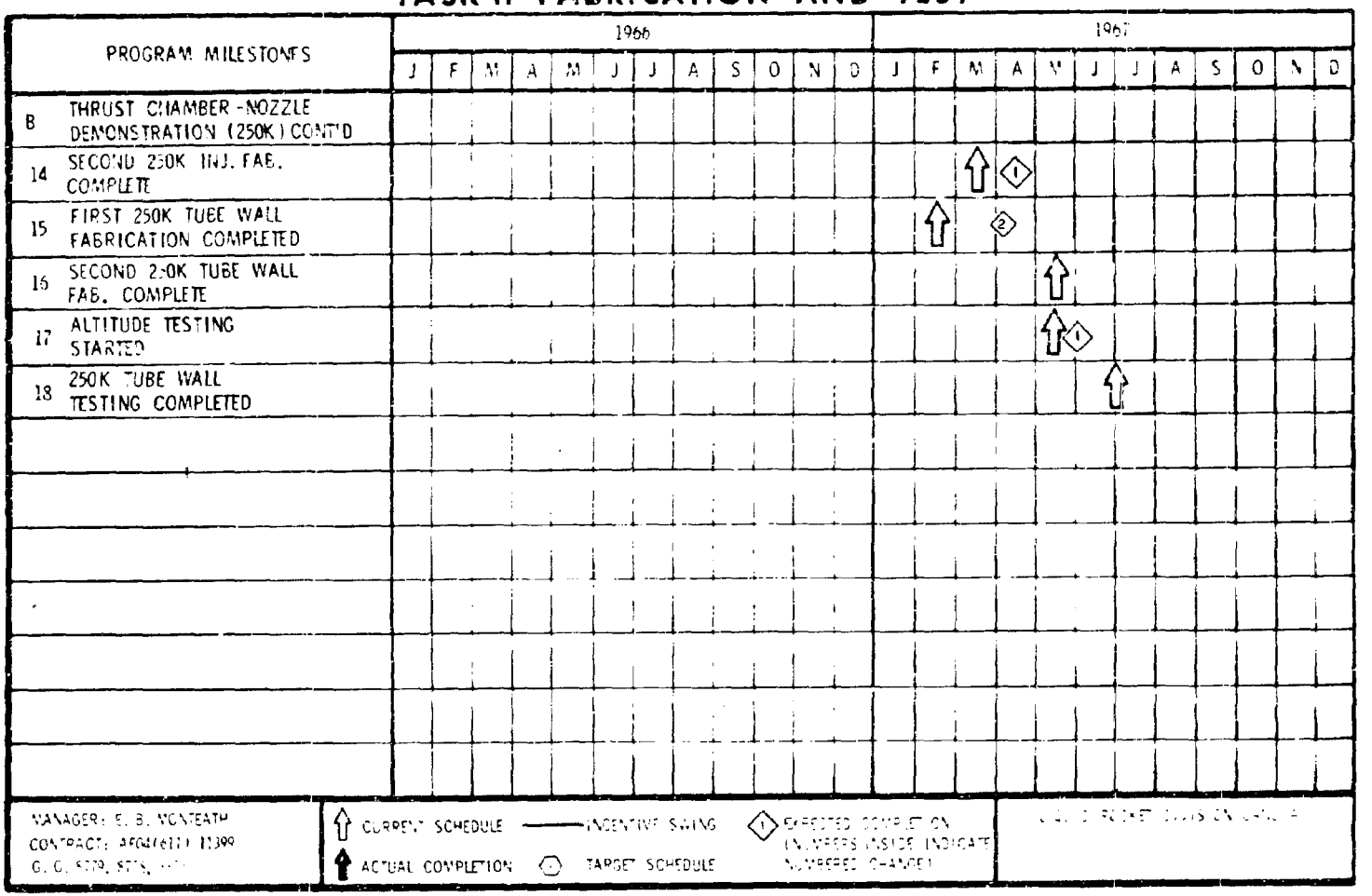

Figure 1. (Continued)

CONFIDENTIAL
8
CONFIDENTIAL

195 788
3 OF 3
12 66

CONFIDENTIAL

AIR FORCE
ADP AEROSPIKE ENGINE
SCHEDULE AND REVIEW PROCEDURE (SARP) CHART
TASK II FABRICATION AND TEST

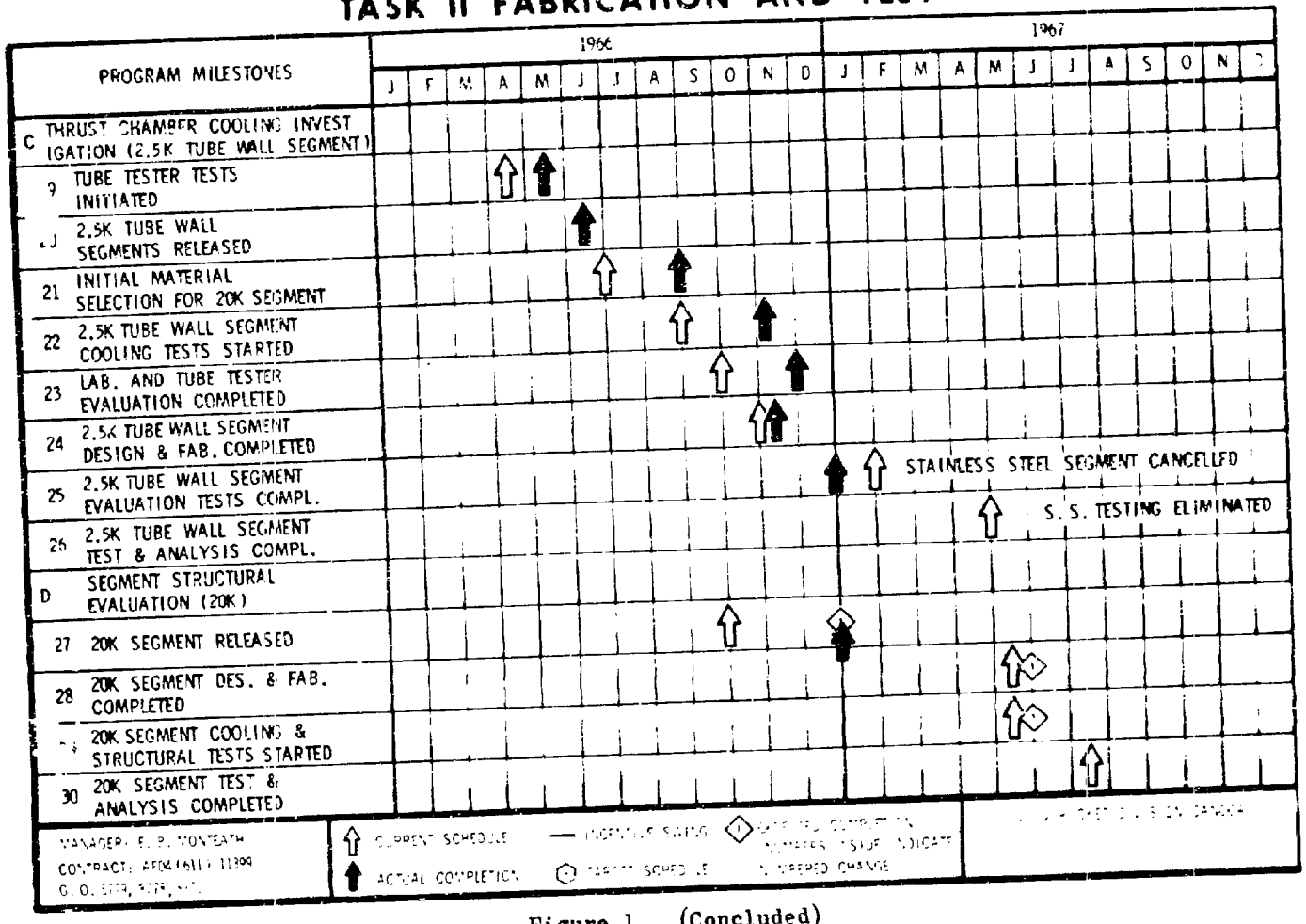

Figure 1. (Concluded)

CONFIDENTIAL

III. PROGRAM STATUS

A. TASK I, DESIGN AND ANALYSIS

1. MODULE DESIGN

a. Status

(C) A final engine balance consistent with the latest component designs was completed which defined the engine and component parameters over the complete range of thrust and mixture ratio requirements. The start sequence was established after resolution of the ignitor temperature problem by a return to a two-step main oxidizer valve. The mathematical model predicts a start transient from hot-gas ignitor ignition to full thrust of 3.5 seconds. The shutdown sequence and transients were also established indicating a satisfactory cutoff in 400 milliseconds.

(C) The second iteration of the module system design was completed, and subsystem design was completed on the pump mounts and base closure configurations. The turbine drive system hot-gas ducts were resized and rerouted to accommodate the series hot-gas valve arrangement.

(C) Preliminary turbopump layouts were made with the resolution of several design tradeoff studies. Curvic couplings and integral turbine blades were selected for the turbine wheels, and a pinned strut support was selected for the outboard turbine bearings. A rotating diffuser at the pump discharge has been incorporated into the LOX pump design replacing the hydraulic turbine and high-speed inducer, resulting in a decrease in balance drum diameter and seal speed.

(U) The thrust chamber layout was completed after defining the injector and baffle structural design and completion of the tube splice study. An oblate spheroid base closure design was selected, and the overall thrust chamber assembly sequence established.

(U) The control valve layouts were completed for the main propellant valves and the tapoff throttle valve. Heat transfer and poppet contour analyses were conducted on the tapoff valve.

b. Progress During Report Period

(1) System Analysis

(a) Engine Balance

(C) During this report period, engine balance analysis was performed at the intermediate thrust levels between 20- and 100-percent thrust and over the mixture ratio (MR) range from 5 to 7. The data are useful in determining the component performance requirements in the throttled area. Some

selected turbomachinery parameters are presented in Fig. 2 through 7 as a function of thrust and mixture ratio. The latest system nominal (MR = 6, P_c = 1500 psia) pressure distribution for both the liquid and hot-gas systems is presented in Tables 1 and 2. This data is based upon nominal propellant pump inlet conditions of 32 psia and 41.7 R temperature for the hydrogen and 37.5 psia and 175.5 R for the oxygen. The complete range of inlet conditions over which the pumps and system must operate is shown in Fig. 8.

(b) Start Dynamics

(C) A simple and rapid tank head start was achieved on the mathematical start model with the thrust chamber at the worst anticipated environmental condition of 620 R prior to initiation of start. The latest sequence utilizes the thrust and mixture ratio control system, thereby eliminating the need for an additional start control system, and will achieve 100-percent thrust from the hot-gas ignitor ignition in approximately 3.5 seconds.

(C) To start the engine, only a mainstage thrust command signal, a mainstage mixture ratio command signal, and a start signal are required. The time sequencing of the propellant and hot-gas valves will then follow as shown in Fig. 9. The various stages of start (time zero, start initiation, ignition, and mainstage) are shown in the schematics of Fig. 10.

(C) The main fuel valve and hot-gas ignitor fuel valve open first and fuel flow is established. The thrust control system senses no thrust and drives the tapoff throttle valve to the full-open stop. Similarly, the mixture ratio control system senses zero mixture ratio (no LOX flow and positive fuel flow) and drives the oxidizer turbine throttle valve to the full-open stop; thus when power becomes available, maximum energy is provided to the turbopumps for breakaway torque.

(C) After an appropriate length of fuel lead (no fuel lead is indicated on the transients presented; but realistically 0.5 to 1.0 seconds will probably be required), start is initiated by opening the hot-gas ignitor oxidizer valve, and combustion is established in the ignitor. Hot gas is supplied to the turbines and to the main chamber (Fig. 10b). The turbines begin to spin, and the pump discharge pressures begin to rise. The mixture ratio in the hot-gas ignitor is controlled by the LOX pressure regulator, thus maintaining the desired combustion temperature.

(C) Approximately 0.8 seconds following hot-gas ignitor ignition, the main oxidizer valve will be opened to the first step position. (A return to a two-step main oxidizer valve was made to improve the hot-gas ignitor temperature start transient. This subject is treated further in the Problem Areas and Solutions section.) Main propellant ignition will be achieved with oxygen in the gaseous state being injected shortly after the main oxidizer valve leaves the fully closed position (Fig. 10c). The high-temperature oxygen will exist for only a very short period and only at low chamber pressures, and therfore will not present an injector face cooling problem.

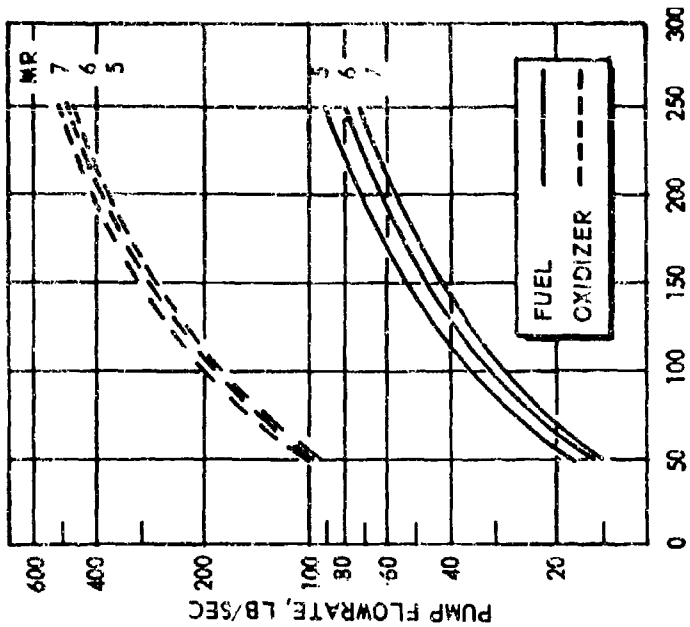

Figure 3. Pump Flowrate vs Thrust

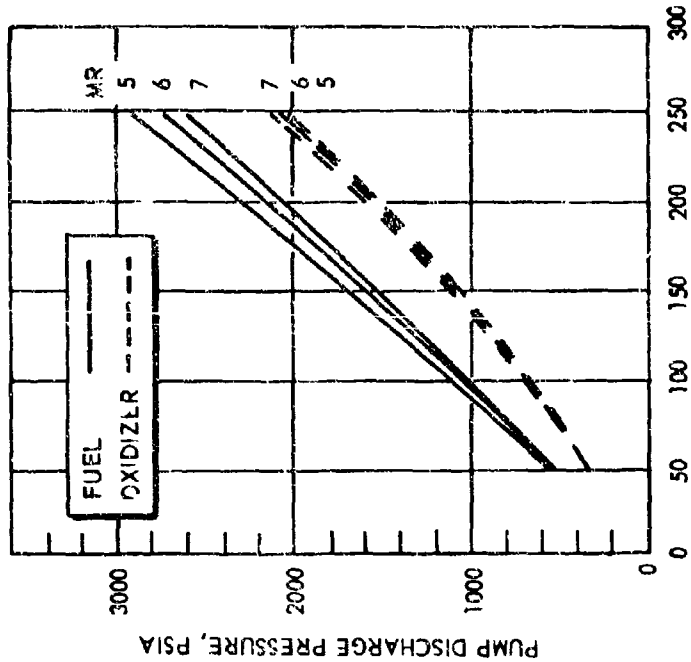

Figure 2. Pump Discharge Pressure vs Thrust

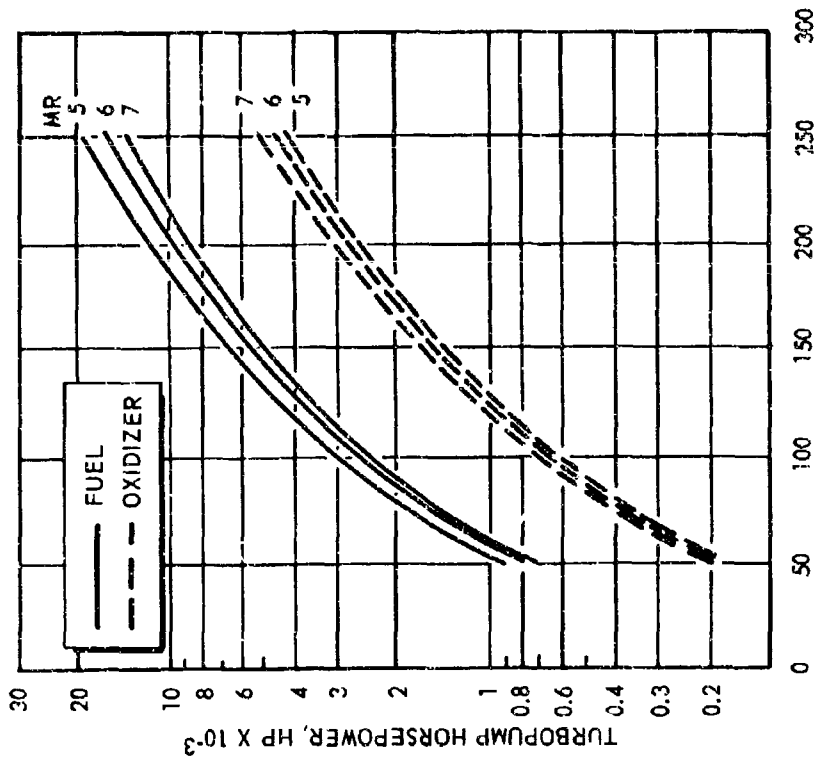

Figure 5. Turbopump Horsepower vs Thrust

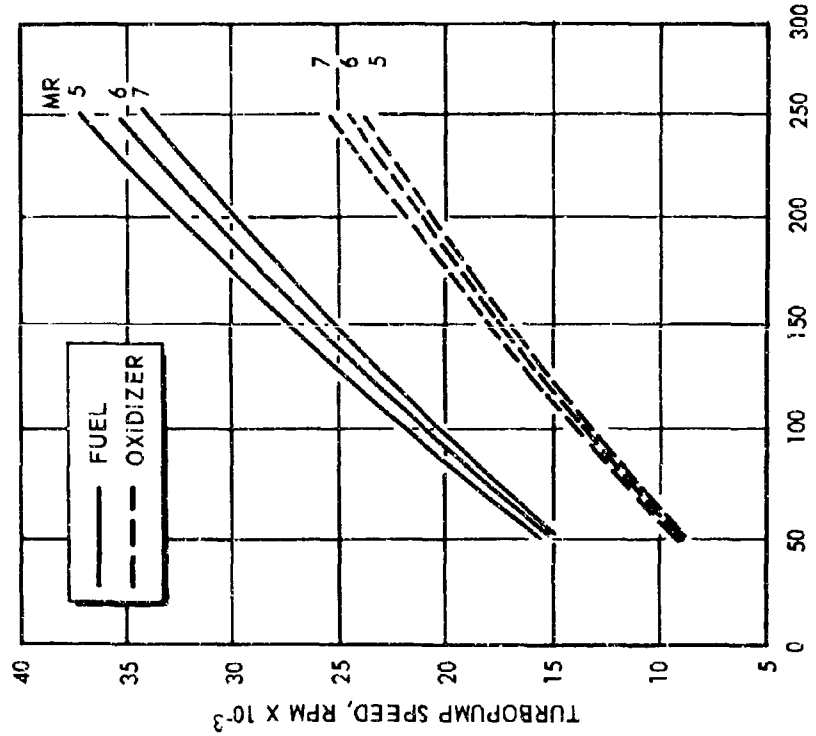

Figure 4. Turbopump Speed vs Thrust

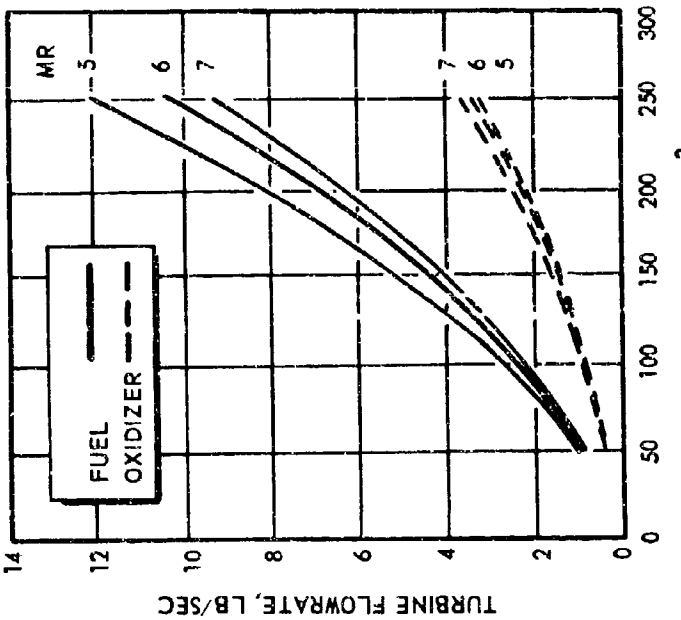

Figure 7. Turbine Flowrate vs Thrust

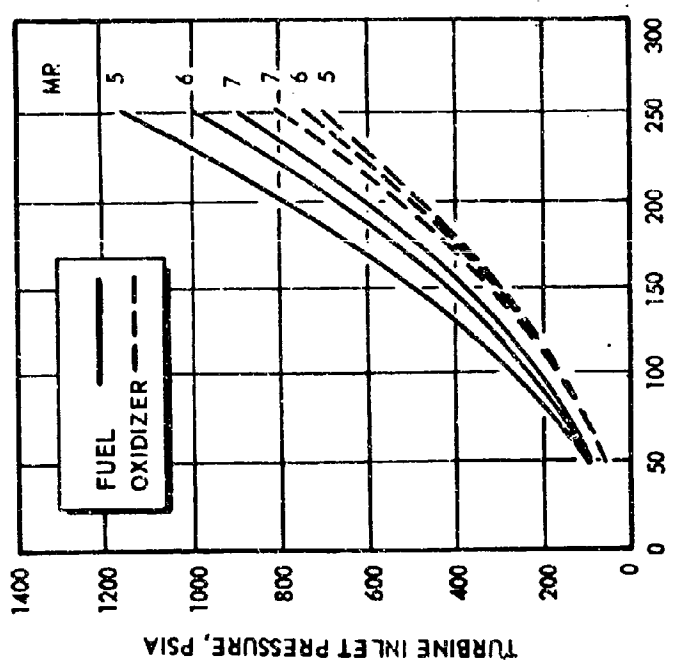

Figure 6. Turbine Inlet Pressure vs Thrust

TABLE 1

PROPELLANT FEED PRESSURE BUDGET

Nominal Budget (F=250K, MR=6:1)	Differential Pressure, psi	Downstream Pressure, psia	Weight Flowrate, lb/sec
Liquid Fuel Side			
Fuel Pump Discharge Pressure	-	2735	79.7
Main Fuel Valve	15	2720	79.7
Fuel High-Pressure Duct	91	2629	79.7
Fuel Flowmeter	5	2624	79.7
Regenerative Coolant Circuit	700	1924	79.7
Injector	394	1530	79.7
Chamber Pressure (Injector End)	-	1530	79.7
Liquid Oxidizer Side			
Oxidizer Pump Discharge Pressure	-	2056	478.3
Oxidizer High-Pressure Duct	23	2033	478.3
Oxidizer Flowmeter	5	2028	478.3
Main Oxidizer Valve	10	2018	478.3
Propellant Distribution Ducts	34	1984	239.1
Oxidizer Thrust Chamber Manifold	60	1924	478.3
Injector	394	1530	478.3
Chamber Pressure (Injector End)	-	1530	478.3

TABLE 2

TURBINE DRIVE SYSTEM PRESSURE BUDGET

Nominal Budget (F=250K, MR=6:1)	Differential Pressure, psia	Downstream Pressure, psia	Weight Flowrate, lb/sec
Injector End Pressure	-	1530	14.39
Tapoff Ports and Manifold	67	1463	14.39
Tapoff Ducts	13	1450	14.39
Tapoff Throttle Valve	258	1192	14.39
Distribution Manifold	8	1184	14.39
Fuel Turbine Drive Duct	14	1170	10.48
Fuel Turbine Calibration Orifice	170	1000	10.48
Fuel Turbine Inlet Pressure	-	1000	10.48
Fuel Turbine Exit Pressure	923	67	10.48
Oxidizer Turbine Drive Duct	8	1176	3.91
Oxidizer Turbine Throttle Valve	256	920	3.91
Oxidizer Turbine Calibration Orifice	170	750	3.91
Oxidizer Turbine Inlet Pressure	-	750	3.91
Oxidizer Turbine Exit Pressure	713	37	3.91
Base Closure Internal Pressure	-	30	14.39

TABLE 2

(Concluded)

Nominal Budget (F=150K, MR=6:1)	Differential Pressure, psia	Downstream Pressure, psia	Weight Flowrate, lb/sec
Injector End Pressure	-	324	1.27
Tapoff Ports and Manifold	2	322	1.27
Tapoff Ducts	0.9	321.1	1.27
Tapoff Throttle Valve	211.0	110.1	1.27
Distribution Manifold	0.8	109.3	1.27
Fuel Turbine Drive Duct	1.1	108.2	0.96
Fuel Turbine Calibration Orifice	16.9	91.3	0.96
Fuel Turbine Inlet Pressure	-	91.3	0.96
Fuel Turbine Exit Pressure	84.6	6.7	0.96
Oxidizer Turbine Drive Duct	0.6	109.5	0.31
Oxidizer Turbine Throttle Valve	27.9	81.6	0.31
Oxidizer Turbine Calibration Orifice	14.7	66.9	0.31
Oxidizer Turbine Inlet Pressure	-	66.9	0.31
Oxidizer Turbine Exit Pressure	63.2	3.7	0.31
Base Closure Internal Pressure	-	3	1.27

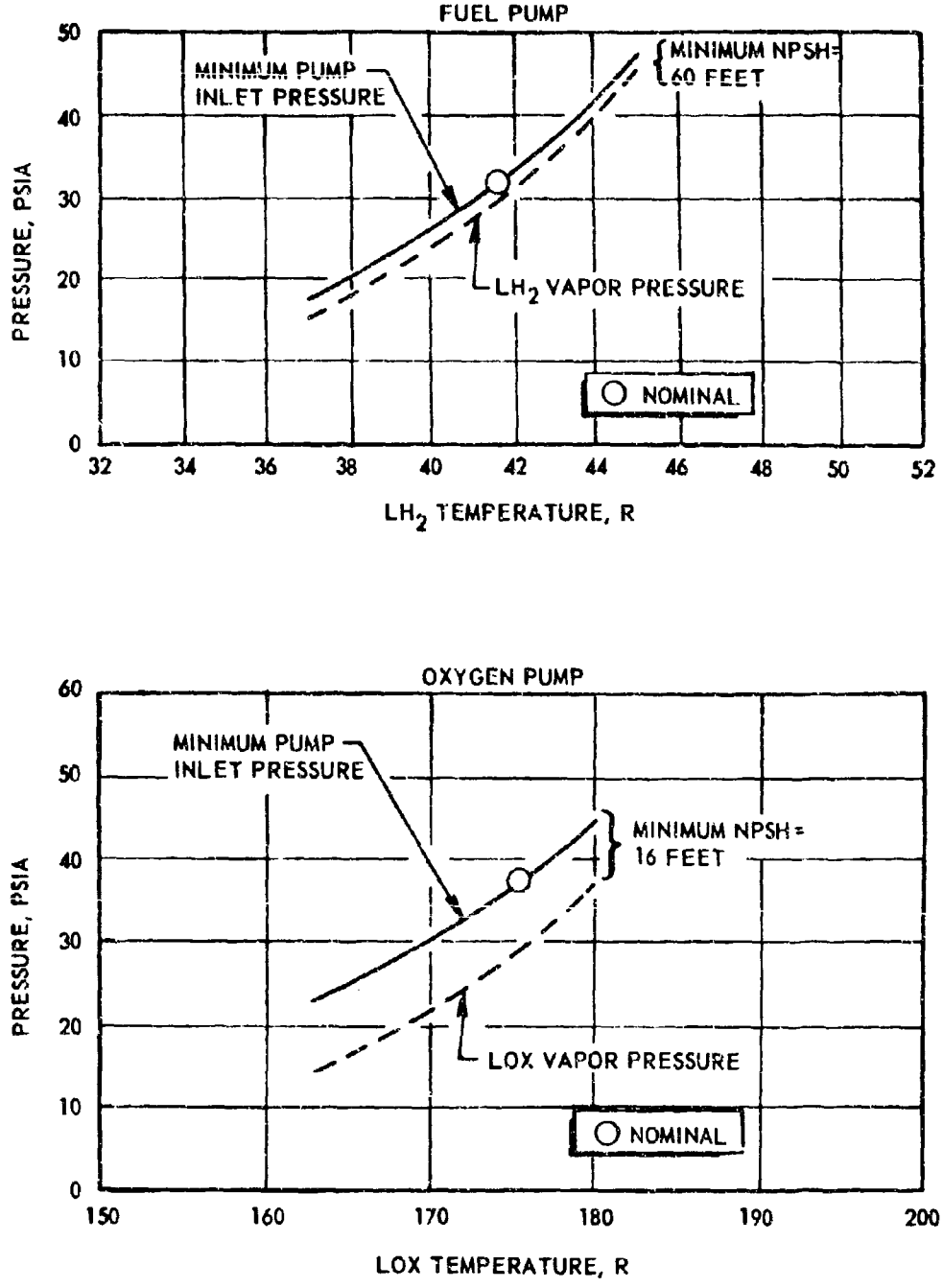

Figure 8. Propellant Pump Inlet Conditions

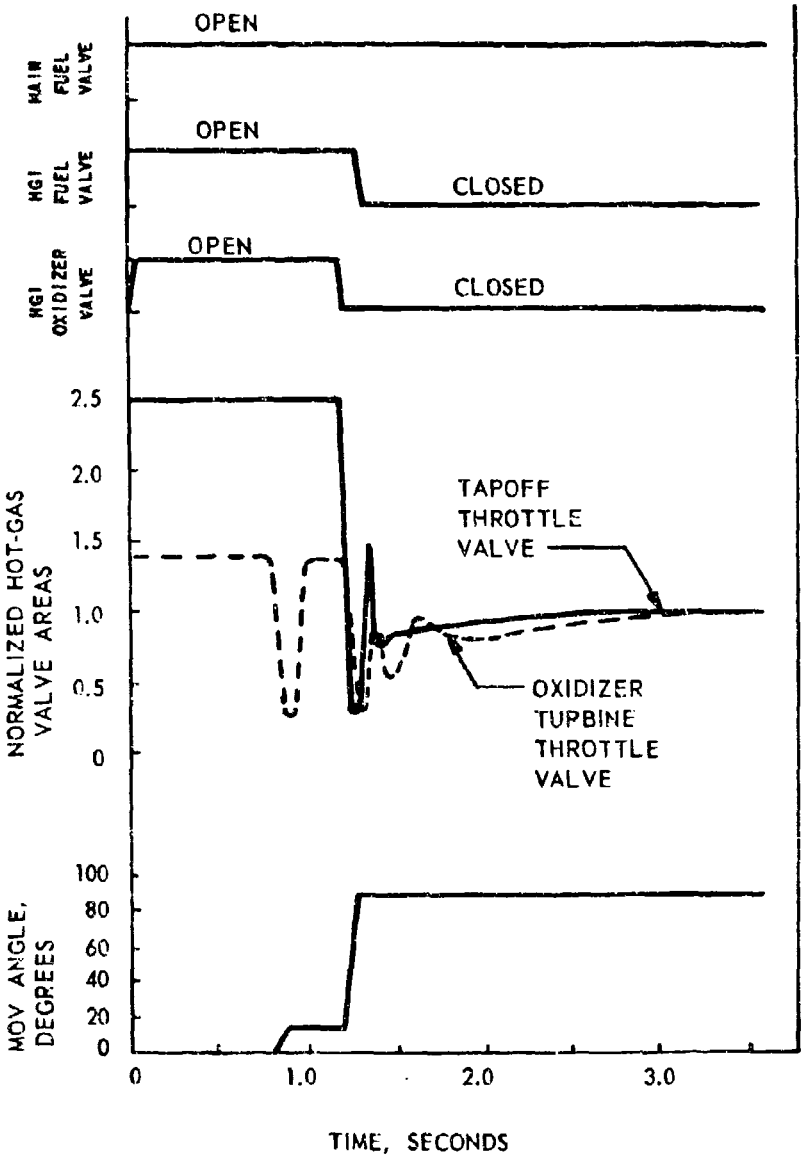

Figure 9. Start Transient Valve Sequencing

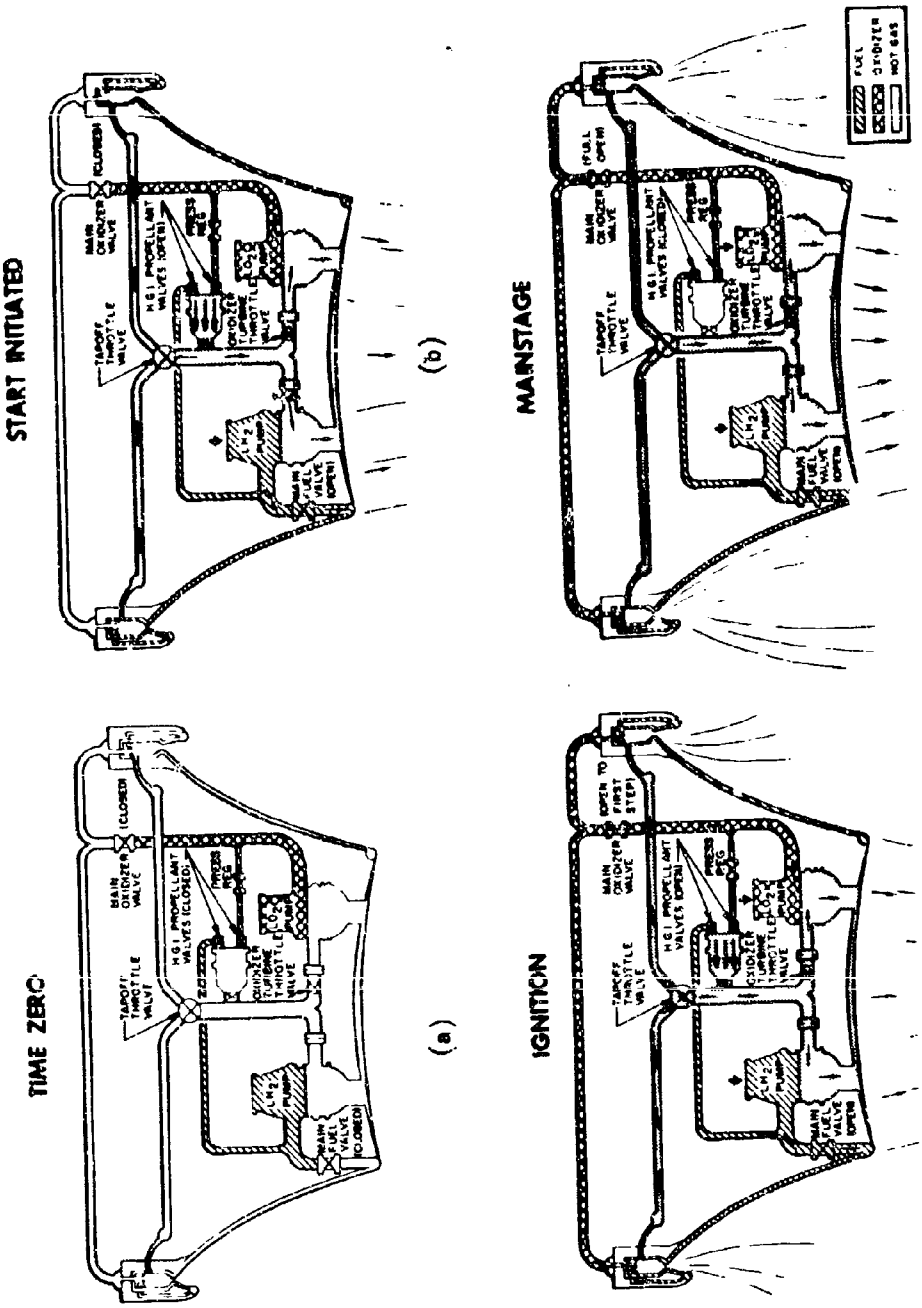

Figure 10. ADP Module Start Sequence

(C) After approximately 0.4 seconds, full LOX prime will be achieved, the main oxidizer valve is ramped to full open, chamber pressure begins to rise steeply, the hot-gas ignitor valves are closed, and the engine commences mainstage operation with the turbines driven by main chamber tapoff flow (Fig.10d). The remainder of the transient to command thrust level is governed by the thrust control system.

(C) The transient pump flowrates and pressures, and main chamber pressure are shown in Fig. 11 and 12. Studying these curves together with the valve sequence (Fig. 9) will explain the action of the hot-gas throttle valves. During the interval when the LOX manifold is being primed (0.8 to 1.2 second), oxidizer flowrate through the liquid feed system will rise rapidly. The active mixture ratio controller will sense a high engine mixture ratio and begin to control the oxidizer turbopump speed by closing the oxidizer turbine throttle valve. This effect causes the LOX pump discharge pressure to decay momentarily but the fuel pump is unaffected, and the mixture ratio will slightly undershoot. The oxidizer turbine throttle valve then returns to the full-open position until the main oxidizer valve moves to the full-open position. At that time, the oxidizer flowrate again rises rapidly and the mixture ratio controller reacts by closing the oxidizer turbine throttle valve. Meanwhile, main chamber ignition has occurred and chamber pressure rises steeply. This causes the thrust controller to react to prevent a thrust overshoot, and hence the tapoff throttle valve area is decreased. From this point, the two valves react to bring the system to the command thrust level.

(c) Shutdown Dynamics

(C) Engine shutdown is achieved in a manner insuring fuel-rich thrust chamber mixture ratio by closing first the tapoff valve, then the main oxidizer valve, and finally the main fuel valve. The tapoff throttle valve is signaled to close by a zero thrust command at the same time as the main valves are signaled to close. The tapoff throttle valve has the fastest closing time (approximately 35 millisecond), while the main valves are considerably delayed (150 millisecond for the oxidizer valve and 400 millisecond for the fuel valve). In this shutdown sequence, turbine power is cut off just prior to main valve closure thus reducing cutoff surges in the propellant feed systems. The cutoff pressure and speed decays are shown in Fig. 13 and 14, and mixture ratio vs time in Fig. 15. Almost 95 percent of chamber pressure is lost in the first 150 milliseconds. An oxidizer feed system pressure surge is exhibited between 100 and 150 milliseconds, after which the chamber pressure decay rate is more gradual. Complete shutdown is achieved after 400 milliseconds.

(d) Controls

(C) Figure 16 illustrates the throttling and mixture ratio control systems for the ADP demonstrator module. All components of the control systems with the exception of the two hot-gas valves are test stand facility items.

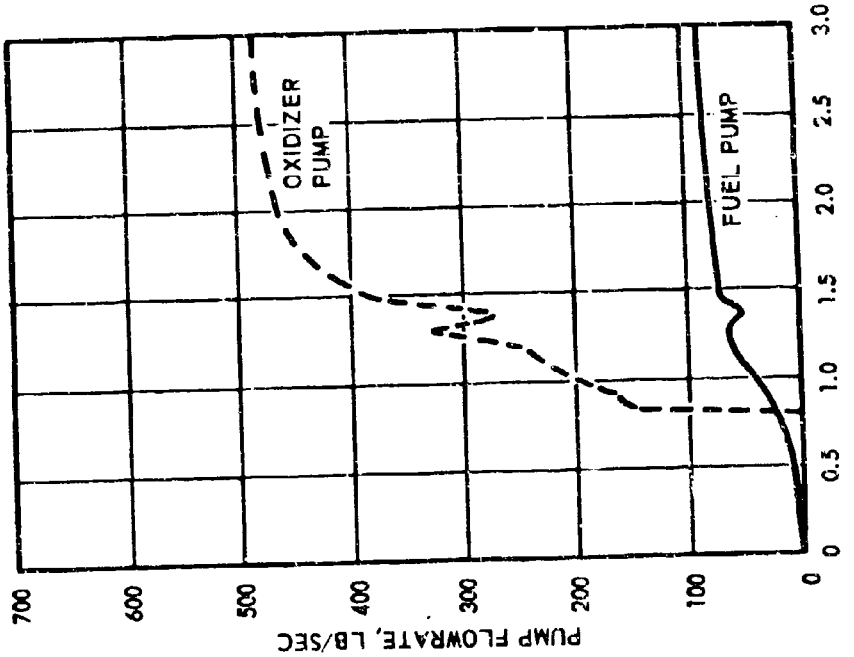

Figure 12. Start Transient Flowrate Buildups

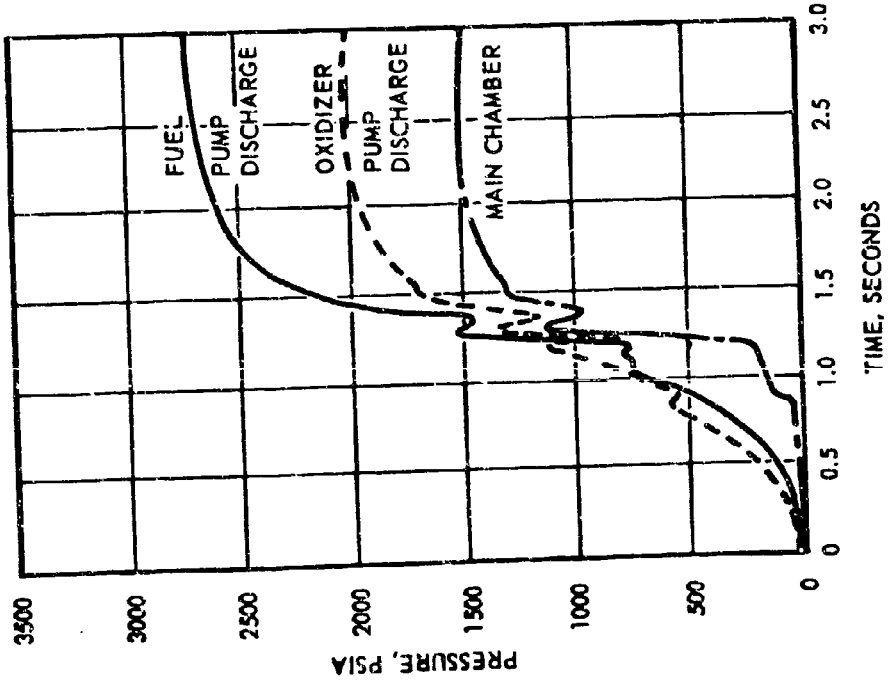

Figure 11. Start Transient Pressure Buildups

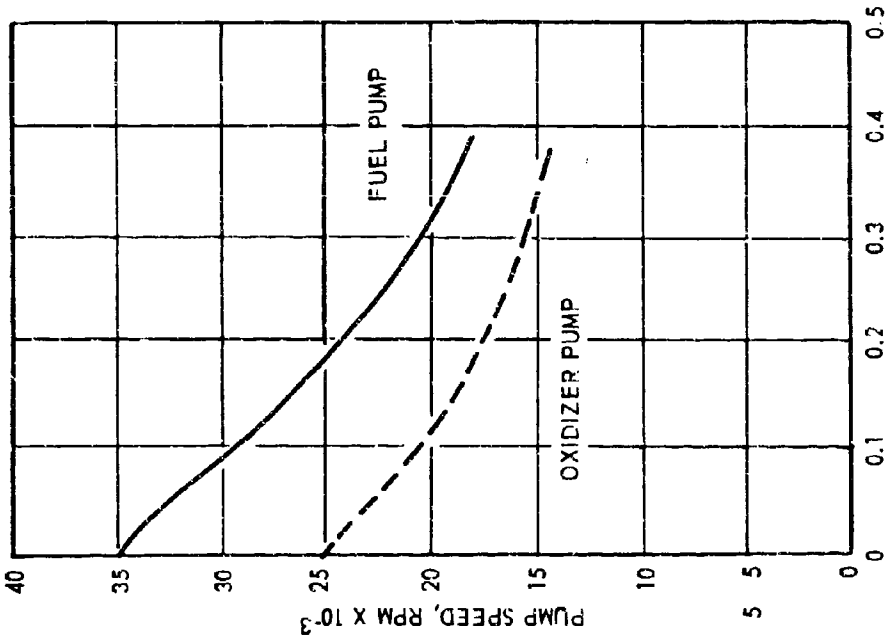

Figure 14. Pump Speed Cutoff Decay

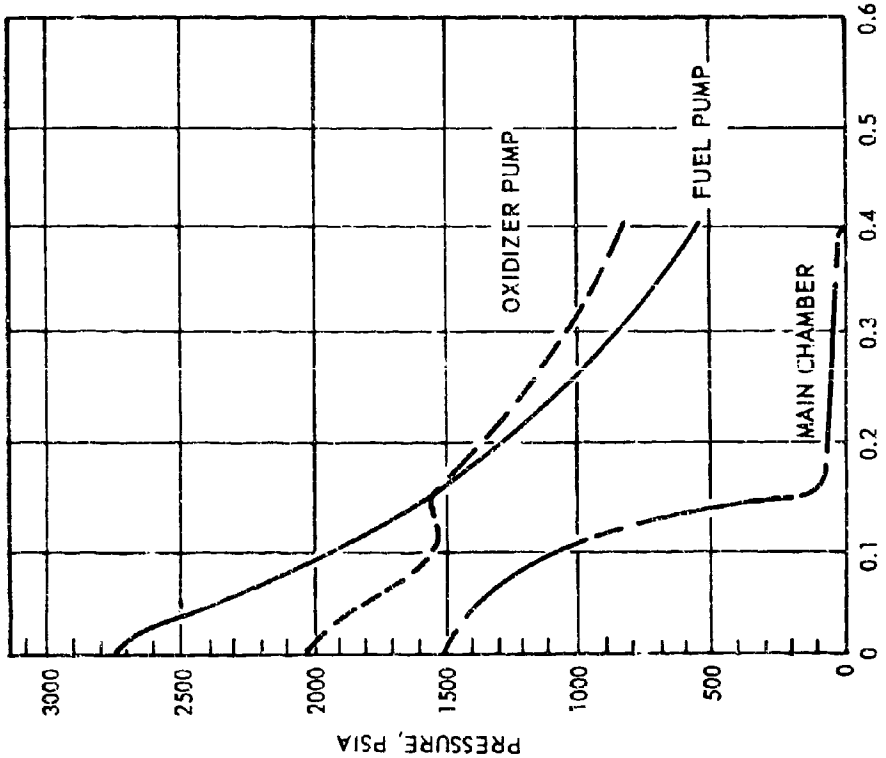

Figure 13. Pressure Cutoff Decay

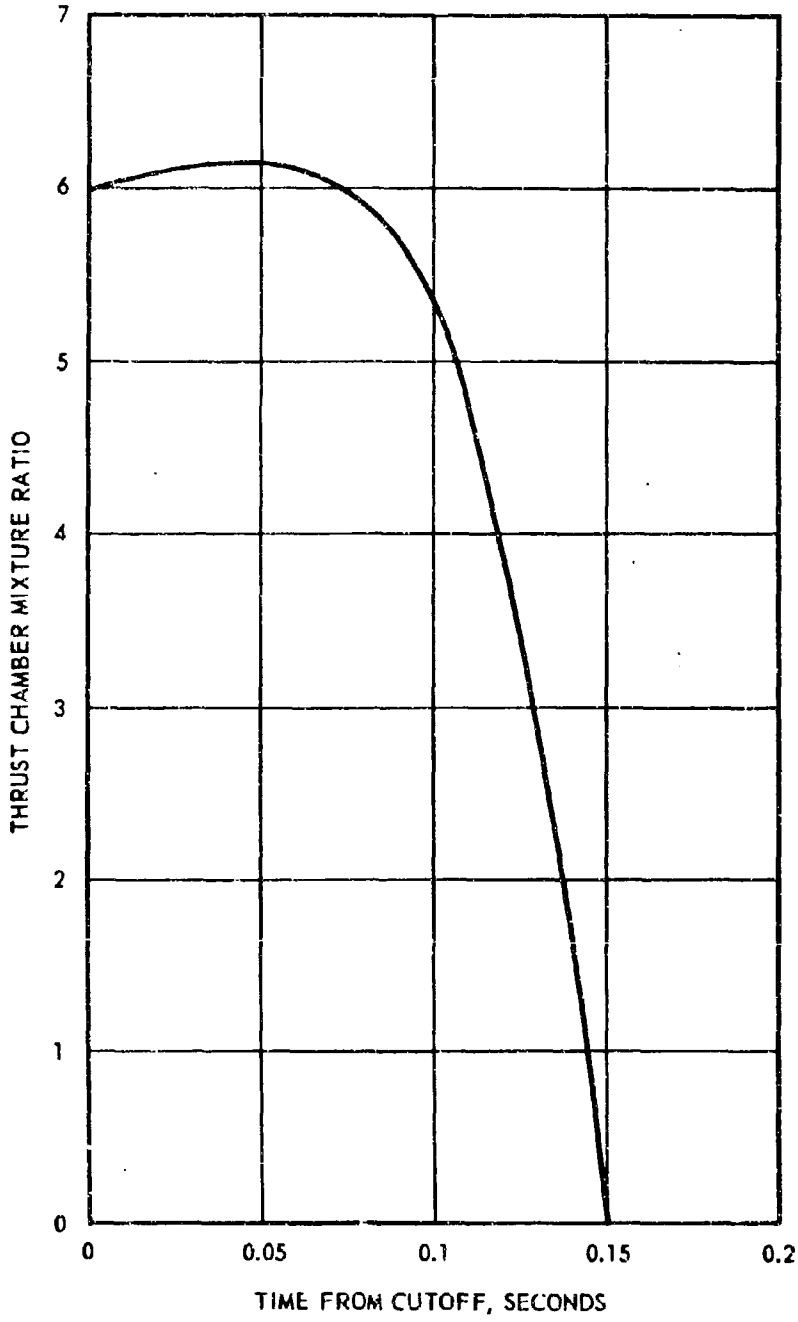

Figure 15. Thrust Chamber Mixture Ratio vs Time From Cutoff (150 milliseconds MOV Closing Time)

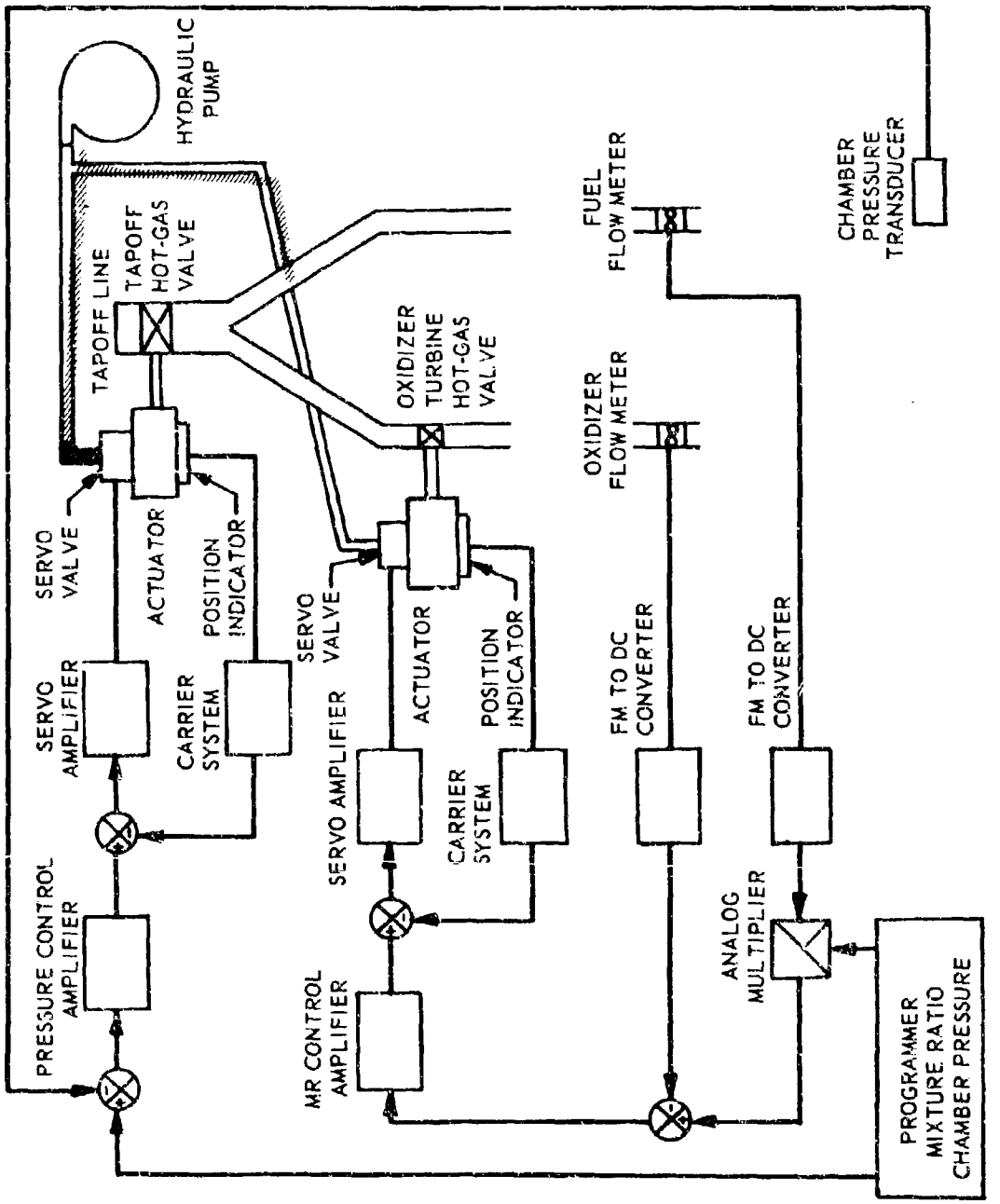

Figure 16. Preliminary Layout and Functional Diagram, ADF Closed-Loop Throttling and Mixture Ratio Controls

(C) The chamber pressure control loop senses chamber pressure and compares this signal with a reference value supplied by the programmer. The difference signal which is proportional to the error is integrated by the chamber pressure controller to produce a position reference for the tapoff hot-gas valve position control loop. This position control loop operates by sensing the position of the valve, comparing the sensed position with the reference, and amplifying the resultant signal to operate a hydraulic servovalve which supplies oil to the valve actuator. The logic of the position loop is such that the valve is positioned according to the position reference input.

(C) To illustrate normal chamber pressure control operation, an increase in the pressure reference will cause the tapoff hot-gas valve to start opening. This will result in a chamber pressure increase which will continue until chamber pressure equals the new reference level.

(C) The mixture ratio control loop operates by comparing measured oxidizer flow with a generated reference value. If oxidizer flow is lower than the reference value, then the error is integrated to cause opening of the oxidizer turbine valve until oxidizer flow has increased to the desired value. This control loop has a valve position loop which operates in a manner identical to that of the pressure control loop.

(C) The oxidizer flow reference is generated by multiplying the measured fuel flow by a factor which is a function of the desired mixture ratio.

(2) System Preliminary Design

(a) Demonstrator Module Design

(U) During this report period, the second iteration of the module layout was completed. The general arrangement shown in Fig. 17 incorporates the new thrust structure design, series arranged hot-gas control valves, propellant flow meters, resized liquid and gas ducts, and a new base closure configuration. The details evaluation of this layout is not completed. A schematic of the demonstrator module system and breakout of the system into subsystems is shown in Fig. 18. A discussion of the effort accomplished on each of the major subsystems is presented below.

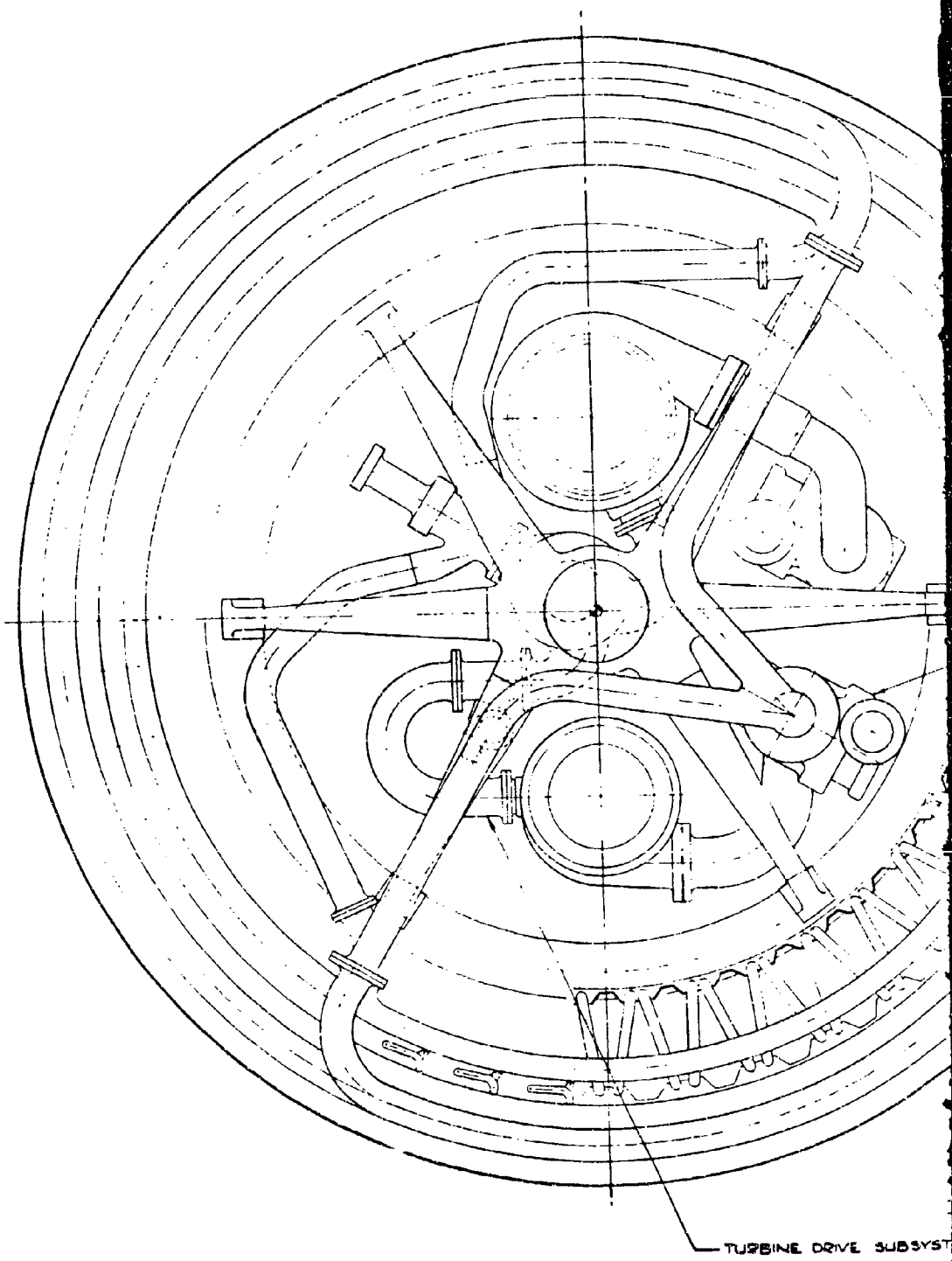
TURBINE DRIVE SUBSYST

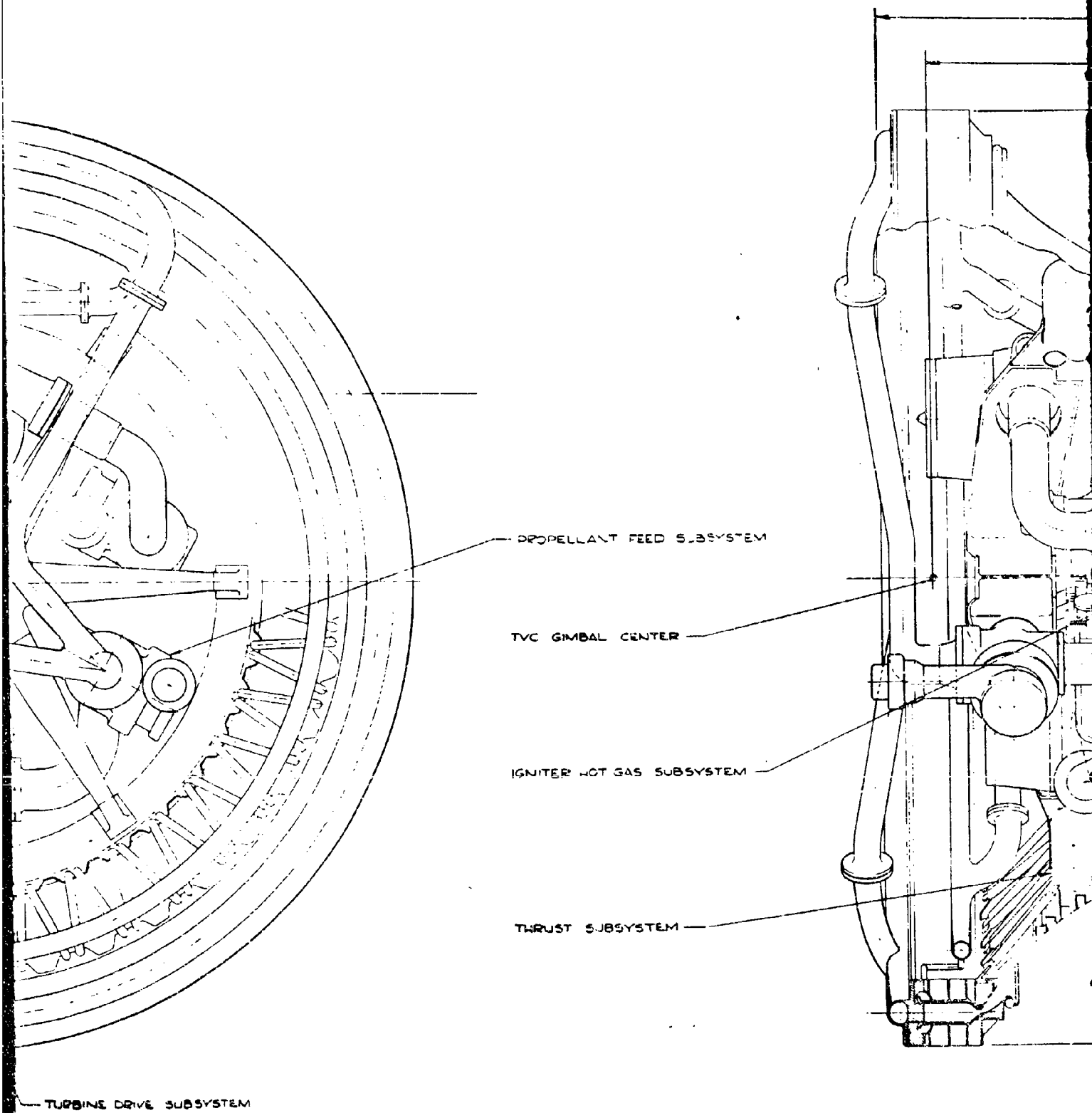
PROPELLANT FEED SUBSYSTEM
TVC GIMBAL CENTER
IGNITER HOT GAS SUBSYSTEM
THRUST SUBSYSTEM
TURBINE DRIVE SUBSYSTEM

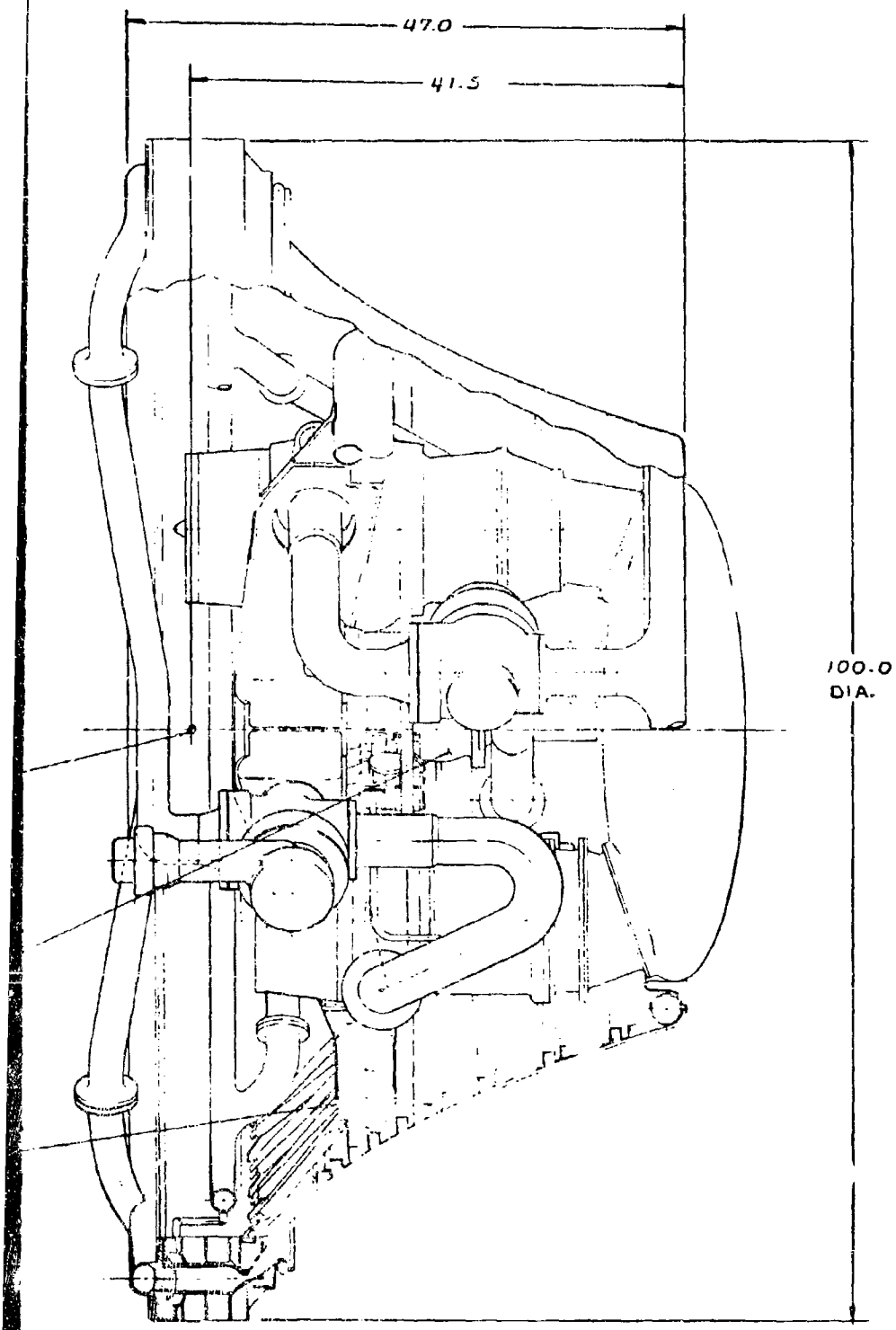

Figure 17. Demonstrator Module, Layout

3

CONFIDENTIAL

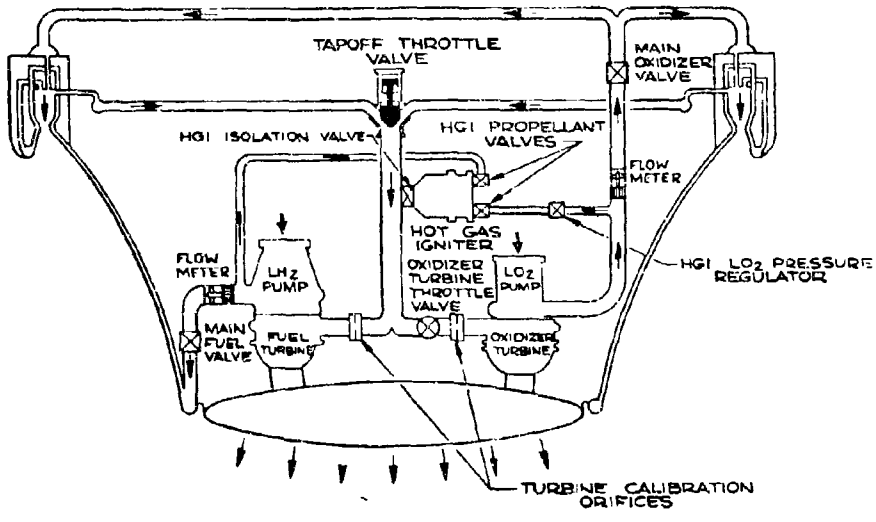

ADP DEMONSTRATOR MODULE SCHEMATIC

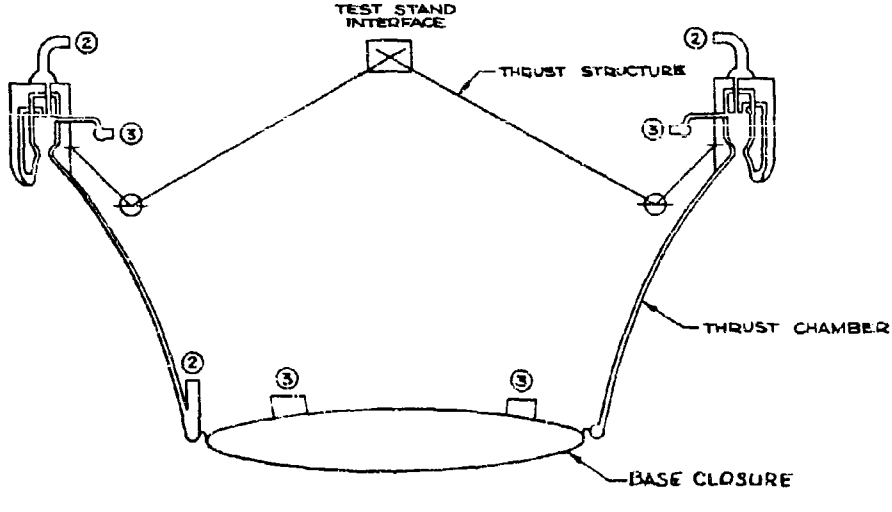

①—THRUST SUBSYSTEM

③—TURBINE D

②—PROPELL

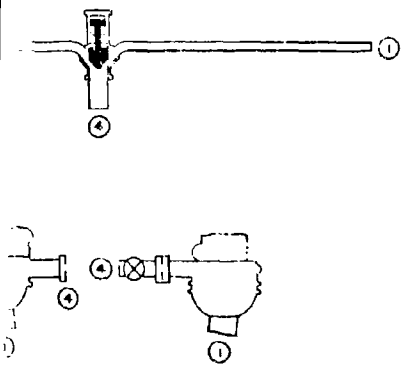

RIVE SUBSYSTEM

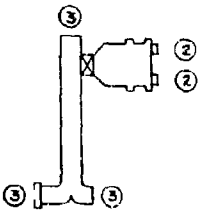

④–IGNITER HOT GAS SUBSYSTEM

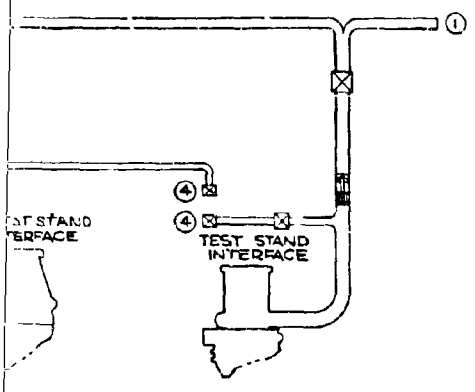

ANT FEED SUBSYSTEM

SUBSYSTEM INTERFACE
LEGEND:

① — THRUST SUBSYSTEM
② — PROPELLANT FEED SUBSYSTEM
③ — TURBINE DRIVE SUBSYSTEM
④ — IGNITER HOT GAS SUBSYSTEM

Figure 18. System and Subsystem Schematic

2

CONFIDENTIAL

(b) Thrust Subsystem

(U) The thrust subsystem, Fig. 18 and 19, is comprised of the Aerospike thrust chamber, the thrust structure, and the base closure. The thrust chamber is discussed in subsequent paragraphs of this report and therefore will not be covered at length in this section.

(U) The thrust structure configuration reported in the previous quarterly progress report (AFRPL-TR-66-348) has been integrated into the design. The intermediate ring of the thrust structure has been reduced 2 inches in diameter to clear the thrust chamber nozzle bands, and adjustment has been made in the ring elevation to maintain the radial beam profile geometry.

(U) A conceptual design for trunion-type turbopump mounts was prepared as shown on the thrust subsystem drawing (Fig. 19). It was studied for the system as a second candidate design in addition to the previously reported adjustable mount because of weight, thrust structure and pump structural considerations, and mechanical simplicity.

(U) In this design, the fuel turbopump is provided structural support from the thrust structure at the fuel discharge flange (Section C-C, Fig. 19) and by a structural pad and fitting (Section D-D) on the fuel volute opposite the discharge flange. In the manner shown in Fig. 19 fittings with spherical surfaces permitting angular misalignment are incorporated on the centerlines of the radial beams adjacent to the pump. The fitting at the flange provides a fixed point of support, and the opposite fitting is fixed in two directions allowing motion in a radial direction from the pump centerline through the fitting. A third support point fixed in one direction is provided between the thrust chamber base closure and the pump shell as shown in Fig. 20 to prevent motion of the pump about the axis formed by the two fittings on the thrust structure.

(U) The trunion design for the oxidizer pump provides structural support at two structural pads and fittings 180 degrees apart on the volute in the manner shown in Fig. 19. The other aspects of the oxidizer pump mounts are identical to those of the fuel pump. In addition to the turbopump loads, the turbopump mounts transmit the base closure thrust loads to the thrust structure.

(U) A structural and interface concept for the base closure design has been selected based upon carrying the base closure thrust loads in the turbine ducts and turbopump shells to the thrust structure. A gas-tight flexure provides the seal between the base closure and the thrust chamber, and is a minimum thrust-load carrying member. The flexure, besides providing a seal, deflects to relieve thermal loads and accommodate assembly tolerance stackup. The base closure is an oblate spheroid composed of two thin Inconel 718 shells joined by welding at their edges. The forward surface is provided with flanges to mate with the turbine discharge ducts, and the outer periphery has mechanical fasteners to permit closure removal for inspection and maintenance. The interior volume serves as a plenum for the turbine discharge gases, and the aft surface is perforated to

CONFIDENTIAL

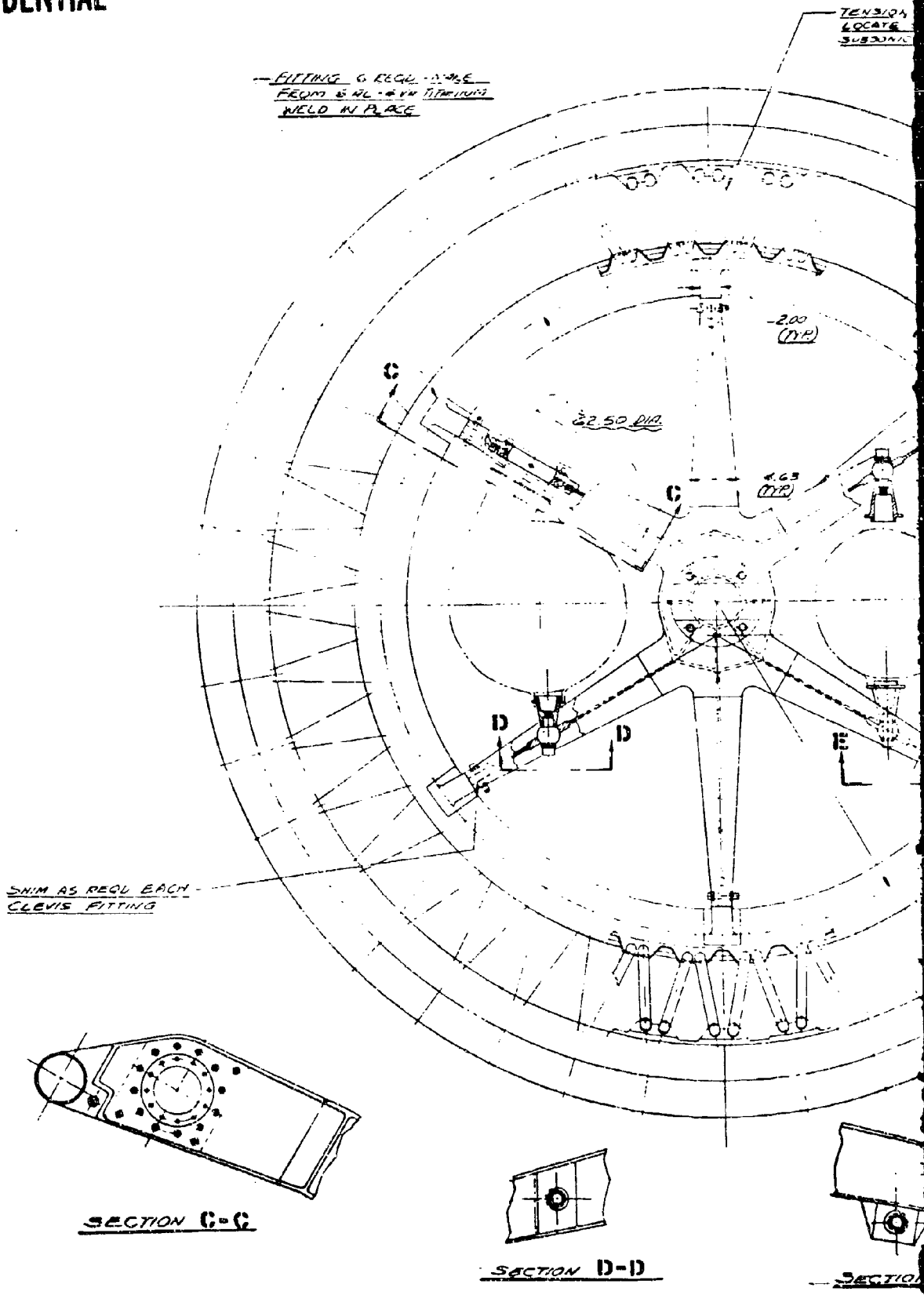

TENSION TUBE, 80 REQD
LOCATE 1 IN AT EACH
SUBSONIC BAFFLE ℄
SPACER RING - MADE FROM
6AL - 4VN TITANIUM
WELD AS SHOWN
℄ SUBSONIC BAFFLE
THRUST STRUCTURE TO
THRUST CHAMBER
WELDED INTERFACE
UPPER CONE
MADE FROM 6 AL
2.00
(TYP)
4.63
(TYP)
.250 TYP
E
E
MAKE FROM 6AL-4V
TITANIUM TUBE
1.000 OD x .032 WALL
4.150
3.35
3.00 (TYP)
WELD (TYP)
.250
.300
(TYP)
A
A
B
B
45°30'
5.00
.125 WALL
10.186
THROAT
COMBUSTION CHAMBER
SUBSONIC
BAFFLE
WELD (TYP)
VIEW A-A
SCALE - ½ SIZE
.500 DIA HIGH STRENGTH
SHEAR BOLT 6 REQD
SECTION E-E

2

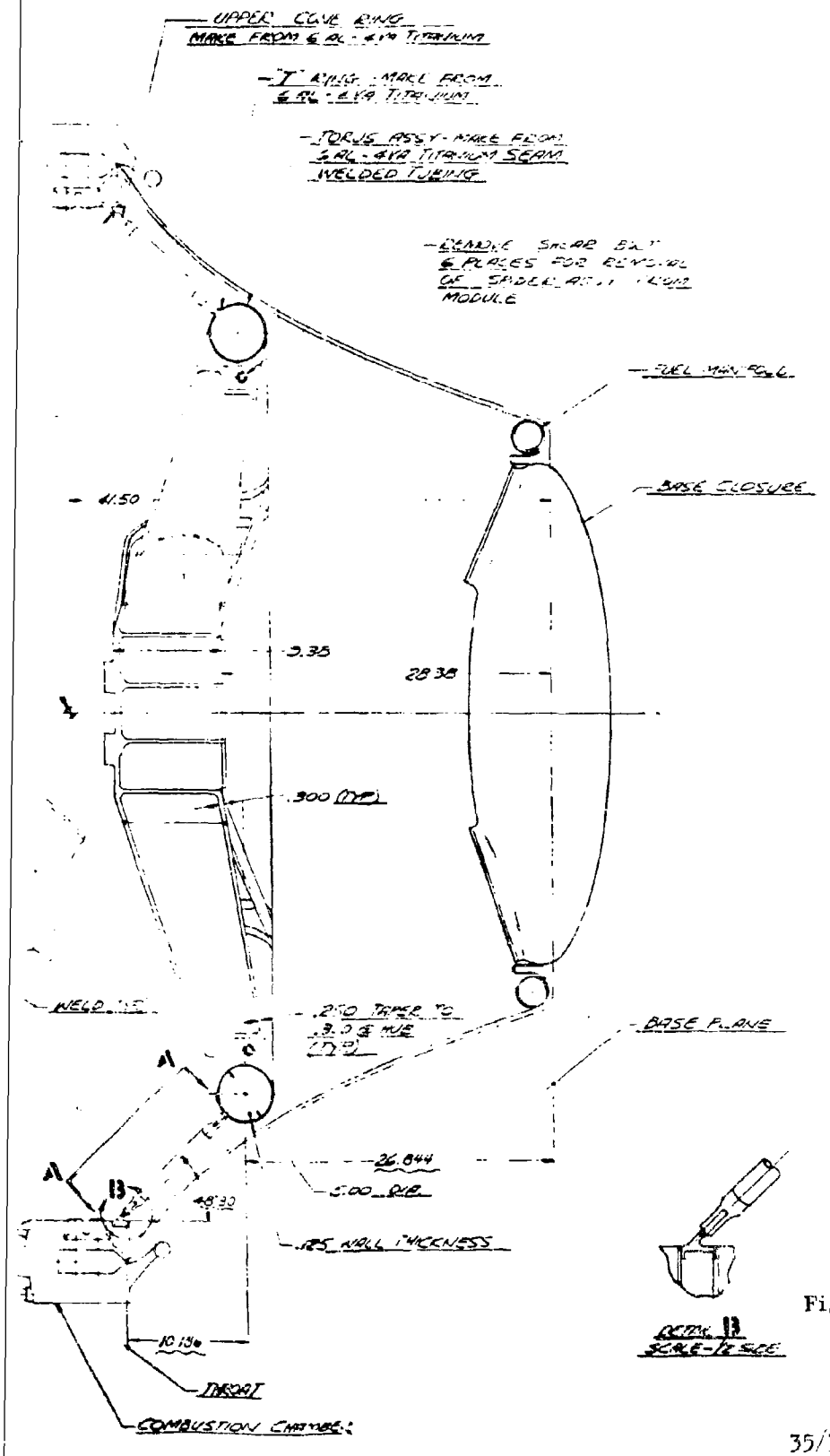

Figure 19. Thrust System Layout

CONFIDENTIAL

CONFIDENTIAL

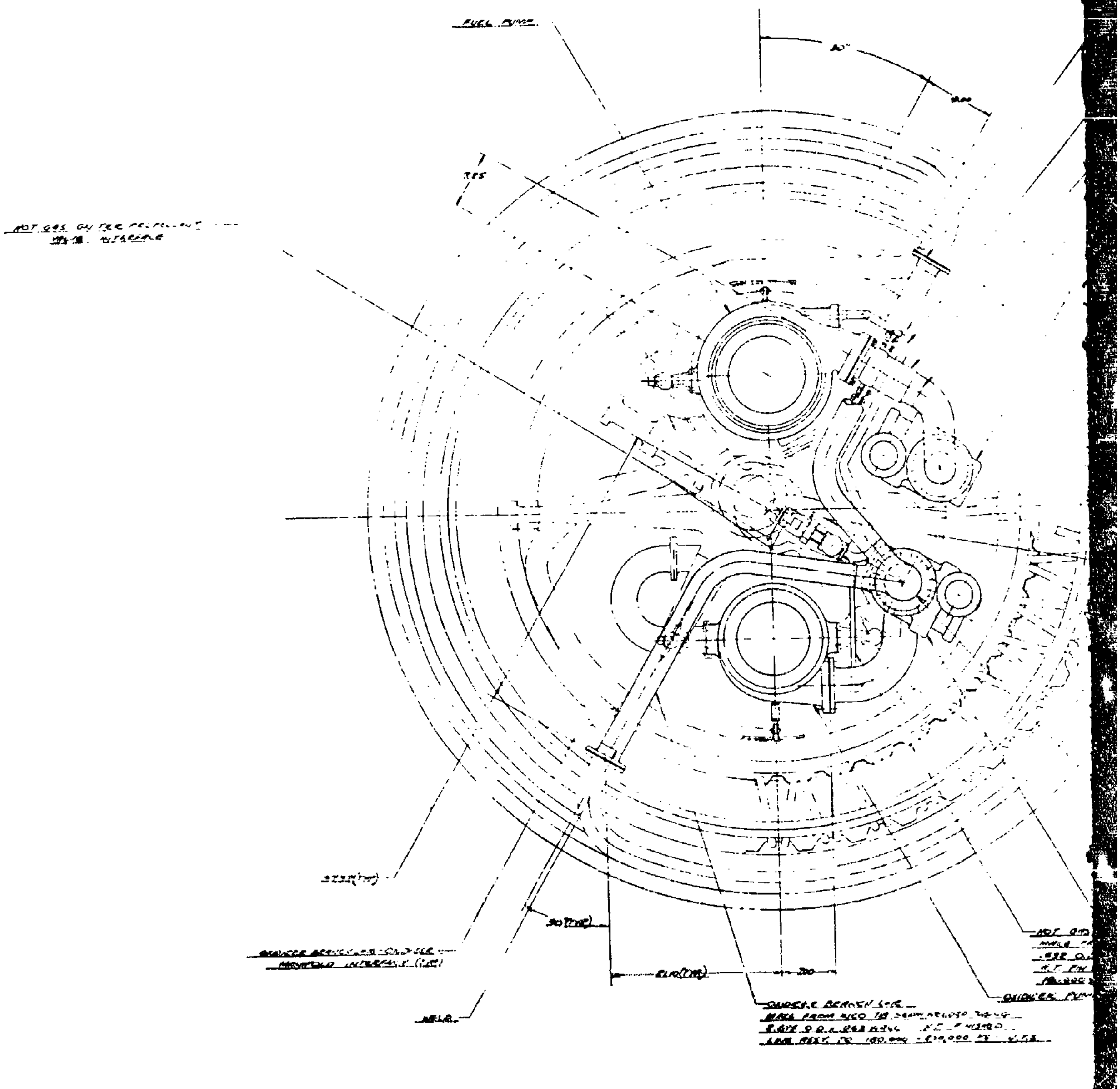

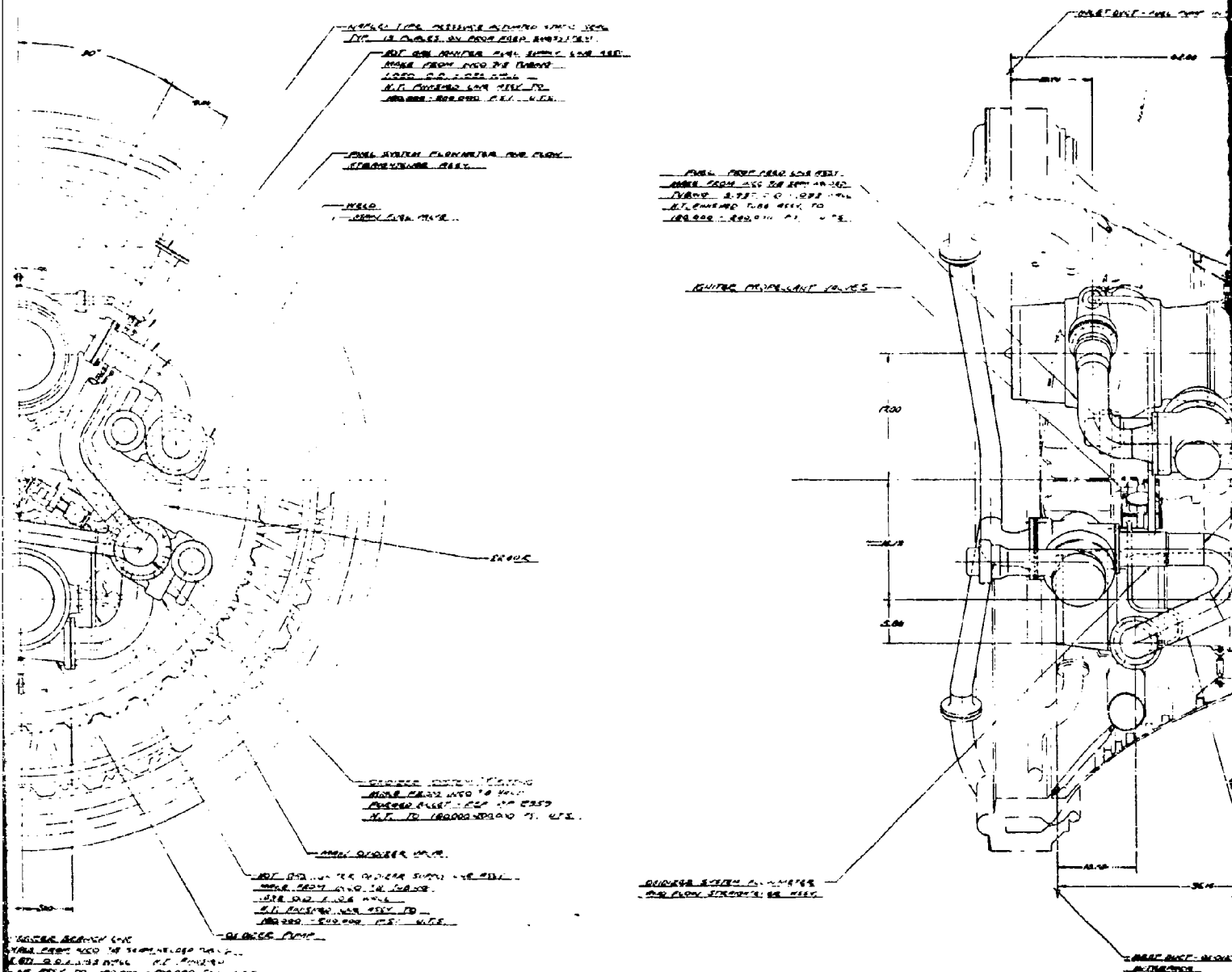

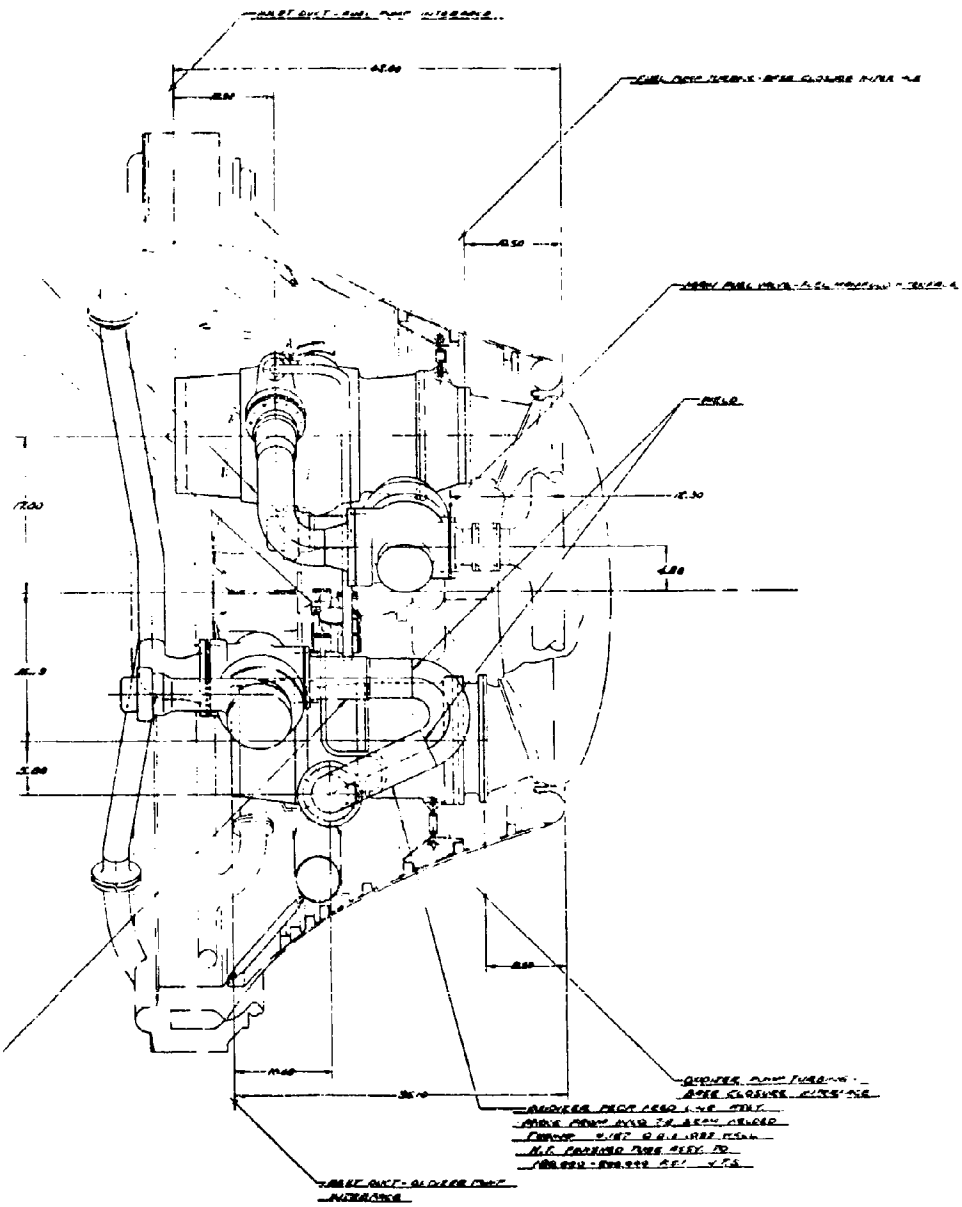

Figure 2C. Propellant Feed Subsystem Layout

CONFIDENTIAL

inject these gases into the base region of the truncated spike nozzle. The thrust loads imposed on the pump shells during engine operation are comparable to the loads they would experience from bellows reactions in the flexible turbine exhaust duct configuration.

(U) The turbopump mounts and base closure design presented require more complete structural sizing and dynamic and thermal analysis before detailing can be initiated.

(c) Propellant Feed Subsystems

(U) The propellant feed subsystem, Fig. 18 and 20, is comprised of the fuel and oxidizer turbopumps, the main fuel and oxidizer valves, flow meters, the igniter LOX pressure regulator, the igniter propellant valves, and the propellant ducting. The turbopump and main propellant valve designs reported in AFRPL-TR-66-348 have been integrated into the design. Deletion of the fuel bypass was also accomplished, and flow meters are included in the main propellant ducts. As previously reported, it is a design objective to eliminate the need for all line bellows. The location of the turbopump centerlines and the main oxidizer valve position remain unchanged. The main oxidizer duct is split downstream of the main oxidizer valve to the two inlets of the oxidizer injector manifold 180 degrees apart. (See Demonstrator Module Thrust Chamber Design section for further discussion of oxidizer manifold design.) The main oxidizer duct upstream of the valve is increased in length to accommodate a turbine-type flow meter in the duct.

(U) The main fuel valve has been relocated and a straight length of fuel duct added to accommodate a turbine-type flow meter at the fuel pump discharge. A clearance hole is provided in the web of the thrust structure radial beam to permit the routing which also accommodates the new fuel pump discharge configuration. A honeycomb flow straightener is included in the flow meter assemblies which provides nonswirl, uniform, straight flow characteristics at the rotor.

(U) The sizing of the main propellant ducts for flow and pressure drop has been accomplished. Preliminary structural sizing of the ducts has been accomplished and the ducting and component interfaces identified dimensionally.

(d) Turbine Drive Subsystem

(U) The turbine drive subsystem, Fig. 17 and 18, is comprised of the tapoff throttle valve, the oxidizer turbine throttle valve, the fuel and oxidizer turbine orifices, and ducting. The tapoff and turbine drive ducts have been rerouted to accomplish the series valve arrangement. The tapoff throttle valve is located in the "Y" joining the two tapoff ducts and its discharge flange interfaces with the tapoff/igniter distribution manifold. The concept of locating the valve in an existing system Y-joint

permitted the selection of a poppet-type valve which has a considerably lower open flow pressure loss than conventional 90-degree poppet valves, thus permitting the system to realize the advantages of low weight and low cost inherent in the poppet design.

(U) Equal length tapoff ducts extend from the two tapoff manifold interface flanges to the valve and are routed to provide adequate length and shape to permit deflection with thermal growth. The oxidizer turbine control valve upstream interface is attached to the distribution manifold, and the oxidizer turbine drive duct is attached to the downstream face. The duct is routed to permit deflection with thermal growth. The system calibration orifices are located in the flange joint interface between the distribution manifold and the fuel turbine inlet and at the interface between the oxidizer turbine throttle valve and the duct. Sizing of the ducts for flow and pressure drop has been accomplished. Preliminary structural sizing of the ducts is complete, and the ducting and component interfaces have been identified dimensionally.

(e) Igniter Subsystem

(U) The igniter subsystem, Fig. 17 and 18, is comprised of the igniter combustor assembly, the igniter isolation valve, and the igniter/turbine drive hot-gas distribution manifold. The igniter combustor and distribution manifold have been relocated to conform to duct routing of the series hot-gas valve system configuration. The distribution manifold has been changed to a three-port configuration as shown in Fig. 21. The fuel turbine port interfaces directly with the fuel turbine inlet, the oxidizer turbine port with the oxidizer turbine control valve, and a single port with the tapoff throttle valve. The igniter isolation valve is a poppet type located in the base of the distribution manifold. The poppet position is normally open to offer low resistance to gas flow from the igniter for turbine spin at tank head start condition, and held closed by control pressure during maintage after igniter shutdown. The manifold passages and port from the igniter are sized for low resistance for turbine spin and ignition under start conditions. Structural sizing is based on Hastelloy-C cast material. A limited design analysis of the isolation valve has been accomplished.

(3) Turbomachinery Design

(a) Fuel Turbopump

Design Layout

(C) During the current quarter, a design review was held and review board recommendations have been incorporated in the completed preliminary layout of the fuel turbopump shown in Fig. 22. The turbopump consists of a three-row hot-gas turbine straddle mounted on rolling contact bearings and directly connected to a two-stage centrifugal pump and a high-speed inducer running at a nominal speed of 35,000 rpm. The high-speed inducer,

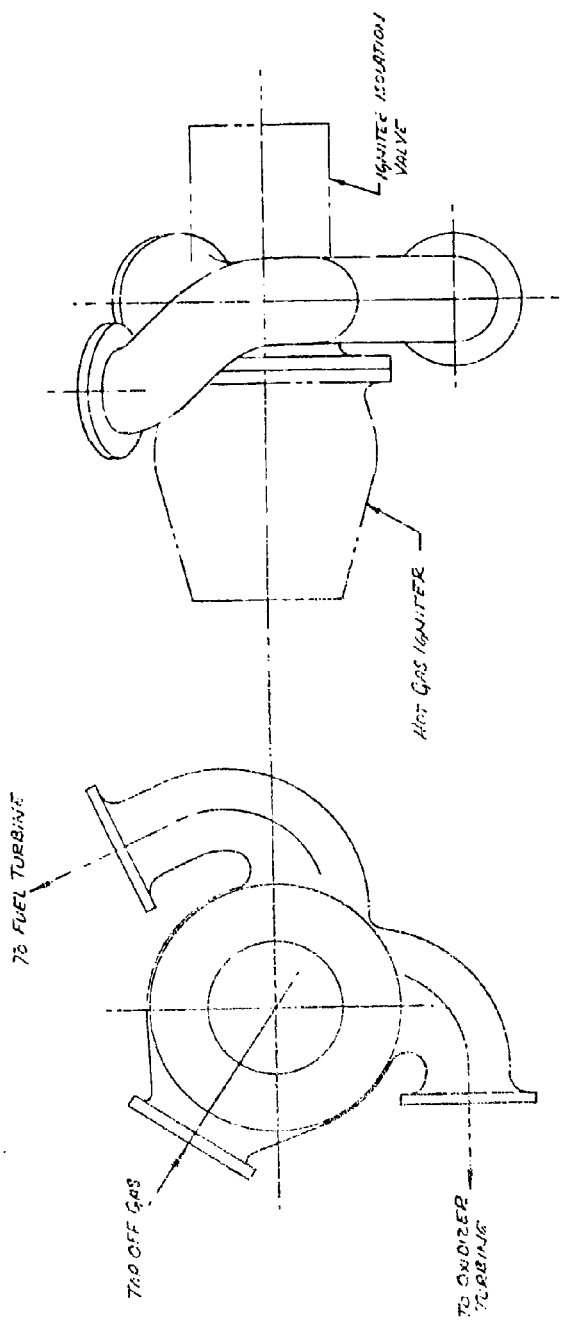

Figure 21. Igniter/Hot-Gas Distribution Manifold

CONFIDENTIAL

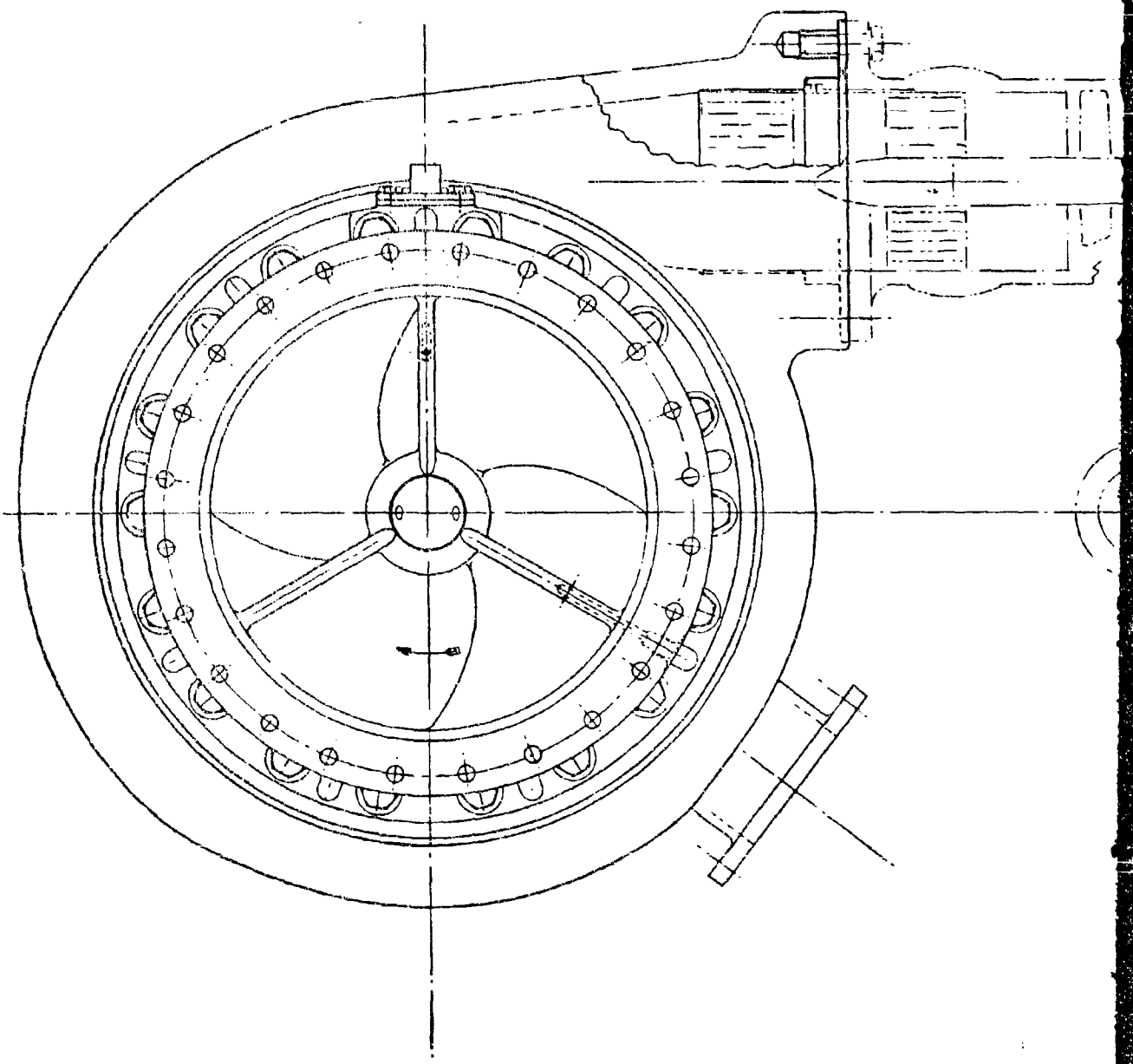

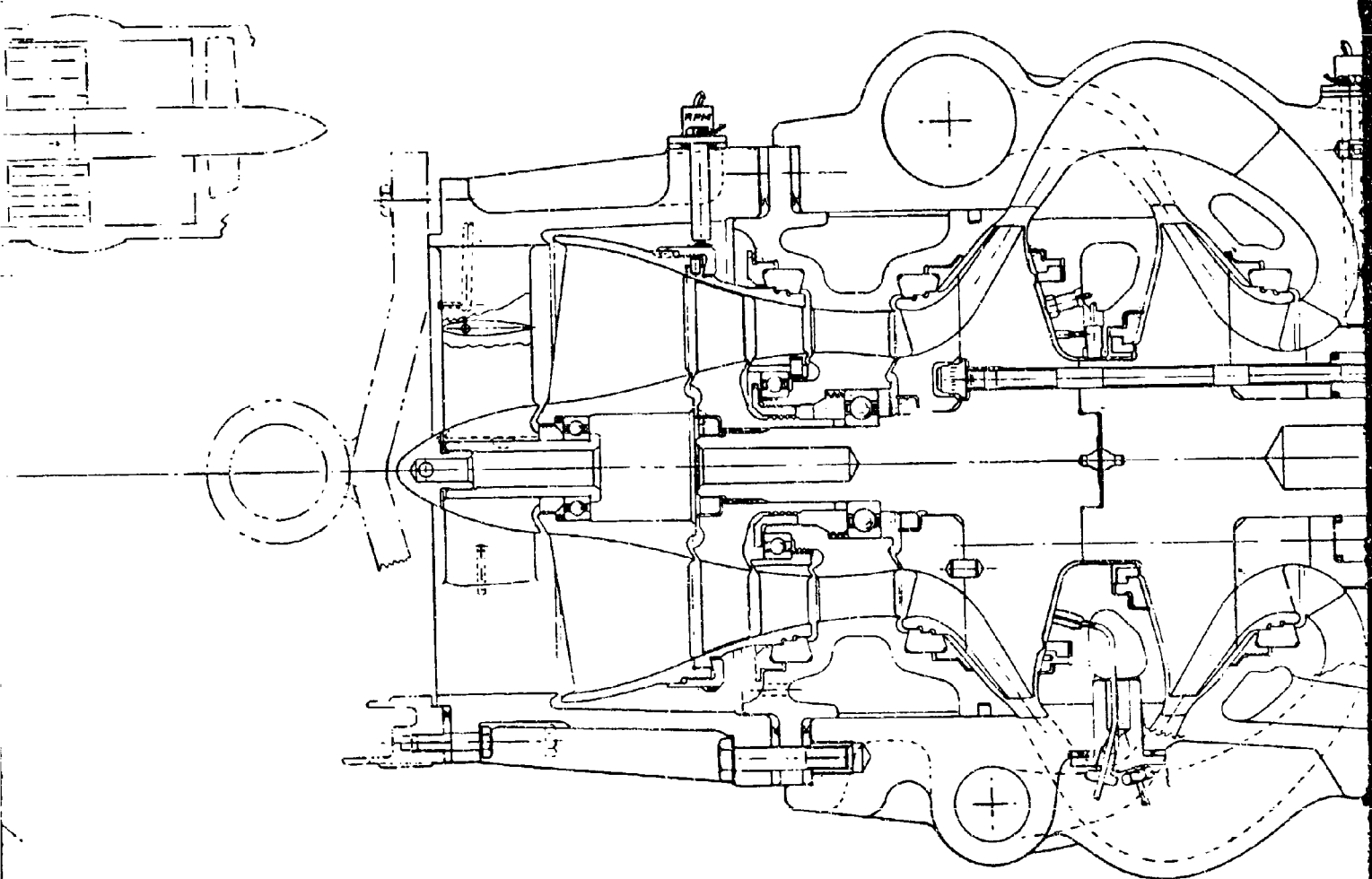

2

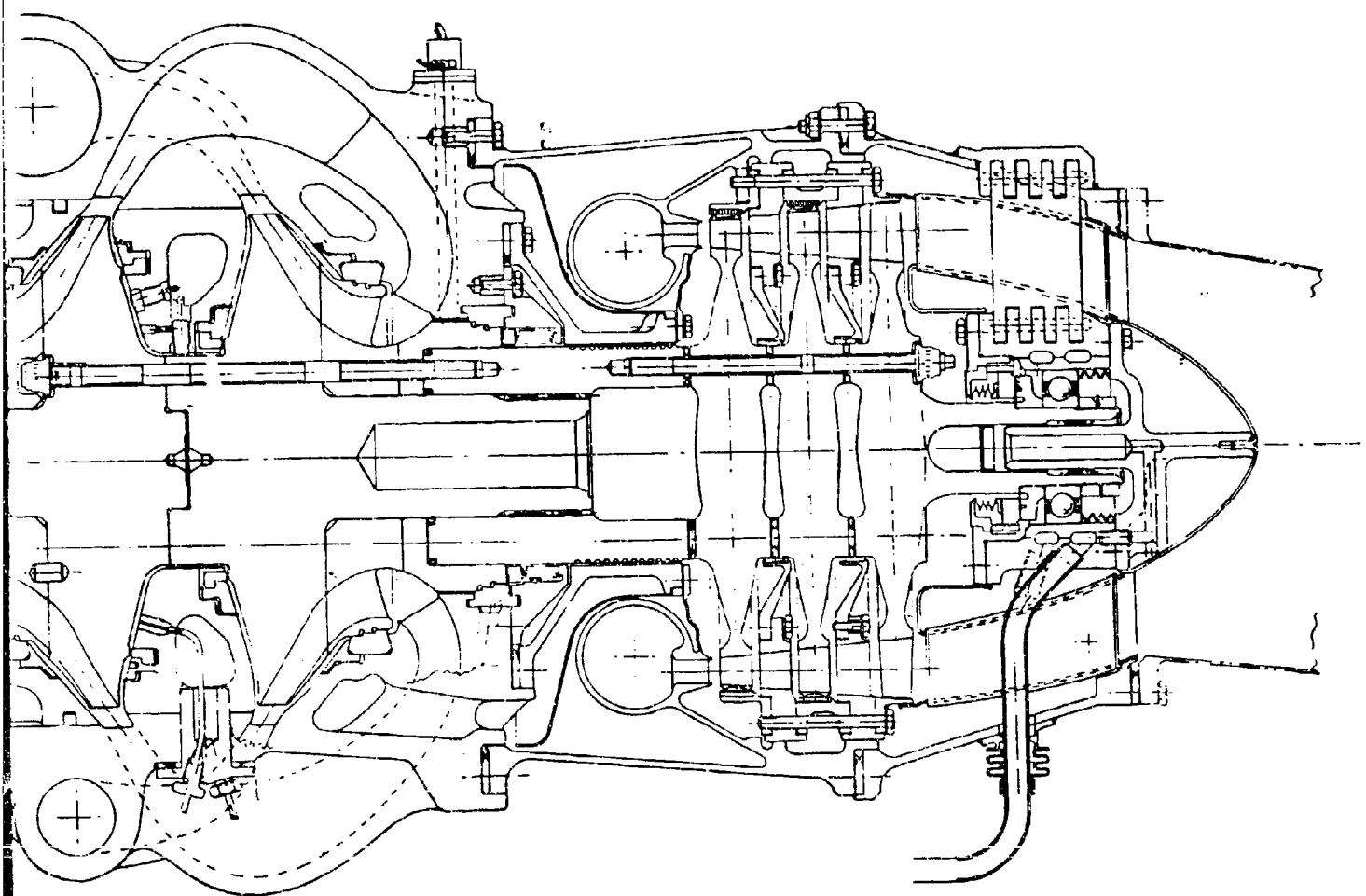

Figure 22. Mark 30 Fuel Turbopump

3

CONFIDENTIAL

driven by the hot-gas turbine, provides the head to drive the low speed hydraulic turbine which in turn is connected to the low speed inducer which provides the capability of meeting the NPSH requirements of 60 feet. The low speed inducer and hydraulic turbine drive is mounted on its own propellant-lubricated rolling contact bearings and operates at a nominal speed of 14,500 rpm. The pump impellers are mounted back-to-back and fastened together by a ring of through bolts and driven by the turbine through a splined coupling. Propellant enters the pump axially, passes through the low-speed preinducer, high-speed inducer, hydraulic turbine, and into the first-stage impeller. A series of five crossover ducts carry the flow from the discharge of the first-stage impeller to the inlet of the second-stage impeller. After passing through the second-stage impeller, five crossover ducts direct the flow into a single discharge duct. Axial thrust of the turbopump is balanced by means of a balance piston arrangement located between the back-to-back impellers. The outboard turbine bearing is supported by a series of pinned supports which provide a high spring rate and allows for the thermal distortions expected in the turbine discharge area. Around each support is a streamlined vane to insulate the support and provide for minimum flow disturbance in the discharge area. Three additional vanes are provided (total of nine) through which the bearing coolant flow is circulated into and out of the turbine bearing.

Impeller Attachment Study

(U) A design study was made to determine the best method of fastening the two back-to-back impellers together. Two methods were considered: a bolt ring at the maximum diameter allowed by the hydrodynamic passages, and a central hole. Both methods were found to be feasible from a stress standpoint. However, the central hole arrangement resulted in a smaller shaft diameter (less rigid rotating assembly) and a piloting problem; therefore, the bolt ring configuration was selected.

Turbine Wheel and Blade Attachment Study

(U) An additional study was made to arrive at the best method of attaching the blades to the turbine wheels and the turbine wheels to each other to achieve an optimum design to meet the requirements of minimum weight, long life, and maintainability. Two methods of attaching the turbine discs were studied: (1) electron beam welding of wheels and shaft into a single structure and, (2) attaching shaft and individual wheels by bolting and transmitting the torque through curvic couplings. Fir tree attachments and machining the blades integral with the discs were the two types of blade attachments studied.

(C) Fir tree blades with the discs fastened together with curvic couplings results in the heaviest design but it allows both individual blade and wheel replacement. The lightest design would be the integrally machined blades combined with a welded wheel assembly; however, it complicates the maintenance problem and also requires segmented stator assemblies, increasing the sealing problem between wheels. The integrally machined blade with the curvic coupling design was selected because it offers the advantages of

being able to disassemble and replace turbine wheels with a weight penalty of approximately 9 pounds compared to the welded discs and no increase in length (in a comparison of the welded and the integrally machined blades and curvic designs the turbine stator axial width, not the disc thickness, sets the length of the unit). Fir trees on rows, 1 and 2 were not selected as this increases the length of the unit at least 1 inch. Figure 23 shows a comparison of the disc profiles for the curvic coupling attached turbine wheels with fir tree blades and with integrally machined blades for all three blade rows.

(C) The third row disc was sized with integral blades only, because blade fir trees would cause excessive rim load, increasing the required disc thickness to greater than 2 inches. Blade stresses of the third row wheel are marginal with a shroud. If a shroud becomes necessary to control blade frequencies, the disc thickness will have to be increased from 1.4 to approximately 1.6 inches.

Outboard Bearing Support Design

(U) A study of the design of the outboard turbine bearing support for both turbopumps was completed. The support must be capable of maintaining bearing alignment while subjected to the turbine discharge environmental conditions. Of the designs considered, two basic configurations were selected for detailed analysis. These were a fixed strut support, and a pin-ended strut support.

The designs of fixed strut supports were subdivided into: radial struts fixed at both the housing and the bearing carrier, angled struts fixed at both the housing and the bearing carrier, and radial struts fixed at the bearing carrier and allowed to move radially at the housing. Two sizes of struts were analyzed: a minimum size with a thickness of 0.15 inch and an axial length of 1.00 inch, and a maximum strut size dictated by the size of the allowable airfoil section in the turbine exhaust passage. A summary of the spring rates and stress analysis for the fixed strut support is shown in Fig. 24.

(U) The designs of the pin-ended strut supports were subdivided into: radial struts pinned at both the housing and the bearing carrier, angled struts pinned at both the housing and the bearing carrier, and radial struts fixed at the bearing housing and pinned and allowed to both move radially and rotate at the housing. The same two strut sizes picked for the fixed struts were analyzed for the pin-ended struts, and a summary of the spring rates and stress analysis for the pin-ended strut supports is shown in Fig. 25.

(U) Figure 26 is a compilation of the spring rates for both the fixed strut and pinned strut supports for configurations of three, six, and nine struts. Also shown are the spring rates and thickness of fixed struts made of Hastelloy-C and Inconel-X.

(C) Although either design (fixed struts or pinned) is adequate, the fixed end struts are subjected to considerable bending stress at the ends, and for this reason the pin ended supports were selected for both turbopumps.

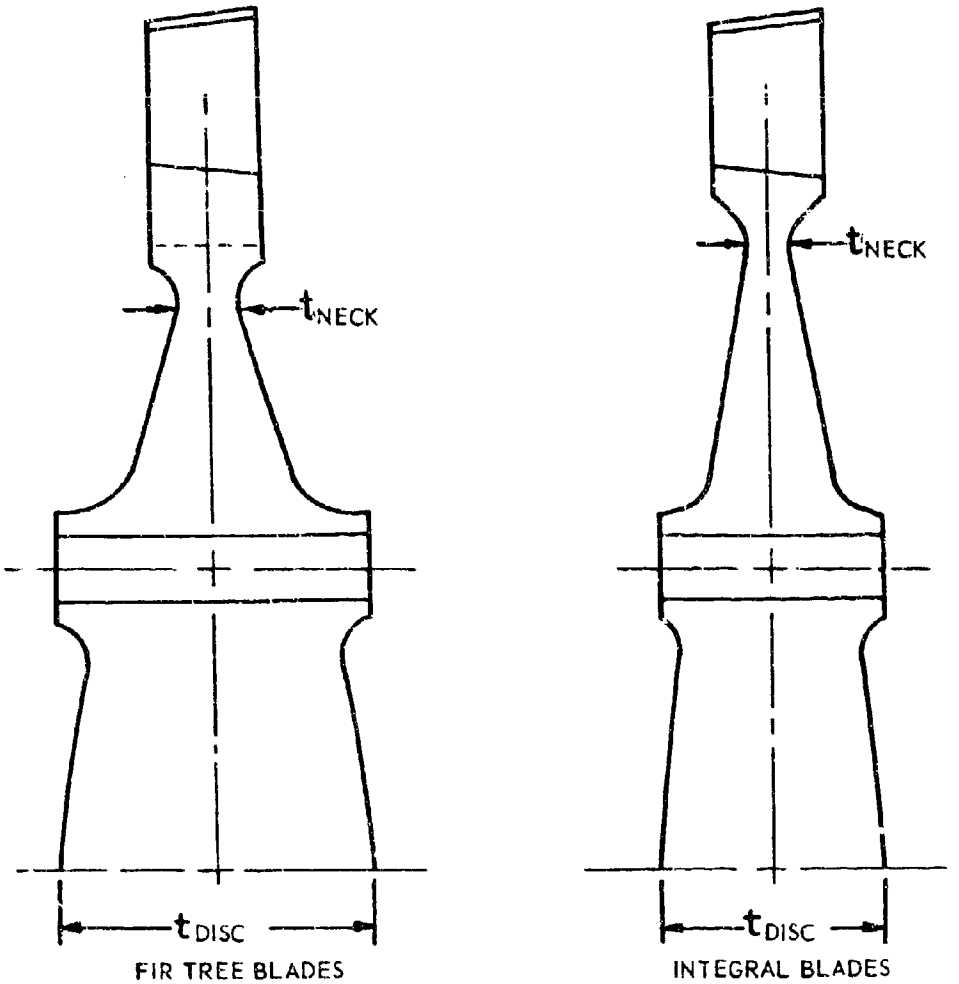

DESIGN CRITERIA :
MATERIAL - INCO 718
RM TEMP F_{tu} 180 KSI
ELONGATION 15 PERCENT
MAX RPM 38,900

MAXIMUM ALLOWABLE OPERATING SPEED=75-PERCENT BURST SPEED

* UNSHROUDED DESIGN

	FIR-TREE BLADES			INTEGRAL BLADES		
	FIRST STAGE	SECOND STAGE	THIRD STAGE	FIRST STAGE	SECOND STAGE	THIRD * STAGE
t_{NECK}	0.36	0.37	—	0.25	0.26	0.37
t_{DISC}	2.0	1.75	—	1.4	1.25	1.4
GAS TEMP F	1320	1100	--	1320	1100	945

Figure 23. Mark 30 Turbine Disc Profiles

	Summary of Springrates for Fixed-Fixed Struts					
	$A = 0.15 \times 1 = 0.15$ in.^{2} $I = 2.81 \times 10^{-4}$ in.^{4}			$A = 0.4 \times 2.25 = 0.90$ in.^{2} $I = 1.20 \times 10^{-2}$ in.^{4}		
	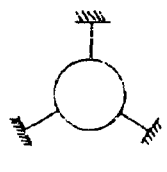	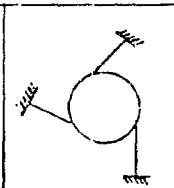	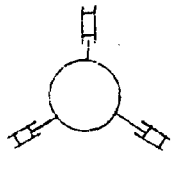	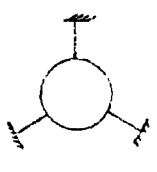	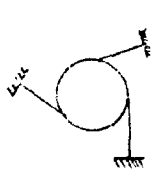	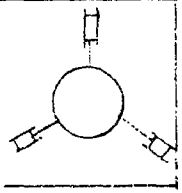
k_{xx} k_{yy} $k_{xy}=k_{yx}$	1.89×10^6 1.89×10^6 0	1.71×10^6 1.71×10^6 0	0.0037×10^6 0.0037×10^6 0	11.46×10^6 11.46×10^6 0	10.34×10^6 10.34×10^6 0	0.161×10^6 0.161×10^6 0
Thermal Stress*	258,000 psi	155,000 psi	0	258,000 psi	413,000 psi	0
Stress Due to 1000 lb F_x, F_y, F_{45} Load	3800 psi 4440 psi 4560 psi	4350 psi 3610 psi 2980 psi	298,000 psi 268,000 psi 287,000 psi	767 psi 730 psi 777 psi	770 psi 700 psi 610 psi	41,900 psi 35,300 psi 40,400 psi

Figure 24. Summary of Springrates for Fixed-Fixed Struts

Summary of Springrates for Pinned-Pinned Struts						
	$A = 0.15 \times 1.0 = 0.15$ in.^{2} $I = 2.81 \times 10^{-4}$ in.^{4}			$A = 0.3 \times 2.25 = 0.90$ in.^{2} $I = 1.20 \times 10^{-2}$ in.^{4}		
	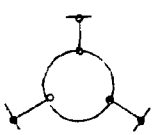	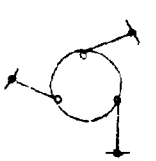	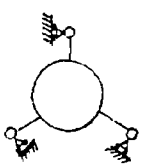	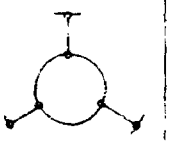	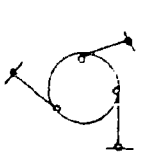	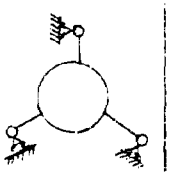
k_{xx} k_{yy} $k_{xy}=k_{yx}$	Unstable	1.71×10^6 1.71×10^6 ∞	0.00004×10^6 0.00004×10^6 -0.133×10^6	Unstable	10.25×10^6 10.25×10^6 ∞	0.040×10^6 0.040×10^6 ∞
Thermal Stress*	258,000 psi	0	0	258,000 psi	0	0
Stress Due to 1000 lb F_x, F_y, F_{45} Load	Unstable	4350 psi 4220 psi 4440 psi	620,000 psi 516,000 psi 559,000 psi	Unstable	725 psi 703 psi 746 psi	83,800 psi 72,300 psi 80,900 psi

*Assumes a radial thermal gradient only

Figure 25. Summary of Springrates for Pinned-Pinned Struts

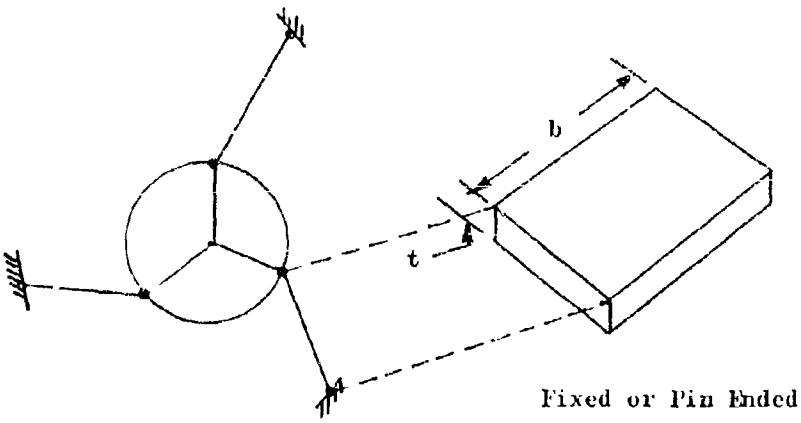

t	b	3 Struts	6 Struts	9 Struts
0.15	1.00	1.71×10^6	3.42×10^6	5.13×10^6
0.40	2.25	10.23×10^6	20.46×10^6	30.69×10^6
0.07	2.25	1.80×10^6	3.60×10^6	5.40×10^6
0.10	2.25	2.57×10^6	5.14×10^6	7.71×10^6

k; lb/in.

NOTE: For the configuration, the springrates are approximately proportional to the area, where

A = x-sectional area of strut

= t x b

b_{max} = maximum allowable width of strut = 2.25 inches

t_{max} = Maximum allowable thickness of strut

= 0.07 inch for Hastelloy-C
= 0.10 inch for Inconel-X
= Determined by Thermal Stress

} Fixed End Only

Figure 26. Radial Springrates

A final design will be incorporated into the layout during the next report period. Materials for the pins and struts will be selected to ensure thermal compatibility and prevent galling and seizing.

Fuel Pump Thermal Contraction Effects

(U) The location of the fuel pump bearing with relation to the balance piston imposed a problem of establishing proper balance piston clearances after chilldown, because of the differential contraction between the aluminum pump housing and the titanium pump impeller and main shaft. Solutions studied were: (1) the use of an invar spacer between the aluminum housing and the titanium bearing support structure, (2) relocation of the bearing under or closer to the balance piston, and (3) allow the bearings to float axially.

(U) Relocation of the bearing under or closer to the balance proved impractical because it resulted in an increase in diameter of the inner balance piston orifice such as to make the balance piston ineffective.

(C) Both the invar spacer and the free floating bearing designs were found to be satisfactory, and the free floating bearing was selected because it was less complex and thus a more reliable method. The balance piston is capable of handing throttling and operating transients, and ring materials will be selected to allow for possible rubbing during the start transient.

(b) Oxidizer Turbopump

(U) A preliminary drawing of the oxidizer turbopump was presented in the third quarterly report. This layout was modified but not completed in this period.

Axial Thrust Balance

(C) Axial thrust analysis on the through flow inducer on the LOX pump resulted in the requirement for either a balance piston or a large diameter balance drum. Because a balance piston would complicate the design, and the large diameter balance drum rotating at pump impeller rpm results in a high labyrinth rubbing velocity, a rotating diffuser (impeller tip turbine) drive was investigated as a replacement for the through flow turbine drive. The rotating diffuser design resulted in a slight savings in overall turbopump length, one less high-pressure seal, and reduced the balance drum rubbing velocity from 700 to 600 ft/sec. Because of these improvements, the rotating diffuser design was selected over the through flow design. Although the balance drum rubbing velocity was reduced by 100 ft/sec, it is still considerably higher than current practice and could be considered a state-of-the-art technology advance. Provisions will be made for future empirical evaluation of possible seal materials.

(4) Thrust Chamber Design

(U) Thrust chamber design effort during the current report period terminated with design resolution of problem areas which have been under study during the last quarter. Included are resolution of design approaches to combustor and structural configurations and selection of materials of fabrication. The completed thrust chamber design layout for the demonstrator module is shown in Fig. 27. The layout incorporates the design decisions listed below.

Selected Items for Demonstrator Module Thrust Chamber

Ni 200 Tube Walls (Inner and Outer)

Segmented Titanium (6 Al 4V) structure, Mechanically Jointed

Removable Baffles (40)

Structural Tie Bolts (2 per Baffle - 200 KSI, 1.12-inch Diameter)

Membrane-Type Centerbody

Axially Bolted Injector

Adhesively Bonded Tube Wall to Structure

Hot-Gas Ignition Through Baffles

Two-to-One Inner Nozzle Splice (Brazed)

360-degrees Brazed Inner and Outer Bodies

Tapoff Configuration and Location

(a) Thrust Chamber

Tubes

(C) The tube bundle for the demonstrator module thrust chamber has been designed with a number of factors in mind. These include operation over the operating envelope of 300- to 1500-psia chamber pressure and mixture ratios of 5 to 7, tube-wall temperatures held to meet the life requirements of 300 cycles and 10 hours of operation, and minimization of coolant

CONFIDENTIAL

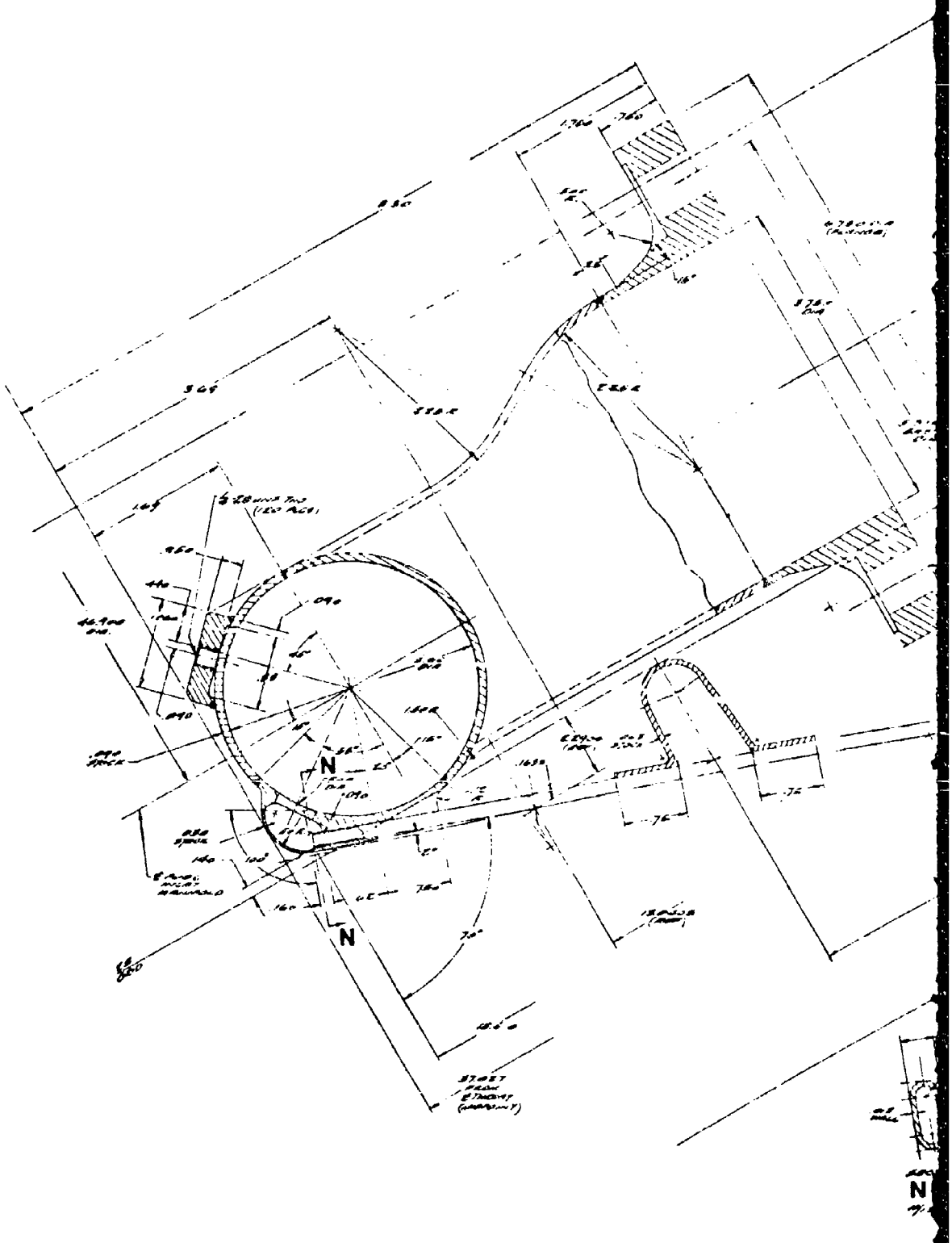

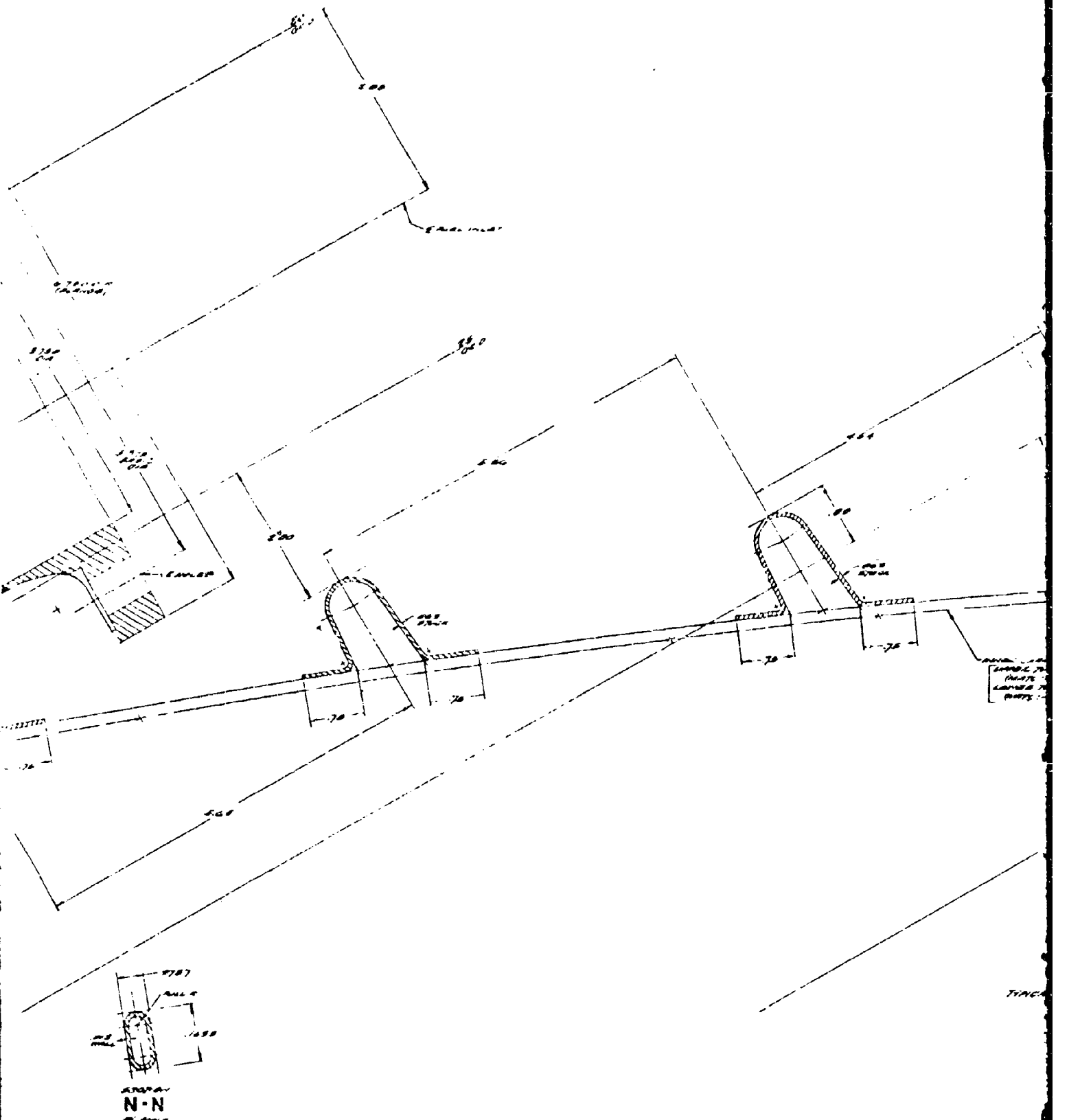

N-N

2

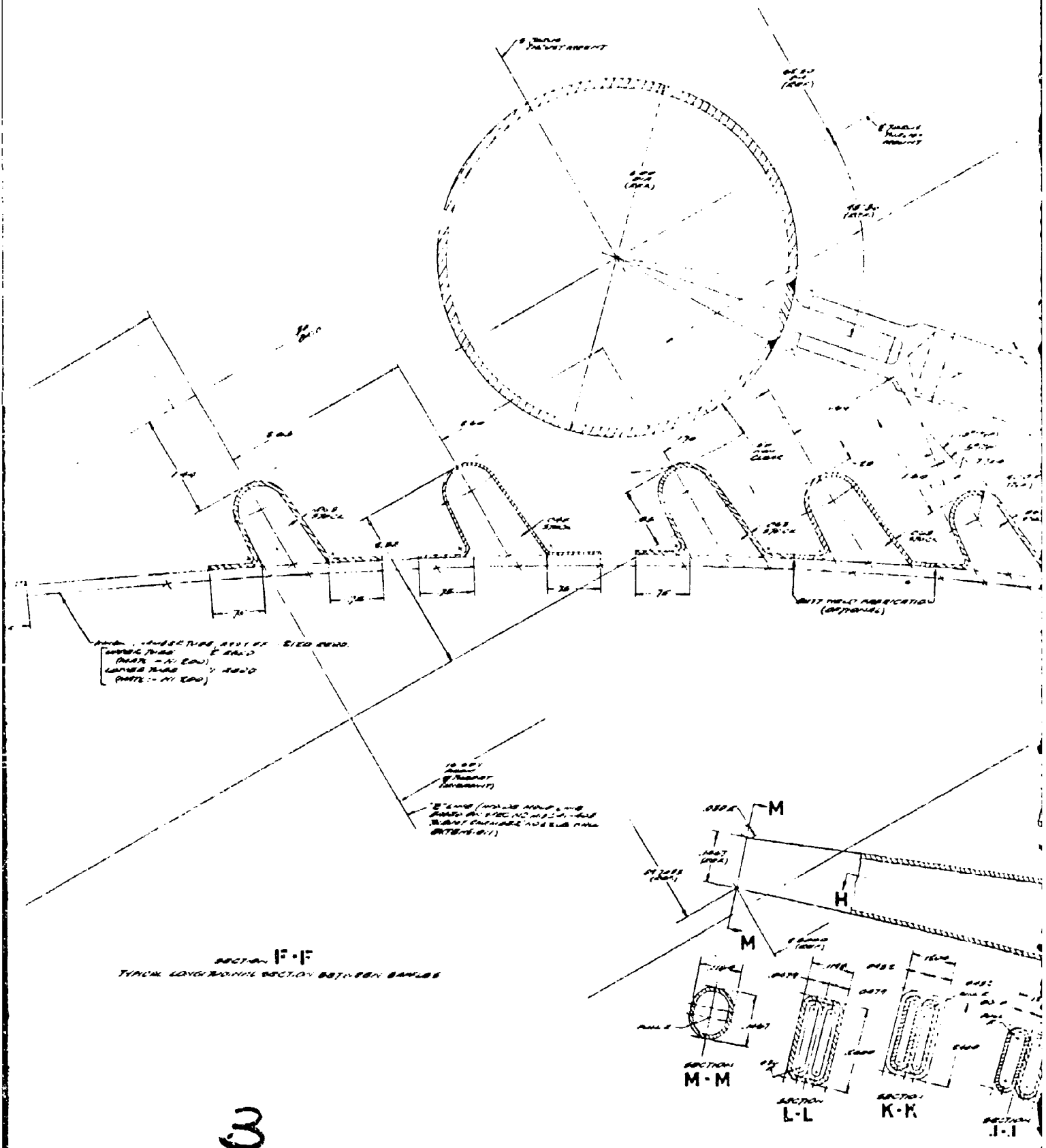

SECTION F-F

TYPICAL LONGITUDINAL SECTION BETWEEN BAFFLES

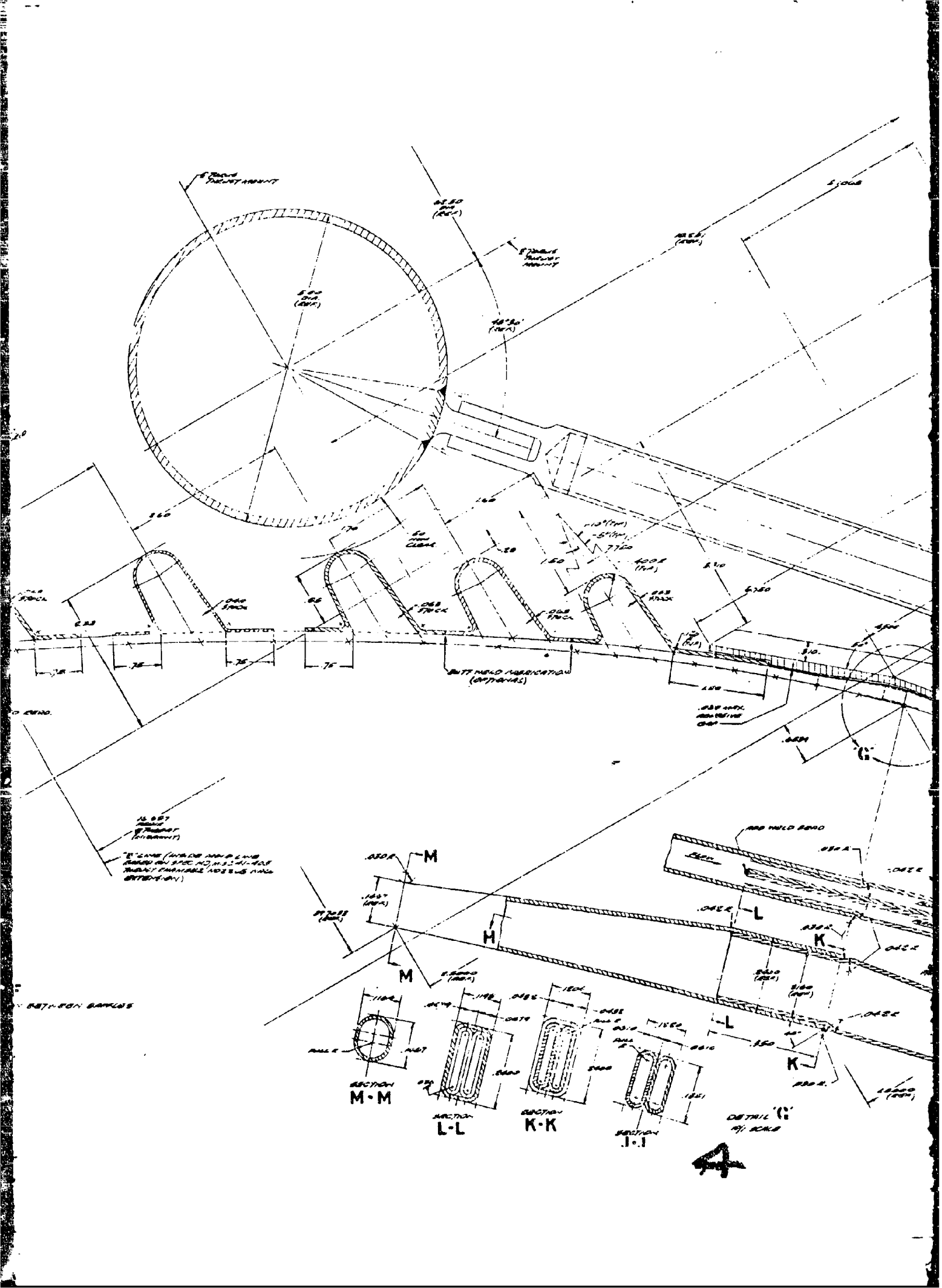
BUTT WELD FABRICATION (OPTIONAL)
M
H
M
L
K
L
K
SECTION M-M
SECTION L-L
SECTION K-K
SECTION J-J
DETAIL 'G'
4

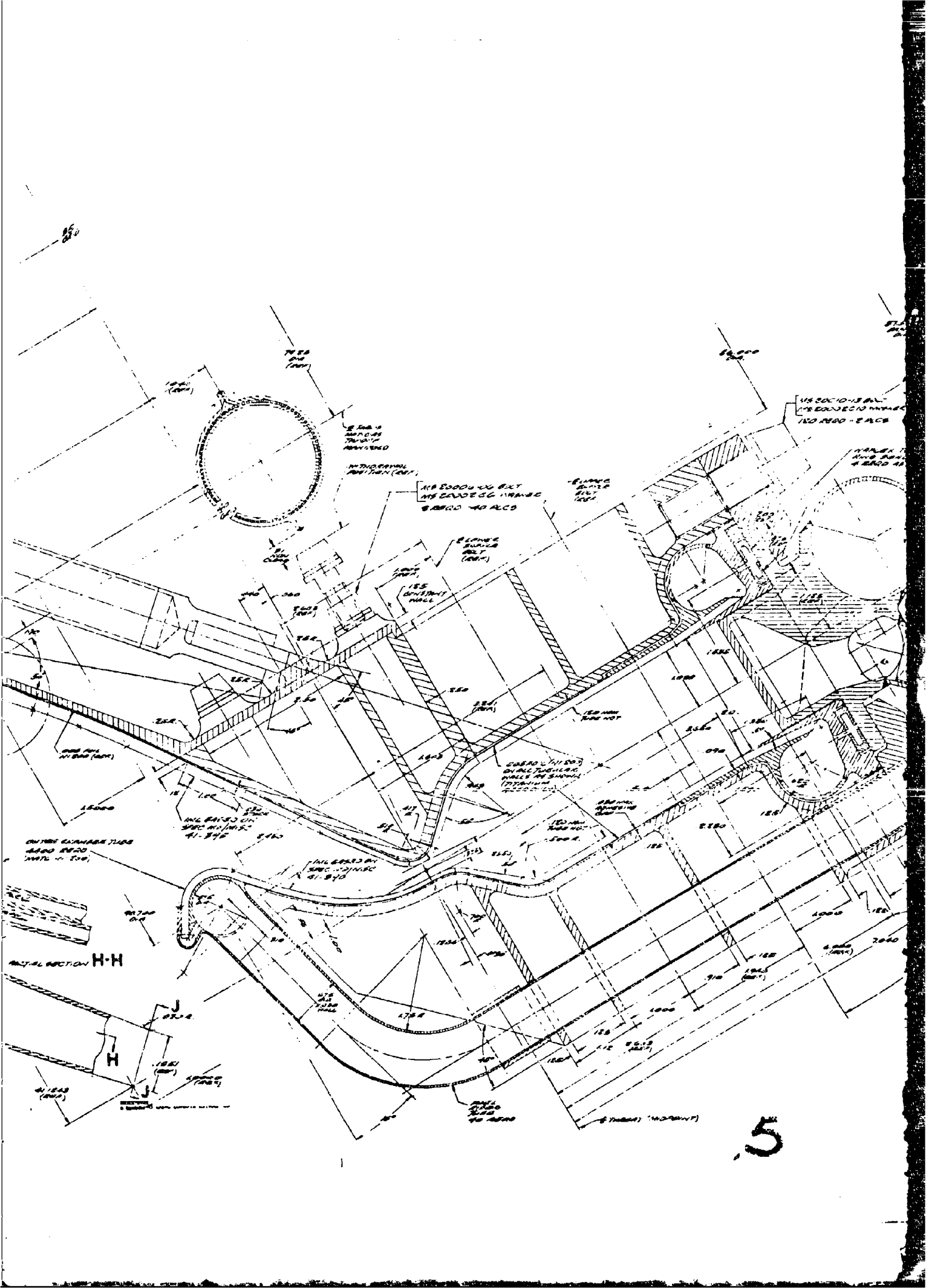
SECTION H-H
H
J
J

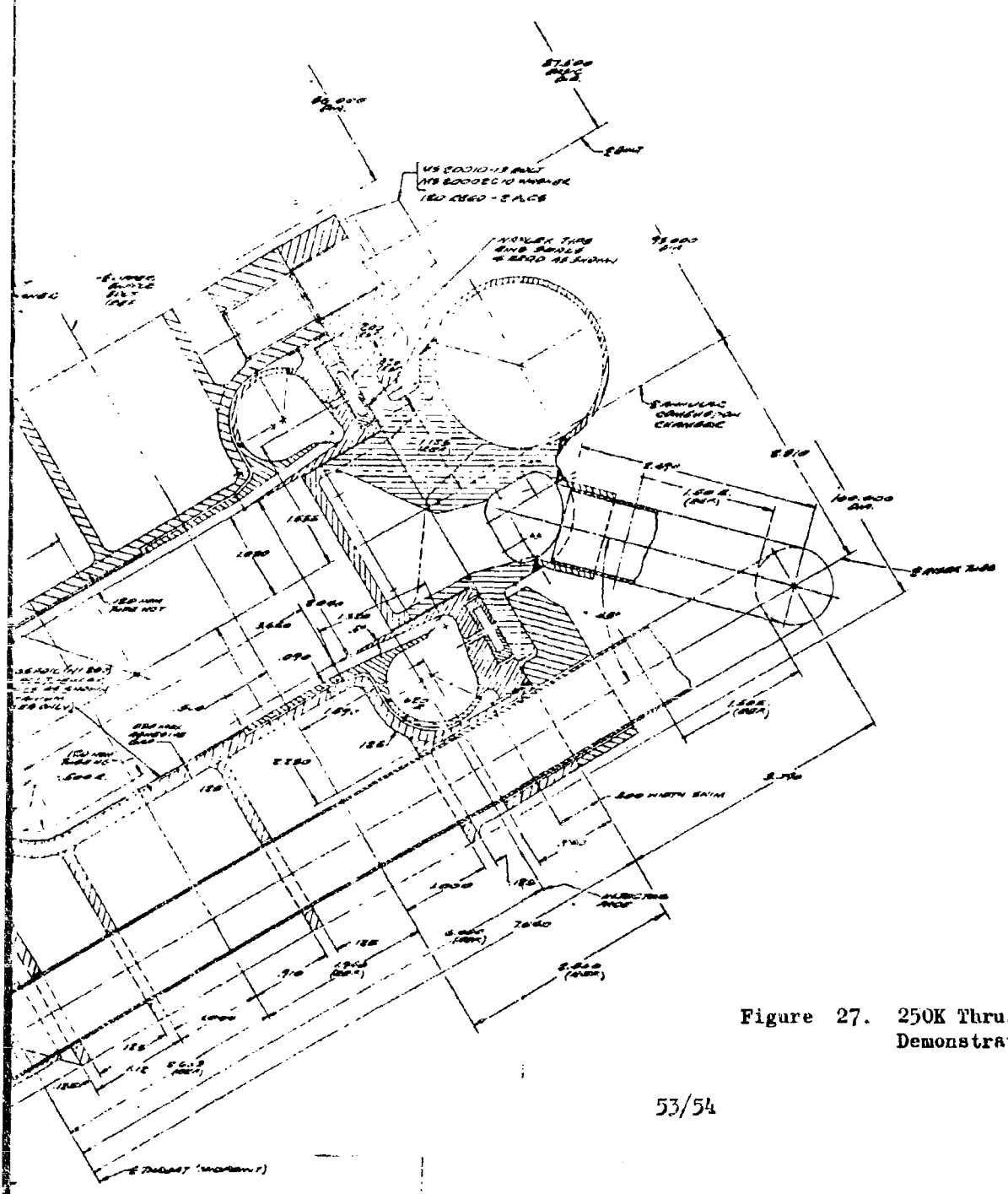

Figure 27. 250K Thrust Chamber Demonstrator Module

CONFIDENTIAL 6

pressure drop and module weight. Heat transfer data obtained from the 2.5K solid-wall and tube-wall chambers have been utilized. Hydrogen cooling requirements are based on extensive data taken at Rocketdyne at high pressures and high heat fluxes. Recent curvature enhancement data (reported elsewhere in this report), taken with an experimental chamber inner and outer tube, have also been used to the fullest extent.

(C) The selected design utilizes a single up pass on the inner body followed by a single down pass on the outer body. Nickel 200, which was previously selected as the basic tube material, was likewise selected as the tube material for the tube below the splice on the inner body. Inco 625 was selected as a long-range substitute, pending the accrual of brazing and formability data for this material. Substantial weight savings are available by use of the latter material.

(C) The tube splice was studied in a heat transfer/presssure drop/hydraulic stress tradeoff analysis. It was determined that a 2:1 splice shown in Fig. 27 approximately 1 inch below the shroud tip was the most feasible. The chamber is designed with approximately 2120 tubes in the nozzle and 4240 tubes above the splice in the combustor region. Currently both tubes consist of 0.012-inch nickel 200 tubing operating at a maximum temperature of 1450 F. The tube upstream of the splice is designed to a mixture ratio of 6 at 1500-psia chamber pressure which will produce slightly reduced wall temperatures at MR = 7. The tube below the splice is designed to operate at 300-psia chamber pressure and a mixture ratio of 7 at sea level conditions, this being the most stringent condition for this part of the inner body. This results from the recompression which occurs at sea level in conjunction with the low coolant flowrates. Elimination of the tube splice by tapering the tube wall thickness is feasible but was not selected because of the penalty in fuel pressure drop.

(C) The outer body consists of approximately 4400 tubes of 0.010-inch nickel 200 material. To achieve wall temperatures under 1500 F (life requirement), the inner body was displaced 3/16-inch downstream starting at the beginning of the chamber convergence. This effectively moves the sonic point on the outer body 3/16-inch downstream. This change permits utilization of the maximum obtainable coolant curvature enhancement at the high heat flux region of the throat (58 Btu/in.^{2}-sec for 1450 F wall temperature).

(C) Hydrogen injection temperatures at nominal operating conditions will be approximately 630 R based on theoretical predictions. Coolant pressure drops are currently being optimized. Additional coolant circuits are being examined to determine what advantage, if any, these circuits may have. However, since this is to some extent a function of the hydrogen coolant temperature rise, the circuit optimization will not be made until data from the 250K tube-wall chambers have been analyzed to obtain hydrogen temperature rises below the throat.

(b) Structural and Seat Assembly

(U) During the current report period, resolution of tapoff, baffle seat, and structural tie relationship was made firm. The selected configuration utilizes a 360-degree inner and outer brazed tube bundle through which baffle seats are installed through EDM holes. With this technique, the number and orientation of tubes during the braze cycle is not critical. The technique for installation of the seat through the tube walls enables in-process pressure check and repair, and precludes entry of braze alloy into the tubes. A pictorial definition of the process is shown in Fig. 28.

(U) Tapoff gases are extracted and hot gas for ignition is introduced through the baffle and directed through insulated ducts in the inner wall in an area not bonded by the adhesive. Orientation of this system with respect to the injector strips is identical to that tested on the 2.5K segment and is awaiting final testing demonstration on the 250K experimental thrust chamber

(c) Injector

(U) The injector configuration was fixed as an axially bolted design (Fig. 29) with removable baffles. The injector body is held in place by two titanium retainer rings which are axially bolted to the combustor body. The concept is shown in Fig. 30a in comparison to an alternate method of attaching the injector as shown in Fig. 30b. In the latter design, the axial bolts are placed through a steel flange extension of the injector. The retainer ring design was selected in preference to the steel body flange design because of lower weight and cost estimates.

(U) The decision to use the axially bolted concept was made after comparison with an integral baffle-injector design which utilized the upper structural tie bolt as a shear connection. The integral concept provided restraint against hydraulic and pneumatic separating loads and offered a potential large weight reduction. The concept, shown in Fig. 31 will be analyzed for growth from the bolted concept for application on the flight configuration. Alignment, the necessity for injector preload and line drilling for installation, and questionable component interchangeability are problems which must be solved before this light-weight configuration can be adopted.

(d) Assembly

(U) An assembly concept using 360-degree continuous titanium structure for inner and outer bodies and segmented tube sections was compared to the chosen 360-degree brazed tube bundle and segmented titanium structure. The former combination made mandatory braze and weld operations after the adhesive application and magnified segment tolerance and fit-up problems. Until technology in these areas is advanced, the adoption of the potentially lower-cost segmented-tube bundle concept will be deferred.

CONFIDENTIAL

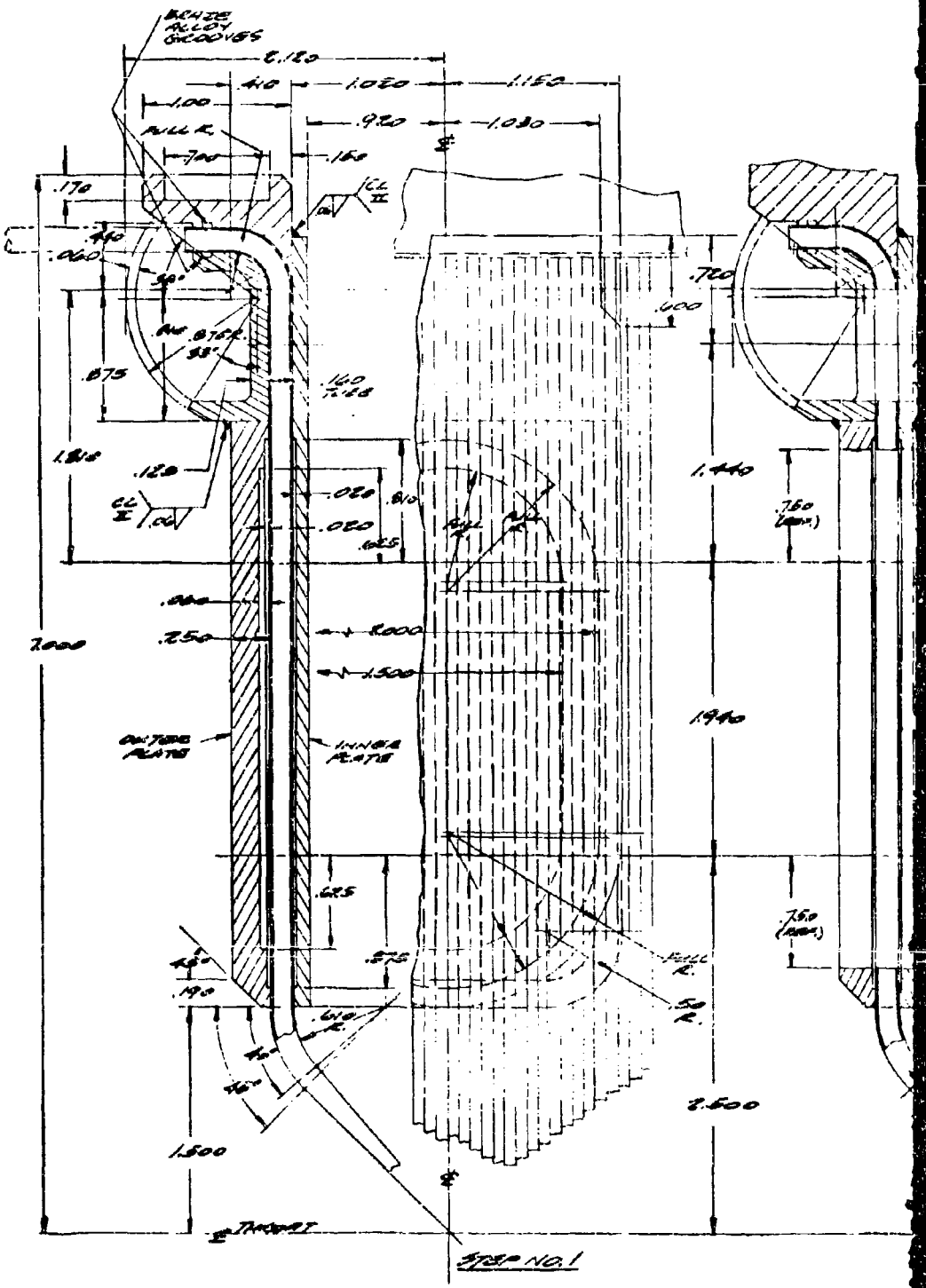

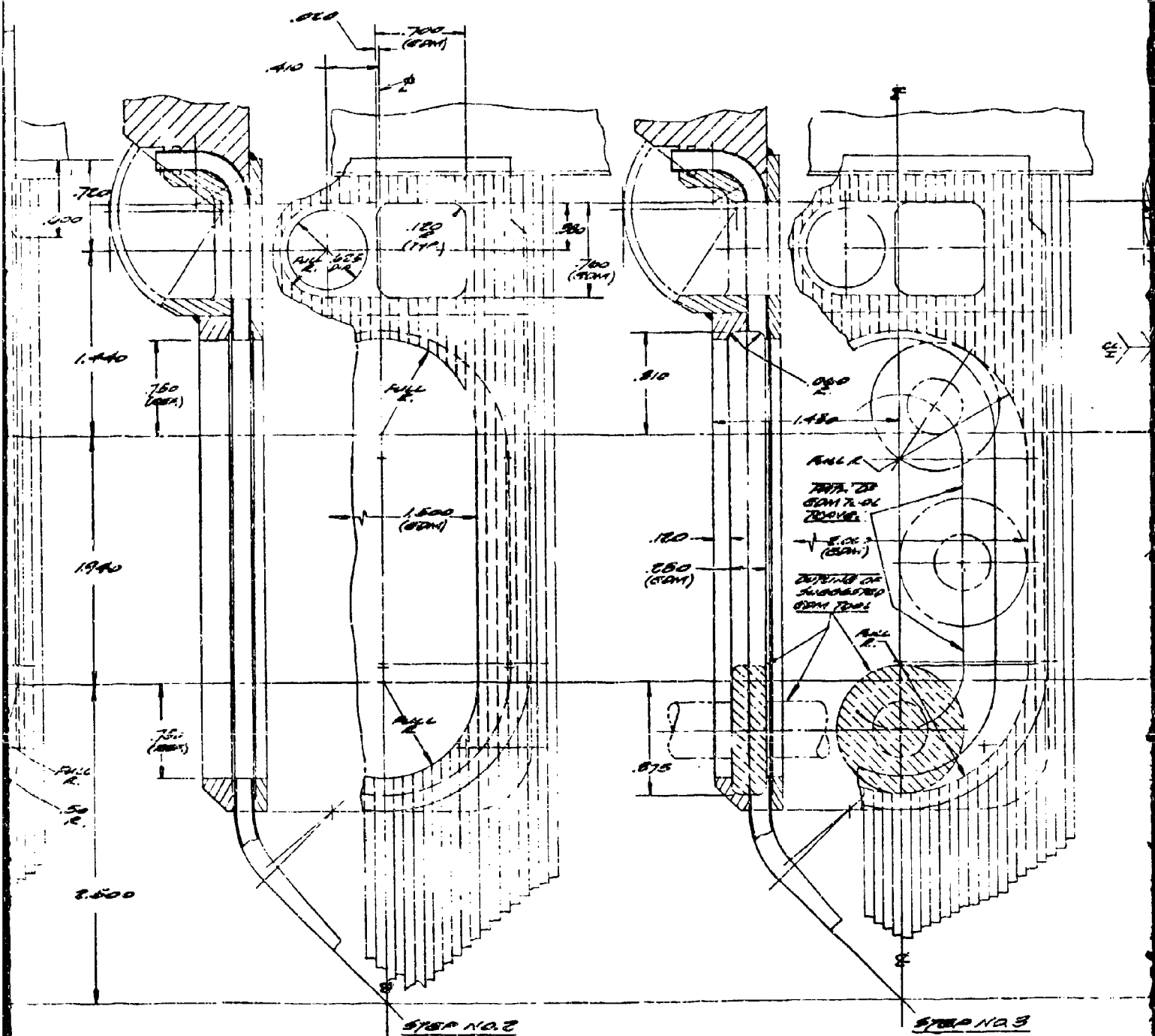
.700 (STAM)
.410
.700 (STAM)
.720
.000
1.440
.750 (STAM)
1.500 (STAM)
1.940
.750 (STAM)
.810
1.480
.180
.250 (STAM)
.875
8.500
STEP NO 2
STEP NO 3

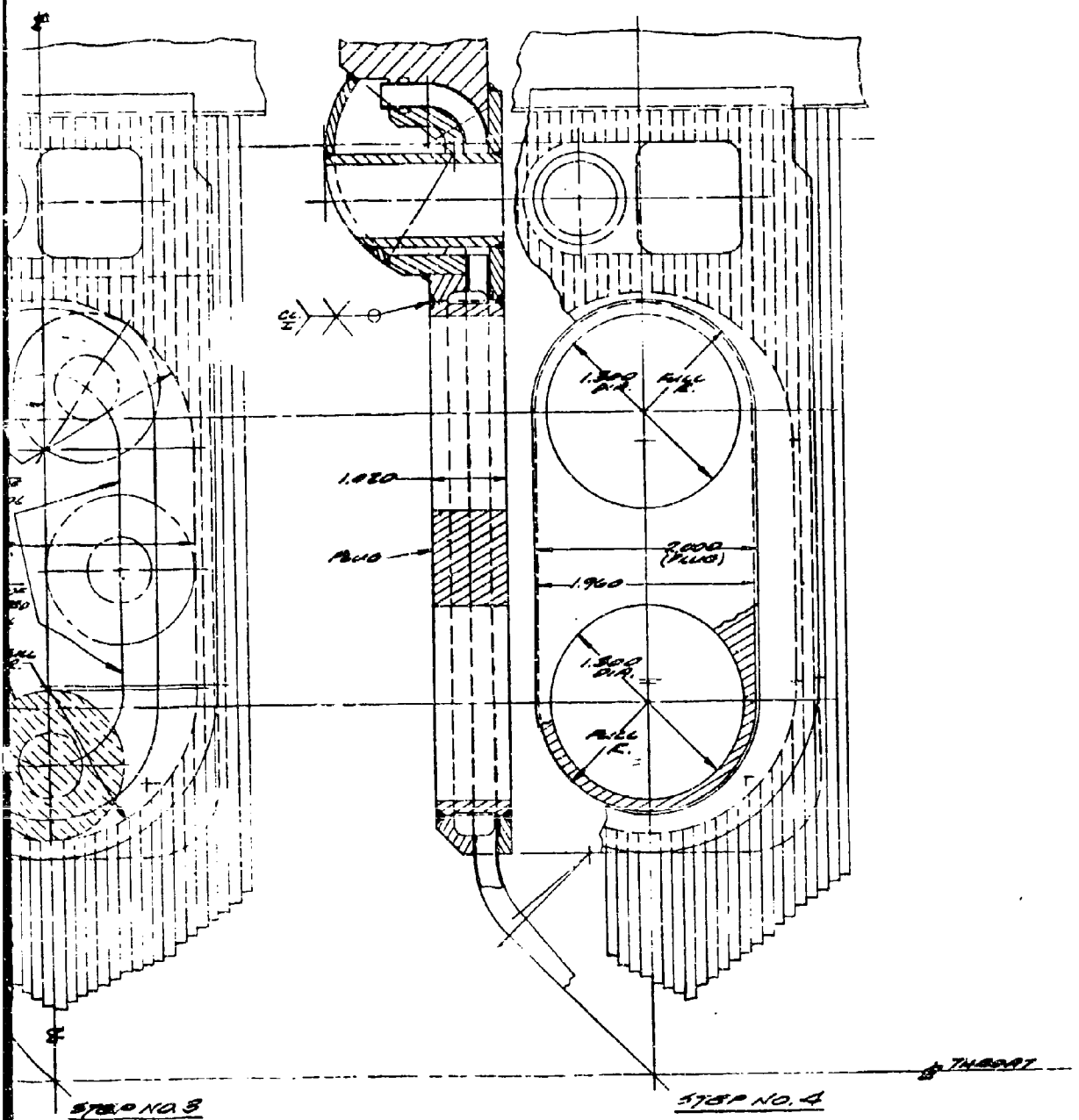

Figure 28. Step Method of Installing and Machining Baffle Seat

CONFIDENTIAL

CONFIDENTIAL

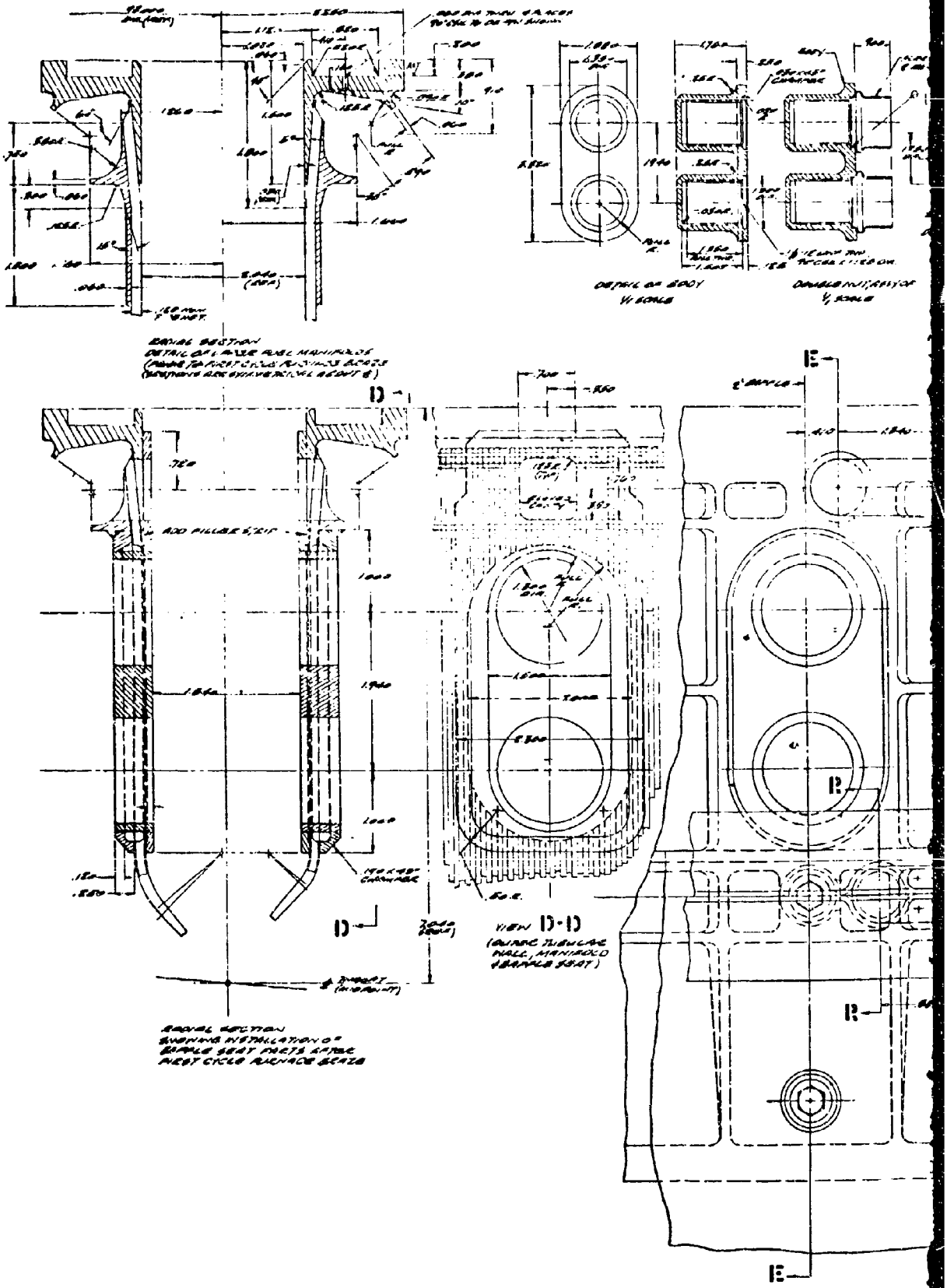

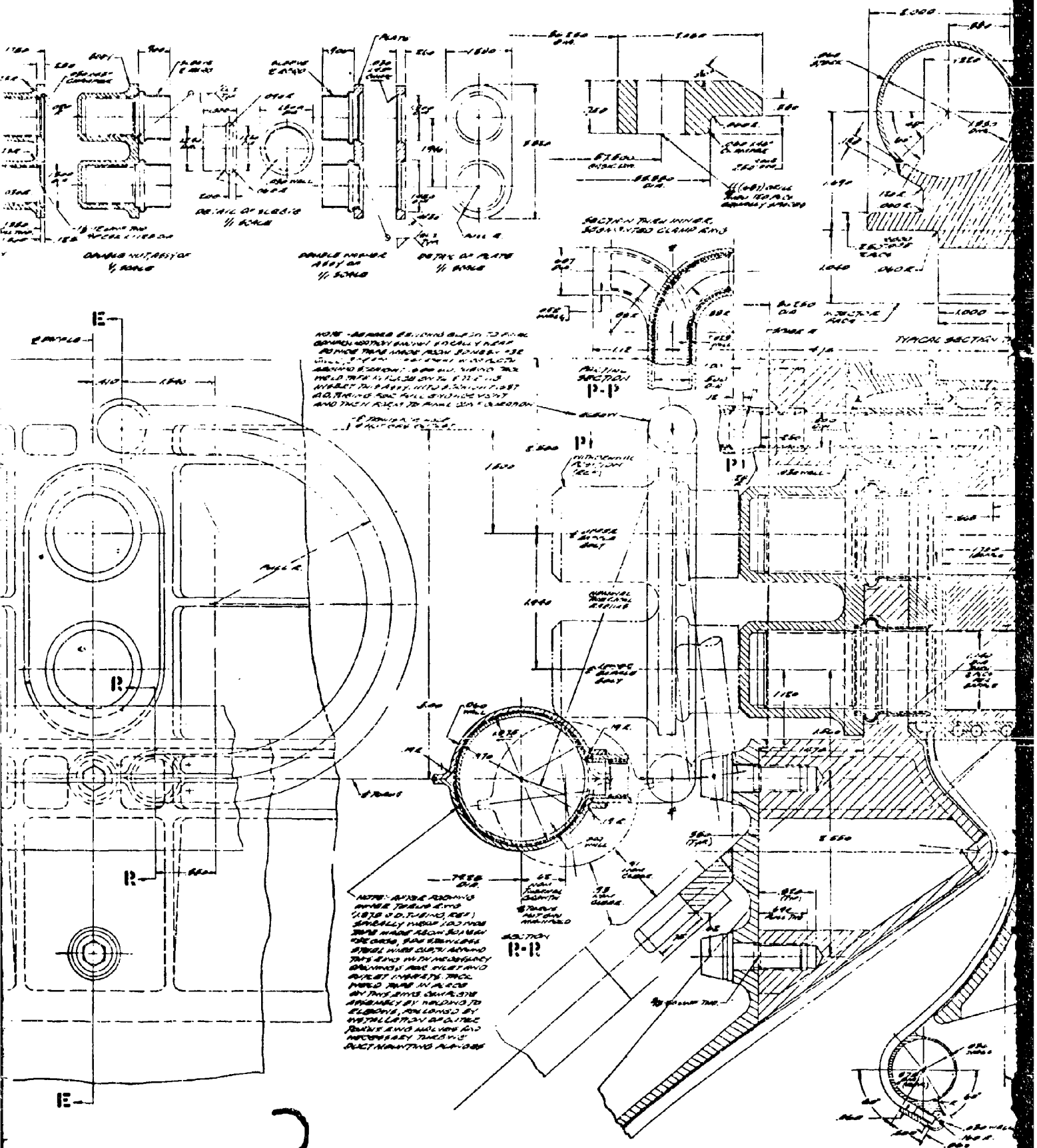

2

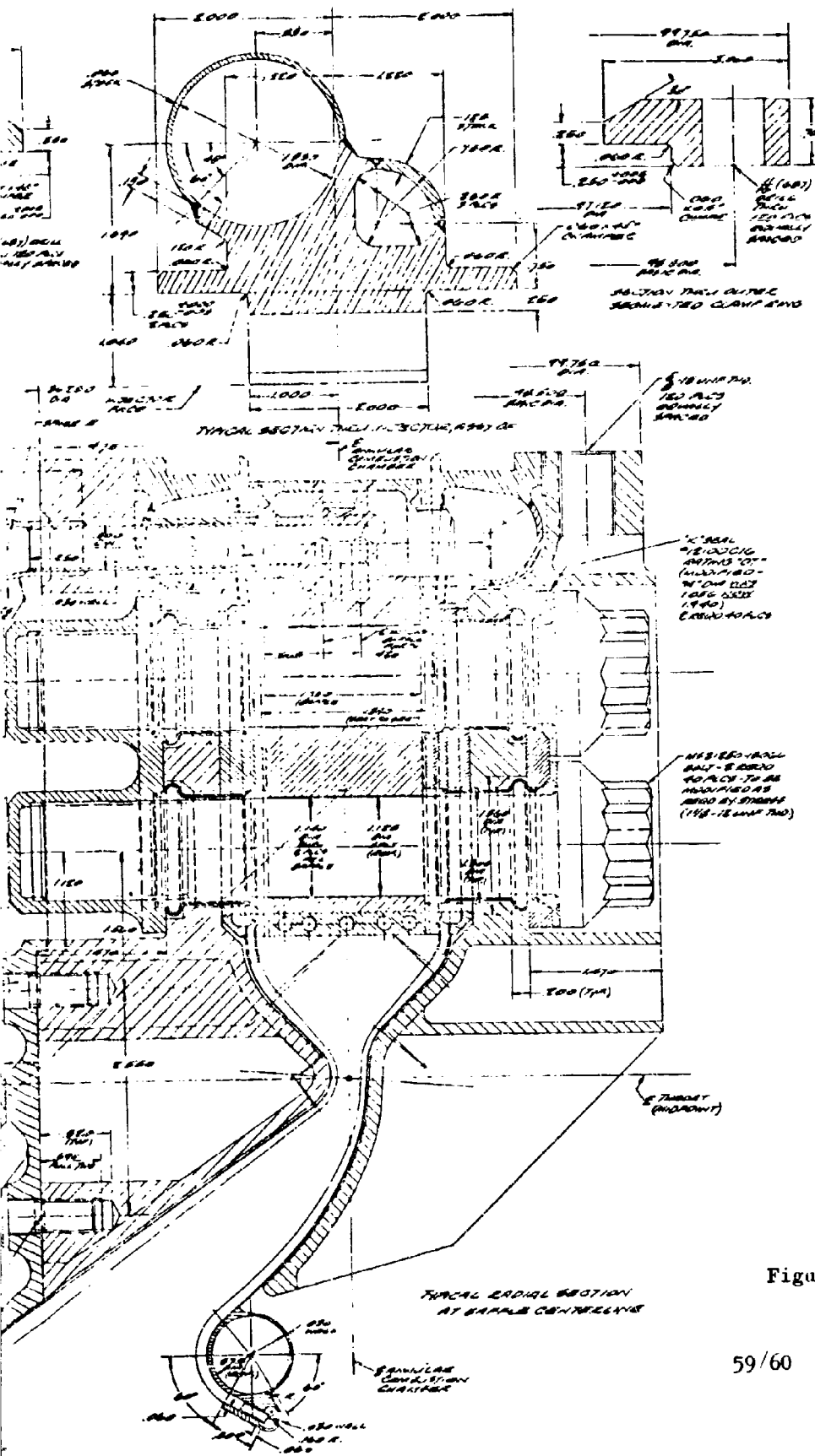

Figure 29. Injector and Baffle Assembly Design

CONFIDENTIAL
3

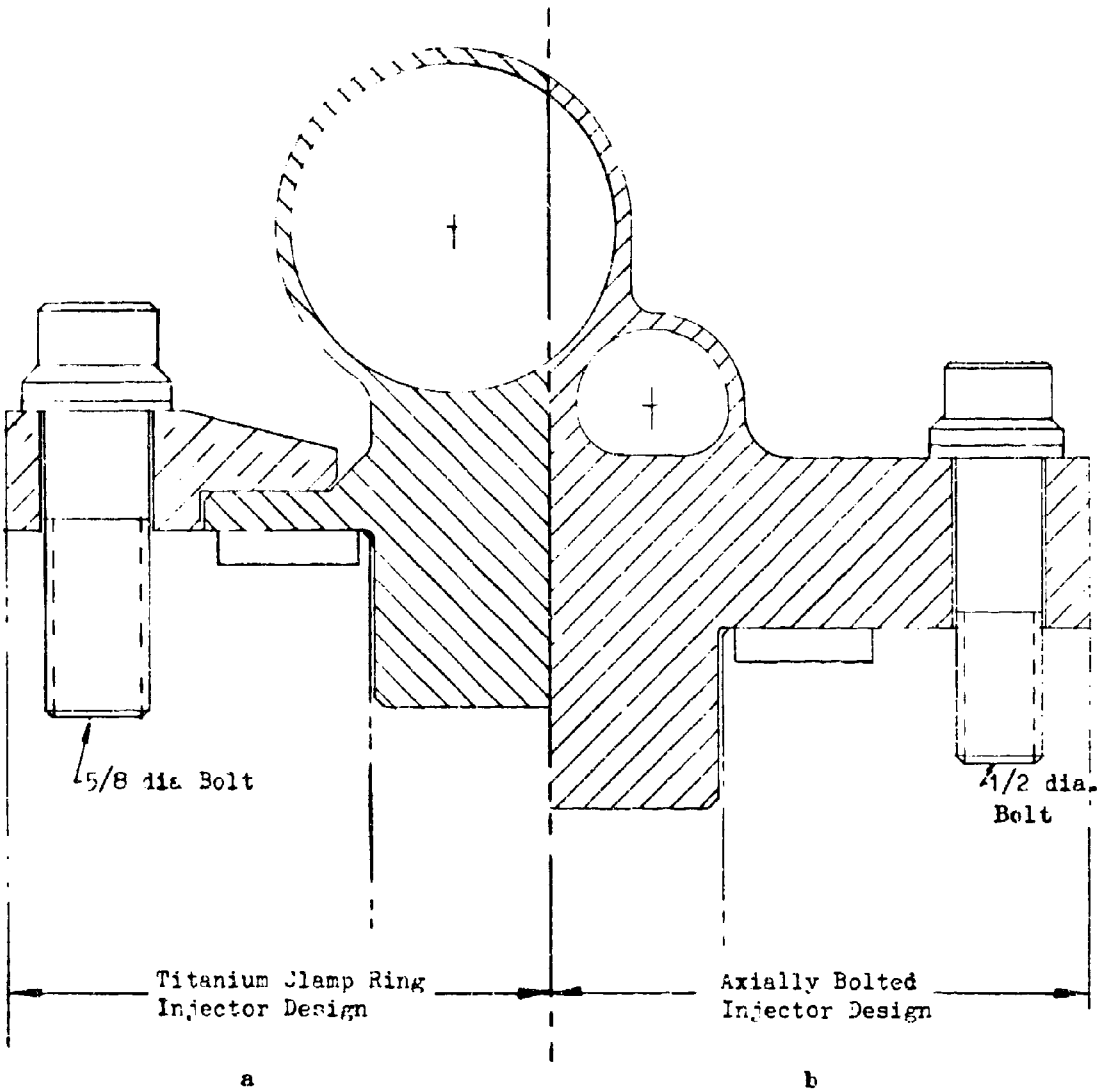

Note: AISI 347 used for injector body in both configurations

Figure 30. Axial Bolted Injector Design Concepts

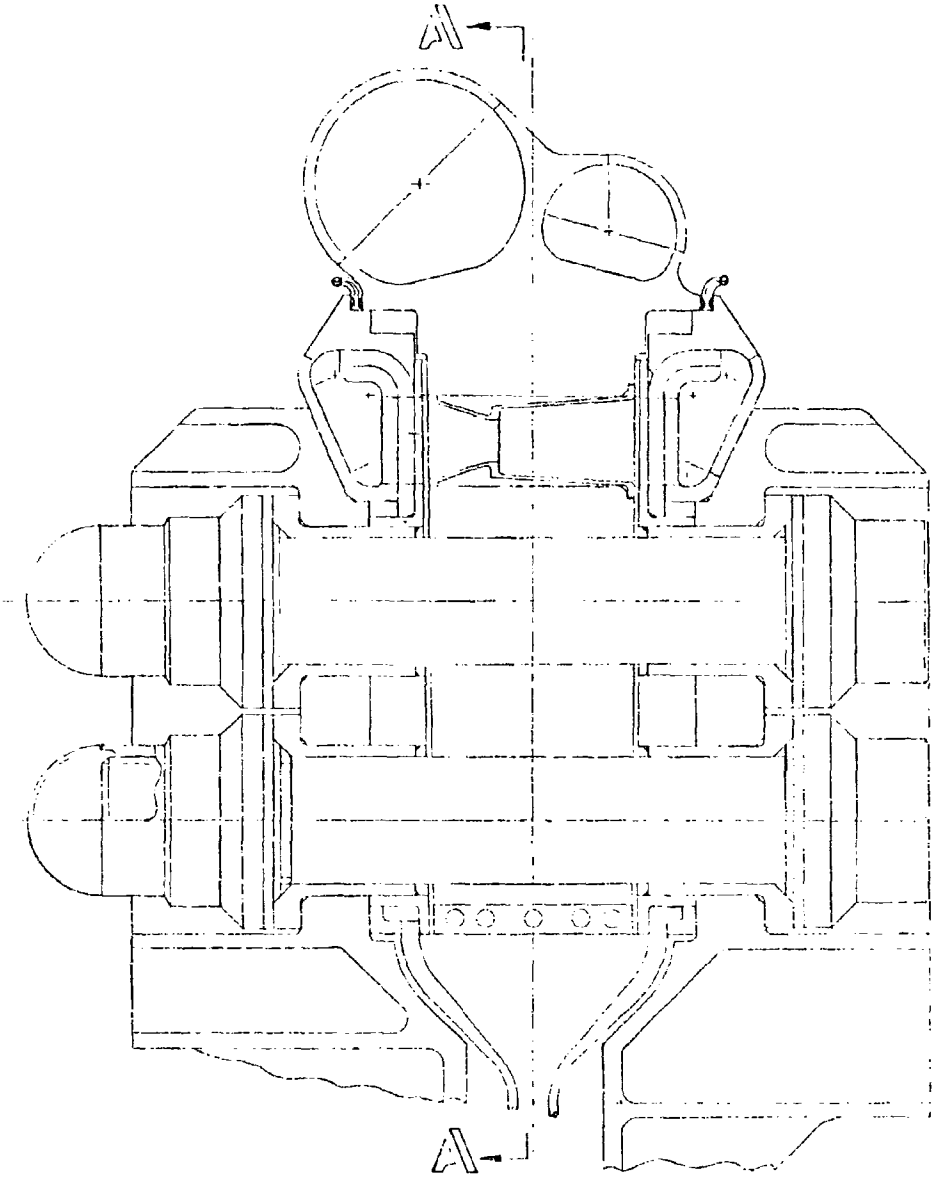

Figure 31. Integral Baffle Injector

(U) Mechanical joining of segments has been substituted for the electron beam welding which had been selected earlier. This was done in spite of a potential weight increase, because of manufacturing and processing problems defined in a more detailed investigation. Among these are dimensional control of the segment fit to assure a satisfactory joint penetration control of the electron beam to preclude adhesive and tube damage, and control of the welding atmosphere in the presence of adhesive to assure a sound joint. Technological advances during Phase II efforts will enable application of the electron beam welding technique to flight configurations for a weight saving. But for the demonstrator module, the mechanical joints will be used. The mechanical joint contemplated employs tensile bolts between the titanium segment flanges and line drilled shear pins for alignment and shear carrying capability.

(e) LOX Manifold

(U) The design requirements for the 250K demonstrator module LOX manifold have been developed based on the following generalized oxidizer manifold design criteria.

Item	Criterion
Oxygen Quality for Ignition	Gas
Differential Priming Time	Balanced ignition
Design	No pockets for gas or dead ends
Static Pressure Distribution	±4 percent
Torque	No additional system weight
Roll Impulse (volume), ft-lb sec	1000

(C) These criteria are based on experimental coldflow (LN_2) and water flow results of a full-scale four tangential inlet manifold, and 1/4-scale transparent models of the four tangential, the two tangential, and the two radial inlet types tested under the NASA System and Dynamics Investigation AEP. Based on these criteria, the following specific design requirements for the 250K demonstrator module LOX manifold have been developed:

1. The manifold torus should be a constant cross-section manifold.
2. There should be no dead ends in any section. With a constant cross-section manifold this would imply complete circulation from one sector to the other.
3. The inlets should be of the tangential type.

4. The number of inlets to the torus depends on the desired volume of the manifold, the maximum velocity, and the allowable differential prime time.

5. The inlets may be located on either the top or the inside of the manifold, and the inlet should intersect the manifold torus in a tangential manner.

6. The inlet should have the same diameter as the manifold torus, and the transition zone between the inlet and the torus should occur in a minimum of 25 degrees of arc.

7. Central location for the origin of the inlet ducts or a uniform length of all lines will not be required. Acceptability of a given design will be evaluation on the individual merits of the design. However, as a general ground rule, all inlet line configurations should have one-half engine symmetry and the differential line length between the shortest and longest pair should not differ by more than 30 percent.

8. To maintain a ±4 percent static pressure distribution, the maximum manifold velocity should be 60 ft/sec.

9. The number of downcomers will be controlled by the injector requirements. For the current injector design, three downcomers per baffled compartment should be employed.

10. The downcomers should be located in the outside section of the manifold.

11. The mass of the manifold with respect to the vapor forming potential must be considered and maintained at a minimum.

(C) The specific design requirements were based on criteria developed from LN_2 cold flow testing of the LOX manifold. It is possible that hot-firing engine data could modify these criteria which in turn could lead to modification of the specific design requirements. One of the more stringent requirements, from the standpoint of engine system design, is the number of inlets. In general, more inlets produce smaller manifold volumes and/or lower manifold velocities. In addition, the greater number of inlets produces the smaller differential prime times. (The differential prime time is defined as the time between ignitable quantities of oxidizer discharged through all orifices.) While there is strong experimental evidence to indicate that the minimum number of inlets (from an operational standpoint) should be no less than four (and possibly more), final evaluation of both the minimum number of inlets and the minimum manifold volume will depend on the hot-firing test results.

(f) Base Closure Design

(C) The two basic concepts studied for the module base closure design are shown in Fig. 32 and 33. The first was a conventional flat plate base closure (similar to that used in the experimental chamber) attached rigidly to the LH_2 thrust chamber manifold at the nozzle exit (Fig. 32). Approximately 9000-pound-thrust load would be transmitted through the closure to the thrust chamber. The necessity of flexible connections between the closure and the pump turbines required the assumption that a modification of the oxidizer turbine flange was feasible. Even with the assumed diminishing of the oxidizer turbine flange diameter, available space precluded the effective utilization of a bellows section. A slip joint was less desirable but could be made to fit in the space limitation. The 7-inch depth of the base closure was determined by the available geometry. The configuration itself contained a flat predrilled bottom plate and an upper dish-shaped plate of Inconel 718. The internal reinforcing structure consisted of eight radial ribs and 16 partial radial ribs. The ribs were connected by three circumferential rings at the bottom and three circumferential ribs at the top. All radial ribs contained large orifices to allow the distribution of the internal gases. Plate stress considerations determined the rib and ring spacing. Estimated weight of this configuration significantly exceeded its budget. Furthermore, there was difficulty in dispersing turbine gases because of the restrictive internal structure.

(U) The second design considered was an oblate spheroidal, membrane structure base closure mounted directly to the pump turbine flanges (Fig. 33). The closure thrust would thus be transmitted directly through the pumps into the thrust structure and no load would be transmitted through the chamber itself. A flexible omega joint seals the connection between the bottom of the chamber and the base closure.

(U) A membraine-type closure using an oblate spheroid configuration was employed using a minor-to-major axis ratio consistant with the space available. After conducting a trade study analyzing pressure vessel head shape vs weight, a minor axis dimension of 6 inches was chosen as the minimum probable head dimension capable of achieving the weight budget.

(U) The oblate spheroid was drawn in its position at the bottom of the thrust chamber indicating the bottom of the closure to extent approximately 5 inches past the chamber exit plane. This additional height does not increase the gimbal excursion, and the light weight and unimpeded internal flow advantages exceed the disadvantage of increased engine height.

(C) The configuration shown assumes curved turbine adapter sections to allow an interface compatible with removal of the base closure from the bottom. Internal flanges on the top head allow removal of the turbine bolts internally. Cone-shaped orifice plates are utilized to create sidewards propogation of the gas flow within the closure as well as reducing the 70- and 40-psi turbine pressures to the 30-psi closure internal pressure. The bottom head is perforated with orifices that comprise approximately 125 $in.^2$ of orifice area. A representative orifice size and spacing would consist of 0.257-inch-diameter orifices 0.875 inches apart.

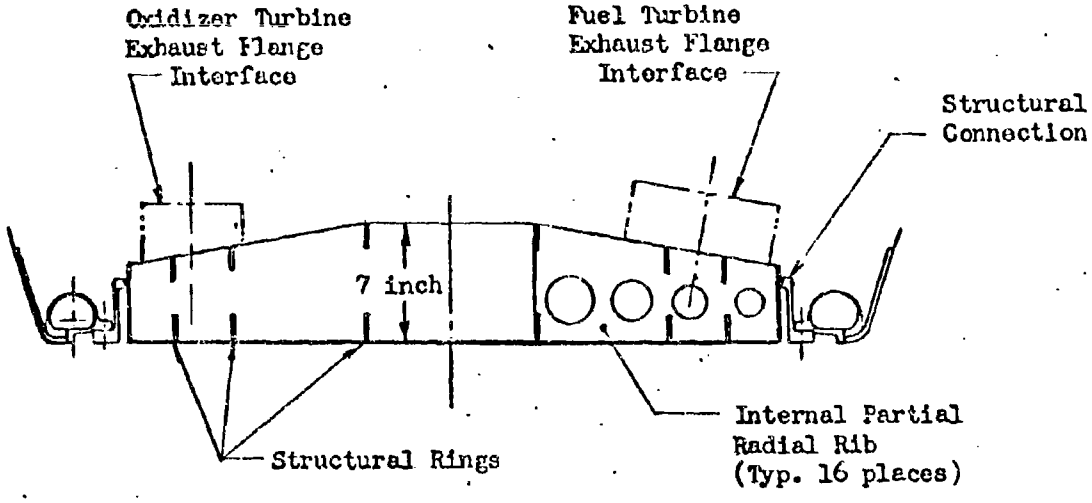

Figure 32. Flat Plate Base Closure

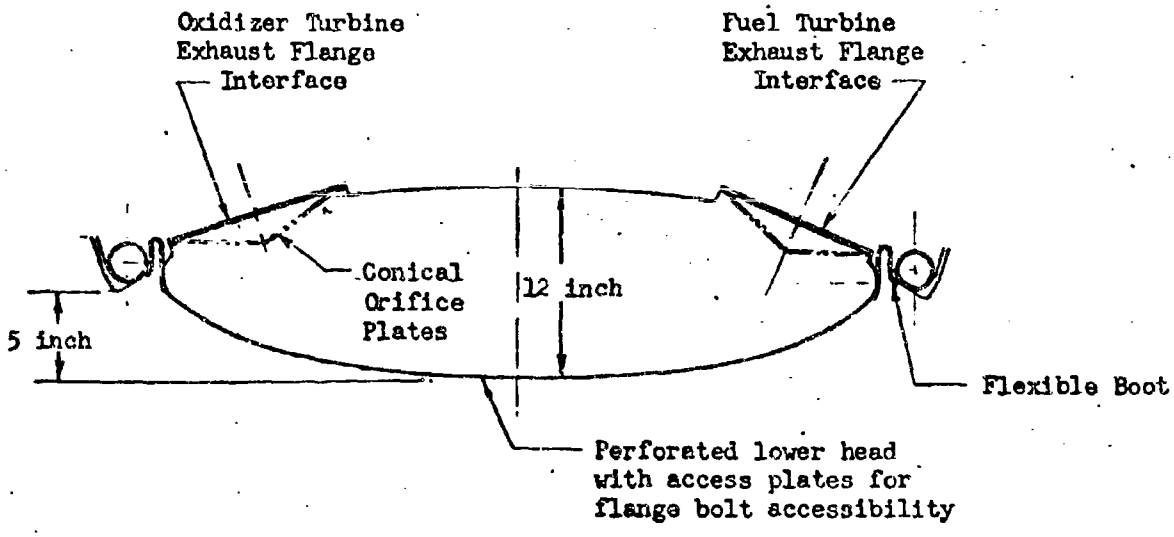

Figure 33. Oblate Spheroidal Membrane Base Closure

(C) The bottom and top heads can either be welded together or bolted. If welded, access plates would be required in the bottom head to allow removal of the turbine flange bolts. A metallic flexure or boot will prevent gas intrusion into the pump and component area. The boot will also accommodate both pump and base closure movements.

(U) The oblate spheroid configuration was therefore tentatively selected for the demonstrator module, because of its advantages in weight, performance, and operability.

(5) Controls Component Design

(a) Main Propellant Valve Design

(U) During the last quarter, a design review was held to review the main propellant valve configuration, materials, and the capability of meeting the system requirements. Design requirement specifications were written for both of the main valves, and the conceptual layouts were completed based on a 4-inch-diameter line.

(U) The layouts for the two valves are shown in Fig. 34 and 35 with no detail presented for the facility provided actuator. A hollow ball is used to minimize the flow forces acting on the ball, and the bearings are designed to run wet to locate them as close to the ball as possible and minimize the shaft overhang and bending loads. Dual Naflex seals are provided for the exterior seals, and machined plastic pressure-actuated seals are planned for the shaft. The ball seal is a pressure-loaded bellows seal, with low-pressure sealing provided by the bellows-installed spring load. The flow direction of the fuel valve is opposite from that of the oxidizer valve to provide moisture protection for the primary seal bellows.

(U) Each valve is oriented so as to place the bellows area downstream of the gate from the moisture source to prevent moisture from collecting in the area of the bellows and subsequent seal leakage problems. From studies of the valve locations and feed system plumbing configurations, it was determined that the most probable source of moisture for the oxidizer valve was downstream of the valve through the thrust chamber injector. On the fuel side, because the location of the fuel valve is below the pump, the major source of moisture was considered upstream of the fuel valve. Furthermore, the fuel valve is protected from downstream ambient moisture sources by the thrust chamber tube bundle. By reversing the flow direction of the fuel valve, the bellows area of each valve is thereby protected from moisture by the primary gate seal. However, for the gate seal to function satisfactorily with the new flow direction, a minor modification in the bellows seal design to change the relationship of the bellows neutral axis and the seal area on the ball was necessary. No other design modifications are required to provide for the reversed flow, and no significant change in valve performance or sealing characteristics is anticipated.

CONFIDENTIAL

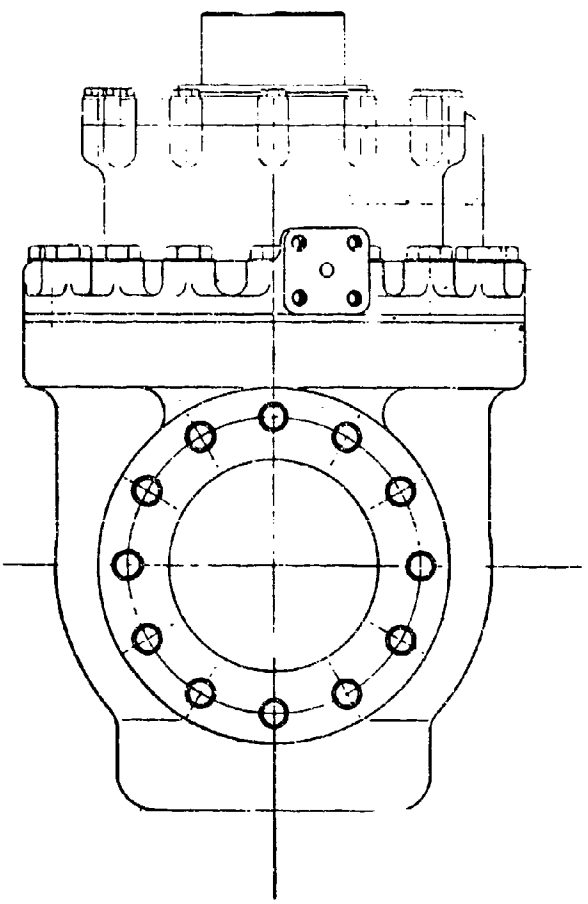

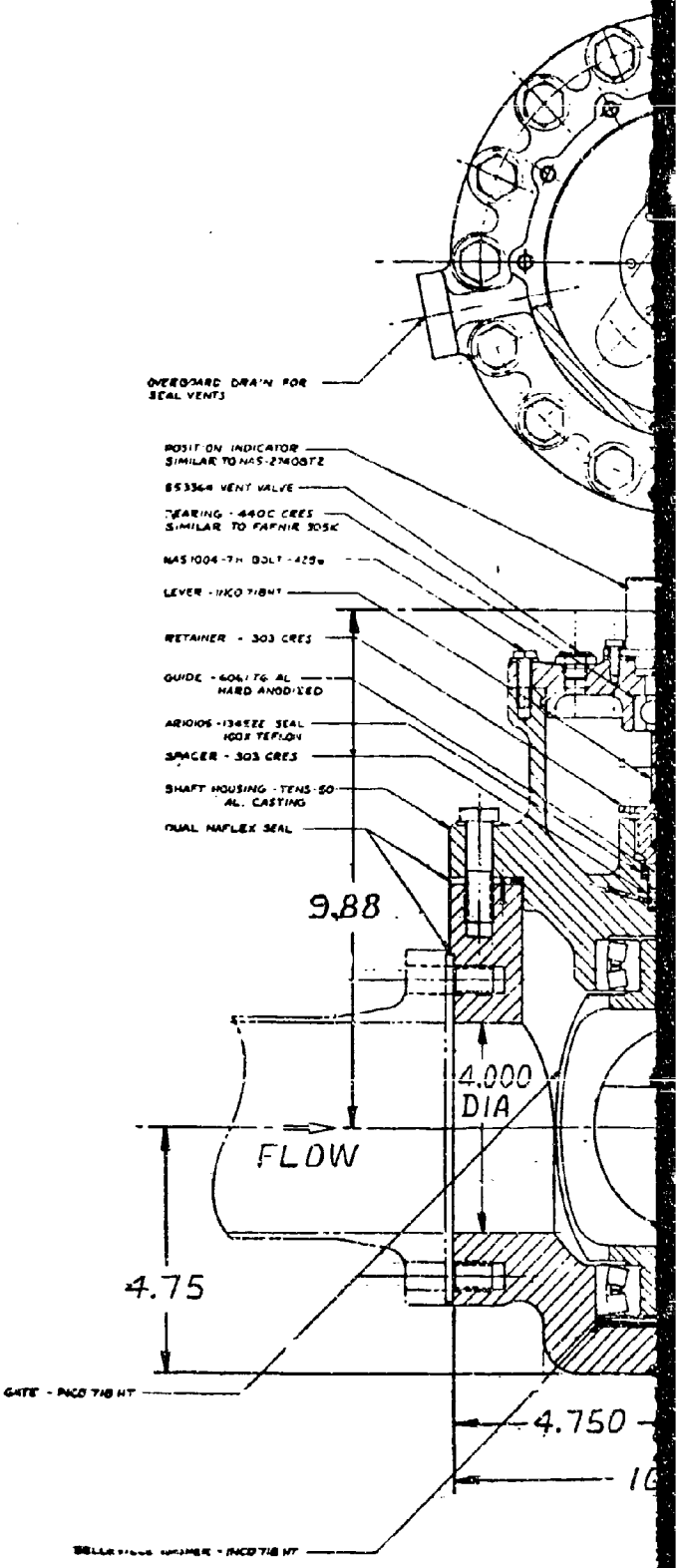

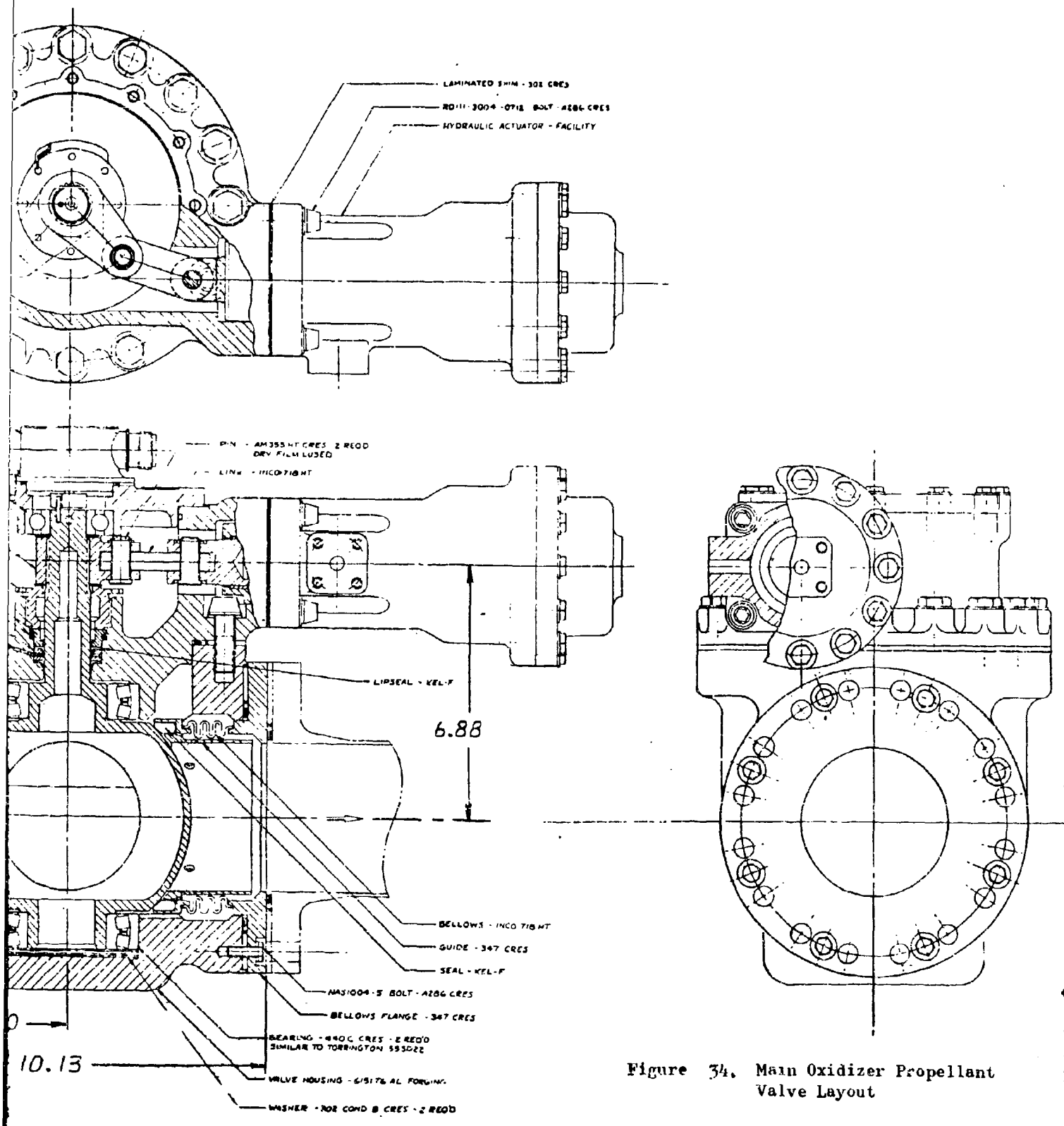

Figure 34. Main Oxidizer Propellant Valve Layout

CONFIDENTIAL

2

CONFIDENTIAL

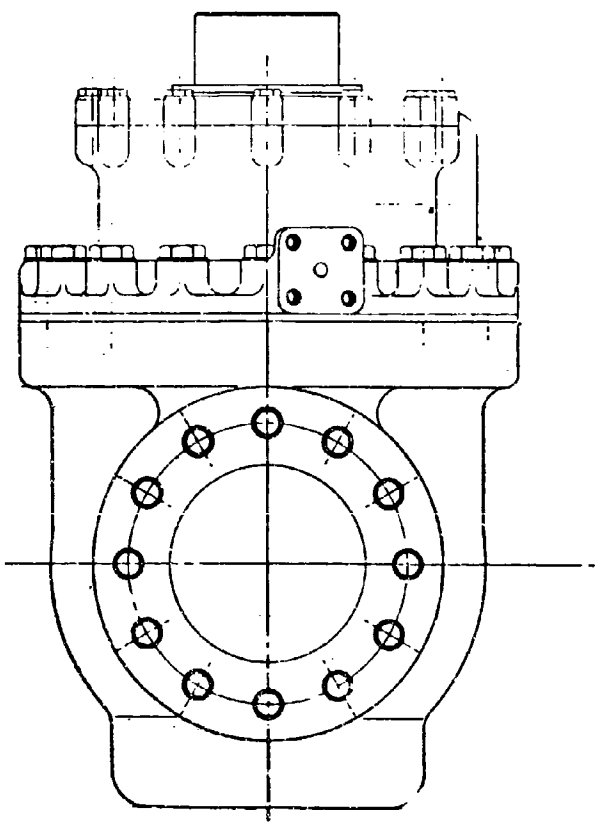

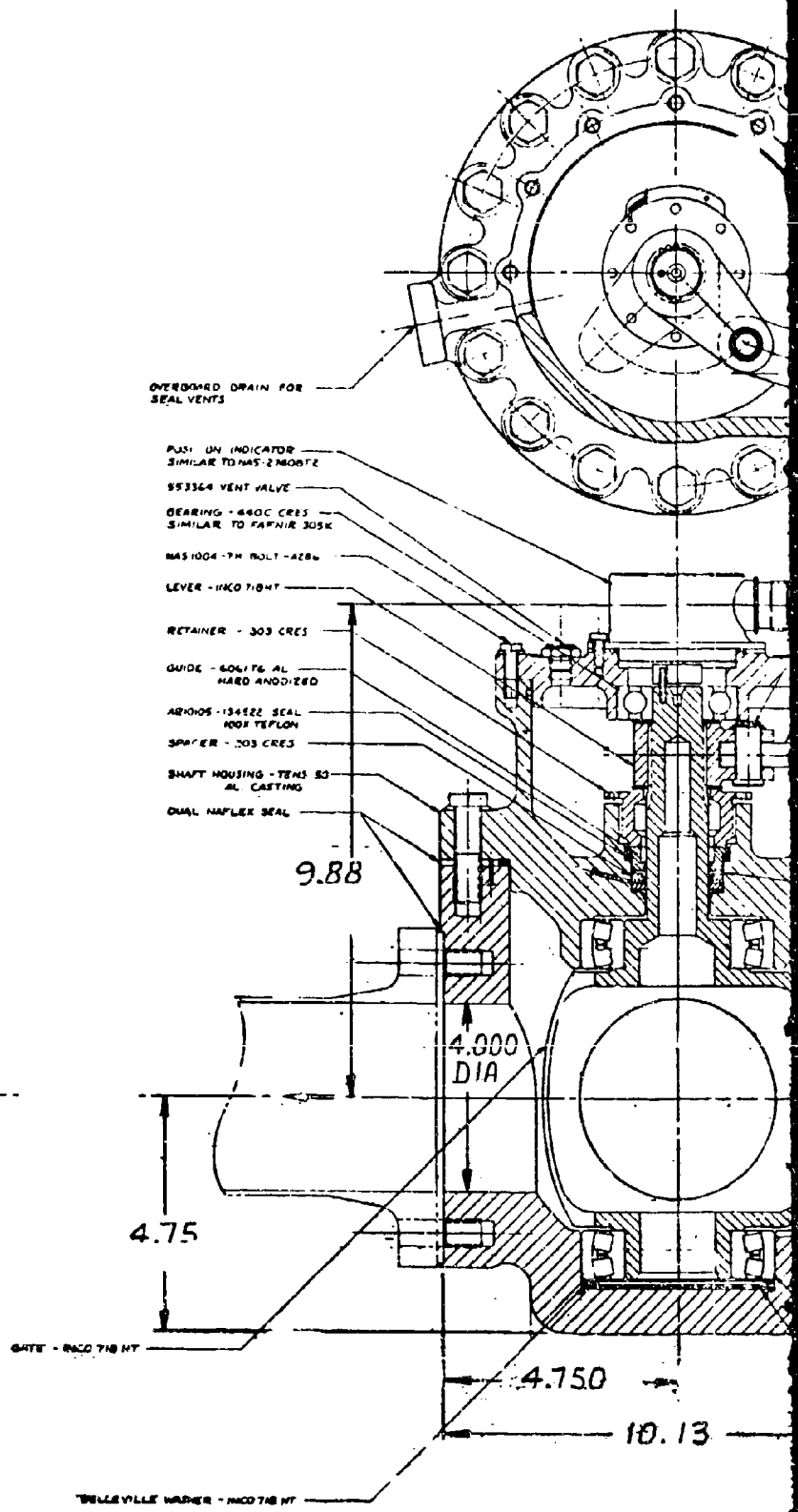

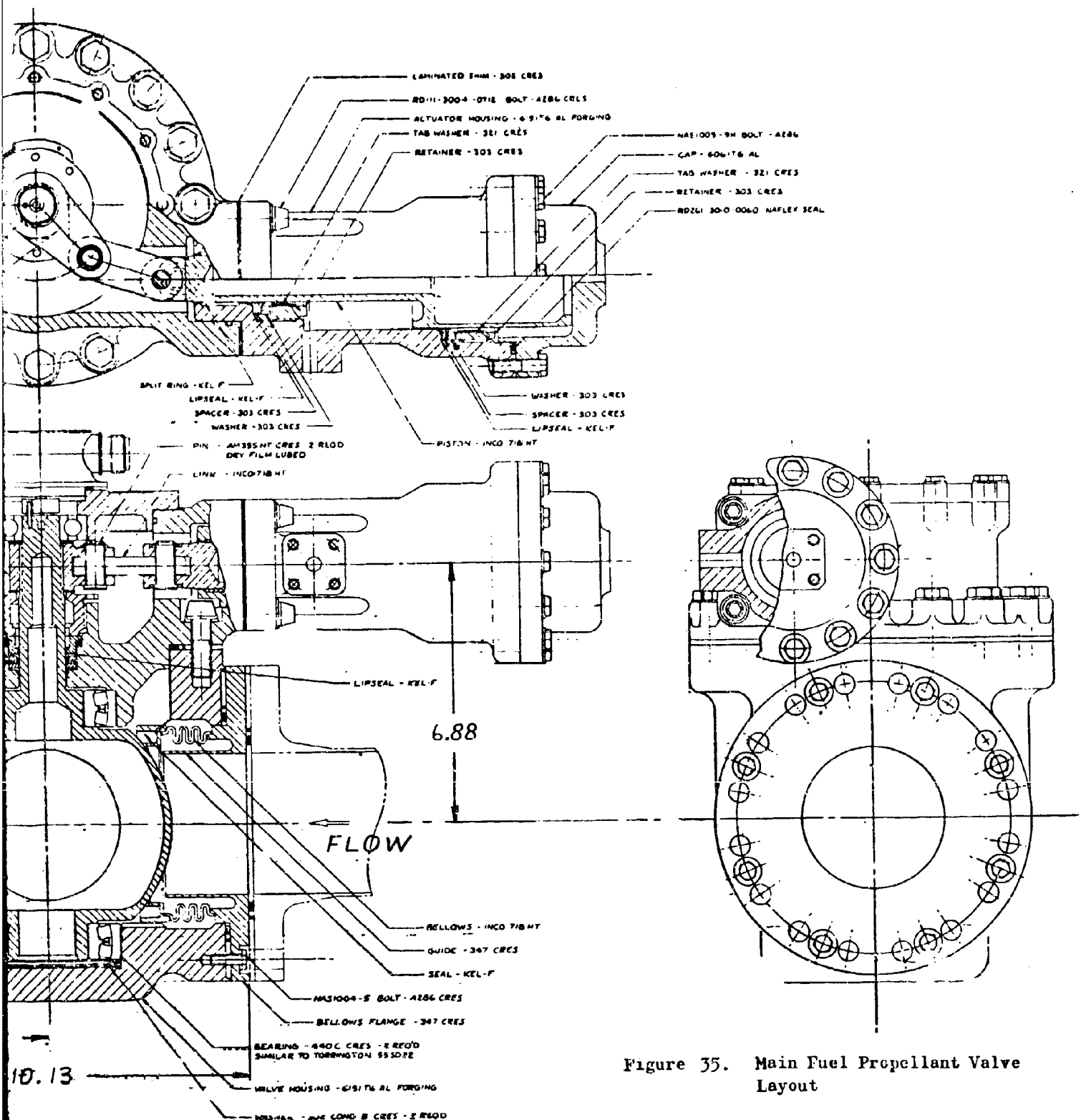

10.13

Figure 35. Main Fuel Propellant Valve Layout

CONFIDENTIAL

2

(b) Tapoff Throttle Valve

A design review was held to evaluate the tapoff throttle valve design configuration, materials, and system requirements. The review board recommendations were studied and refinements were made in the valve design. A design requirement specification was also written for the tapoff throttle valve.

(U) A design layout was initiated during this report period and the maximum and minimum valve flow areas were established to meet the engine operating limits. The poppet nose was contoured to reduce turbulence as the hot gas flows around the poppet. In addition, a slight taper was incorporated to reduce the rate of change of area with stroke as the poppet approaches the closed position. The valve configuration, poppet contour, and relationship of flow area to stroke are shown in Fig. 36.

(U) The design layout was completed through the selection of materials for the parts in the hot-gas flow stream. Because of the 1500F nominal operating temperature, only materials with good mechanical properties and corrosion resistance at elevated temperature are used. Stellite 21 was selected for the poppet because of its high-temperature strength and resistance to erosion. The housing is Hastelloy-C because of its high-temperature strength, ductility, and good casting properties.

(U) A preliminary heat transfer analysis was made to evaluate the transient heat transfer from the poppet into the actuator.

(C) Assuming a heat transfer path through steel, the temperature at the approximate location of the actuator O-rings (assumed to be 6 inches away from a 1500 F heat source) is 81 F after 300 seconds of engine operation with an initial temperature of 70 F. After engine cutoff, this temperature will continue to rise for some time as the component tends toward temperature equilibrium. The heat transfer analysis did not include the transient effect after shutdown; however, the calculations made through cutoff appear to indicate that the maximum tolerable temperature of 350 F will not be approached, and therefore the service life of 10 hours should not present a design problem relative to the actuator O-rings. A more complete heat transfer analysis will be made during Phase II.

(U) Several areas related to the high temperature of the hot gas which should be studied further during Phase II became apparent during the design. The materials required because of the high operating temperature are difficult to machine by conventional methods which precludes the use of threads. Therefore, the joint between the piston rod and poppet cannot utilize a threaded fastener. Brazing appears to be satisfactory; however, some additional analysis is required to ensure that sufficient braze area is provided.

(U) Because the valve will operate with a high degree of throttling with high-temperature gas, erosion of the housing may be critical. This area will be analyzed thoroughly and if necessary, a material such as Stellite 21 which is more resistant to erosion will be welded into the critical area.

CONFIDENTIAL

FLOW AREA VS. POPPET STROKE

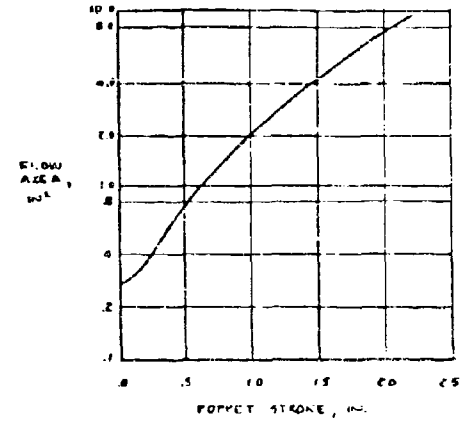

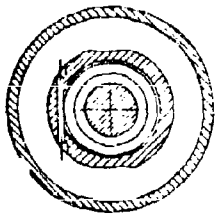

SECTION D-D
(SCALE 1/1)

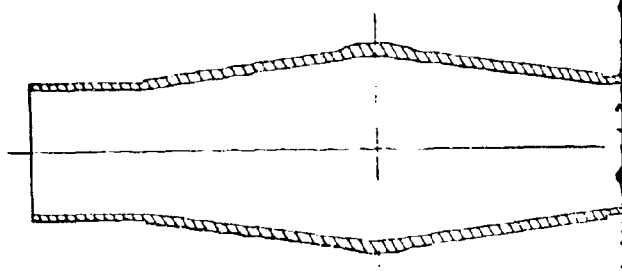

SECTION A-A
(SCALE 1/1)

A DESIGN POINT, VALVE FULL OPEN
B MAXIMUM THRUST ; MF = 7:1
C " " ; ME = 5:1
D MINIMUM THRUST ; ME = 7:1
E " " ; MR = 5:1

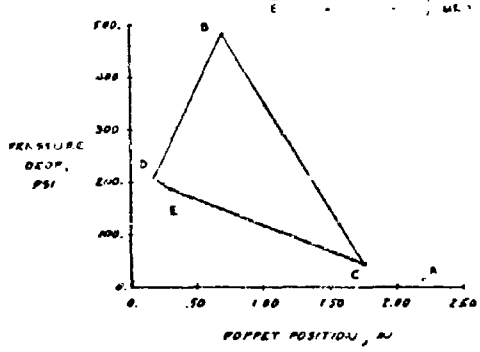

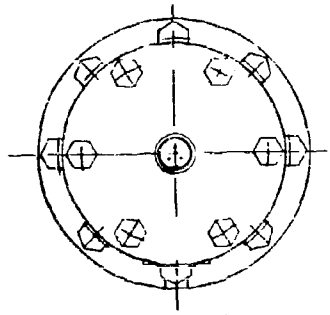

VIEW B-B
(SCALE 1/1)

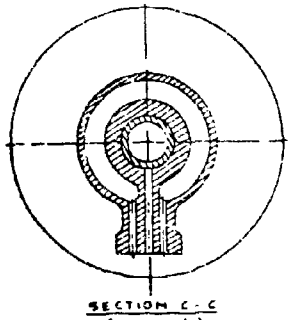

SECTION C-C
(SCALE 1/1)

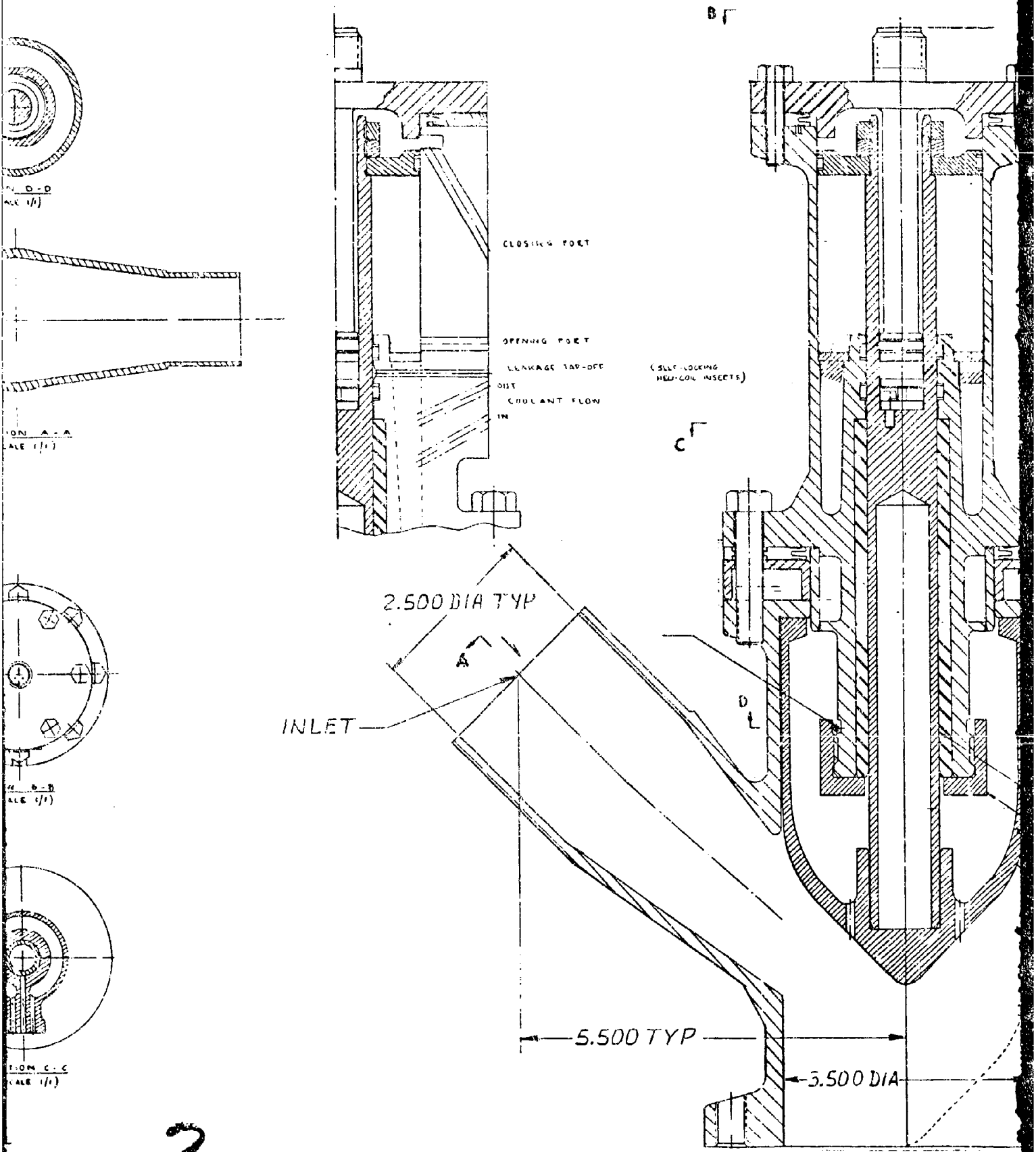
B
C
CLOSING PORT
OPENING PORT
LEAKAGE TAP-OFF
OUT
COOLANT FLOW
IN
(SELF-LOCKING HELI-COIL INSERTS)
2.500 DIA TYP
A
INLET
D
5.500 TYP
3.500 DIA

2

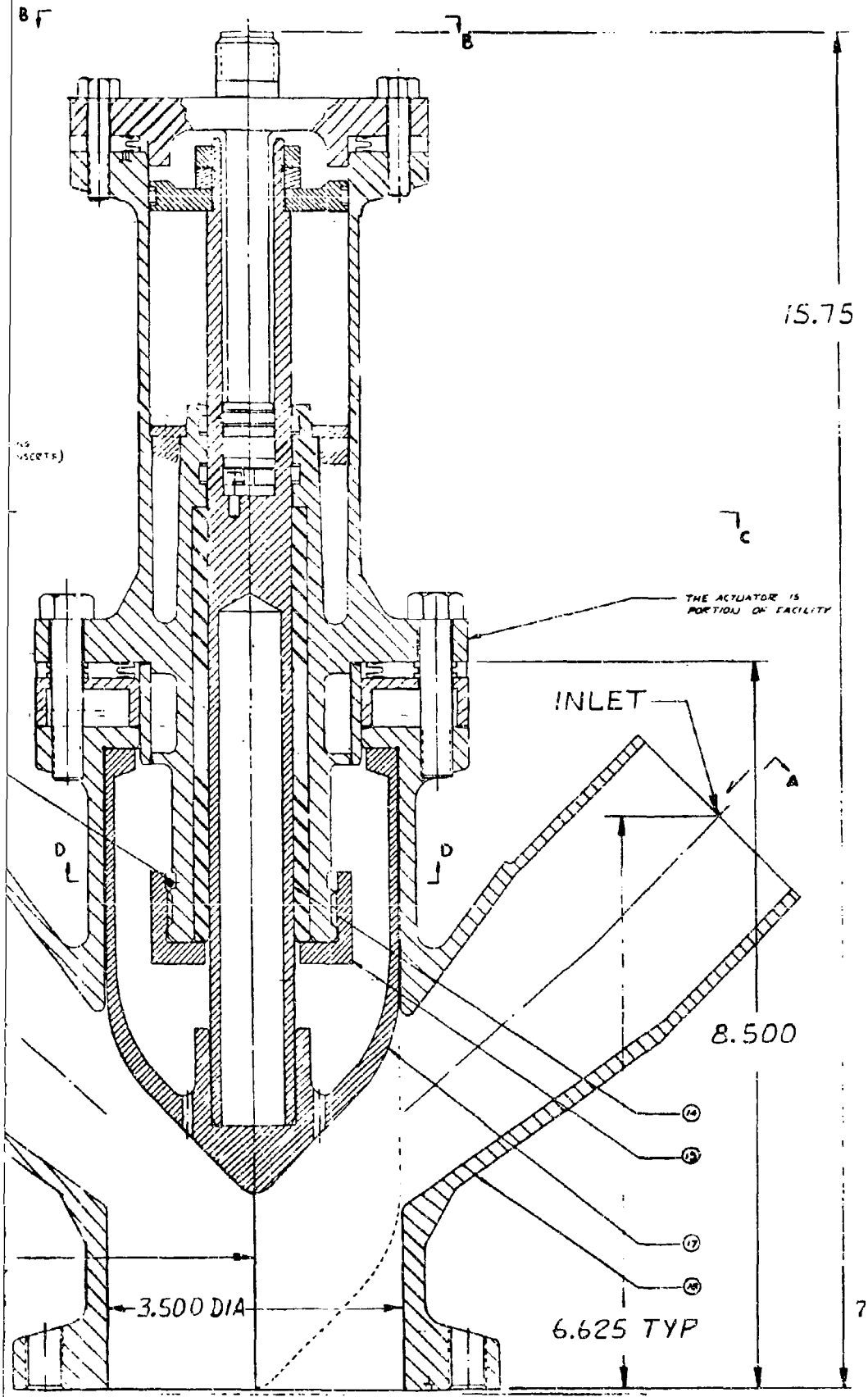

Figure 36. Tapoff Throttle Valve Design

CONFIDENTIAL

3

(U) Heat transfer from the valve housing and poppet into the actuator may also be higher than desirable. Hydraulic fluid circulation can be provided in the facility actuator, insulation can be used wherever possible, and the configuration of the parts in the heat transfer path can be studied to optimize the heat transfer and heat capacity relationship.

C. Problem Areas and Solutions

(C) In the last quarterly report, it was stated that the single-step main oxidizer valve created a main chamber ignition problem by virtue of a temporary drop in the hot-gas ignitor temperature. When the LOX valve was opened, the LOX pump discharge pressure dropped below the fuel pump discharge pressure, and this caused the mixture ratio of the hot-gas ignitor to fall off. The problem was resolved by returning to a two-step main oxidizer valve. This reduces the effect of the opening of the LOX main valve, and the LOX discharge pressure remains above the fuel discharge pressure until after main chamber ignition (Fig. 11). Figure 37 shows the ignitor temperature as a function of time for both the one-step and two-step valves. The transient still exhibits a temperature drop (from 1600 F to 1530 F); however, the minimum temperature is now above the level required for main chamber ignition.

(C) Further analysis of the main chamber ignition conditions was made to assure that the thrust chamber propellant mixture ratio was high enough to obtain satisfactory ignition. Figure 38 indicates the main chamber mixture ratio during the start transient. This curve indicates that the mixture ratio rises rapidly to a value of 1.5 after the oxidizer valve is moved to the first position. (Current test results indicate that a value of 1.0 or higher is desired for ignition.) Ignition is obtained at this point with gaseous oxygen because the oxidizer system is not fully primed. The back pressure of combustion then causes a reduction in the flow of gaseous oxygen, and the main chamber mixture ratio drops until full oxidizer prime is reached. At this point, the main oxidizer valve is moved to the second position and the system proceeds into mainstage. It should be noted that the drop in main chamber mixture ratio does not occur until after ignition is attained, thereby assuring a high ignition mixture ratio.

d. Planned Effort

(U) During the next quarter, design effort will be directed towards the completion of the final turbopump and thrust chamber layouts.

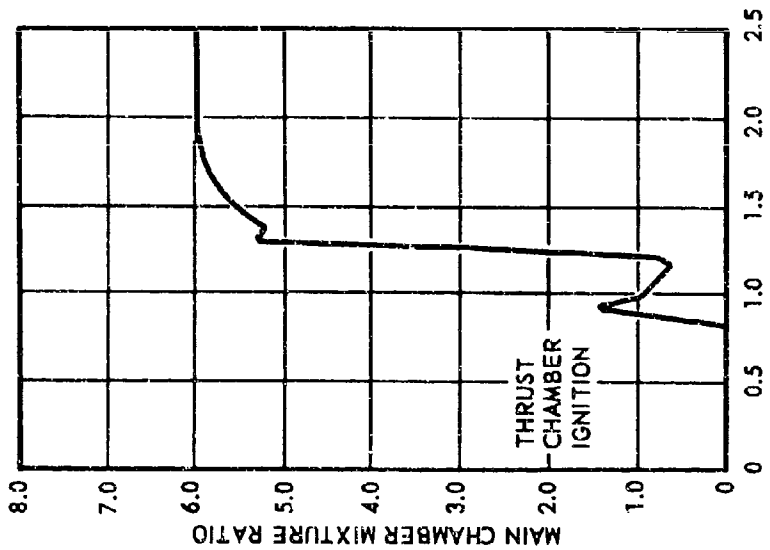

Figure 38. Main Chamber Mixture Ratio Start Transient

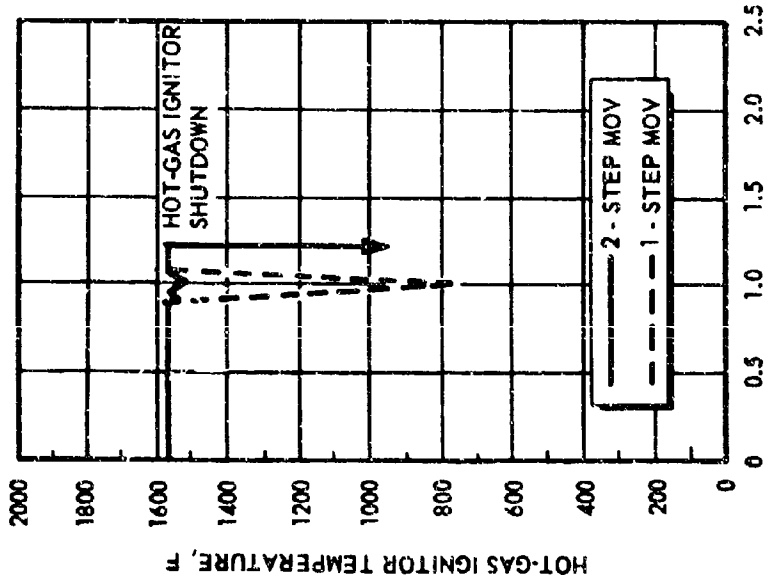

Figure 37. Hot-Gas Ignitor Temperature Start Transient

2. APPLICATION STUDY

a. Status

(C) The generation of all parametric installation weights and vehicle fairing and/or interstage surface areas has been completed for thrust levels of 250,000 and 350,000 pounds. Parametric installation data covers the range of diameters from 68.5 inches to 130 inches for the 250K vehicles (vehicles utilizing 250K-pound-thrust modules) and from 80 inches to 160 inches for the 350K vehicles.

(U) The calculation of performance index values has been accomplished by employment of the above engine/vehicle integration information which was based on "minimum envelope" thrust structure design rather than the previous 15-degree cone limit design.

(C) An individual optimum for each of the 12 vehicle cases has been established. In general, the optimum diameters for the 250K cases are smaller than the optimum diameters for the 350K cases. The 350K modules, however, optimized at approximately the same chamber pressures. Of significance is the fact that all optimum chamber pressures are equal to or less than 2000 psia and the two reusable upper-stage vehicles (No. 5 and No. 6) for both thrust levels optimized at chamber pressures of 1100 psia or less.

(U) Preparation of the Application Study Special Report was initiated. This report will discuss in detail the pertinent information generated during the Applications Study. It is for this reason, only highlights of the progress made in the fourth quarter will be presented here.

b. Progress During Report Period

(1) Installation

(C) During this report period, parametric installation data for both the 250K and 350K cases has been redefined removing prevalves from all vehicles and employing a minimum envelope installation thrust structure in place of the previously assumed 15-degree maximum truncated outer cone angle thrust structure for Cases 1, 3, and 4 (250K and 350K). In these installations, there is a minimum clearance between modules (2 inches) and the mount height is as short as possible consistent with the maintenance of propellant feed system and tank bottom clearance. Layouts of each vehicle case were generated to determine the minimum mount height for each candidate module diameter. Figures 39 and 40 are typical layouts which depict minimum mount height for each clearance criterion (i.e., propellant feed system clearance and thrust structure/tank bottom clearance) for an 80-inch module installation, Case 3, 250K. It is seen that the propellant feed system clearance determines the minimum mount height for this configuration. At the minimum mount height of 100 inches, the fairing area, maximum skirt diameter, and installation weight are all minimum, thus defining the optimum mount height.

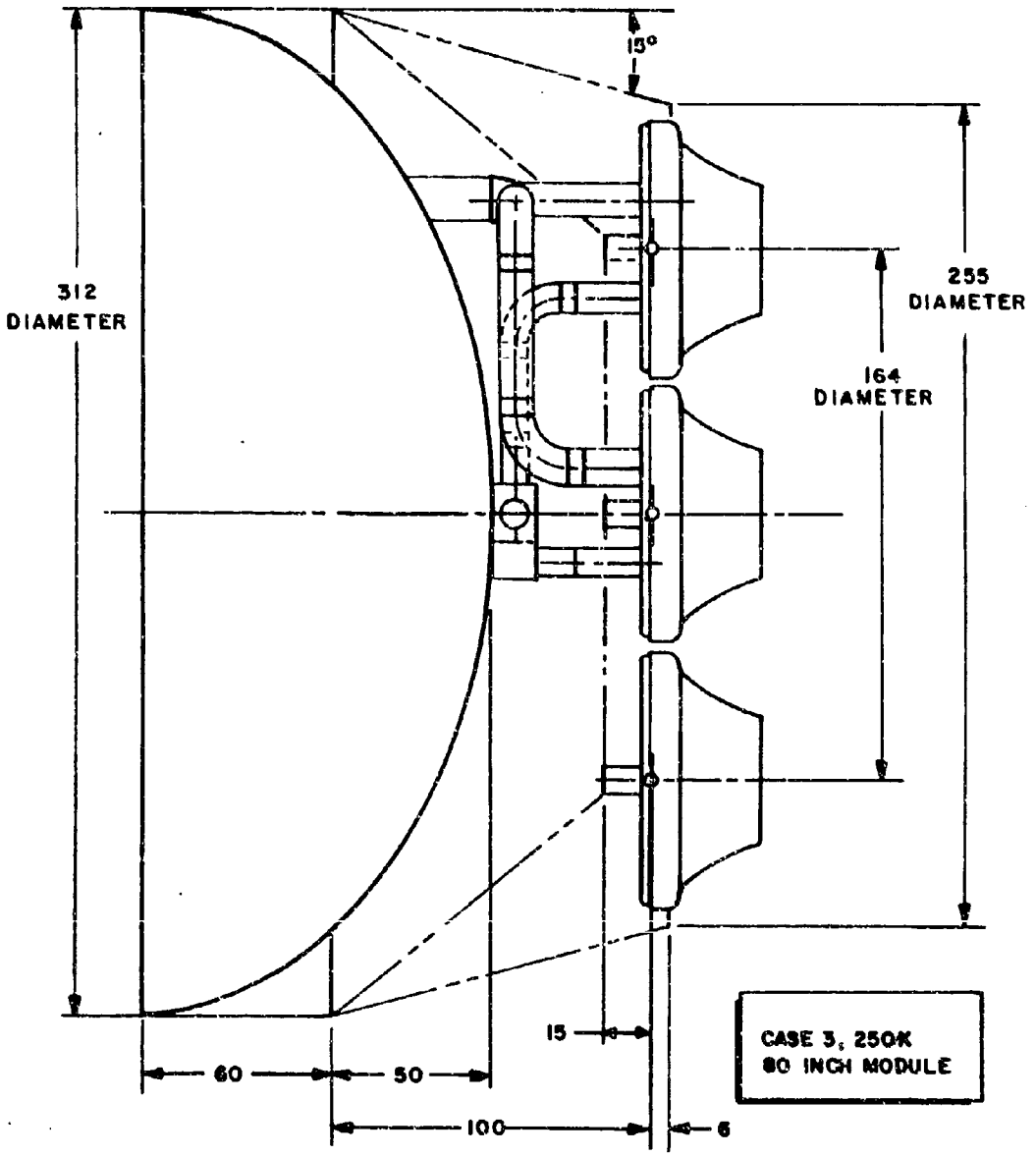

Figure 39. Minimum Mount Height, Propellant Feed System Limit

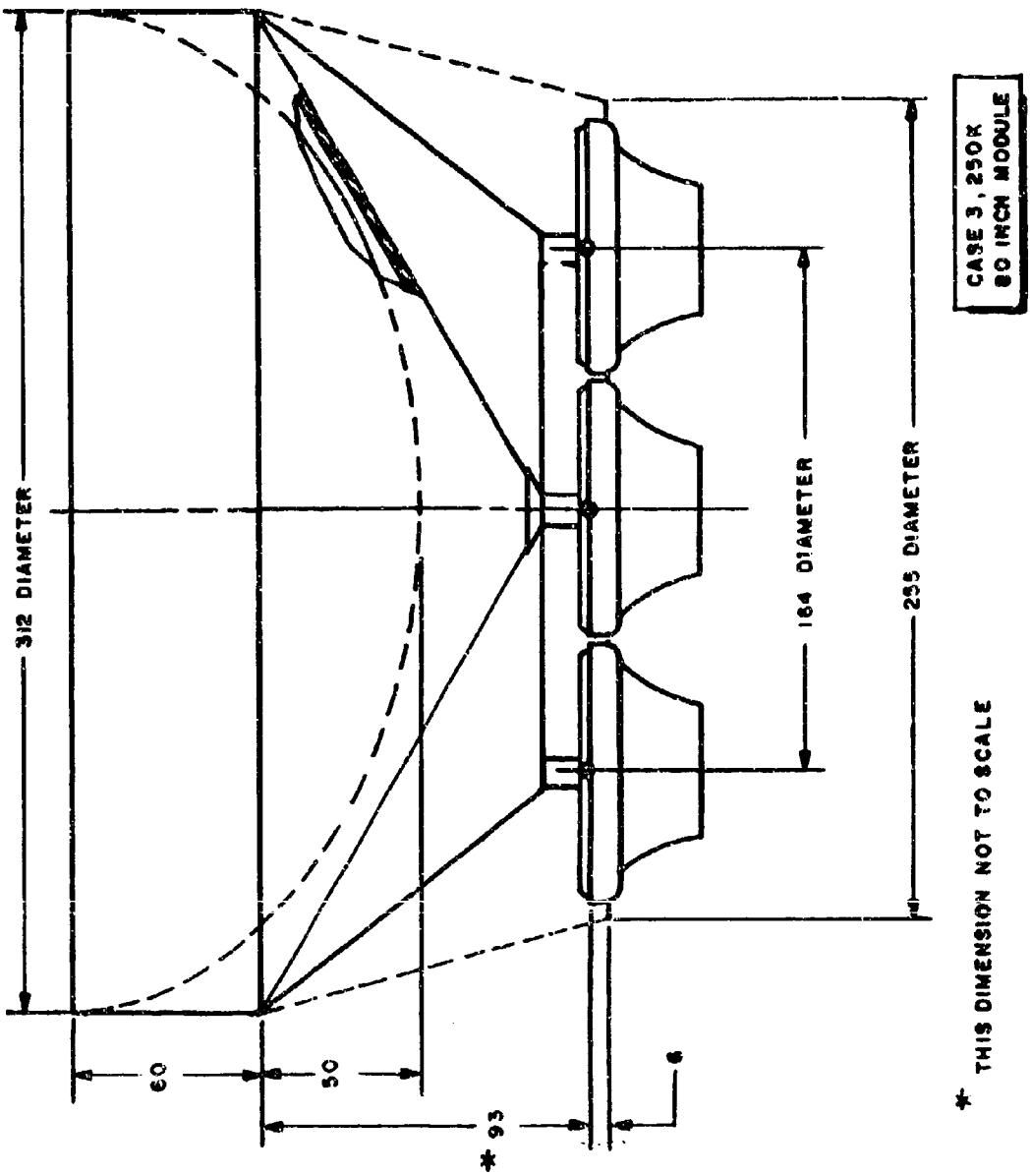

Figure 40. Minimum Structural Mount Height Limit

(U) The revised thrust structure parametric weights were determined wi .h thrust structure angles varied as necessary to provide a minimum diameter mount ring. The configurations are similar to the previous design. Cases 1, 3, and 4 have inner cones and radial beams to provide lateral support for the truncated cone during gimbaling. Figure 41 shows a typical thrust structure for vehicle Cases 1 and 3, 250K. The thrust structure in Case 4, 250K, is similar except for the number of radial beams. Vehicle Cases 2, 5, and 6 did not employ a truncated cone thrust structure and therefore are not affected by the foregoing revision. Radial loads induced by the angle of the thrust structure cone at the vehicle main attach frame are carried by a hoop ring integrated with the thrust structure, thus precluding transfering of radial and torsional loads into the vehicle. The vehicle is subjected to axial loads only.

(U) The revision to the truncated cone thrust structure reflects upon the following:

1. Propellant feed system
2. Heat protection system
3. Fairing area

(U) The change in propellant feed system weights for the revised thrust structure heights is directly proportional to the change in line lengths resulting from the lower mount heights.

(U) Heat protection system basic weight analysis is unchanged by the revised thrust structure design. Only the area of the base heat shield is affected. The area of the heat shield is a function of the joining diameter at the plane of the heat shield. Thus, reduction in fairing diameter achieved through the revised thrust structure installation lowers heat shield weight.

(U) Reductions in fairing and/or interstage areas occur in the lower mount height regions in those vehicle cases which employ the revised minimum envelope thrust structure. In addition to determining the minimum envelope defined by the revised thrust structure, all vehicle cases, both 250K and 350K, were investigated to more clearly define the minimum envelope attainable considering the effects of propellant feed system installations. Figures 42 through 53 illustrate the effect of mount height and module diameter on installation weight and fairing area for the 350K vehicle cases. Limits of installation effects are depicted on each curve. As noted, the propellant feed system installation effects occur only with the smaller module diameters.

(U) A limited study of secondary injection thrust vector control (SITVC) systems and their effect on performance index was initiated during this report period.

(U) A screening of candidate SITVC systems resulted in the selection of a configuration utilizing propellants tapped off the turbopump outlets and combusted at low mixture ratio as being most representative of an

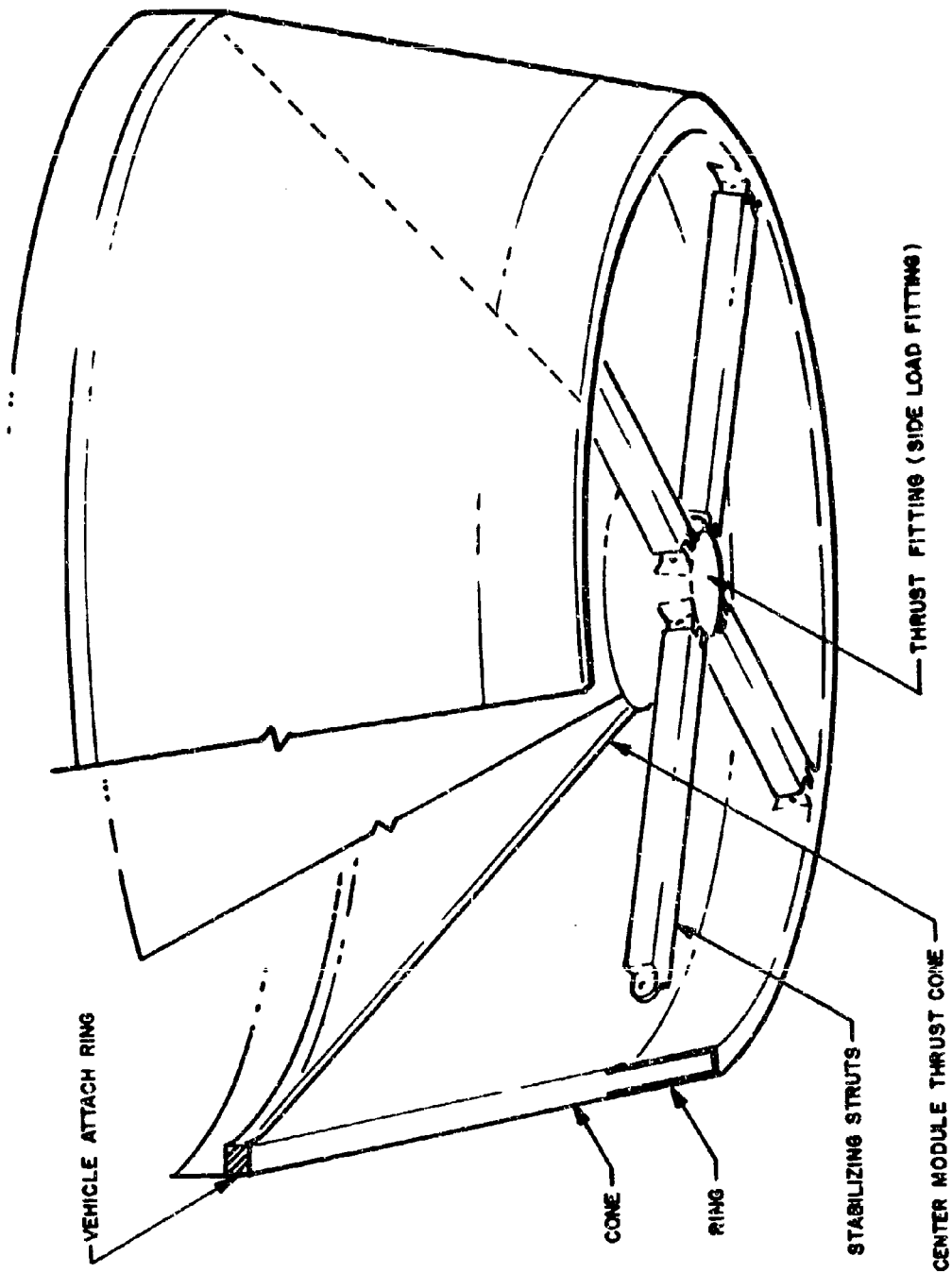

Figure 41. Cases 1 and 3 Thrust Structures

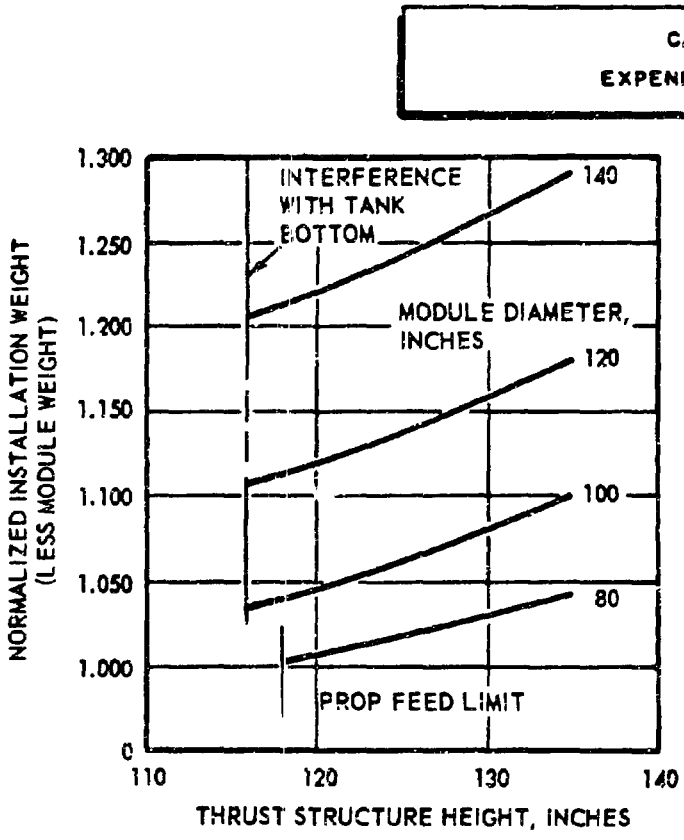

Figure 42. Normalized Installation Weight Variation With Thrust Structure Height, Case 1

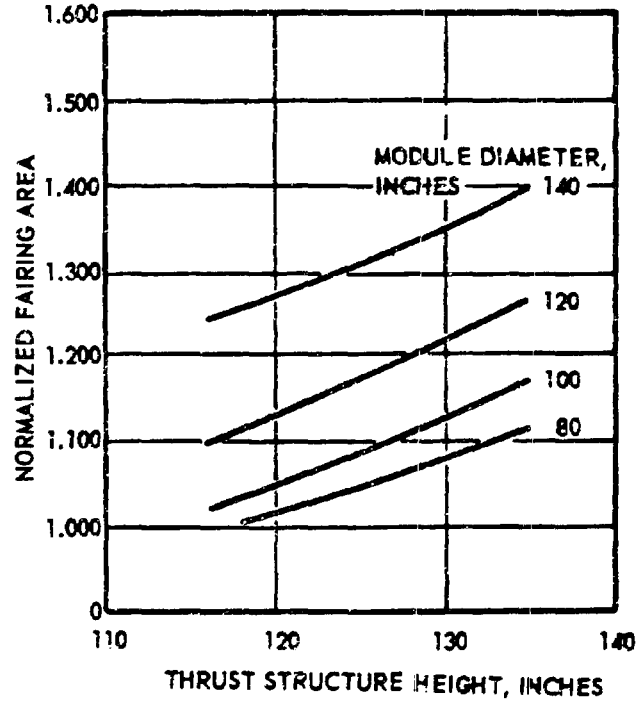

Figure 43. Normalized Fairing Area Variation With Thrust Structure Height, Case 1

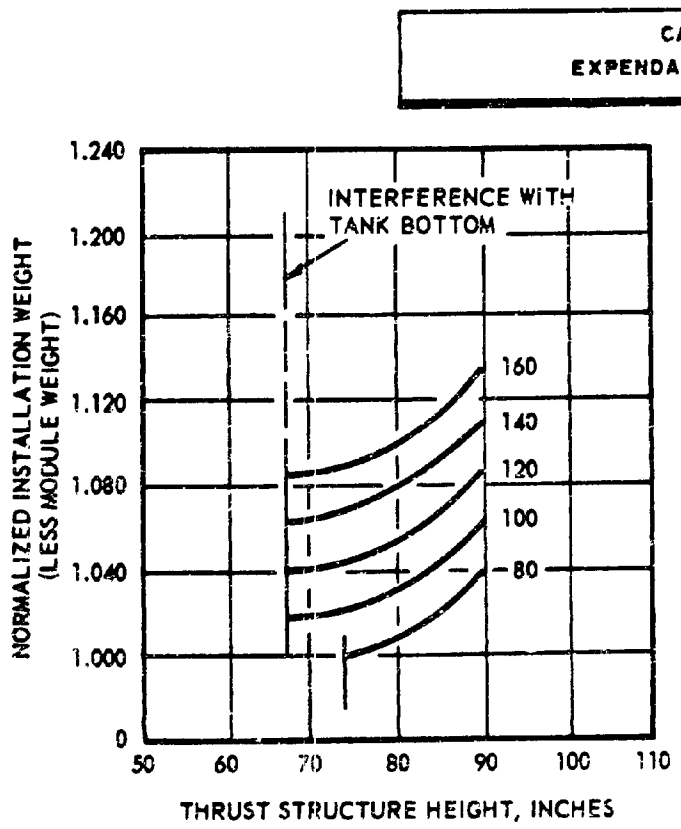

Figure 44. Normalized Installation Weight Variation With Thrust Structure Height, Case 2

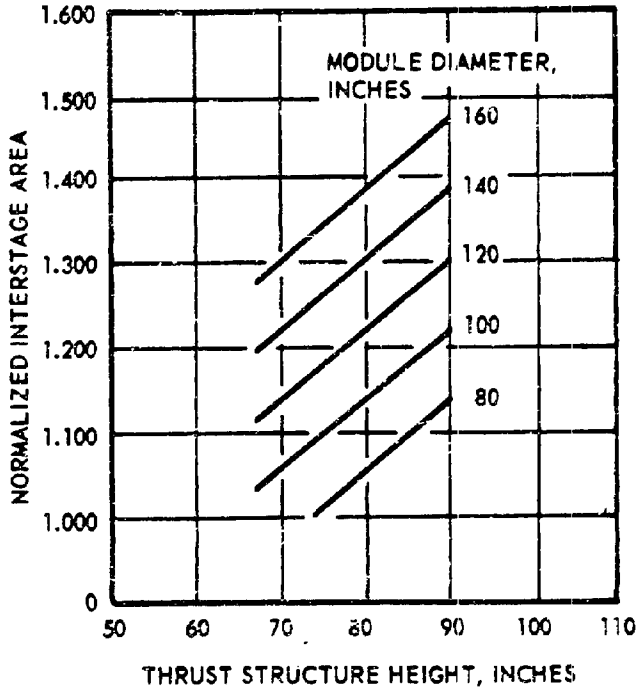

Figure 45. Normalized Interstage Area Variation With Thrust Structure Height, Case 2

CASE 3, 350K

EXPENDABLE SINGLE STAGE TO ORBIT

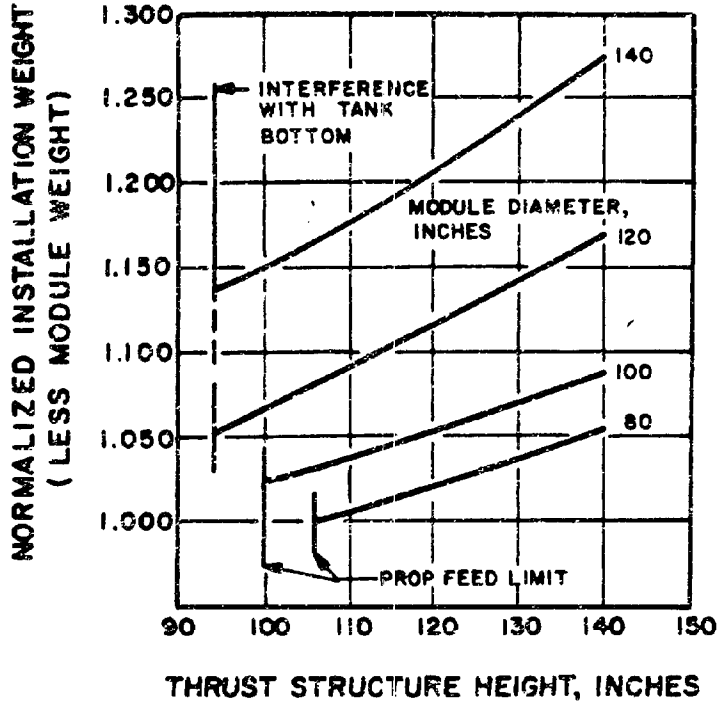

Figure 46. Normalized Installation Weight Variation With Thrust Structure Height, Case 3

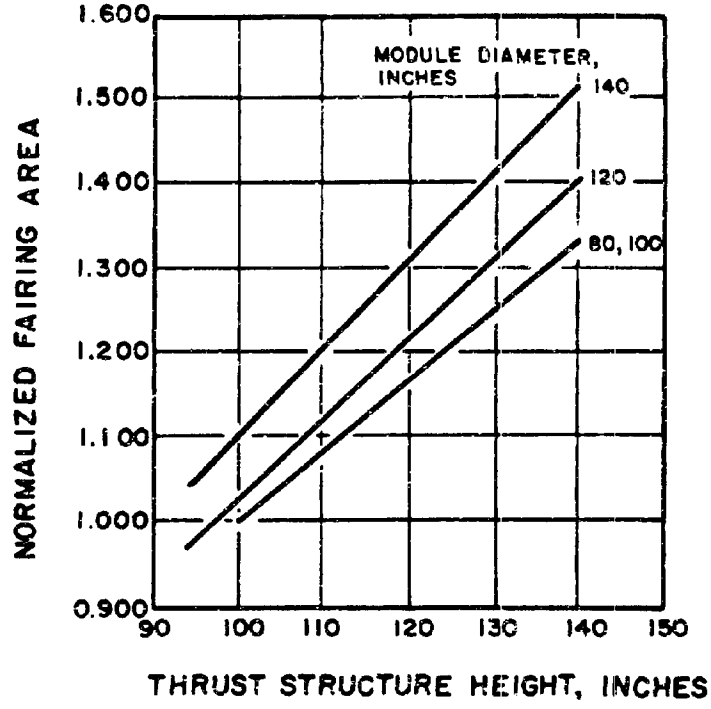

Figure 47. Normalized Fairing Area Variation With Thrust Structure Height, Case 3

CASE 4, 350K
RECOVERABLE FIRST STAGE (VTOHL)

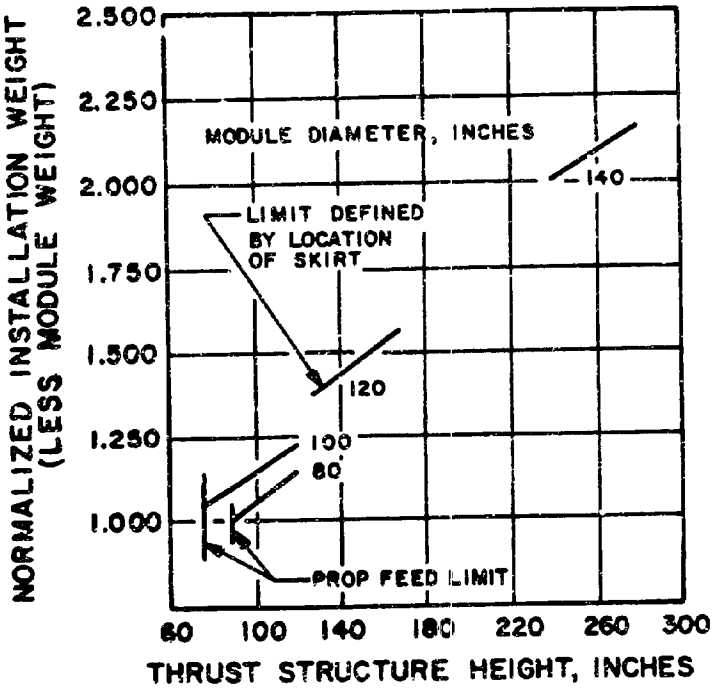

Figure 48. Normalized Installation Weight Variation With Thrust Structure Height, Case 4

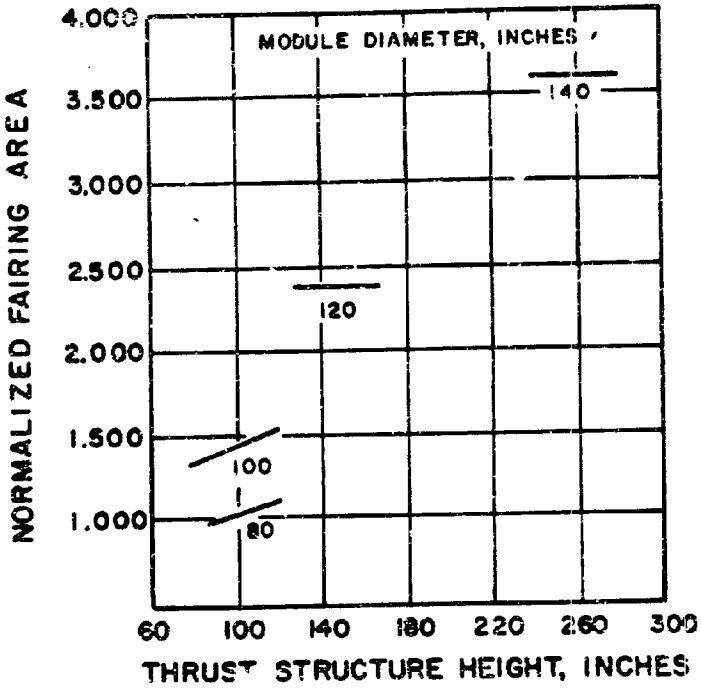

Figure 49. Normalized Fairing Area Variation With Thrust Structure Height, Case 4

CASE 5, 350K

RECOVERABLE SECOND STAGE, PICKABACK

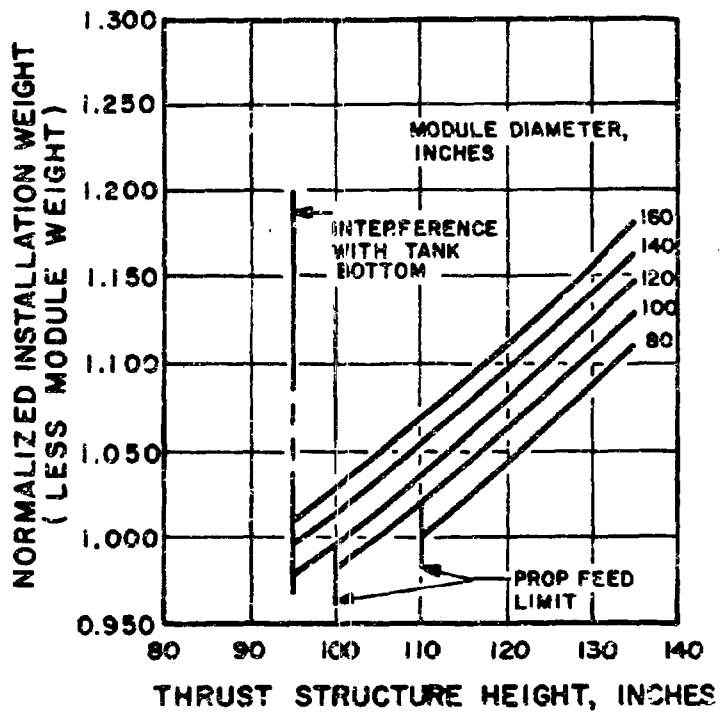

Figure 50. Normalized Installation Weight Variation With Thrust Structure Height, Case 5

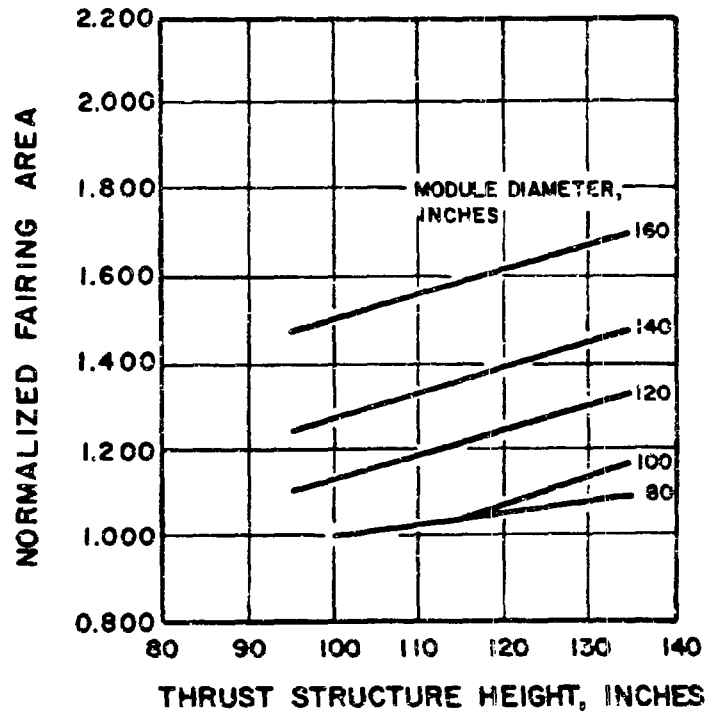

Figure 51. Normalized Fairing Area Variation With Thrust Structure Height, Case 5

CASE 6, 350K

RECOVERABLE SECOND STAGE, TANDEM

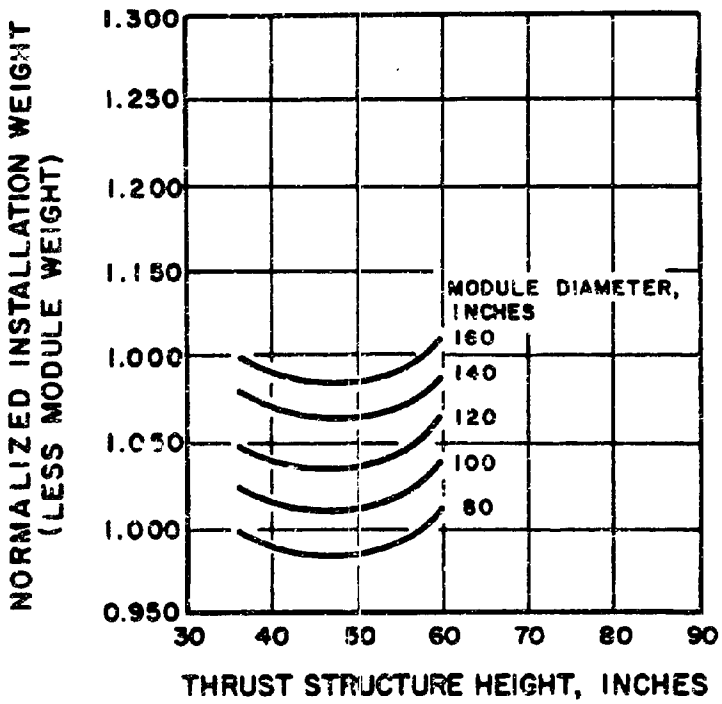

Figure 52 . Normalized Installation Weight Variation With Thrust Structure Height, Case 6

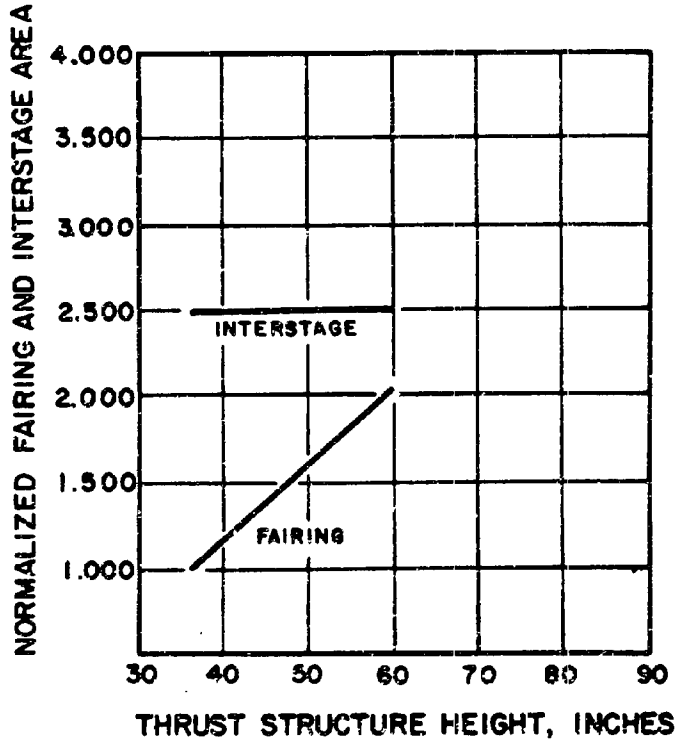

Figure 53. Normalized Fairing and Interstage Areas Variation With Thrust Structure Height, Case 6

advanced light-weight, high-performance system. This system uses four low-temperature multiple thrust uncooled combustors located one in each of four quadrants in the inner body at the plane of TVC injection.

Combustor nominal design parameters are:

Chamber Pressure, psia	1200
Mixture Ratio, o/f	1:1
Characteristic Velocity, ft/sec	6840
Total Flowrate, lb/sec	31.6
Total Throat Area, sq in.	5.60
L*, inches	25

(C) Comparison of this selected design in the Case 2 installation (potentially the vehicle most complementary to an aerospike module utilizing SITVC) with a mechanically gimbaled installation resulted in an engine weight increase, an interstage area reduction, a vehicle thrust structure weight decrease and a resulting performance index loss with the SITVC design. Listed below are the differences in module weight, installation weight, and interstage area brought about by using a SITVC system in lieu of mechanical gimbaling for Case 2, 250K.

Engine Module Weight, pounds	+19
TVC System, pounds	-173
Injectant and Tank Weight, pounds	+1468
Vehicle Thrust Structure, pounds	-114
Propellant Feed System, pounds	-210
Net Weight Differential, pounds	+990
Interstage Area, sq ft	-68

(2) Performance Index Analysis

(C) The performance index has been used as the resultant figure of merit in evaluating engine modules for use in the advanced vehicles. The diversity of stage concepts necessitates individual parametric optimization before selection of a common module. The optimization of the individual cases was performed in accordance with the ground rules and procedures detailed in the Application Packages. One of the inputs, the engine/vehicle installation weight data, was refined during this report period. Based on these data, performance index values for the 250K cases were recalculated. In the determination of the individual optima, only the nominal mixture ratio (6:1) was used. Previous study has indicated that operating mixture ratio does not significantly affect the optimum operating parameters.

(C) The normalized performance of the six 350K vehicle cases are presented parametrically in Fig. 54 through 65. In general, the lower-stage vehicles tend to optimize at higher chamber pressure and lower module diameter than the upper-stage cases. It is noted that the optimum chamber pressures, as was the case for the 250K vehicles previously reported in AFRPL-TR-66-348, are $\leq$ 2000 psia. It is also noted that the reusable vehicles optimize at lower chamber pressures than the expendable.

(C) The effects of mixture ratio on the performance index of the six 350K cases are shown in Fig. 54 through 65. The data presented here are for 1500-psia chamber pressure, but the general trends are represented for the total range of chamber pressure of interest. Of particular importance is the fact that the peak performing mixture ratio for all vehicles occurs near a mixture ratio of 6:1.

(U) The new parametric performance data for the 250K vehicle cases (with installation changes discussed in preceeding section) indicate the same basic trends regarding the optimum chamber pressure and module diameter as that previously reported. The significant difference is an increase in performance index over that previously reported. The percent performance index increase obtained for each of the 250K vehicles is:

Vehicle	Performance Index Increase, Percent
1	1.74
2	4.23
3	10.27
4	4.93
5	2.72
6	5.58

(U) The versatility of an engine concept can be measured by its adaptability to widely different stage designs without suffering significant performance loss as compared to the case where each stage employs its individual optimum engine. The aerospike engine with its inherent altitude compensation can be designed to power all six vehicle cases with minimum losses and no differences in hardware (one engine for the six 250K vehicle cases and another for the six 350K vehicle cases). In the selection, an average relative performance index was defined as follows:

$$W'_X = \frac{1}{N} \sum_{i=1}^{N} W'_{X_i}, \quad i = 1,2,---N$$

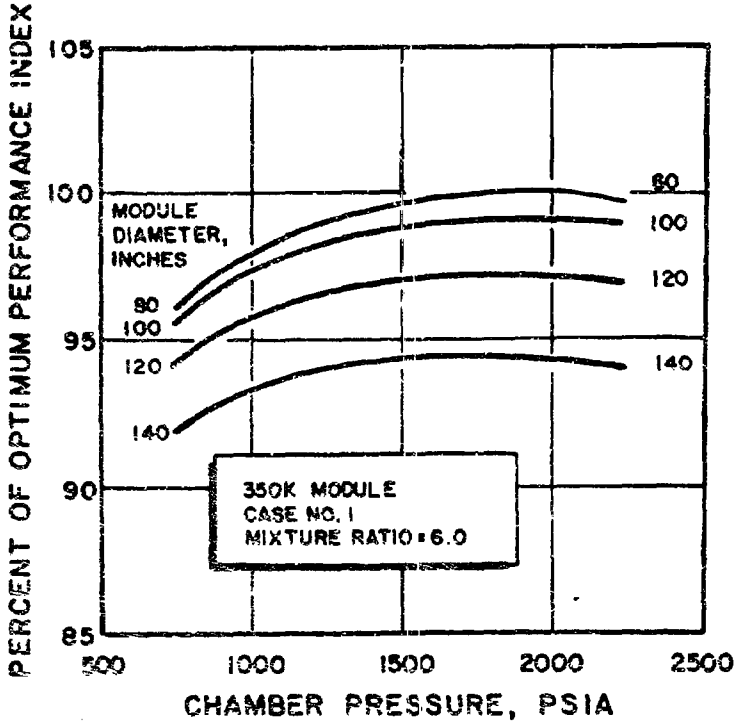

Figure 54. Chamber Pressure Optimization, Case 1

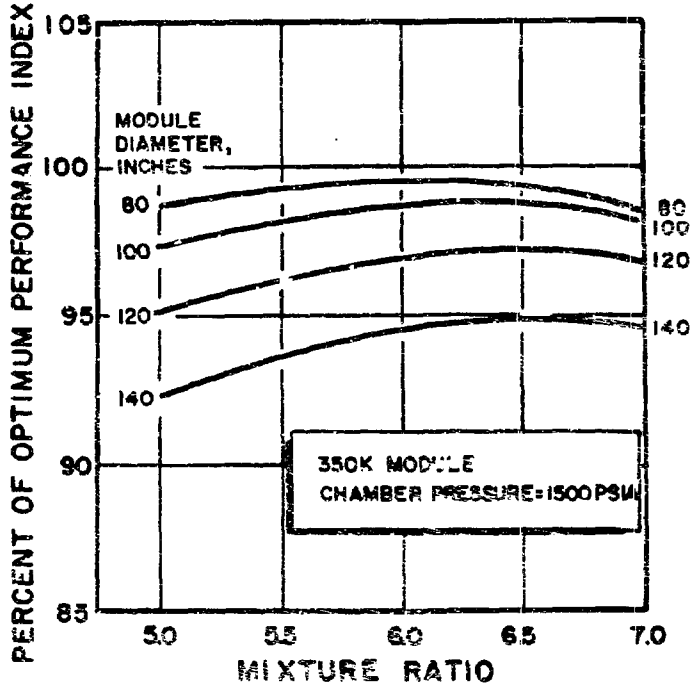

Figure 55. Mixture Ratio Optimization, Case 1

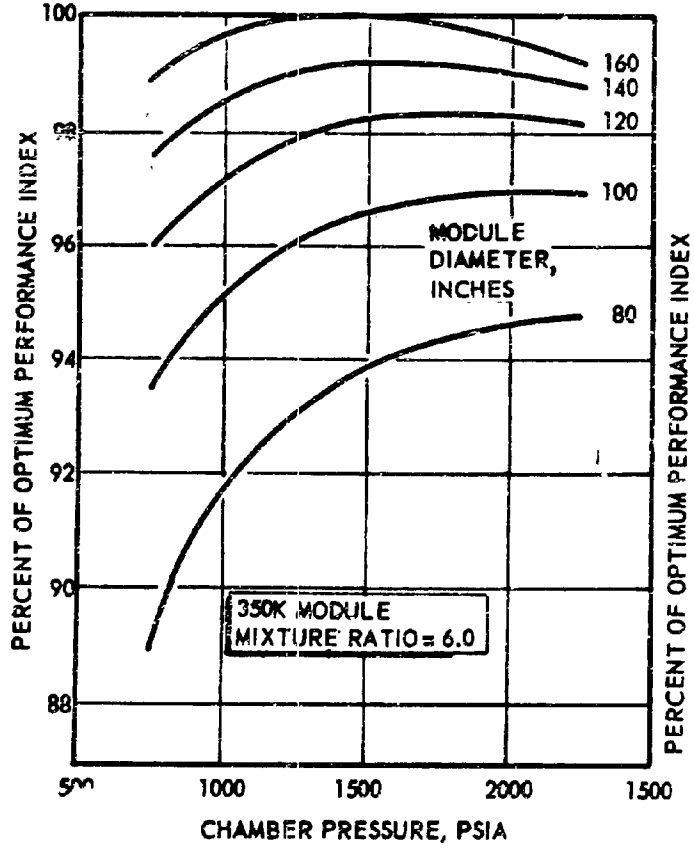

Figure 56. Chamber Pressure Optimization, Case 2

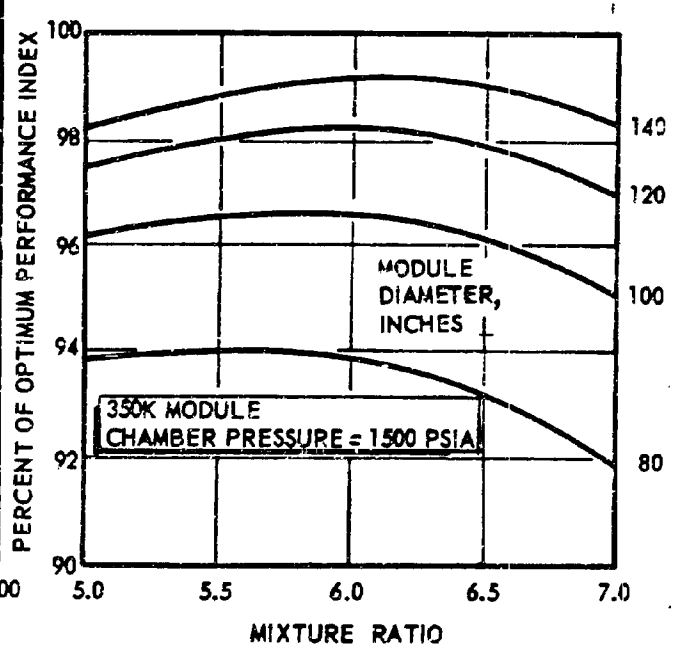

Figure 57. Mixture Ratio Optimization, Case 2

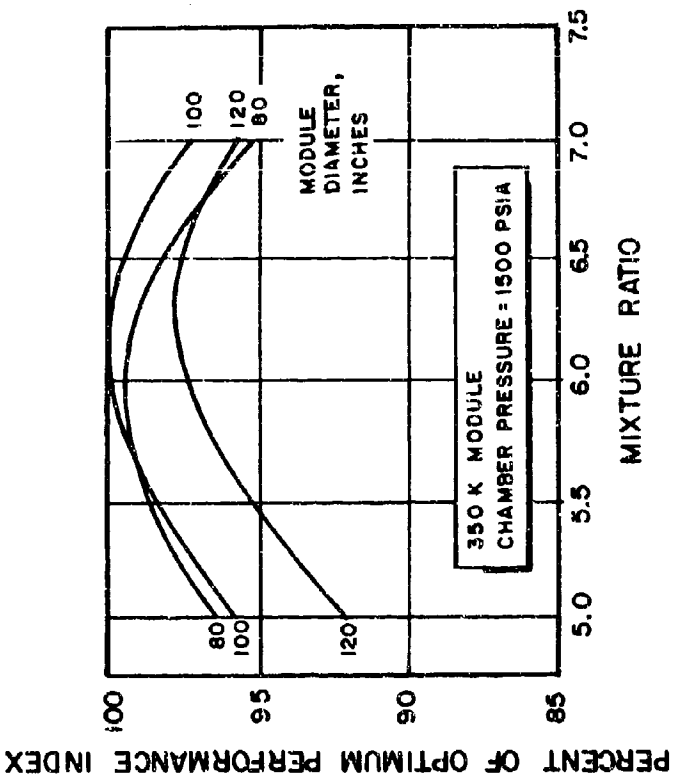

Figure 59. Mixture Ratio Optimization, Case 3

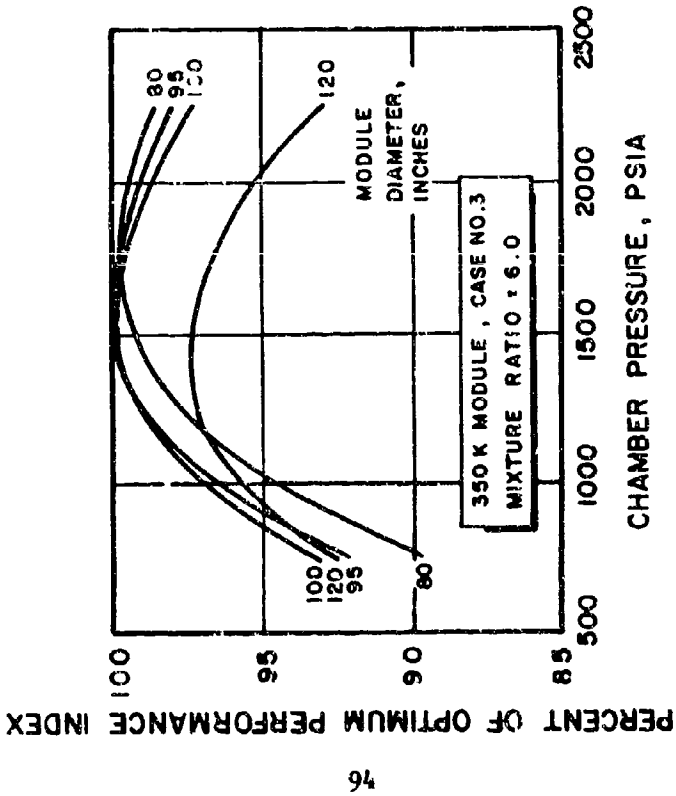

Figure 58. Chamber Pressure Optimization, Case 3

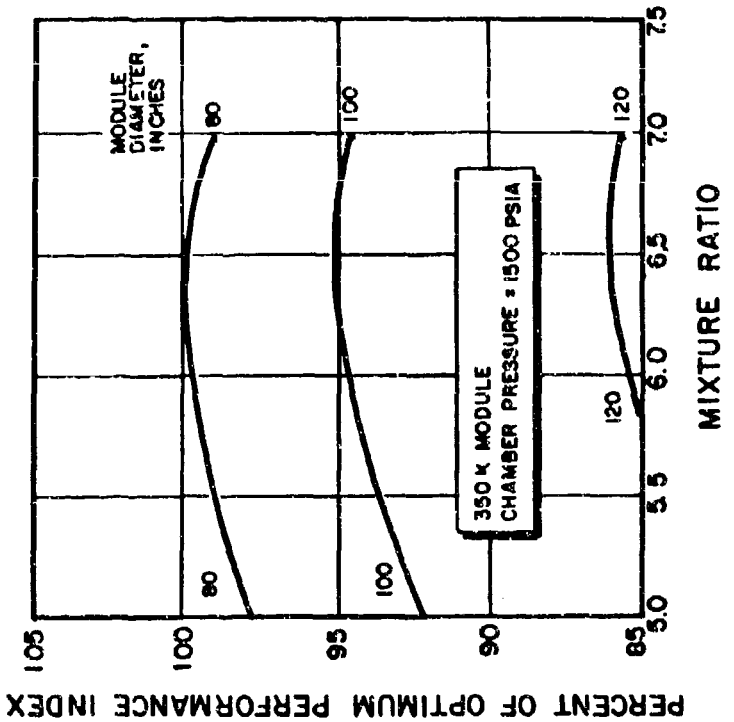

Figure 61. Mixture Ratio Optimization, Case 4

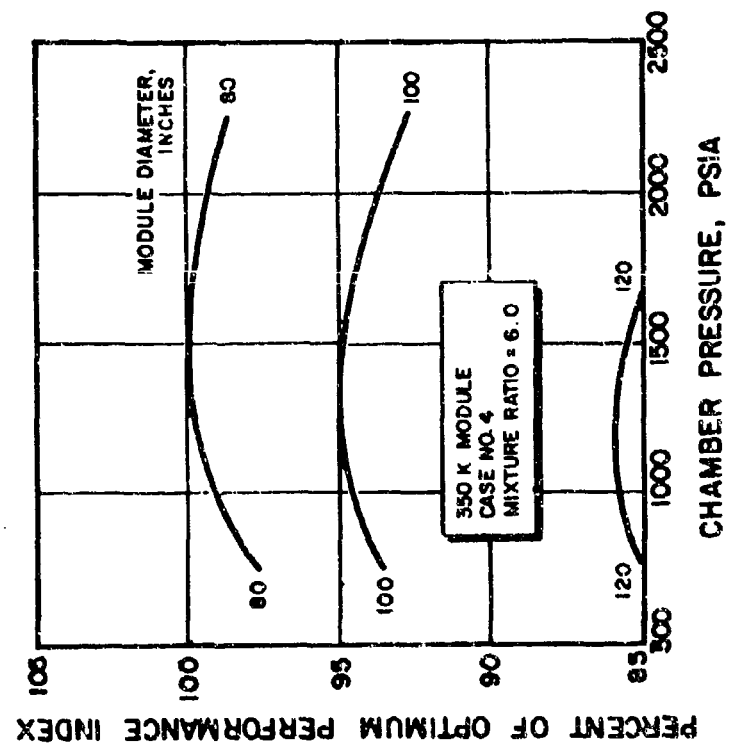

Figure 60. Chamber Pressure Optimization, Case 4

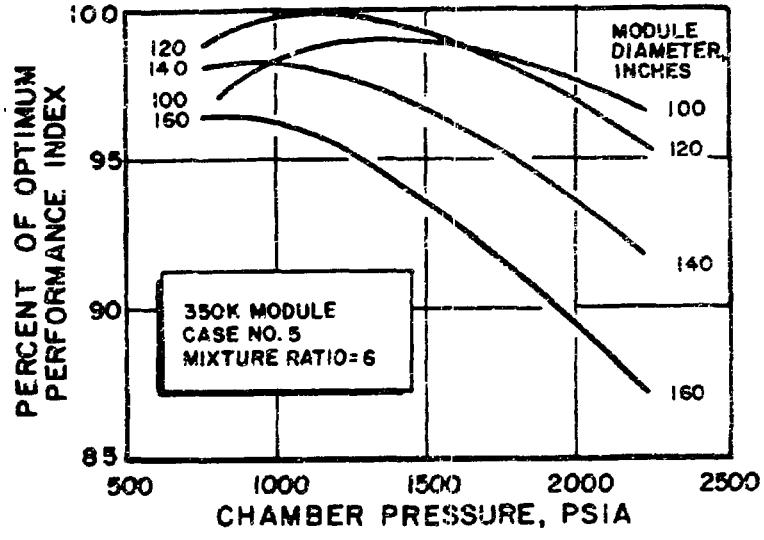

Figure 62. Chamber Pressure Optimization, Case 5

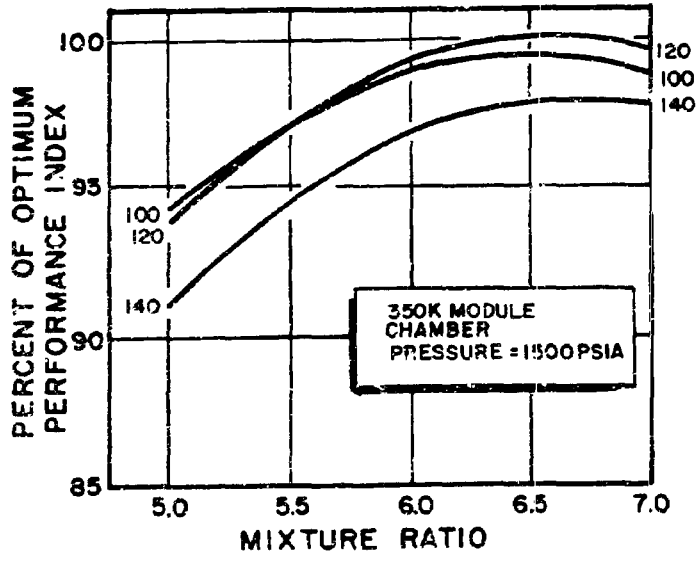

Figure 63. Mixture Ratio Optimization, Case 5

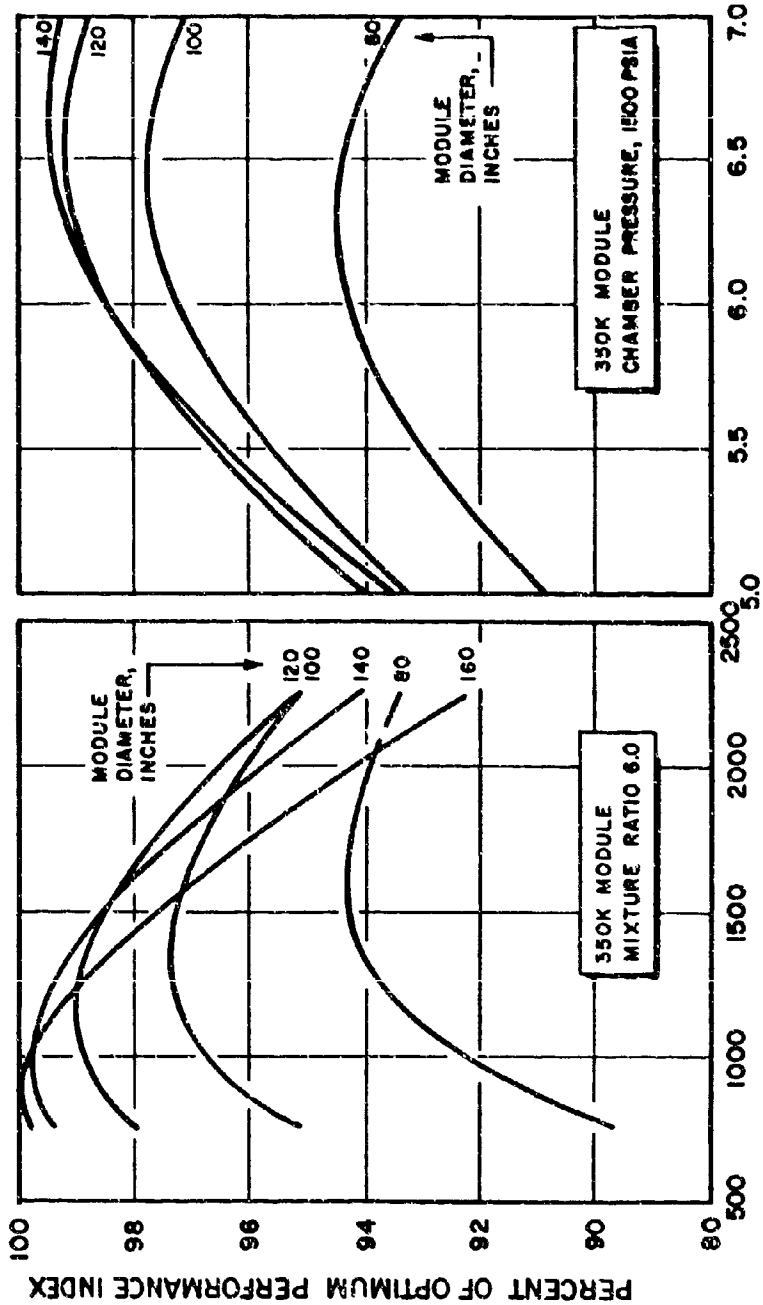

Figure 64. Chamber Pressure Optimization, Case 6

Figure 65. Mixture Ratio Optimization, Case 6

where W_X' = the normalized or relative performance index, or the percent of optimum performance index value obtainable within the ranges of parameters studied

N = number of relative performance indices

(C) To determine the common module for the six vehicle cases, a graphical maximization of W_X' was performed. The resulting best common module for the 250K vehicle cases was determined to be a configuration which has an operating chamber pressure of 1500 psia and a module diameter of 80 inches. The operating chamber pressure of the resulting common module for the 350K is 1500 psia and its diameter is 100 inches. The average relative performance index of these common modules was found to be approximately the same, 97.7 percent. Considering the wide differences in design concepts among the six stages for each of the two thrust levels, this is an indication of the versatility of the aerospike engine concept.

(C) Perturbation analysis has been initiated based on the recommended common module design for the 250K vehicle cases only. The purpose of the analysis is to evaluate the advantages, if any, of several operational and design alternatives, by comparing their effect on the performance index values with the basic plan. In this report, only one of several investigations, the comparison of the constant chamber pressure design and constant vacuum thrust design is included. The constant chamber pressure design requires that the module chamber pressure be held constant when the mixture ratio is varied from its nominal value of 6. The constant thrust design, on the other hand, dictates a constant vacuum thrust during the mixture ratio excursion. Figures 66 and 67 depict the effect of mixture ratio on performance index for modules designed with constant chamber pressure and constant vacuum thrust. The results indicate that when the constant thrust design is used (1) optimum mixture ratio shifts slightly to the lower mixture ratio end of the scale, (2) there is no noticeable change in the values of the maximum performance index, and (3) the optimum operating parameters remain essentially unaffected. The conclusion drawn is that the constant chamber pressure control capability results in a mixture ratio optimization more complementary to vehicle size.

c. Problem Areas and Solutions

(U) No significant problems were encountered in the application study during this period.

d. Summary of Planned Effort

(U) The application study will be completed early in the next quarter and a special report prepared presenting the results.

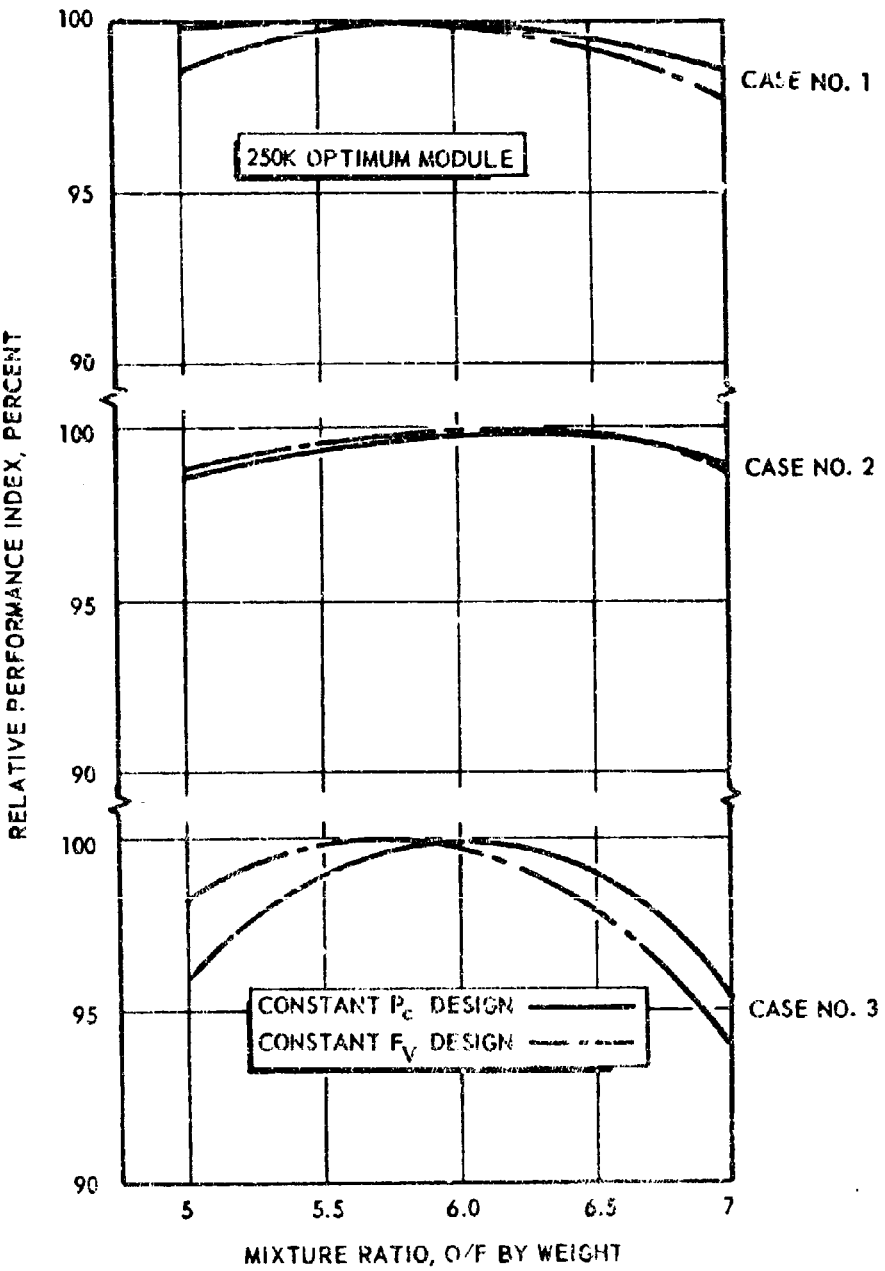

Figure 56. Comparison of Effect of Mixture Ratio on Optimum Performance, Cases 1 Through 3

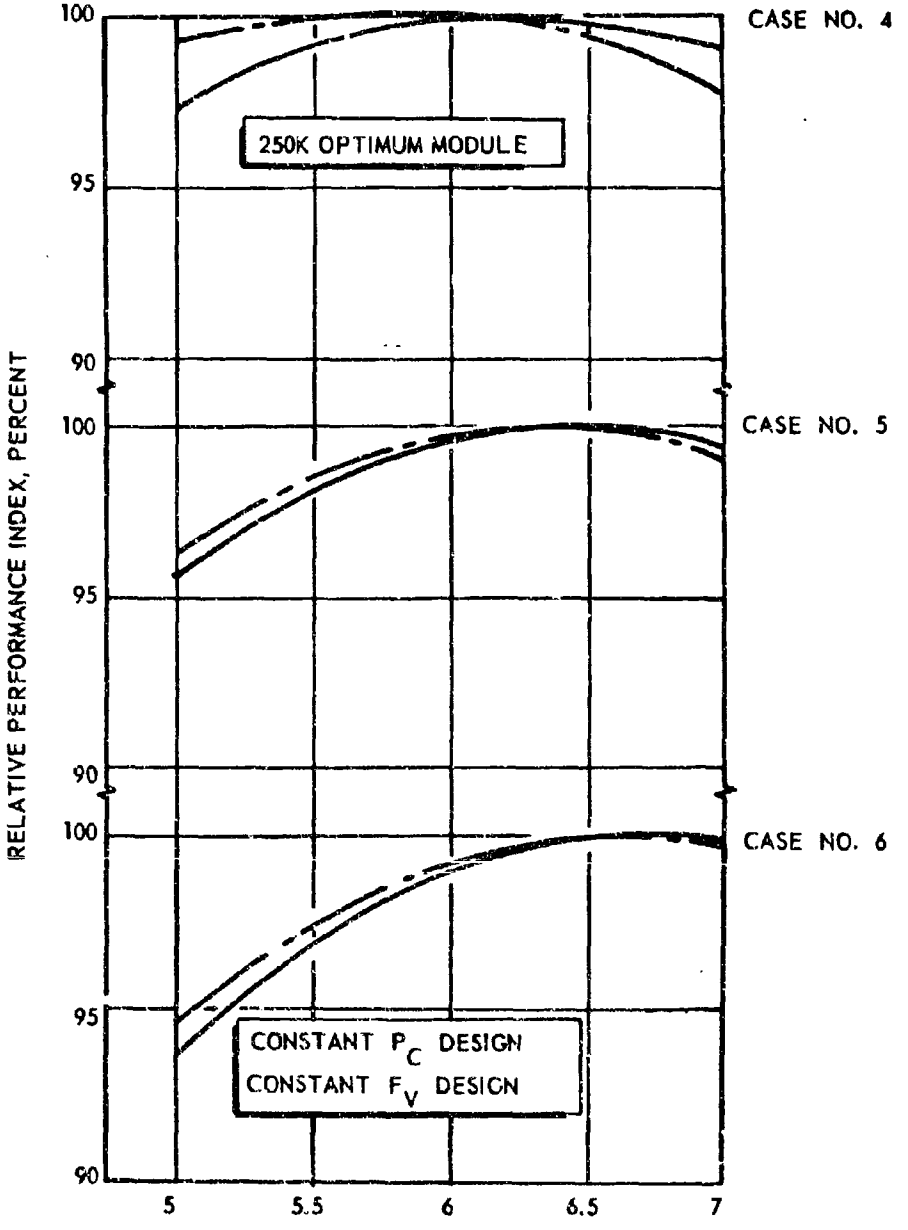

Figure 67 . Comparison of Effect of Mixture Ratio on Optimum Performance, Cases 4 through 6

B. TASK 2, FABRICATION AND TEST

1. INJECTOR PERFORMANCE INVESTIGATION, 2.5K SOLID-WALL SEGMENTS

(C) The 2.5K segment injector investigation effort was designed to utilize the segmentation potential of the Aerospike thrust chamber for the development of candidate injector patterns for the 250K injector with the experimental objectives of: (1) selecting an injector design that delivers characteristic velocity efficiency in excess of 0.96 over the operating range, (2) determining thrust chamber heat transfer characteristics, (3) developing a gas tapoff system that yields gases suitable for use as a turbine working fluid, (4) evaluating injector durability, and (5) determining injector stability.

a. Status

(U) This subtask had been successfully completed in the last quarter except for analysis of certain tapoff data. A final tabulation of performance results has been prepared for this report, completing all aspects of the effort.

b. Progress During the Report Period

(U) The objectives of the test effort were quite varied and several different techniques were required to complete the data analysis. The hardware had heat transfer limitations which imposed definite restrictions on the manner of testing. For example, these tests were conducted with water-cooled copper hardware which had a theoretical burnout heat flux of 55 Btu/in.^{2}-sec. Engineering judgment required that the experimental peak heat flux should be minimized to a value substantially less than the theoretical maximum. Consequently, testing at chamber pressures greater than 900 psia was accomplished by the use of gaseous hydrogen as film coolant in the converging portion of the nozzle. Injector performance in this thrust chamber was evaluated for tests with water-cooled hardware, film-cooled hardware, and gas-tapoff hardware. In each of the aforementioned cases, the data technique was developed such that the physics of each situation were properly described. The data reduction techniques for the water-cooled tests are based upon conventional methods and have been previously reported in Ref. 1 and 2.

(U) Those tests wherein gaseous hydrogen was used as a film coolant were analyzed by application of an energy balance technique, reported in Ref. 3, and checked by several tests which operated both with and without film coolant. Gas-tapoff test data reduction was accomplished by use of a mass-energy balance technique as given in Ref. 2.

(U) The manner of presentation of the results logically follows the experimental techniques in use for the various tests and objectives. Therefore, complete summary performance tables were prepared with the test objectives and techniques serving as guidelines.

c. Problem Areas and Solutions

(U) There were no problem areas encountered during this quarter.

d. Testing

(U) Testing was completed in the last quarter. A listing of all tests performed and associated with this task along with injector line design description is given in Appendix B. This listing provides a complete compilation of the testing effort with basic thrust chamber operational parameters. A tabulation of performance results for water-cooled chamber tests, film-cooled tests, and gas-tapoff tests is presented in this section. These results were initially presented and analyzed in earlier quarterly reports. A summary of performance during high chamber pressure operation is shown in Fig. 68

(U) Table 3 provides a listing wherein only water cooling was utilized. Performance and heat transfer results are given.

(U) Table 4 is a listing of test results for those tests where gaseous hydrogen film coolant was employed. Also indicated are several key tests performed to check the analytical techniques, wherein the film coolant was shut off during the tests to provide characteristic velocity c* data with and without film cooling. As seen, the analytical technique was quite accurate. Also of interest is the fact that the ADP combustor configuration always incurred a substantial performance reduction with the injection of film cooling.

(C) Table 5 summarizes the results from the gas-tapoff testing. As reported in Ref. 2, the final c* efficiencies shown have been determined by fully accounting for gas-tapoff flowrates and resultant combustion mixture ratio shifts. It is seen that thrust chamber operation covered the range of chamber pressures from 274 to 1581 psia and mixture ratios from 3.31 to 9.71 with the bulk of the tests at mixture ratios ranging from 4.0 to 7.0. Eight injectors with a total of 26 modifications were tested in the ADP effort. These modifications were made to optimize injector design and provide fuel bias for gas tapoff.

e. Summary of Planned Effort

(U) There is no further planned effort on this subtask.

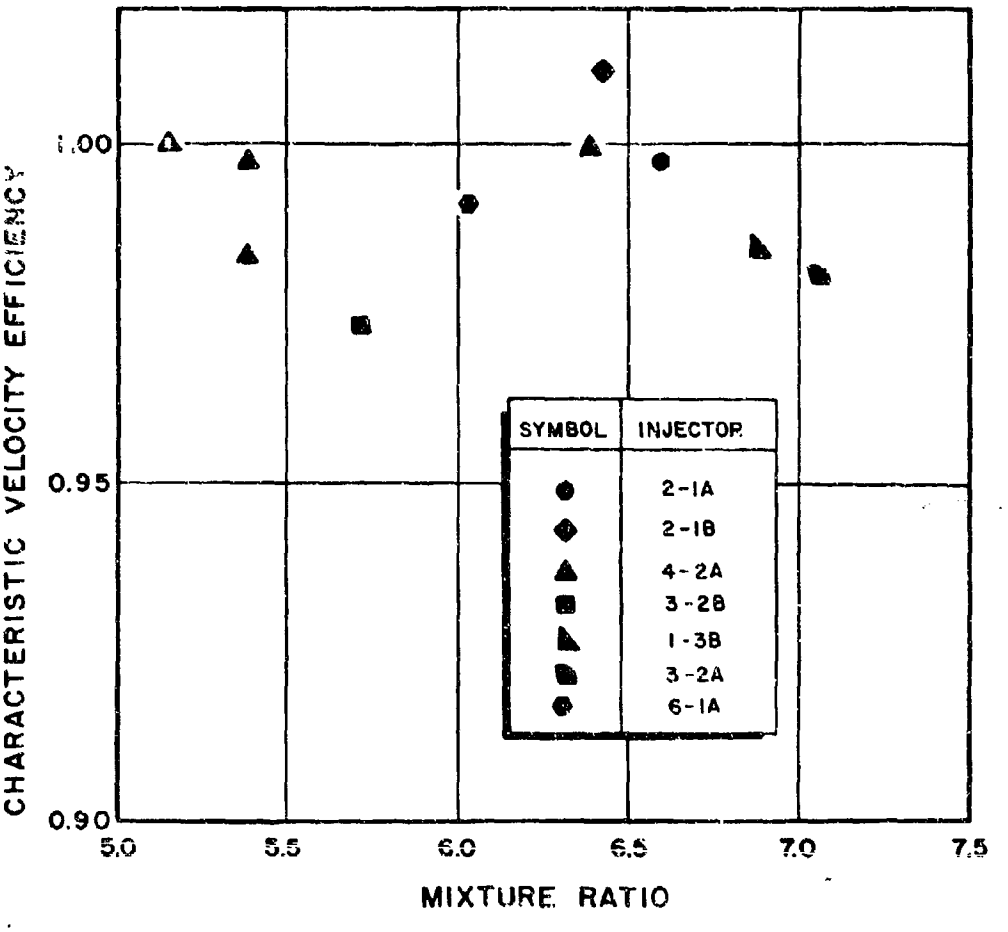

Figure 68. Characteristic Velocity Efficiency Over the Mixture Ratio Range for Chamber Pressures From 900 to 1505 psia

TABLE 3

SUMMARY OF 2.5K WATER-COOLED THRUST CHAMBER PERFORMANCE TESTS

Run Number	Test Date, 1966	Injector Number	Duration, seconds	Throat Area, sq. in.	Thrust, pounds	Chamber Pressure, psia	Mixture Ratio, o/f	Total Weight Flowrate, lb/sec	ΔP Fuel	ΔP Oxidizer	c^*_{tp}	$\theta_{c^*_{tp}}$	c^*_{fl}	$\eta_{c^*_{tp}}$	Throat Heat Flux, Btu/sq. in.-sec	Comments
027	5-21	2-1A	5.7	0.990	937	641	7.81	2.638	233	33	7553	0.989	7788	1.038	30.1	Related program
028	5-23	2-1A	5.9	0.990	1415	971	6.50	4.054	348	175	7535	0.998	7500	0.994	58.5	Related program
029	5-23	2-1A	5.7	0.990	420	306	5.04	1.223	154	9	7750	0.989	7666	1.000	14.4	Related program
031	5-27	4-1A	0.6	0.990	1450	1564	5.71	3.123	ND	ND						Injector erosion
032	5-31	1-2A	0.6	0.990	1450	1614	7.78	6.859	ND	ND						Bomb test
033	6-6	2-1B	4.3	0.990	806	630	5.91	2.545	ND	39	7695	1.000	7716	1.003	25.8	
034	6-6	2-1B	4.3	0.990	1327	974	6.45	3.947	ND	118	7662	1.012	7573	0.988	42.7	
035	6-6	2-1B	1.0	0.990	459	345	5.85	1.340	ND	8	7531	0.979	7688	1.000	15.7	
036	6-6	4-1A	4.3	0.990	1710	1189	6.38	4.956	ND	ND						Coolant leak into thrust chamber
037	6-6															Nozzle throat eroded
038	6-16	2-1D	4.3	0.990	446	334	5.79	1.394	86	16	7573	0.983	7677	0.998	13.2	
039	6-16	2-1D	4.4	0.990	915	680	6.07	2.755	127	55	7696	1.002	7560	0.984	33.1	
040	6-16	2-1D	4.3	0.990	933	665	5.94	2.749	124	54	7677	0.996	7558	0.983	32.9	
041	6-16	2-1D	4.3	0.990	920	658	5.80	2.653	120	54	7659	0.995	7660	0.979	31.4	
050	6-21	2-1E	4.2	0.965	427	326	5.58	1.304	57	15	7525	0.980	7595	0.994	13.9	
051	6-21	2-1E	4.3	0.965	909	653	5.62	2.599	121	55	7879	0.988	7654	0.985	43.2	
052	6-21	2-1E	4.3	0.965	911	658	5.67	2.631	123	55	7648	0.984	7579	0.975	25.7	
053	6-23	2-1E	4.2	0.965	418	318	5.31	1.254	61	12	7736	0.994	7693	0.989	12.5	
054	6-23	2-1E	4.3	0.965	672	495	5.79	1.970	86	30	7665	0.994	7547	0.982	21.1	
055	6-23	2-1E	4.3	0.965	898	654	5.90	2.666	116	52	7525	0.977	7592	0.994	27.4	
056-057																Injector strip-to-land separation, burn induced by brare failure
072	7-5	1-3A	4.0	0.950	745	544	6.84	2.270	128	53	7270	0.979	7205	0.971	33.8	
073	7-5	1-3A	4.3	0.950	1062	779	5.70	3.034	234	95	7595	0.977	7452	0.960	55.0	
074	7-5	1-3A	4.3	0.950	1057	773	5.15	2.992	243	88	7058	1.003	7383	0.995	41.9	
075	7-6	1-3A	NM	NM	NM	NM	NM	NM	NM	NM						Nozzle throat eroded
076	7-8	1-3B	4.4	0.950	820	634	5.64	2.522	174	64	7567	0.975	7583	0.977	24.1	
077	7-14	1-3B	4.4	0.950	886	647	5.88	2.602	172	65	7577	0.999	7435	0.984	28.9	
078	7-14	1-3B	4.4	0.950	845	621	5.79	2.488	174	58	7527	0.987	7511	0.993	26.6	
079	7-12	1-3B	14.3	0.940	1079	779	6.11	3.094	196	91	7500	0.980	7358	0.988	26.8	
080	7-12	1-3B	14.3	0.940	1061	760	6.21	3.055	183	83	7484	0.982	7557	0.999	32.0	
081	7-13	3-2A	0.5	OP	1906	1514	7.05	6.614	ND	ND						Uncooled hardware
082	7-15	3-2A	12.7	0.950	1111	805	6.52	3.172	260	37	7570	1.004	7540	1.000	35.5	
083-104																Facility malfunction
105	10-20	6-1A	3.6	0.970	444	347	4.74	1.350	66	12	7887	0.990	NT	NT		
106	10-20	6-1A	3.8	0.970	446	344	4.78	1.318	68	12	8004	0.999	NT	NT		

NOTES: ND - No data; NM - Main stage not achieved extensive nozzle damage due to erosion; OP - Orifice plate nozzle eroded

TABLE 4

SUMMARY OF 2.5K FILM-COOLED THRUST CHAMBER PERFORMANCE

Run Number	Test Date, 1966	Injector Number	Duration, seconds	Throat Area sq in.	Thrust, pounds	Chamber Pressure, psia	Mixture Ratio, o/f	Total Weight Flowrate, lb/sec	ΔP Fuel	ΔP Oxidizer	% Film Coolant / Total	η_{c^*} (By Heat Balance)	η_{c^*} (After Film Coolant Shutoff)	η_{c^*} (With Film Coolant Flowing)	Throat Heat Flux, Btu/in.^{2}-sec	Comments
100	8-2	1-3B	ND	ND	ND	ND	ND	ND	ND	ND	ND					
101	8-2	1-3B	3.4	0.950	982	720	5.28[a]	2.556	187	55					7.6	Coolant water leak into combustion chamber
102	8-2	1-3B	3.5	0.950	1385	1004	4.94[a]	3.401	277	101					14.2	Coolant water leak into combustion chamber
103	8-2	1-3B	3.5	0.950	1617	1169	5.16[a]	4.052	315	150					16.4	Coolant water leak into combustion chamber
104	8-5	1-3B	3.6	ER	1902	1394	5.81[a]	4.584	ND	ND						Nozzle throat eroded
105	8-5	1-3B	3.5	0.950	2105	1494	6.89[a]	6.001[b]	288	293	0.073	0.985			20.0	
106	8-5	5-2A	3.2	0.950	2139	1505	7.07[a]	6.152[b]	441	214	0.072	0.981			23.2	
107	8-9	4-1B	3.5	0.950	2151	1504	8.05[a]	6.474[b]	251	163	0.062	0.965		0.884	20.4	
108	8-9	4-1B	2.7	0.950	1022	741	6.19[a]	3.066[b]	175	40	0.052	0.913	0.907	0.870	30.6	
109	8-9	5-1A	4.6	0.950	527	385	5.74[a]	1.696[b]	134	33	0.078	0.912	0.899	0.820	20.7	Data pertinent to ADP program, related program
110	8-9	5-1A	0.8	0.950	2176	1491	6.87[a]	6.135[b]	330	405	0.074	0.955		0.892	20.7	Data pertinent to ADP program, related program
111	8-12	3-2A	4.9	0.970	390	294	4.55[a]	1.289[b]	174	6	0.105	0.979	0.969	0.959	17.4	
112	8-12	3-2A	4.8	0.970	496	364	5.34[a]	1.569[b]	135	8	0.097		0.977		19.4	
113	8-12	3-2A	4.6	0.970	1378	969	6.68[a]	3.992[b]	337	58	0.061	0.977		0.939	QN	
114	8-12	3-2A	3.4	0.970	1340	946	6.11[a]	3.769[b]	331	56	0.034	0.988		0.958	QN	
115	8-12	3-2A	3.4	ER	2308	1762	8.13[a]	6.762[b]	401	237	0.054				QN	Nozzle throat eroded
116	8-17	2-2A	ND	0.970	ND	ND	ND	ND	ND	ND	ND					Igniter malfunction
117	8-19	3-2A	3.9	0.925	860	630[c]	5.12[a]	2.583[b]	274	26	0.077	0.957	0.977	0.944	QN	
118	8-19	3-2A	3.9	0.925	874	650	6.93[a]	2.811[b]	192	31	0.069	0.986	0.981	0.939	QN	
119	8-19	3-2A	4.5	0.925	411	324	5.90[a]	1.263[b]	147	2	0.116	0.944	0.943	0.916	QN	
120	8-19	3-2A	4.5	0.925	598	437	5.03[a]	1.213[b]	106	3	0.124	0.979	0.974	0.925	QN	
121	8-23	3-2B	3.5	0.925	887	666	5.24[a]	2.526[b]	145	27	0.080	0.953	0.976	0.935	QN	
122	8-23	3-2B	2.9	0.925	1012	1046	5.72[a]	3.973[b]	178	77	0.097	0.973	ND	0.936	QN	
123	8-24	4-2A	3.0	0.925	838	633	5.12[a]	2.320[b]	145	41	0.074	1.004	0.990		QN	
124	8-24	4-2A	3.8	0.925	810	614	4.88[a]	2.214[b]	150	42	0.085	1.002	0.997		QN	
125	8-24	4-2A	2.7	0.925	1354	1005	5.39[a]	3.692[b]	201	103	0.109	0.998			QN	
126	8-24	4-2A	2.0	0.925	1782	1320	5.16[a]	4.881[b]	306	201	0.091	1.002			QN	
127	8-24	4-2A	2.6	0.925	2032	1496	6.39[a]	5.671[b]	265	280	0.077	1.002			QN	
128	8-26	4-2A	ND	0.925	ND	ND	ND	ND	ND	ND	ND					Sequence malfunction
129	8-26	4-2A	1.7	0.955	1231	982	5.39[a]	3.426	191	65			0.984		QN	
130	8-28	3-2B	1.7	0.955	1020	762	5.88[a]	2.999	170	53			0.975		QN	
197	10-20	6-1A	3.9	0.970	1316	950	5.58[a]	5.231[b]	163	61	ND					Film-coolant instrumentation error
198	10-24	6-1A	4.2	0.970	2208	1548	6.04[a]	6.171[b]	199	228	0.044	0.991			QN	
199	10-24	6-1A	4.2	0.970	1341	959	5.64[a]	3.858[b]	135	81	0.065	0.963			QN	

NOTES: ER = Nozzle throat eroded, throat area varied during test
ND = No data
QN = Heat flux not determined, data generally similar to previous film-cooled tests

a = Mixture ratio based on injector flowrates
b = Flowrate includes film-coolant flow
c = Indicated instrumentation error

CONFIDENTIAL

TABLE 5

2.5K WATER-COOLED THRUST CHAMBER GAS TAPOFF SUMMARY

Run No.	Test Date, 1958	Injector No.	Duration, seconds	Throat Area, sq in.	Thrust, pounds	Chamber Pressure, psia	MR, o/f	Weight Flowrate, lb/sec	ΔP Fuel	ΔP Oxidizer	Tapoff Weight Flowrate, lb/sec	Tapoff Temperature, F	η_{c*}	Comments
083	7-18	1-5B	1.2	0.940	360	271	4.61	1.120[a]	ND	ND				Data unstable, no tapoff temperatures or pressures
084	7-18	1-5B	0.8	0.940	369	285	5.96	1.419[a]	106	ND				
085	7-18	1-5B	1.4	0.940	400	304	6.16	1.457[a]	95	17				No tapoff temperatures or pressures
086	7-18	1-5B	1.4	0.940	572	440	5.22	1.860[a]	160	28				
087	7-18	1-5B	1.2	0.940	822	615	5.78	2.534[a]	169	60				
088	7-21	1-5B	1.5	0.940	410	317	5.87	1.575[a]	95	39				No tapoff pressure, tapoff temperature decayed during test
089	7-21	1-5B	1.3	0.940	650	609	5.32	2.489[a]	195	70				No tapoff pressure, tapoff temperature out of instrument range
090	7-22	1-5B	1.5	0.940	547	412	5.43	1.683[a]	127	37				No tapoff pressure, tapoff temperature decayed during test
091	7-22	1-5B	1.7	0.940	905	587	5.20	1.574[a]	128	28				No tapoff pressure
092	7-22	1-5B	1.8	0.940	679	506	5.63	2.104[a]	156	45				
093	7-27	1-5B	1.5	0.940	964	665	5.72	2.777[a]	195	87				
094	7-27	1-5B	1.4	0.940	929	678	6.96	2.744[a]	242	86				
095	7-27	1-5B	1.3	0.940	957	688	6.52	2.916[a]	171	104				
096	7-27	1-5B	1.4	0.940	924	668	5.74	2.818[a]	200	87				Tapoff temperatures out of instrument range, no tapoff pressure
097	7-29	1-5B	1.8	0.880	856	705	5.10	2.595[a]	194	77				
098	7-29	1-5B	1.8	0.880	856	698	4.52	2.565[a]	259	81				
099	7-29	1-5B	1.9	0.880	892	709	6.28	2.765[a]	158	105				
133	8-31	4-2A	2.2	0.925	401	326	4.53	1.368[a]	119	8				
134	8-31	4-2A	2.5	0.925	411	330	4.60	1.330[a]	120	8				Excessively low tapoff temperatures
135	8-31	4-2A	1.8	0.925	470	333	6.41	1.379[a]	ND	ND				
136	8-31	4-2A	2.4	0.925	1261	969	4.97	3.579[a]	257	62				
137	8-31	4-2A	2.6	0.925	1264	988	6.58	3.791[a]	152	72				
138	9-1	4-2B	1.7	0.925	460	324	5.43	1.370[a]	ND	ND				
139	9-1	4-2B	1.6	0.925	1259	966	5.23	3.670[a]	225	64				Tapoff temperatures greater than 2500 F
140	9-6	4-2C	1.9	0.925	490	334	5.52	1.382[a]	ND	ND				
141	9-6	4-2C	2.0	0.925	372	319	4.86	1.228[a]	73	10				
142	9-6	4-2C	1.6	0.925	373	335	4.45	1.145[a]	72	7				
143	9-6	4-2C	ND	0.925	ND	ND	ND	ND	ND	ND				
144	9-6	4-2C	1.8	0.925	448	326	4.68	1.387[a]	45	17				Tapoff temperatures out of instrument range
169	9-26	4-2C	3.5	0.925	442	324	4.14	1.164[a]	ND	ND		1015		
170	9-26	4-2C	1.3	0.925	415	341	5.45[d]	1.234[a]	50	5		1120		
171	9-26	4-2C	1.3	0.925	461	378	6.21[d]	1.361[a]	42	7	0.022	1350	0.976	
172	9-26	4-2C	1.3	0.925	613	645	7.39[d]	2.226[b]	94	23	0.039	1460	0.980	
173	9-26	4-2C	1.2	0.925	1100	871	6.70[d]	3.046[b]	70	54	0.053	1350	0.992	
174	9-26	4-2C	1.3	0.925	687	597	6.98[d]	1.446[b]	34	6	0.023	1475	0.971	

NOTE:

a - Flowrate includes gas tapoff flow
d - Mixture ratio based on injector flowrates
ND - no data

CONFIDENTIAL

CONFIDENTIAL

TABLE 5

(Concluded)

Run No.	Test Date, 1965	Injector No.	Duration, seconds	Throat Area, sq in.	Thrust, pounds	Chamber Pressure, psia	MR, o/f	Weight Flowrate, lb/sec	ΔP Fuel	ΔP Oxidizer	Tapoff Weight Flowrate, lb/sec	Tapoff Temperature, F	η_{c^*}	Comments
175	9-28	A-45	1.5	0.925	377	331	5.27[d]	1.142[a]	50	ND	0.018	1395	0.893	
176	9-29	A-35	2.5	0.925	377	331	5.07[d]	1.099[a]	48	ND	0.018	1520	0.926	
177	9-29	A-35	2.5	0.925	378	330	5.09[d]	1.097[a]	52	2	0.018	1440	0.904	
178	9-29	A-35	2.5	0.925	390	321	5.35[d]	1.170[a]	50	4	0.019	1600	0.958	
179	9-29	A-35	2.5	0.925	385	335	5.27[d]	1.300[a]	54	7	0.018	1480	0.950	
180	9-28	A-35	1.1	0.925	2005	1851	5.90[d]	5.460[a]	182	143	0.094	1705	0.940	
181	9-30	A-35	0.7	0.925	1977	1854	5.99[d]	5.447[a]	255	56	0.060	1700	0.824	
182	9-30	A-36	1.0	0.925	1697	1398	6.60[d]	4.037[a]	221	91	0.071	1760	0.991	
183	9-30	A-36	1.0	0.925	1805	1618	6.40[d]	4.695[a]	294	99	0.076	2010	0.962	
184	10-1	A-35	1.5	0.925	409	331	7.29[d]	1.018[a]	127	3	0.018	1915	1.040	
185	10-1	A-35	2.2	0.925	390	338	6.36[d]	0.949[a]	146	4				Injector rotated 180 degrees, tapoff thermocouples destroyed
200	10-26	A-18	1.4	0.980	371	295	4.05[d]	1.206[a]	82	14		1273		Oxidizer-rich tapoff
201	10-26	A-10	1.5	0.980	387	299	4.28[d]	1.243[a]	72	ND		1850		Oxidizer-rich tapoff
202	10-26	A-19	1.5	0.980	366	288	4.13[d]	1.212[a]	72	19		1040		Fuel-rich tapoff, c^* data not calculated due to unmetered hydrogen addition to tapoff
203	10-26	A-19	1.6	0.980	1275	868	5.94[d]	3.849[a]	143	110		1250		
204	10-26	A-19	1.6	0.980	1676	1295	7.00[d]	5.963[a]	184	280		1360		

NOTES:

a = flowrate includes gas tapoff flow
d = mixture ratio based on injector flowrates
ND = no data

CONFIDENTIAL

CONFIDENTIAL

2. THRUST CHAMBER COOLING INVESTIGATIONS, 2.5K TUBE-WALL SEGMENTS

(U) The thrust chamber cooling investigations were designed to provide data on the regenerative cooling limits of the Aerospike chamber, fatigue life capability, and operating point for cyclic life of 100 reuses and 10 hours between overhauls, and a selection of tube material to meet the operating requirements. The 2.5K tube-wall segments were designed to provide cooling data, and other pertinent data were provided through combined analytical and laboratory techniques.

a. Status

(C) The ADP test effort on the copper tube-wall segment encompassed seven successful hot firing tests over the pressure range of 540 to 1500 psia, terminating with a regeneratively cooled 1500-psia demonstration.

(U) Laboratory metallurgical work has been fully completed and reported in the earlier progress reports. Pertinent tube tester effort was continued and is reported herein. The subtask is now completed, except for continued analysis of related d ta.

b. Progress During the Report Period

(C) During this report period, all experimental testing and data analysis on this subtask was completed. The copper turbular segment test series was successfully accomplished with mainstage operation over the nominal chamber pressure range of 540 to 1500 psia. All the heat transfer data were reduced and found to compare favorably with previously obtained 2.5K copper solid-wall hardware. Additional tube tester data and analysis strongly supported the selection of nickel 200 as the candidate material for design requirements of 300 restarts.

c. Testing

(1) 2.5K Tube-Wall Segments

(C) Seven hot tests were conducted on the 2.5K copper tube-wall segment on the ADP test effort. The test series consisted of six mainstage tests between 540- and 1500-psig chamber pressure, plus an ignition checkout test. Inspection of the hardware after the test series revealed the copper tubes were in good condition. The performance was typical of that obtained on the solid-wall segment performance evaluation and is shown in Table 6 and 7.

(U) A summary of the test results is presented in Table 8 . These data were reviewed to define the heat transfer distribution of the tube-wall segment. The overall heat transfer characteristics (end point data) were well-behaved and showed that the heat transfer was of an expected turbulent nature (Fig. 69) throughout the chamber pressure range. Unfortunately, the local coolant bulk temperature measurements were not within

TABLE 6

2.5K COPPER TUBE-WALL SEGMENT PERFORMANCE DATA

Test No.	Chamber Pressure, psig	Mixture Ratio, o/f	$\dot{w}_{LO_2}$	$\dot{w}_{GH_2}$	η_{c^*}	Coolant Mixture Ratio*	Tube Condition
030	Ignition only						Excellent
031	540	4.70	1.87	0.398	0.953	3.00	Excellent
032	880	5.06	3.02	0.596	0.987	3.25	Excellent
033	600	4.80	1.95	0.408	1.025	2.00	Excellent
034	985	5.20	3.50	0.673	0.960	3.07	Excellent
035	1300	5.00	4.47	0.895	0.974	4.03	Excellent
036	1500	5.10	5.20	1.02	0.970	5.04	Excellent

*Contoured tube Mft = $\dot{w}_{LO_2}/\dot{w}_{GH_2}$ coolant per tube bundle

TABLE 7

2.5K COPPER SEGMENT ADP TEST SERIES

Test No.	Thrust Chamber					Contoured Tube				
	Chamber Pressure, psig	Mixture Ratio	$\dot{w}_{LO_2}$	$\dot{w}_{GH_2}$	η_{c^*}	Mixture Ratio	Δ T, F	Δ P, psi	Inlet Temperature, F	Inlet Pressure, psig
030	Ignition only									
031	540	4.70	1.87	0.398	0.953	3.00	133	230	-216	1980
032	880	5.06	3.02	0.596	0.987	3.23	136	430	-216	2220
033	600	4.80	1.95	0.408	1.025	2.00	117	420	-215	2175
034	985	5.20	3.30	0.673	0.960	3.07	145	540	-255	2220
035	1300	5.00	4.47	0.895	0.974	4.03	180	540	-255	2250
036	1500	5.10	5.20	1.02	0.970	5.04	210	530	-260	2180

NOTE: Contoured tube mixture ratio = $\dot{w}_{LO_2}/\dot{w}_{GH_2}$ coolant per tube bundle

CONFIDENTIAL

CONFIDENTIAL

TABLE 8

SUMMARY OF CYCLING TEST DATA

		Thrust Chamber				Contoured Tube				
Test No.	No. of Cycles	Chamber Pressure, psig	Mixture Ratio	$\dot{w}_{LO_2}$	$\dot{w}_{GH_2}$	Mixture Ratio	Δ T, F	Δ P, psi	Inlet Temperature, F	Inlet Pressure, psig
037	1	1540	5.25	5.30	1.01	4.90	205	320	-260	2230
038	3	1600	6.0	6.10	1.02	5.70	210	340	-252	2280
039	15	1500	5.05	5.20	1.03	5.0	215	333	-255	2235

NOTE: Test No. 038 data is for cycle No. 3
Test No. 039 data is for cycle No. 1

CONFIDENTIAL

CONFIDENTIAL

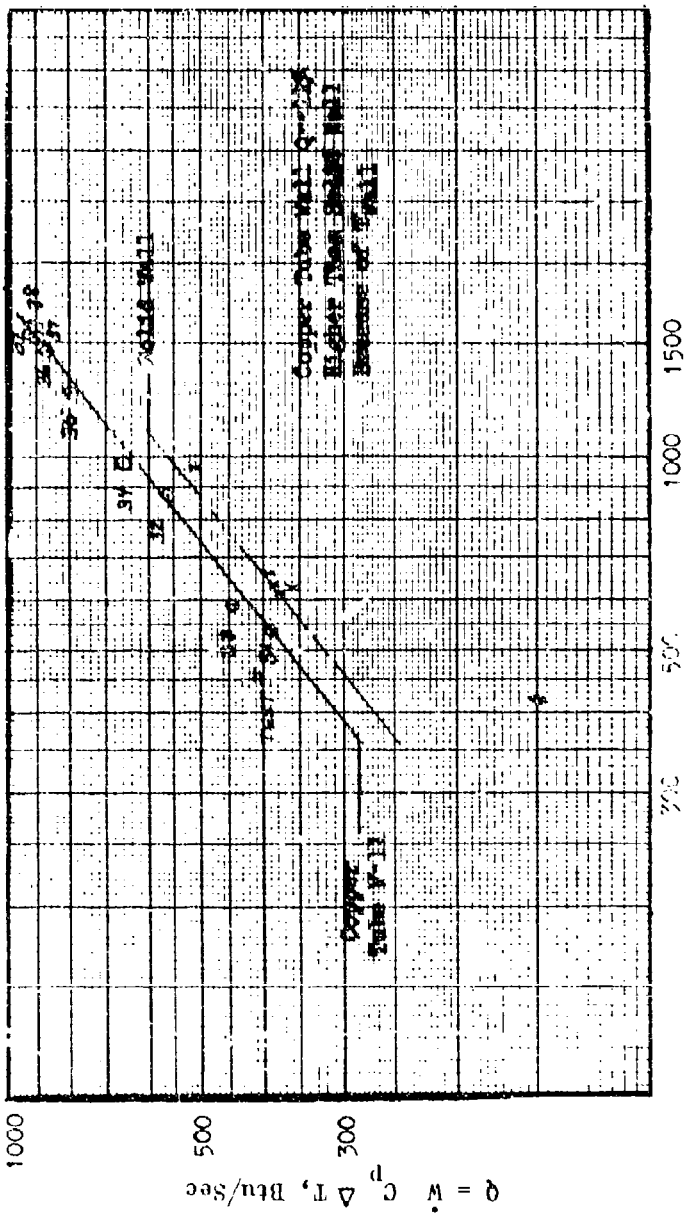

Figure 69. 2.7K ADP Copper Tube-Wall Overall Heat Transfer Characteristics

the required accuracy to assess the heat transfer distribution. Therefore, the solid-wall water-cooled data (Q_{local}) employing the same injector were reviewed. The ΣQ_{local} of solid-wall segment tests (Ref. 2) are compared with tube-wall Q_{total} in Fig. 69 . As noted in Fig. 69, a difference of approximately 11 percent between solid-wall and tube-wall data exists which is attributable to the difference in local gas-side wall operating temperatures. Using the established heat transfer distribution of the solid-wall segment, the local heat transfer distribution of the copper tube-wall chamber was determined and is shown in Fig. 70 . The associated gas-side tube-wall temperature profile, utilizing a maximum coolant curvature enhancement of 1.5, is also presented in Fig. 70 The data show that regenerative cooling capability was definitely determined.

(2) Tube Tester

(C) The electrically heated, hydrogen-cooled, thermal fatigue tube tester has been used to evaluate four 0.012-inch wall tubular specimens. The first two samples were cycled at a planned 1400 F wall temperature with penetrating crack failures occurring on both samples at 142 cycles. The failure mode was of multiaxial intergranular separations, resulting in coolant leaks where these separations penetrated the wall. Both of these specimens were of large grained material (1850 F braze temperature).

(C) Subsequent metallographic examination revealed no grain boundary contamination of the tube material. The overall failure mode was not of pure transverse crack nature; however, it is apparently still of a general fatigue nature which may be typical of high-temperature, low-cycle fatigue, where temperatures are well into the creep range of the material. The posttest metallurgical examination showed the presence of remelted braze alloy on the crown. These observations led to a suspicion that the actual peak tube-wall temperatures during the test were about 1700 to 1800 F. Fast-response microminiature thermocouples were obtained and installed on the next test series adjacent to the standard size thermocouples, lying parallel to the tube crown. In this manner, more surface contact area between the thermocouple and heated crown was obtained and the tube crown temperature was more accurately controlled.

(C) During the current report period, two specimens were tested: These specimens were designed to evaluate the effects of processing (i.e., enlarged grain size) on the fatigue life. One sample was purposely process annealed at 1800 F while the other was taken in the "as received" small grain condition. Both samples were hand brazed in the test fixture at a nominal 1200 to 1400 F temperature.

(C) At the start of the test, large differences in the recorded temperatures from the microminiature and standard size thermocouples were noted. The peak cyclic wall temperatures for the tests were therefore established using the indicated higher values (200 to 400 F higher) by the microminiatures. The cyclic wall temperatures were then programmed for 100 to 1400 F. Testing continued to 270 cycles for both specimens, with no tube failure. The test specimens were removed for inspection, which revealed that multiaxial microcracks were initiated, but none had penetrated the hot wall of

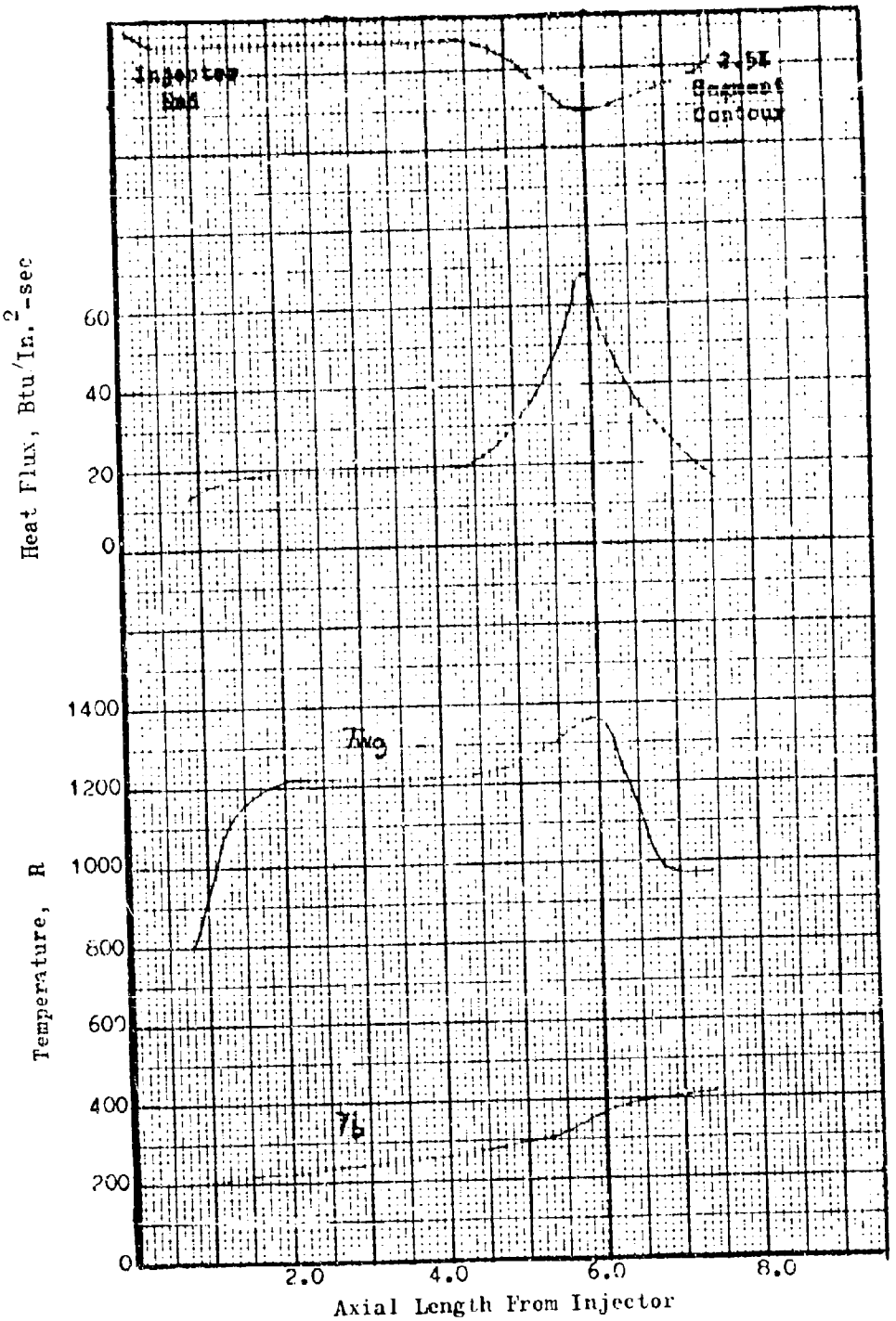

Figure 70. 2.5K Copper Tube-Wall Thrust Chamber Heat Transfer Distribution

the tube (Fig. 71). The higher temperature-processed specimen, however, had developed two microcracks in a colder portion of the tube adjacent to some large braze fillets. These cracks seem to be associated with the large braze fillets in some way. Metallographic examination revealed that these cracks are both of the transgranular and intergranular type.

(C) Subsequently, the small-grained specimen which had experienced 270 thermal cycles was reinstalled in the test apparatus and cycled to complete rupture. A total of 315 cycles was accumulated on this specimen. The large-grained specimen has had the cracked tube crown removed and patches installed. A total of 320 cycles was accumulated on this specimen when failure occurred in the patch area.

(U) Metallographic examination of the removed tube crowns, and also of the small-grained specimen, is in progress. The results of the tests to date are summarized in Table 9 . These results give strong support to the choice of nickel 200 to meet the ADP cyclic-life requirements. The unexpected multiaxial failure mode is under investigation.

TABLE 9

SPECIMEN TEST SUMMARY

Specimen Description	Cyclic Wall Temperature, F	Coolant Heat Flux Btu/in.^{2}-sec	Cycles to Failure	Type of Failure
Large Grained	1700 to 1800 (estimated)	30	142	Intergranular separation
Large Grained	1700 to 1800 (estimated)	30	142	Intergranular separation
Small Grained	1400 F	30	315	Under investigation
Large Grained	1400 F	30	320	Under investigation

(U) Although testing is complete on this program, future plans for related programs in Rocketdyne call for the testing of four additional specimens with higher wall-temperature gradients. Two of these tests will explore the effects of hydraulic stress on the fatigue life, while the remaining two tests will be used to obtain an indication of the effects of steady-state thermal cycling, in an effort to duplicate the H-1 type failures of pure transverse cracking.

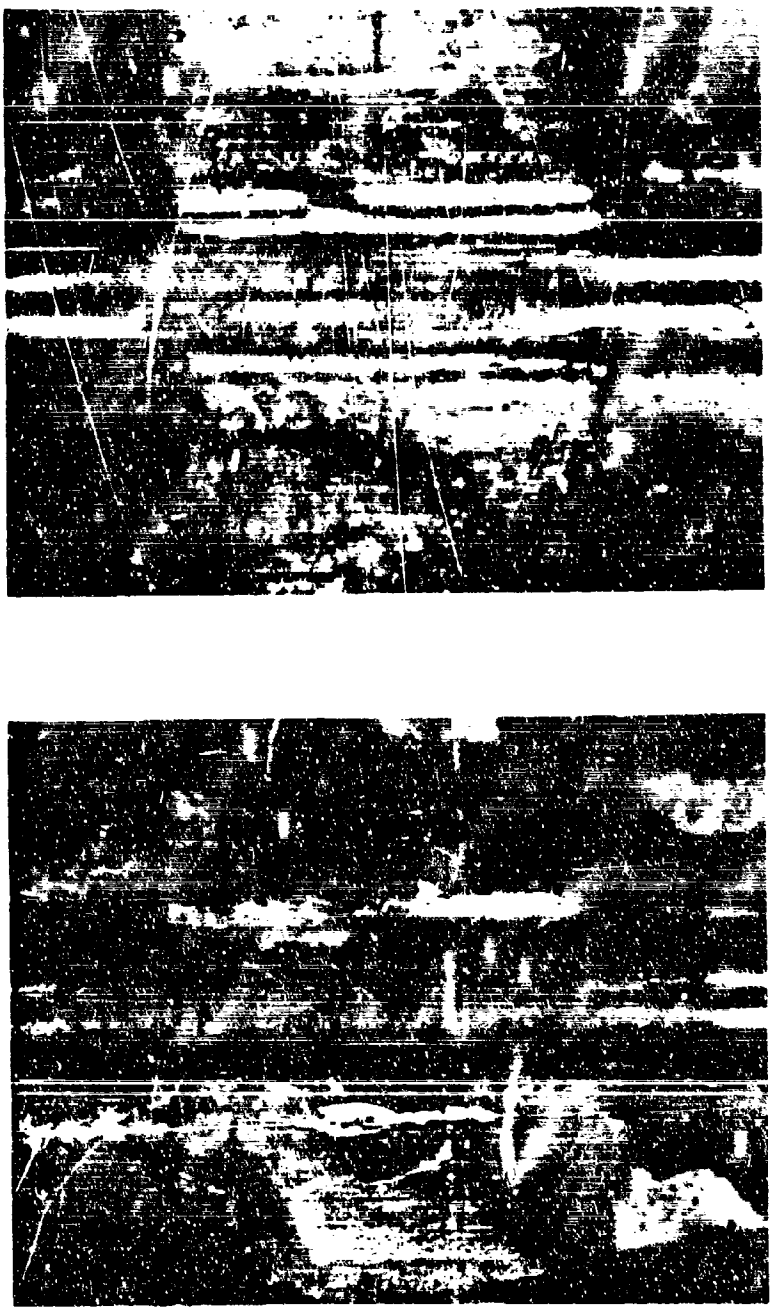

Large Grain

Figure 71. Nickel 200 Tube Tester Specimens After 270 Thermal Cycles

d. Problem Areas and Solutions

(U) There were no problem areas in this subtask during this reporting period.

e. Summary of Planned Effort

(U) This report effort concludes this subtask with the exception of analysis of related data.

3 THRUST CHAMBER NOZZLE DEMONSTRATION, 250K

(U) Full-scale, 250K thrust chambers duplicating the combustion and nozzle expansion features of the demonstrator module thrust chamber are being used to demonstrate the performance capability of the Aerospike thrust chamber. One solid-wall 250K chamber is being fabricated for the following purposes:

1. Verify injector integrity and compatibility before exposing the tube-wall chamber
2. Evaluate hypergolic and hot-gas ignition
3. Rate the injector-combustor stability by pulse gun as well as operational test
4. Provide a preliminary means of evaluating combustor and nozzle performance
5. Evaluate tapoff gases and demonstrate feasibility of tapoff source of turbine power on the Aerospike chamber

(U) In addition, the inherent ruggedness of this type of hardware will make it a valuable tool during test facility shakedown periods.

(U) Two 250K tube-wall chambers are being fabricated to provide long-duration capability for performance measurements. These chambers will be operated with varying degrees of base bleed at site conditions and in a diffuser for simulating altitude conditions. Injector and combustor features simulate those presently being designed into the demonstrator module chamber.

a. Status

(U) During the past quarter, the first injector and all components for the solid-wall assembly were completed. The 250K solid-wall thrust chamber was assembled and delivered to the test site. Installation of the hardware to the test stand was completed and preparations for pretest blowdowns and the test series are currently under way.

(U) The tube-wall assemblies, including the tubular inner and outer bodies, the base closure, and supporting ducting, are all progressing satisfactorily. The inner and outer combustors for the first tube-wall assembly have both successfully completed their first braze cycle. The second set of combustor bodies has completed prebraze machining operations and is currently being prepared for the first braze cycle. The second injector unit is approximately 60 percent complete and is in its final fabrication steps prior to the braze cycle.

b. Progress During Report Period

(1) Solid-Wall Thrust Chamber

(U) The solid-wall thrust chamber utilizes a water film-cooled inner and outer body. This chamber assembly which is designed primarily for checkout and stability rating of the injector is capable of short-duration firings. During this report period, the fabrication of all the components for the solid-wall assembly was completed. The chamber was assembled (Fig. 72) and shipped to the test site.

(C) The solid-wall test planning has been completed. The goals of the solid-wall chamber phase of the 250K Aerospike program are:

1. Operation from 20 to 100 percent of rated chamber pressure
2. Mixture ratio operation from 5.0 to 7.0 (o/f)
3. Hot-gas tapoff demonstration
4. Combustion stability evaluation with pulse gun technique
5. Hot-gas ignition

It is anticipated that these objectives can be attained with 11 satisfactory mainstage tests. Prior to these tests, a series of blowdowns will be conducted to verify operation of all propellant systems.

(U) The fit between all mating components during the assembly of the solid-wall thrust chamber was excellent. Of particular interest was the matching of the shear lips on the inner and outer bodies to the injector unit. The matching of these components demonstrated the ability to maintain critical fabrication tolerances at large diameters. Potential leakage of the four injector-to-thrust-chamber seals was checked. In each case, the seals performed considerably better than nominally required. The leakage rates for the two rubber O-rings (these are replaced by Naflex seals on the tube wall assembly) was found to be 0 and 1.2 scim, and no detectable pressure loss in a 1-minute period was observed for the two metal O-ring seals.

(U) The assembly of the solid-wall chamber was conducted on a combustion assembly-shipping fixture placed on the back of a transport trailer. This fixture was designed to permit chamber disassembly and assembly at the site. Transportation of the chamber to the site was accomplished, and a mobile crane was used to transfer the thrust chamber from the shipping pallet to the test stand (Fig. 73).

(2) Injectors

(U) Injector unit No. 1 has been completed and installed into the solid-wall thrust chamber. During this quarter, the injector progressed through the brazing operation; the unit was then leak checked with the aid of an

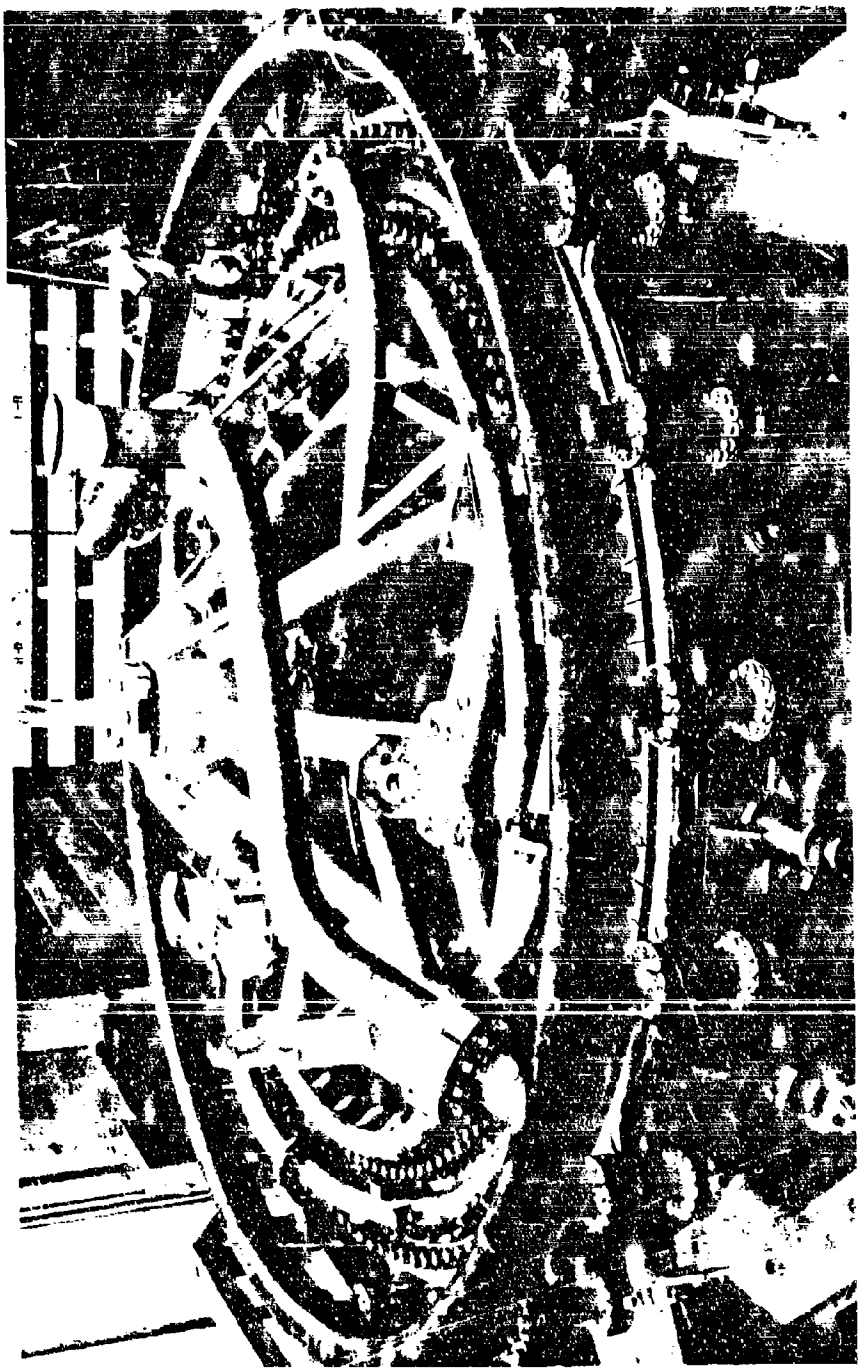

Figure 72. Solid-Wall Thrust Chamber Preparation for Shipment to Reno Test Site

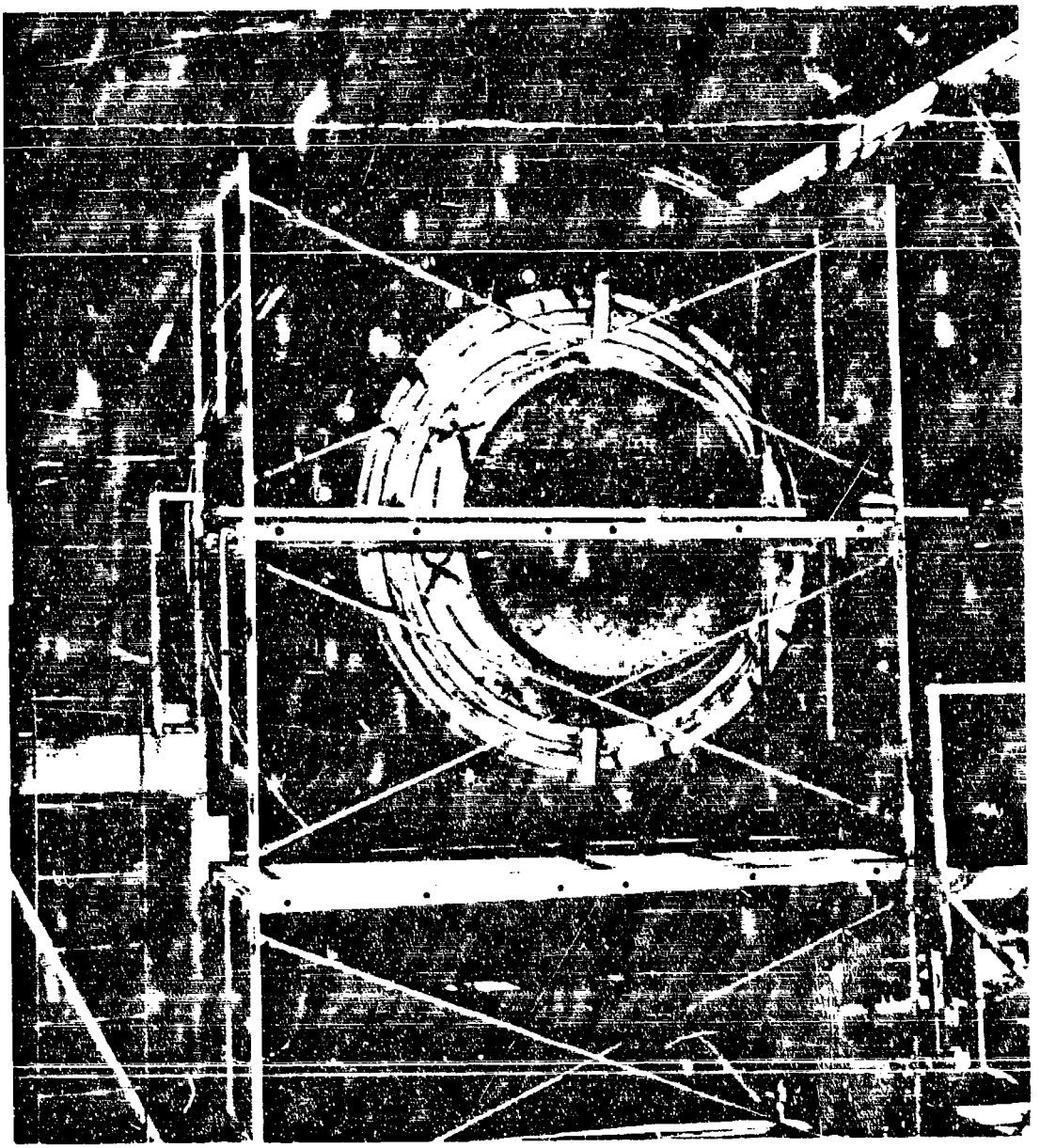

Figure 73. Solid-Wall Thrust Chamber Mounted on Reno Test Stand D-2

epoxy-resin compound, final machining was completed, and calibration and cleaning operations were accomplished.

(U) Subsequent to the initial braze cycle, the appearance of the braze was excellent; however, leakage was observed in several locations. The injector was realloyed and brazed for a second cycle (Fig. 74). Subsequent to this braze operation, the unit was leak checked. The leak check is accomplished by using an epoxy-resin compound which plugs the injector orifices. Use of this simple technique has allowed potential sources of leakage to be accurately located. Subsequent to the final braze operations, a 40-psig helium leak check of the oxidizer, fuel, and baffle braze joints indicated zero leakage. The oxidizer strips were also hydrostatically tested at 650 psig. No leaks were noted.

(U) Final machining of the injector shear lips was accomplished by match machining the shear lip to dimensions taken from the inner and outer solid-wall combustors. Subsequent stacking of these units revealed an excellent fit.

(U) The injector fuel and oxidizer flow circuits were each calibrated with the injector in a face-down position. The oxidizer system was water calibrated over a flowrate range of 1000 to 1900 gpm. The fuel system was calibrated over a flowrate range of 1100 to 2400 gpm. These flow calibrations showed excellent stream impingement and good correlation with analytically predicted pressure drop values.

(U) Injector unit No. 2 (Fig. 75) has completed all rough machining and welding operations. Weld cracks in the propellant closeout manifolds have been detected and are currently being repaired. Subsequent to this repair and the completion of proof-pressure tests, the broaching of baffle and strip grooves and EDM machining of the fuel and oxidizer passages will commence. All baffles and all injector strip fabrication for this unit are currently complete; flow calibration and plating of 50 percent of the strips are the only remaining operations.

(3) Tube Wall Chambers

(U) Two 250K tube-wall chambers are being fabricated to provide long-duration capability for performance measurements. The major components for the tube-wall thrust chamber are the inner and outer bodies. For the first chamber, the inner and outer bodies have completed the first braze cycle with good results and are now being prepared for the second braze cycle (Fig. 76 and 77). The second inner (Fig. 78) and outer bodies have been machined, nickel plated, and are being alloyed preparatory to tube stacking and furnace brazing. All tubes for the second combustor chamber have been completed and are ready for stacking.

(U) All supporting components for the tube-wall assembly are progressing satisfactorily. Welding of the perforated base plate is complete, and final machining of the assembly is currently 85 percent complete (closure instead of plate). Welding of the fuel inlet duct was completed and the component is presently being X-rayed. Fabrication of the fuel ducts for

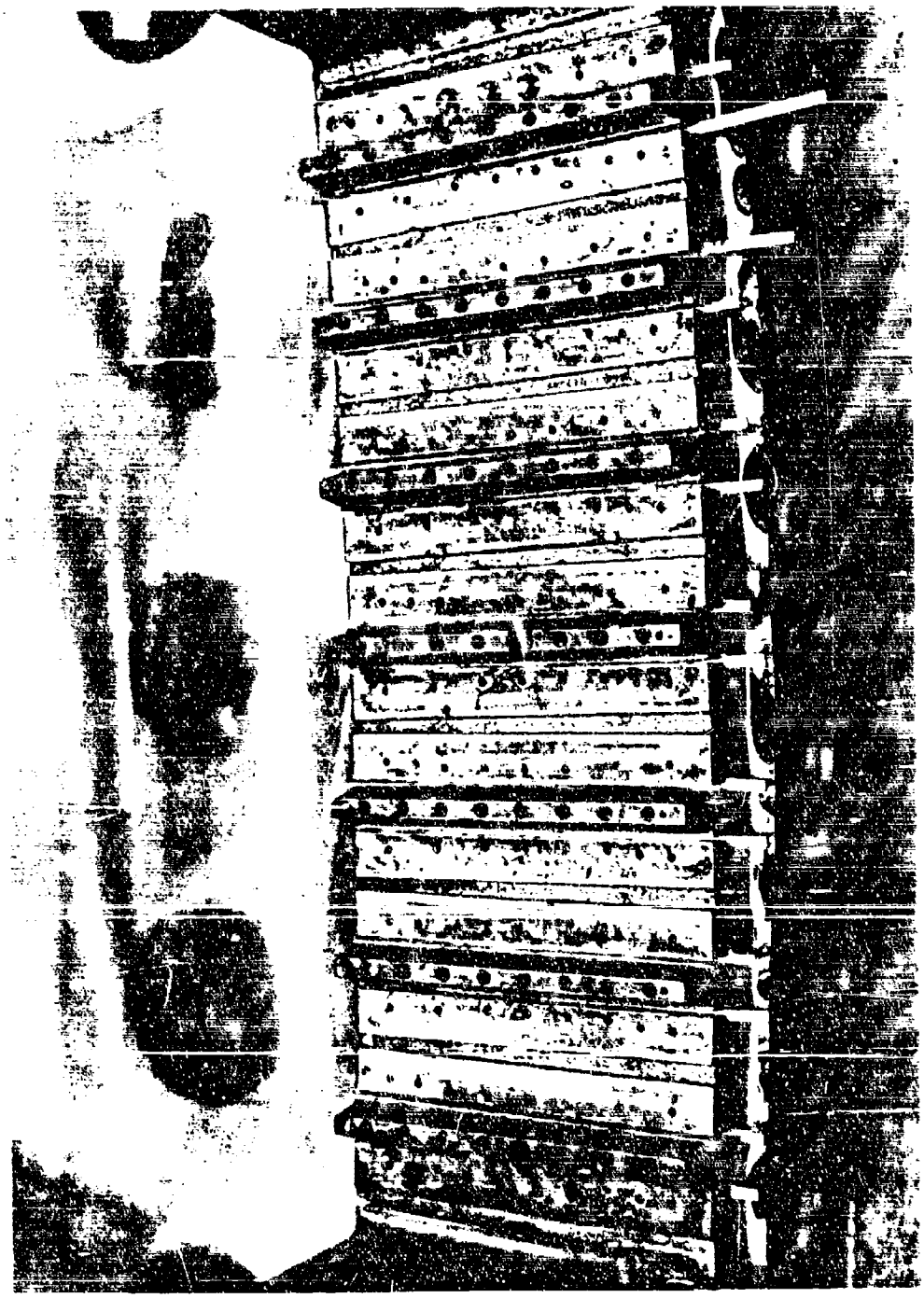

Figure 74. Injector Unit No. 001

Figure 75. Injector Unit No. 002

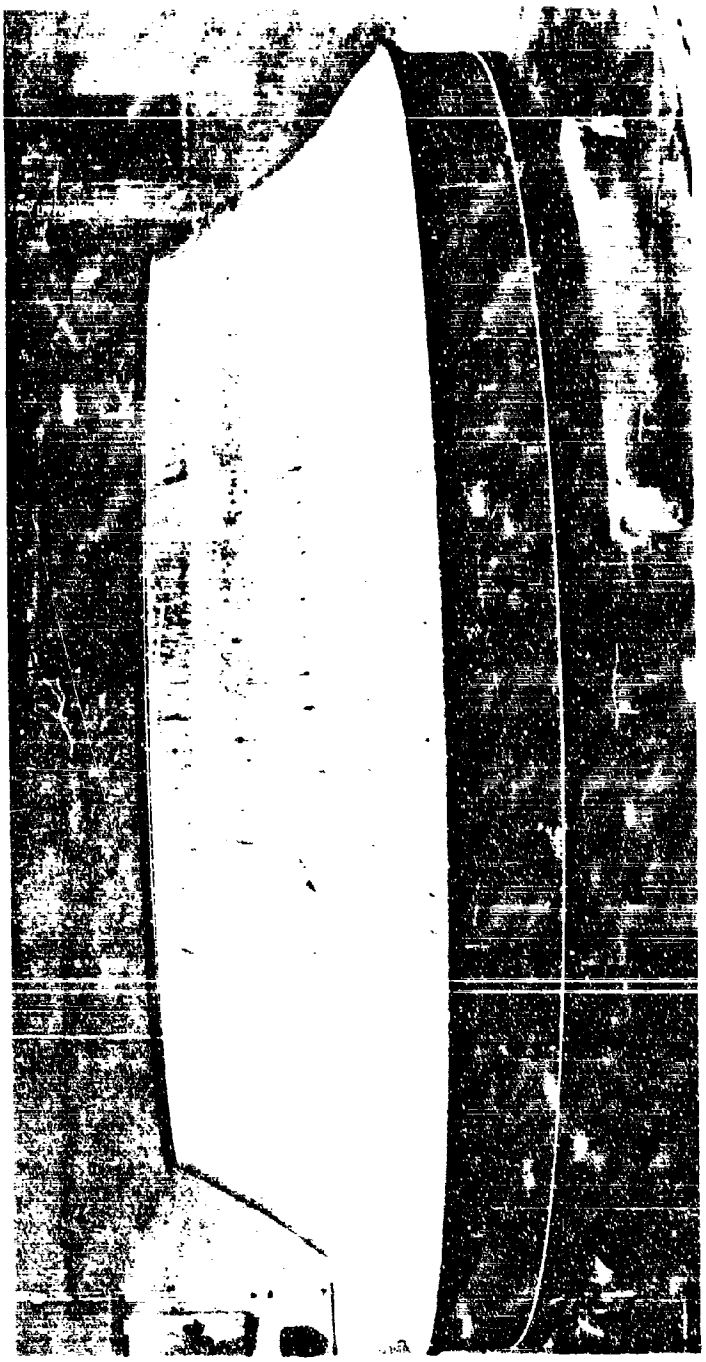

Figure 76. No. 1 Inner Tube Wall

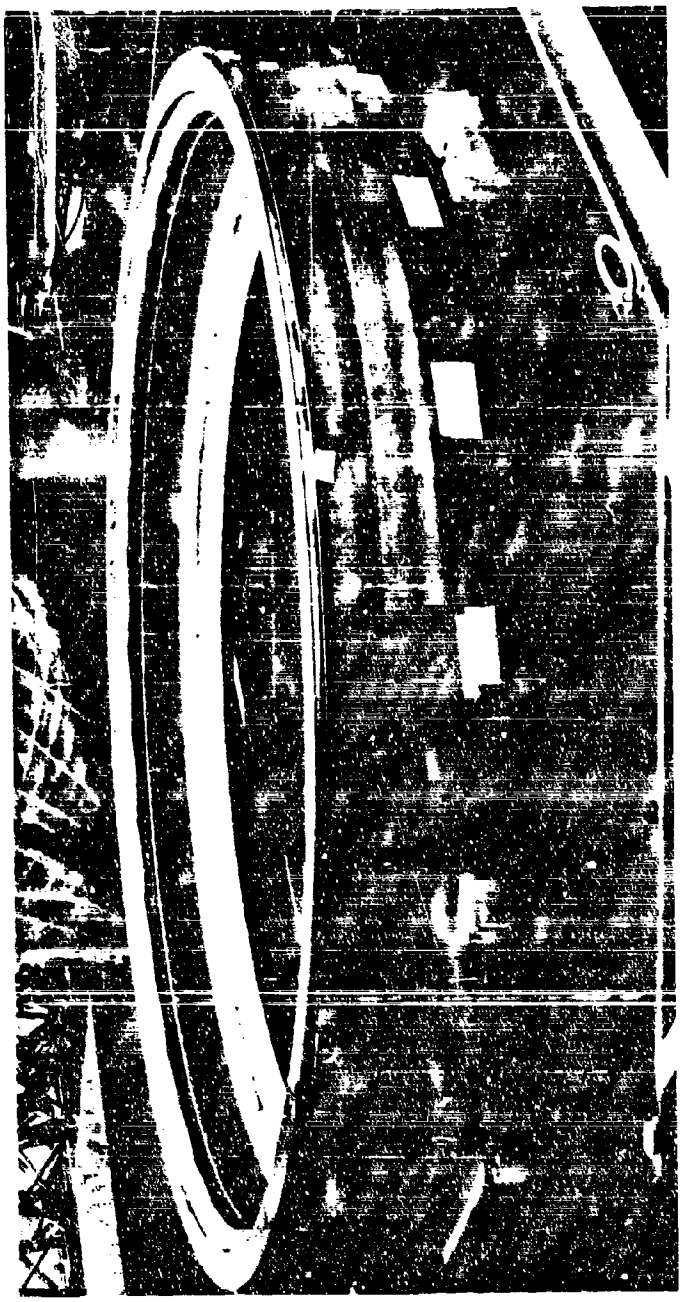

Figure 77. No. 1 Outer Tube Wall

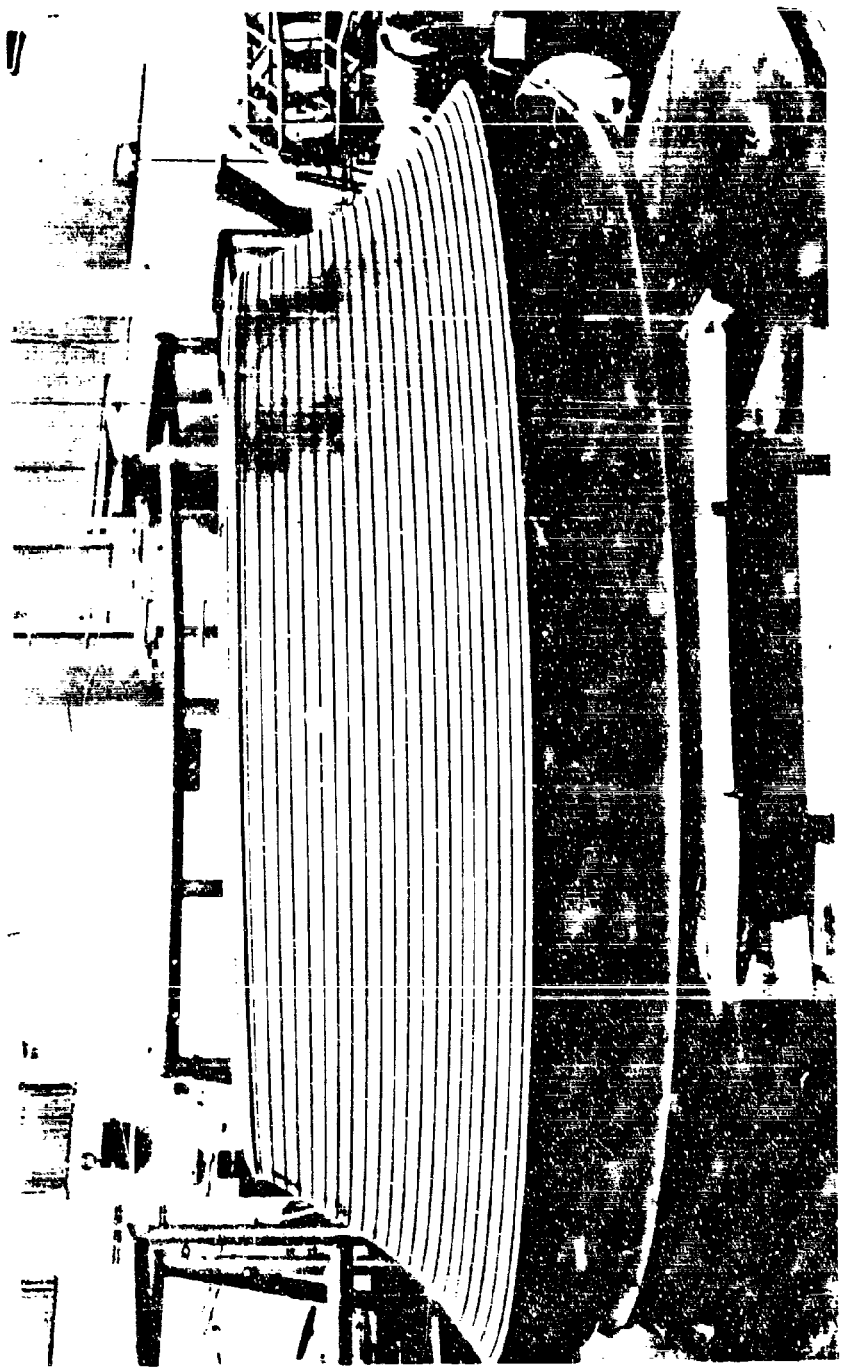

Figure 78. No. 2 Inner Tube Wall

the tube-wall chamber is in progress. The gas generator is in final machining and 90 percent complete. Other components, such as the uncooled nozzle extensions, are complete (Fig. 79).

(U) Hydrogen Heat Transfer Coolant Enhancement Evaluation

(U) A total of 12 electrically heated tests were run on one inner and one outer body tube to develop complete curvature enhancement data. Both tubes were of 347 stainless steel and both had been final formed and contoured to the 250K experimental tube dimensions. The tubes were instrumented with thermocouples on both the gas side and the opposite side of the tube. Voltage taps were placed at appropriate locations to determine the power generation within different sections of the tube. The hydrogen was heated to about 150 R and flowed through the tubes in the same direction as in the 250K tube-wall chambers. Hydrogen inlet pressures ranged between 1500 and 2000 psia. This corresponded to flowrates of 0.015 to 0.021 lb/sec for the outer tube and 0.018 to 0.024 lb/sec for the inner tube. Heat fluxes up to 31 Btu/in.^{2}-sec were generated in each tube with peak heat fluxes being near actual engine operating throat locations. Results of the tests are shown in Fig. 80 and 81 for the inner and outer tube, respectively. The measurement reference stations are shown in Fig. 82 and 83. The reference equation is the McCarthy-Wolf correlation.

(U) Because of a number of effects including roughness, entrance, and contraction (acceleration) effects, the experimental film coefficients are higher than that predicted by the McCarthy-Wolf equation. Station 8 (Fig. 80) has a very high enhancement, probably due, in part, to the low driving potential between the wall and coolant temperature (60 to 90 F for this region) compared to a driving potential of 300 to 800 F in the throat and upstream portions of this tube.

(U) Results of the tests show that a considerable entrance effect exists in both tubes. Also an appreciable increase in heat transfer coefficient occurs in the curved sections of the tube (curvature enhancement), in particular in the throat and at the start of the chamber convergent section. In conclusion, the tests indicate that the curvature enhancements used to date on ADP experimental tube designs are conservative (1.5 on the inner and 1.2 (1.5 with slight stream shift of contour) on the outer). The data are also useful for optimal design of the demonstrator module inner and outer body throat curvature locations.

(5) Oxidizer Manifold Starting Criteria

(U) Experimental investigations of the thermal and hydraulic characteristics of the experimental oxidizer manifold configuration have shown that flow above a minimal value are necessary during manifold priming for satisfactory operational characteristics. It should be noted, however, this minimum flowrate is a function of the manifold temperature, as well as its mass. For the 250K experimental engine, the minimum flowrate during the priming of a warm (ambient) manifold is approximately 115 lb/sec of oxidizer. These investigations have also shown that for flowrates greater than this value, flow overshoots (of the order of 50 percent above the steady-state value) are possible on a pressure-fed test stand. The

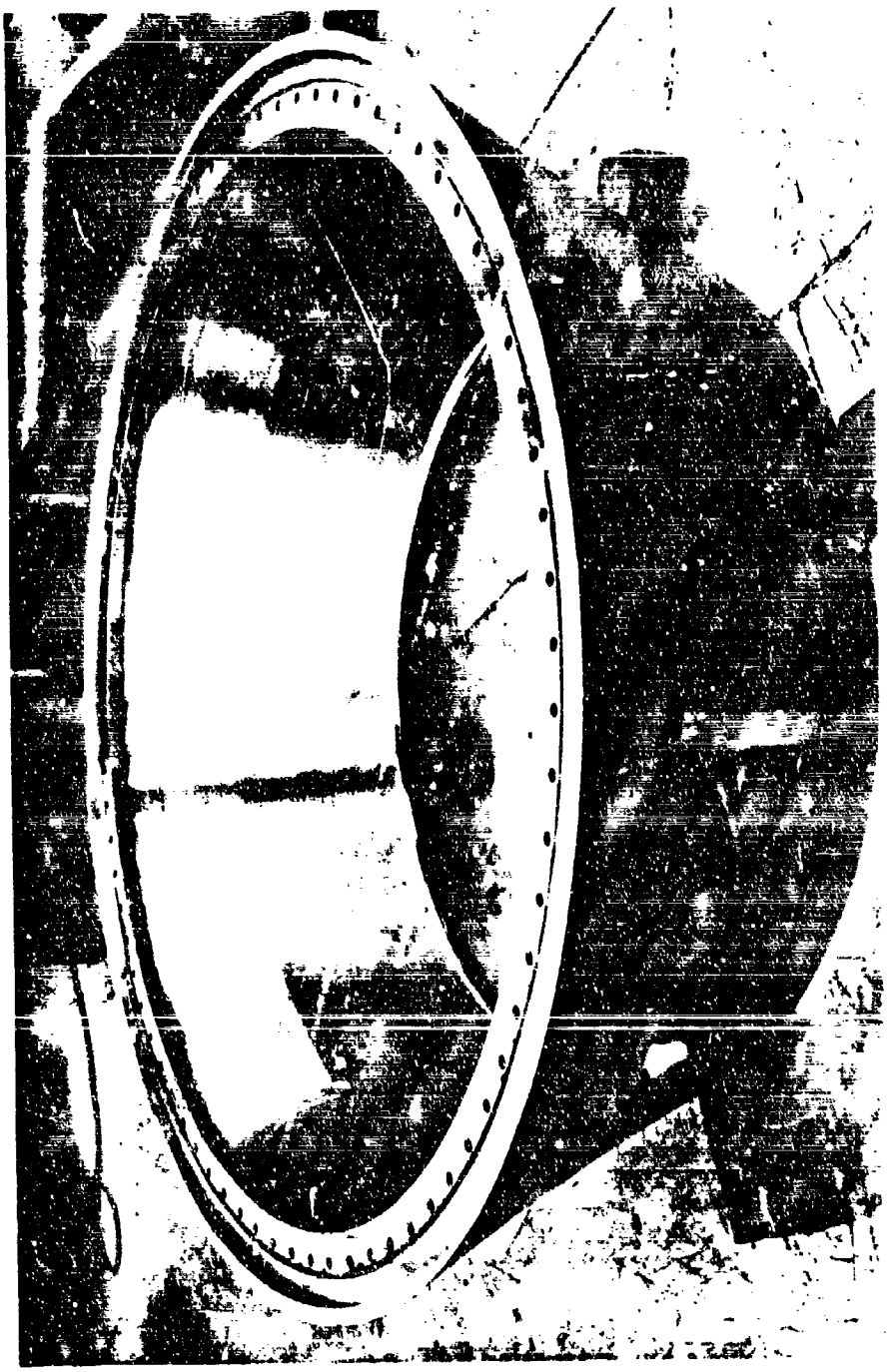

Figure 79. Uncooled Nozzle Extension

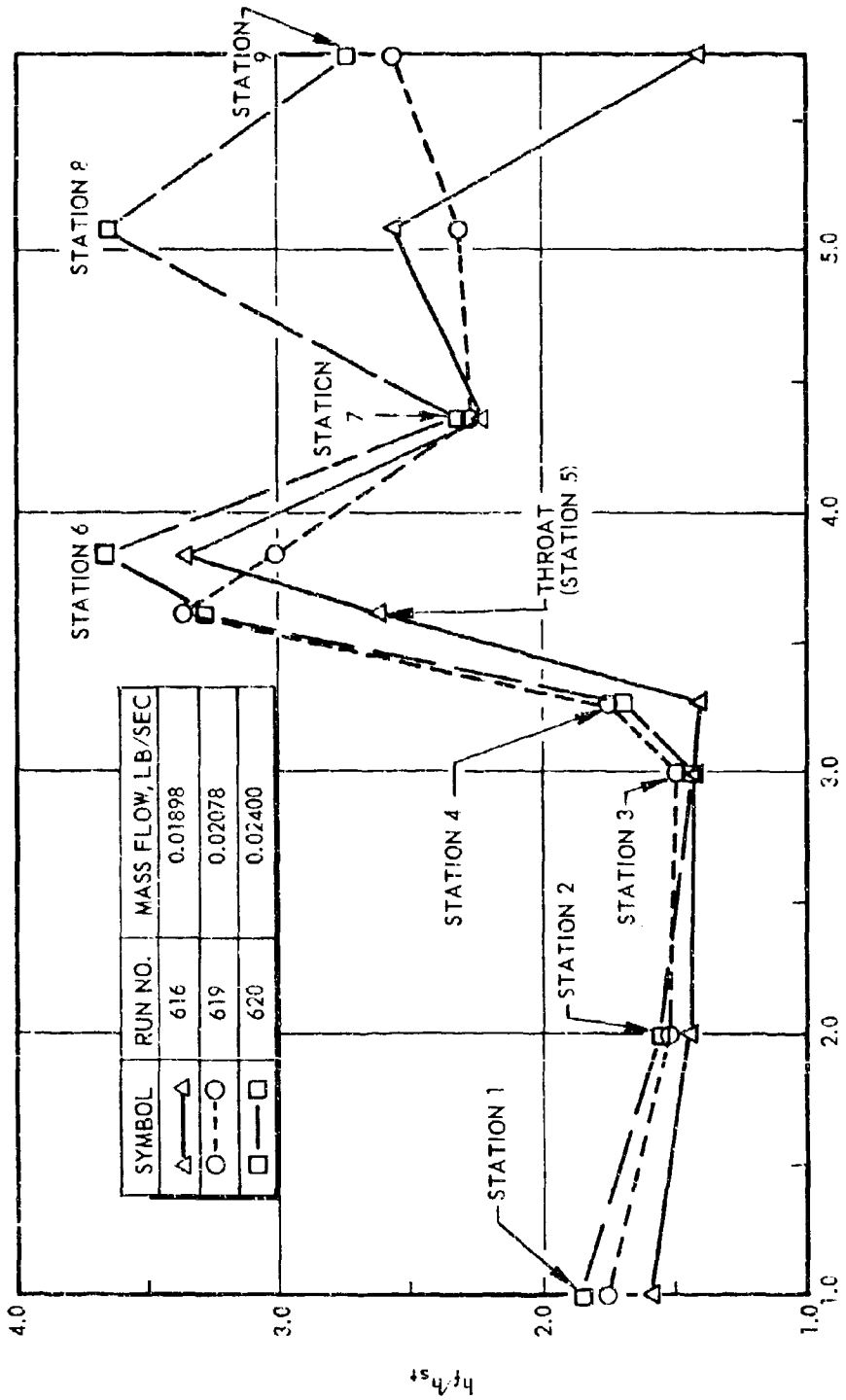

Figure 80. Heat Transfer Results for Inner-Body Coolant Tube; Ratio of Flame-Side Surface to Predicted Straight Tube Heat Transfer Coefficients

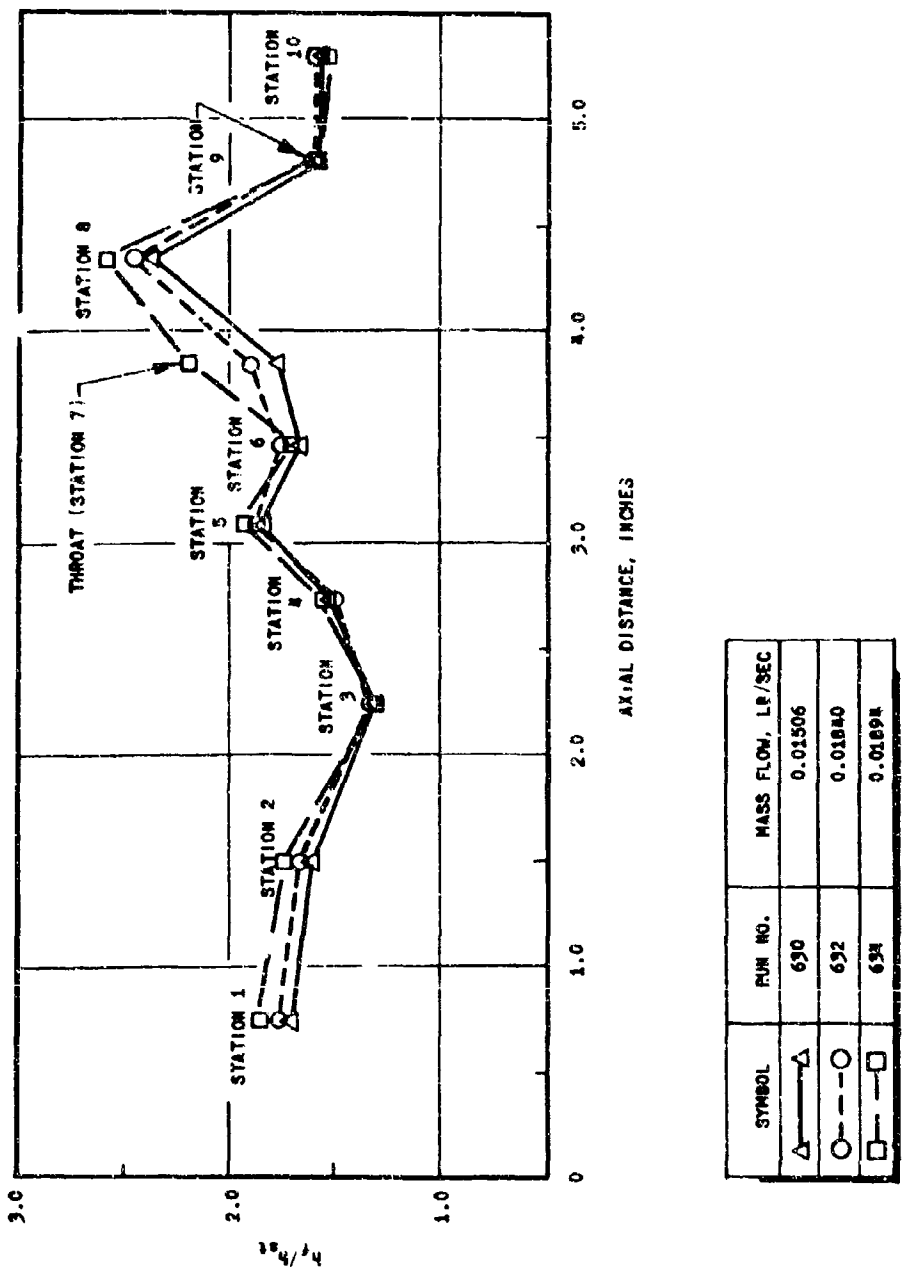

Figure 81. Heat Transfer Results for Outer-Body Coolant Tube; Ratio of Flame-Side Surface to Predicted Straight Tube Heat Transfer Coefficients

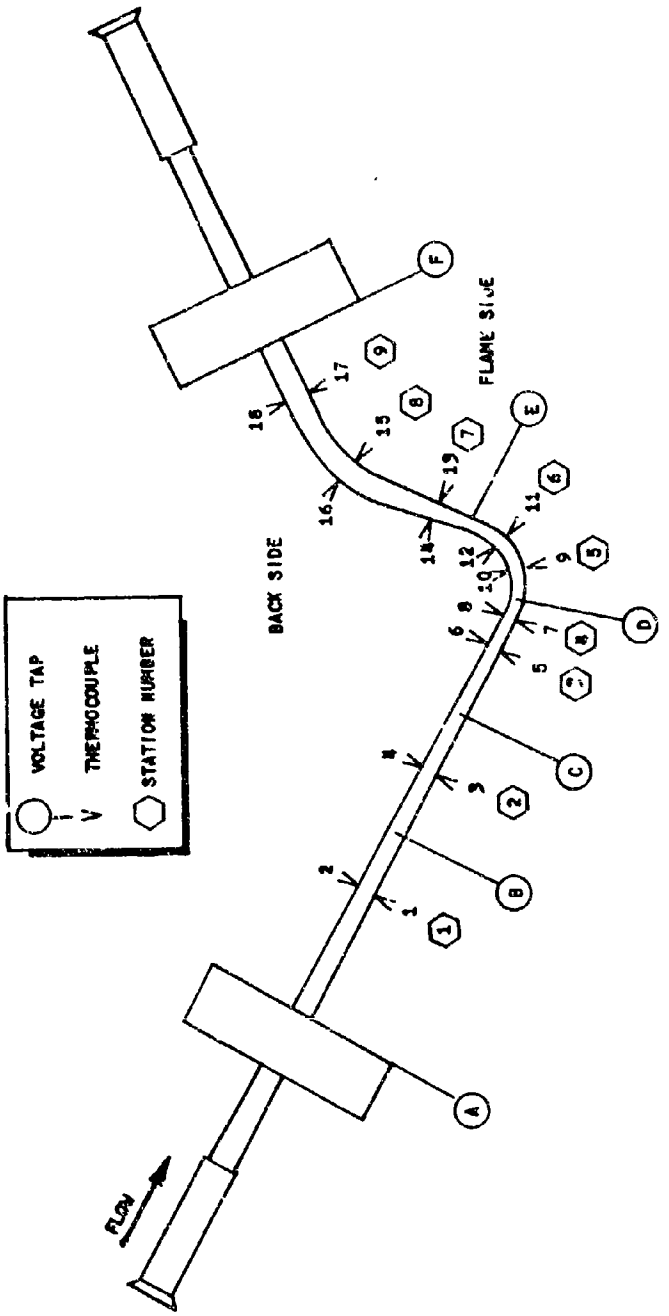

Figure 82. Test Section Fabricated From Inner Body Tube of ADP Aerospike Engine

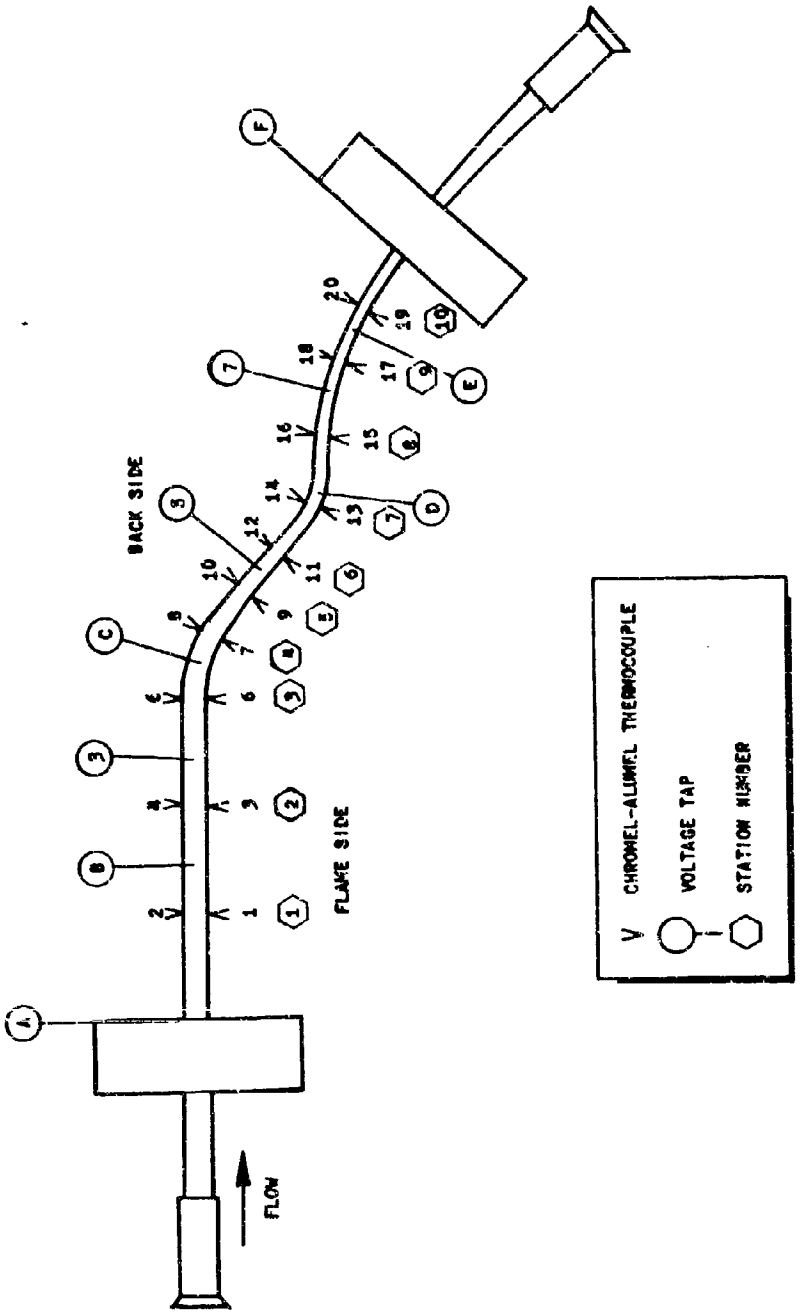

Figure 83. Test Section Schematic for Outer Coolant Tube of ADP Aerospike Engine

operational test plans for the experimental testing of the 250K chamber therefore include the use of cavitating venturii to restrict the possibility of mixture ratio and chamber pressure overshoots. Because these devices provide an extremely rapid acceleration of the flow up to the steady-state value, the average velocity during the manifold priming phase will be essentially the same as the steady-state value.

(6) 250K Solid-Wall Performance Analysis

(U) The 250K solid-wall thrust chamber is water film cooled. Although performance data are not a requirement of this test series, such data may be useful and an analytical procedure is being formulated to evaluate the effect of film coolant on thrust chamber performance parameters.

(U) Two theoretical models which represent upper and lower limits to thrust chamber performance with film coolant were selected for study. In one model, the water film coolant was assumed to remain in the liquid phase throughout the nozzle flow process. The film coolant was assumed to be heated to a temperature that is intermediate between the boiling temperature at a pressure equal to chamber pressure and a pressure equal to nozzle throat pressure. Also, kinetic equilibrium was assumed to exist everywhere in the flow field. In the other model, the water film coolant achieves instantaneous thermal and kinetic equilibrium with the combustion products.

(U) Calculations of the effect on performance of frictional drag, nozzle discharge coefficient, and nozzle divergence are in process. These calculations will yield the values of the influence coefficients, for the aforementioned physical effects, that are appropriate to the 250K hardware configuration.

(7) Base Bleed for 250K Testing

(C) During the experimental evaluations of the 250K tube-wall thrust chamber, gaseous hydrogen will be utilized as the base bleed gas for some of the secondary flow tests. The principle of gas substitution is based on the ability to predict the gaseous hydrogen flowrate required to obtain the same base pressure as that which would be obtained with turbine gas bleed. The dependence of realized values of base pressure on both the secondary and primary gas properties has been well established in experimental investigations (Ref. 4 and 5). Analytical techniques have been developed which permit comparison of isoenergetic (like primary and secondary gases) and nonisoenergetic (unlike primary and secondary gases) base pressure measurements. These techniques are based on the theoretical and experimental observations that choking of the secondary gases is obtained for large bleed rates. (A large bleed rate for the 250K experimental thrust chamber will be obtained with secondary flows greater than 0.5 percent of the primary flow.)

(U) Any of the nonreactive-type gases, such as hydrogen, helium, or nitrogen would be satisfactory as a substitute for the turbine gases; however, hydrogen has been selected because the c* of ambient hydrogen closely approximates the expected c* of turbine exhaust gases. Typical results for the testing of a hydrogen peroxide Aerospike (Ref. 5) obtained with the c* parameter are shown in Fig. 84 and 85. Secondary gas properties employed in the testing are given in Table 10. Figure 86 shows the measured base pressure vs the nominal secondary flow ratio, and Fig. 84 shows the base pressure. The theoretical basis for gas substitution predictability is given in Appendix A.

c. Problems and Solutions

(U) The solid-wall thrust chamber utilizes a water-film-cooled inner and outer body. The design of these bodies also incorporated a welded copper throat section to supplement the film cooling in the throat region. The construction of this welded copper throat section was completed successfully for the outer body. Extremely good conductivity was achieved. Welding of the inner body proceeded in a similar fashion and good conductivity was achieved. However, porosity and weld cracks were prevalent in the throat region. This condition was operationally unsatisfactory. Attempts at repairing the weld and replacing the cracked area with a copper ring were unsuccessful. The throat profile is now achieved by a nickel weld buildup. The duration of the combustor will still be governed by the uncooled stainless steel in the combustion chamber; however, the use of nickel in the throat will not allow operation with the film coolant off.

(U) Inspection subsequent to the thrust mount post-weld stress relief and heat treat revealed cracks in the parent material of three 4340 forgings used to connect the mount to the inner body. Additional cracks were also evident in the area of the calibration lugs on the center forging attaching to the gimbal block. Repair was made by removing the cracked end forgings and fabricating identical fittings of 4130 plate stock heat treated to the required stress level.

(U) To verify the structural integrity of the thrust mount after these operations, a proof load test was conducted using 430,000 pounds applied axially and cycled five times. Inspection between cycles and after testing revealed no propagation of the few remaining surface cracks and adequacy of the structure under the applied load.

d. Testing

(U) Buildup of the Nevada Field Laboratory test facility (described in Ref. 3) in preparation for installation of the 250K Aerospike thrust chamber was completed during this report period. The solid-wall thrust chamber has been installed in the test stand, and all propellant lines connected. The test facility is in a state of readiness to initiate propellant blowdowns. Instrumentation and wiring hookup in preparation for water and fuel blowdowns has been completed. Instrumentation for oxidizer and hot-gas igniter blowdowns is in work.

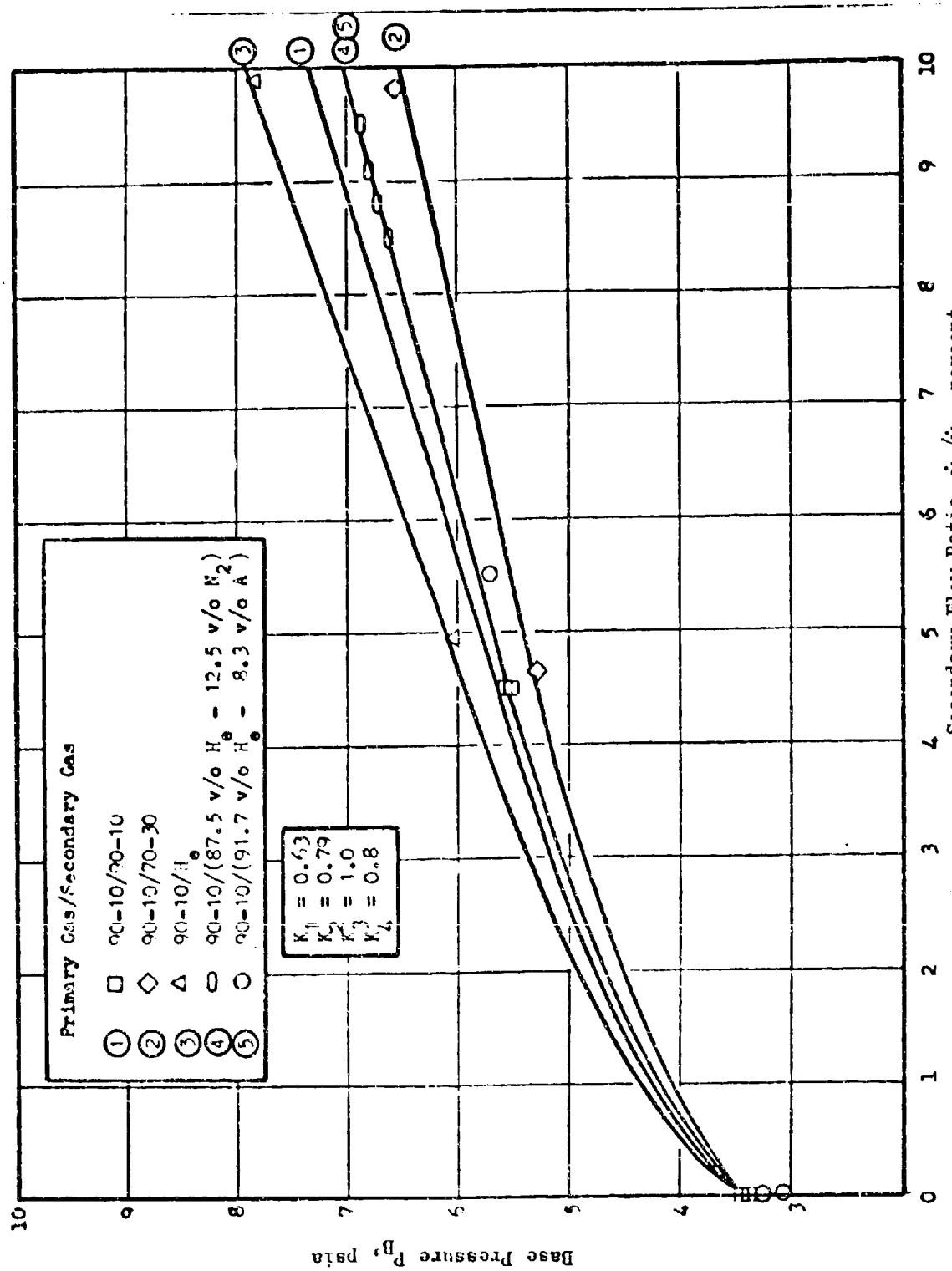

Figure 84. Estimated Base Pressure vs Secondary Flow Ratio

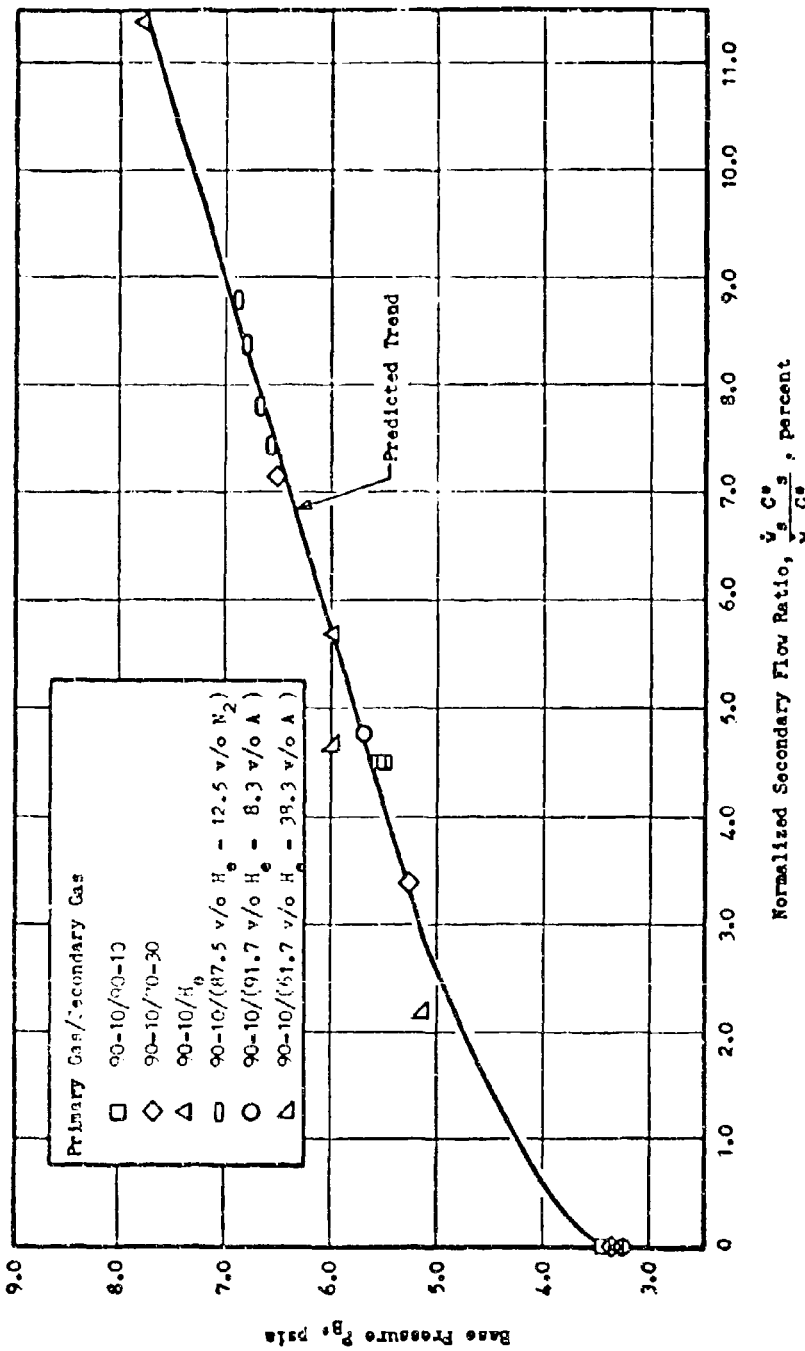

Figure 85. Base Pressure vs Normalized Secondary Flow Ratio

TABLE 10

SECONDARY TEST FLUIDS

Secondary Test Fluid	Molecular Weight	Specific Heat Ratio	Secondary c^*_s	c^*_s/c^*_p
H_2C_2 (10-percent H_2O)*	22.105	1.265	3090	1.0
H_2O_2 (30-percent H_2O)	21.043	1.315	2255	0.73
Gaseous Nitrogen	28.016	1.462	1395	0.45
Gaseous Helium	4.003	1.670	3550	1.15
Mixture 1 (He-87.5%, N_2-12.5%)**	7.0	1.620	2697	0.87
Mixture 2 (He-61.7%, A-38.3%)**	17.8	1.70	1681	0.54
Mixture 3 (He-91.7%, A-8.3%)**	7.0	1.67	2677	0.87

NOTE: Composition in abbreviated form next to gas callout

*Weight Percentage
**Mole Percentage

CONFIDENTIAL

CONFIDENTIAL

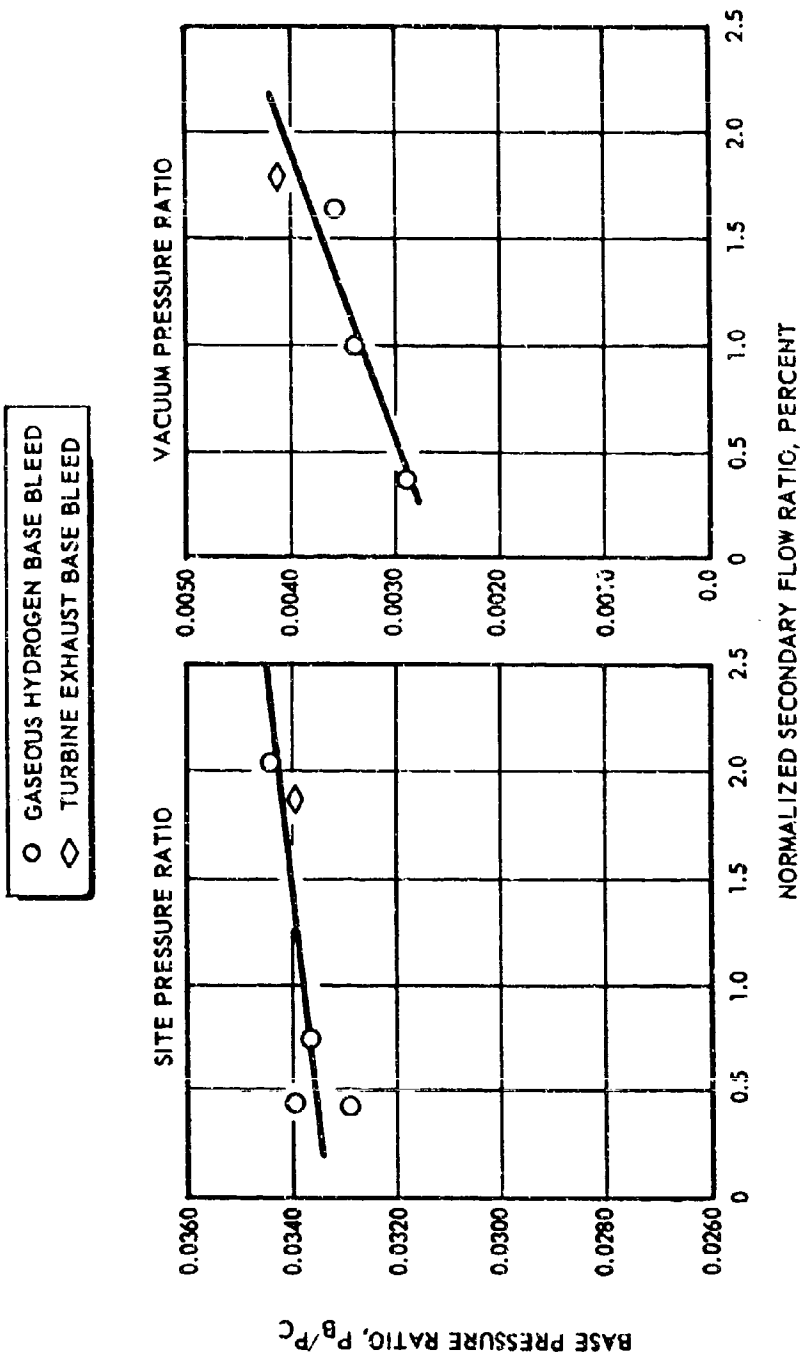

Figure 86. Base Pressure Ratio vs Normalized Secondary Flow Ratio

(U) Data acquisition at the Nevada test site will utilize the Astrodata system. This data acquisition system includes an on-line computer system which may be used for test control. The Astrodata system has been checked out, and the computer programs that control the system and unpacking routines have been verified.

e. Planned Effort

(U) During the next quarter, fabrication of all 250K hardware and testing of the solid-wall thrust chamber will be completed. The assembly of the first tube-wall thrust chamber and the delivery of the hardware to the test facility will be accomplished.

4. 20K SEGMENT STRUCTURAL EVALUATION

(U) The 20K segment chamber is being designed, manufactured, and tested to evaluate structure, cooling, fabrication, and performance over the throttling and mixture ratio range for the demonstrator module chamber design. To satisfy these conditions, a three-compartment rectangular segment is being constructed. The segment includes two subsonic struts but does not include the solid inner body spike or the extended outer body shroud.

(U) The three-compartment segment approach, without the spike or inner body extended shroud, allows use of a symmetrical chamber, with one tube design for the inner and outer bodies, and will provide close simulation of the maximum tube-wall thermal stress which occurs in the throat region, maximum coolant bulk temperature rise in the high heat flux area of the throat and combustion chamber, and a close approximation of pressure loads that will occur in the 250K module.

(U) Three compartments with two subsonic struts represent the shortest segment length required for continuous beam simulation. The rectangular combustor lengths are the equivalent arc length of the module at the throat diameter. The ability of the structure to maintain throat dimensions throughout the chamber pressure range and with repeated firings will be simulated very closely. Also, construction of all structural parts will be closely simulated. The effects of differences between the 20K segment and demonstrator module will be analytically determined and used to interpret the test results.

a. Status

(U) All drawings are complete. Figure 87 is a perspective view of the components in their relation to each other. The fabrication of all components is in process.

b. Progress During Report Period

(U) During this period, all detail and assembly drawings were completed and loose hardware (bolts, nuts, etc.) and purchased items were placed on order.

(U) Fabrication of all components was initiated. All the tubes for the first unit and 75 percent of the tubes for the second unit are complete. Flow calibration and metallographic examination of the finished tubes were conducted. Flows and pressures were uniform and tube quality was excellent.

(U) Work is progressing satisfactorily on the initial braze subassemblies. Four baffle seat subassemblies (Fig. 88) are required for each of the two 20K segments being fabricated; two for each of the contour walls. Fabrication of the first four units is complete. Two of the four units required

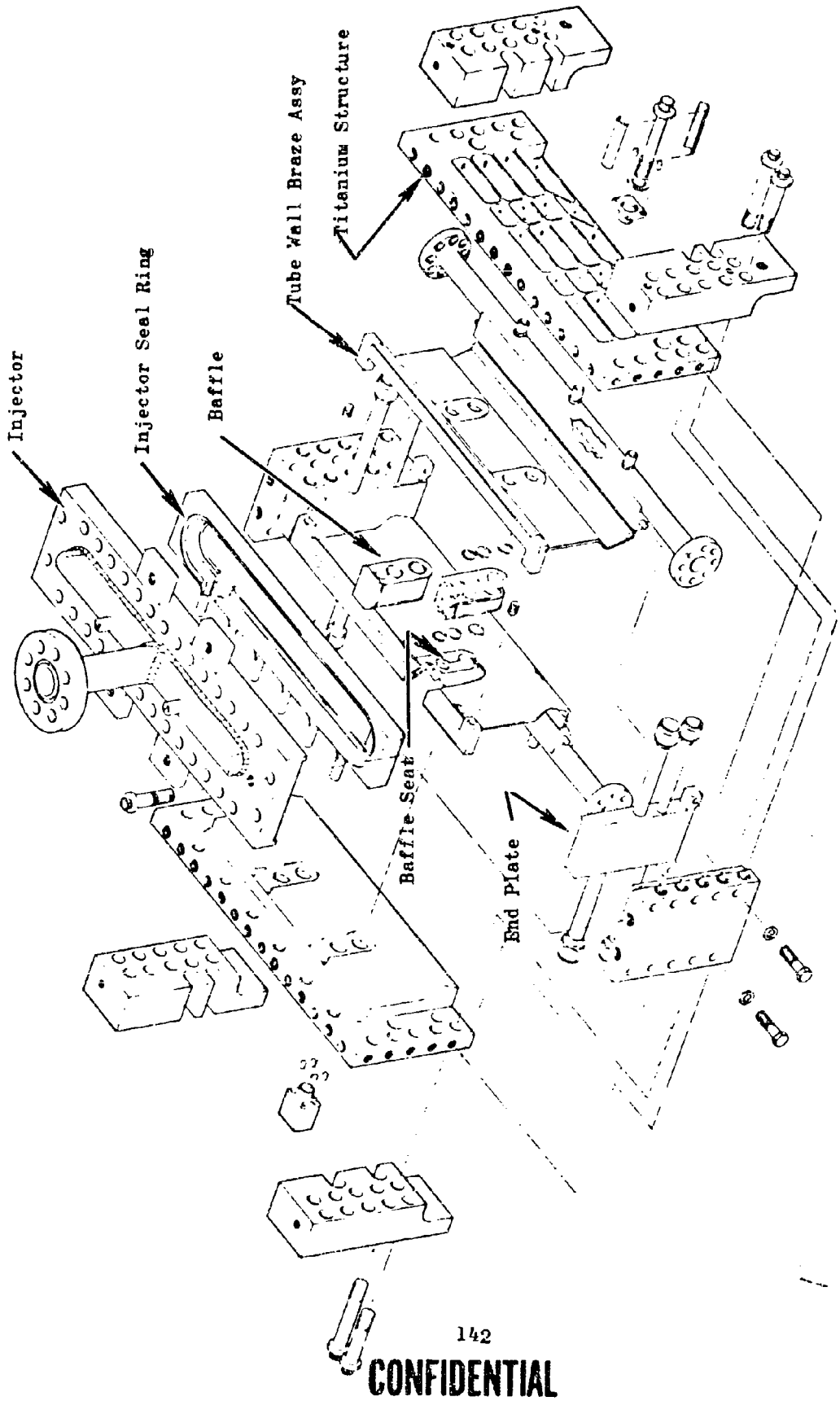

Figure 87. Perspective View of the 20K Segment Thrust Chamber

Figure 88. 20K Baffle Seat

for the second segment are in machining prior to flow calibration. One additional unit has completed its first furnace braze cycle and awaits leak checking; the last unit has been assembled in preparation for its initial cycle. Two tube-wall braze assemblies (Fig. 87, each including two baffle seat subassemblies and sufficient tubes to form a contoured segment wall) are being prepared for the first 20K assembly. The first tube-wall braze assembly has completed its first furnace braze cycle (Fig. 89) and has been leak checked. It is presently being prepared for its second braze cycle. The second assembly is currently being prepared for its initial braze cycle.

(U) Based upon heat transfer data obtained in the solid-wall firing effort and electrically heated tubes, the demonstration module tube design has been improved over the earlier 20K tube design. For comparison purposes, Table 11 has been prepared to indicate the design differences and resultant wall temperature differences for the two designs. It is observed that a symmetrical throat design on the 20K, simulating the outer body, with a series up-pass and down-pass cooling arrangement results in the up-pass side running above design T_{wg} of 1450 to 1520 F, whereas the down-pass side operates at a temperature commensurate with the 250K demonstrator module design.

(U) Two combustion baffles are utilized in the 20K chamber segment (Fig. 87). In addition to providing a stabilizing influence to the combustion process, the baffles are designed to protect the structural tie-bolts from the combustion environment and to transfer the chamber coolant from the inner body to the outer body. The baffles are regeneratively cooled by diverting 25 percent of the coolant from the crossover circuit through passages within the copper shell which surrounds the baffle body. A parametric heat transfer study for the baffle geometry at the anticipated hot firing conditions was conducted. The temperature distribution on the hot-gas side of the 20K baffle being fabricated is shown in Fig. 90.

(U) Fabrication of component details (Fig. 91) for the first two baffles is complete, and these units are being assembled for furnace braze. The details for the remaining units are in work.

(U) Fabrication is underway on all other components. The first injector body assembly has been completed through major machining prior to plating and brazing. The injector strips for this initial test unit are complete and ready for installation into the body. Unit No. 2 is being rough machined prior to welding of manifolds, closeouts, etc. Machining of the strips is in process. The two regeneratively cooled, drilled copper end plates for the first chamber segment are being furnace brazed. The component details prior to assembly for brazing are shown in Fig. 92. Proof of the numerical control tape for mil ing the titanium structural supports has been made on an aluminum trial block. Machining of the titanium structural supports for the initial assembly is in process.

c. Problem Areas and Solutions

(U) The nickel tube-wall braze backup sheet evidenced distortion during prebraze operation. Functionally, the sheet serves to provide a uniform

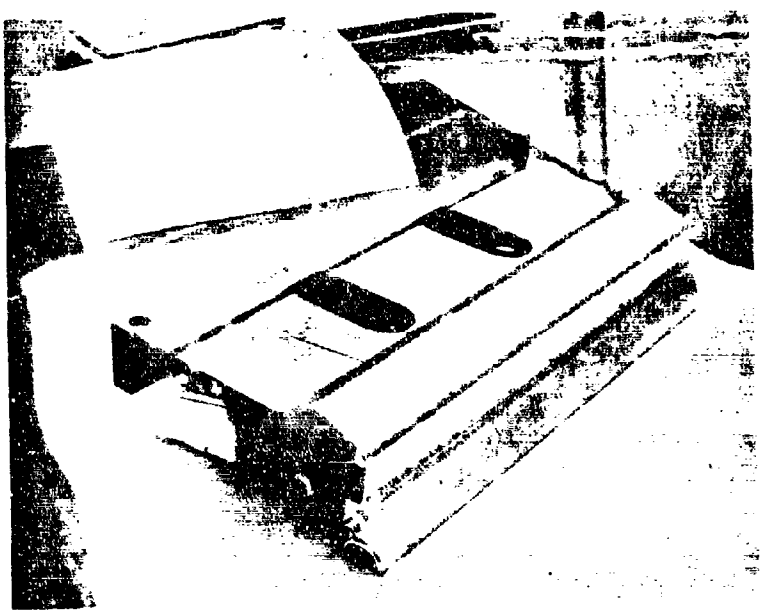

Figure 89. Tube-Wall Brazed Assembly

CONFIDENTIAL

TABLE 11

COMPARISON OF 20K AND 250K DEMONSTRATOR TUBE DESIGN
(P_c = 1500 psia, MR = 6.0)

	Inner Body		Outer Body	
	20K	250K	20K	250K
Tube	Nickel 200		Nickel 200	
Wall Thickness, inch	0.012	0.012	0.012	0.010
Tube Outside Diameter, inch	0.075	0.068	0.075	0.064
Coolant Mass Velocity at 1500 P_c, MR = 6 $\frac{lb}{in.^2-sec}$	11.0	12.3	11.0	10.6
Contour Simulation	Symmetrical with outer body*		Good	
Curvature Enhancement	1.1 to 1.2	1.5	1.2	1.4 to 1.5**
Coolant Inlet Temperature, R	200	60		
Gas-Wall Temperature, F	1800	1450	1800	1520

*For an up-pass, this results in reduced curvature enhancement.
**Shifted outer contour 3/16 inch upstream with respect to inner body to provide maximum curvature enhancement.

CONFIDENTIAL

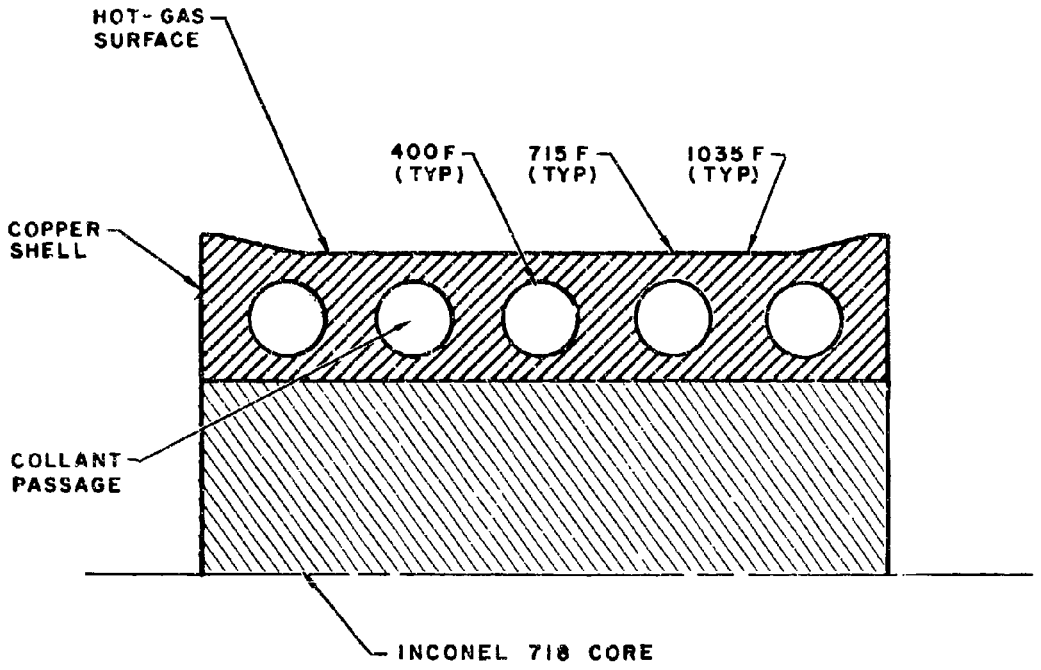

Figure 90. 20K Chamber Segment Maximum Baffle Temperature Distribution at Baffle Ends

Figure 91. Baffle Assemblies

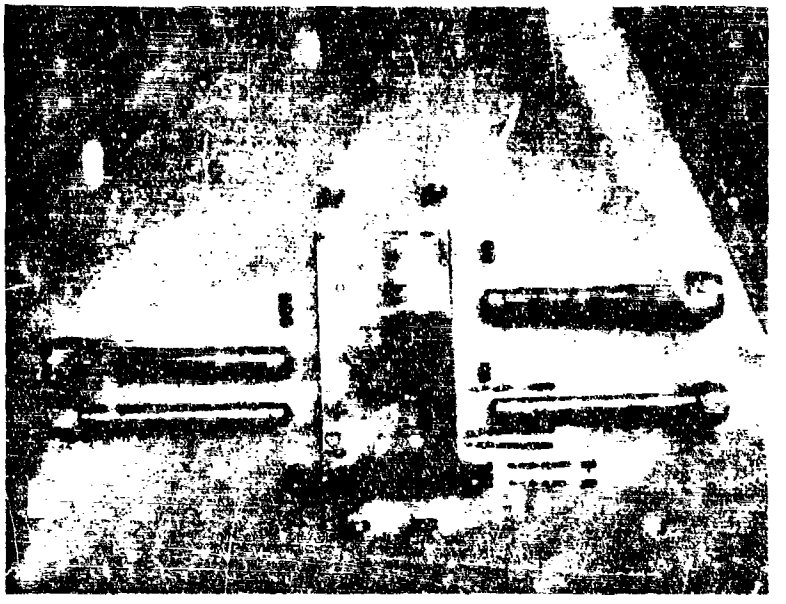

Figure 92. End-plate Assembly Details

adhesive thickness and, therefore, uniform strength of bond. However, analysis and adhesive sample tests have indicated that the adhesive thickness variations attendant to bonding directly to the irregular tube bundle surface would not adversely affect the bond strength. Therefore, this sheet was eliminated.

d. Plans for Next Period

(U) During the next period, fabrication of the initial 20K segment will be completed and preparation for testing completed, test procedures will be established, and testing will be initiated.

C. CONCLUSIONS AND RECOMMENDATIONS

(C) 1. Stabilized operation of a copper tube-wall segment with a high-performance injector from 300- to 1500-psi chamber pressure and a mixture ratio of 5 has demonstrated regenerative cooling of the Aerospike chamber at these levels.

(U) 2. Successful completion of furnace braze of two outer body and two inner body 250K tube-wall assemblies (one each on NASA SDI program) demonstrates the workability of this tooling and fabrication procedure. As the demonstrator module tube bundle is designed to use this same tooling, modified for detailed differences, it is believed that a similar one-for-one success can be achieved for that chamber.

(U) 3. Even though a substantial weight reduction can be realized by making the combustion chamber baffles integral with the injector in the Demonstrator Module, it is concluded that the assembly and inspection ease afforded by separate baffles makes these a better selection for the development level engine. The lighter configuration will be reconsidered for flight engines.

(U) 4. Turbine wheels assembled through curvic couplings and therefore easily replaceable are superior to the all-welded turbines for the Demonstrator Module.

REFERENCES

1. R-6537-1, AFRPL-TR-66-138: First Quarterly Progress Report Advanced Cryogenic Rocket Engine Program, Aerospike Nozzle Concept, Rocketdyne, a Division of North American Aviation, Inc., Canoga Park, California, June 1966, CONFIDENTIAL.

2. R-6537-2, AFRPL-TR-66-242: Second Quarterly Progress Report Advanced Cryogenic Rocket Engine Program, Aerospike Nozzle Concept, Rocketdyne, a Division of North American Aviation, Inc., Canoga Park, California, September 1966, CONFIDENTIAL.

3. R-6537-3, AFRPL-TR-66-348: Third Quarterly Progress Report Advanced Cryogenic Rocket Engine Program, Aerospike Nozzle Concept, Rocketdyne, a Division of North American Aviation, Inc., Canoga Park, California, December 1966, CONFIDENTIAL.

4. R-6582: Aerodynamic Nozzle Study, NAS 8-2654 Final Report, Rocketdyne, a Division of North American Aviation, Inc., Canoga Park, California, July 1966, CONFIDENTIAL.

5. R-6273: Aerodynamic Nozzle Study NAS 8-2054, Interim Report, Rocketdyne, a Division of North American Aviation, Inc., Canoga Park, California, July 1966, CONFIDENTIAL.

NOMENCLATURE

F	Thrust, lbf
P	Pressure, psia
I_s	Specific impulse, $\frac{\text{lbf-sec}}{\text{lbm}}$
C_F	Thrust coefficient
c^*	Characteristic velocity, ft/sec
$\dot{W}$	Mass flowrate, lbm/sec
A	Area, sq in.
ϵ	Expansion area ratio

Subscripts

B	Base
s	Secondary
p	Primary
t	Throat (primary nozzle)
c	Chamber

APPENDIX A

THEORETICAL BASE BLEED PRESSURE CORRELATION TECHNIQUES

With a choking criteria to explain the secondary gas behavior, the change in base thrust with the addition of secondary flow can be described with an equivalent sonic nozzle performance

$$\Delta F_B = \Delta P_B A_B = I_s^{sonic} \Delta \dot{w}_s = \frac{C_F^{sonic} c^*_s}{g} \Delta \dot{w}_s \quad (A-1)$$

Dividing Eq. A-1 by the nozzle stagnation chamber pressure (P_c) and rearranging terms leads to

$$\frac{P_B}{P_c} = \frac{C_{F_s}^{sonic} c^*_s \dot{w}_p}{g P_c A_B} \Delta\left(\frac{\dot{w}_s}{\dot{w}_p}\right) \quad (A-2)$$

substituting

$$\frac{A_t}{c^*_p} \text{ for } \frac{\dot{w}_p}{g P_c} \text{ and } \epsilon_B \text{ for } \frac{A_B}{A_t}$$

the following form is obtained

$$\frac{P_B}{P_c} = \left(\frac{C_{F_s}^{sonic}}{\epsilon_B}\right)\left(\frac{c^*_s}{c^*_p}\right)\Delta\left(\frac{\dot{w}_s}{\dot{w}_p}\right) \quad (A-3)$$

Recognizing that the base pressure at a given $\dot{w}_s/\dot{w}_p$ ratio is equal to the zero bleed base pressure plus the change in base pressure caused by the secondary flow, the following is obtained:

$$\frac{P_B}{P_c} = \left.\frac{P_B}{P_c}\right|_{\dot{w}_s=0} + \frac{P_B}{P_c} = \left.\frac{P_B}{P_c}\right|_{\dot{w}_s=0} + \left(\frac{C_{F_S}^{sonic}}{\epsilon_B}\right)\left(\frac{c^*_s}{c^*_p}\right)\left(\frac{\dot{w}_s}{\dot{w}_p}\right) \quad (A-4)$$

From Eq. A-4 it can be seen that the base pressure ratio P_B/P_c depends on both the primary nozzle aerothermodynamics $\left(P_B/P_c\big|_{\dot{w}_s=0}\right)$ and the ratio of the secondary and primary gas properties and flowrates.

With the aid of the above equation, the details of the gas substitution principle can be shown for a generalized case where the first condition utilizes primary gas as a source of base bleed and the second condition utilizes an auxiliary gas source as the base bleed. This auxiliary gas

could be either a turbine exhaust or a cold gas of the nonactive type. From this equation, it can be seen that to obtain the same base pressures for both types of bleed it is necessary to satisfy the following relationship:

$$\frac{C_F^{\text{sonic}}}{\epsilon_B}\left(\frac{c^*_s}{c^*_p}\right)\left(\frac{\dot{w}_s}{\dot{w}_p}\right)_{\text{aux bleed}} = \frac{C_F^{\text{sonic}}}{\epsilon_B}\left(\frac{\dot{w}_s}{\dot{w}_p}\right)_{\text{primary bleed}} \tag{A-5}$$

As C_F^{sonic} is a weak function of the gas properties, the bleed rate with the auxiliary bleed gases required to give the same base pressure as that obtained with the primary bleed is given as

$$\left(\frac{\dot{w}_s}{\dot{w}_p}\right)_{\text{primary bleed}} = \left(\frac{\dot{w}_s}{\dot{w}_p}\right)_{\text{auxiliary bleed}}\left(\frac{c^*_s}{c^*_p}\right) \tag{A-6}$$

The above equation shows, that for fixed primary flow conditions, base pressure measurements can be normalized by use of the normalized secondary flow ratio parameter $(\dot{w}_s/\dot{w}_p)(c^*_s/c^*_p)$.

APPENDIX B

TABULAR SUMMARY OF 2.5K WATER-COOLED COPPER SEGMENT

(U) A complete listing of all tests conducted with 2500-pound-thrust, water-cooled copper segment is presented in Table B-1. The listing of tests in this table is chronological and as such, represents an experience summary with the segment thrust chamber concept. Table B-1 shows only the pertinent operating parmeters and, where appropriate, explanatory comments are included. Figure B-1 depicts the injector orifice pattern designs corresponding to the injector numbers in Table B-1.

TABLE B-1

TOROIDAL SEGMENT THRUST CHAMBER PERFORMANCE

EXPERIENCE SUMMARY

Run No.	Test Date, 1966	Injector No.	Duration, seconds	Throat Area, sq in.	Thrust, pounds	Chamber Pressure, psia	Mixture Ratio, o/f	Total Weight Flowrate, lb/sec	Comments
016	4-8	1-1A	0.3	0.990	TR	TR	TR	TR	Injector strip survey test *
017	4-8	1-1A	0.3	0.990	TR	TR	TR	TR	Injector strip survey test *
018	4-21	2-1A	0.3	0.990	TR	TR	TR	TR	Injector strip survey test *
019	4-21	2-1A	0.3	0.990	TR	TR	TR	TR	Injector strip survey test *
020	4-21	2-1A	0.3	0.990	TR	TR	TR	TR	Injector strip survey test *
021	4-27	2-1A	0.3	0.990	TR	TR	TR	TR	Injector strip survey test *
022	4-27	2-1A	0.3	0.990	TR	TR	TR	TR	Injector strip survey test *
023	4-28	2-1A	0.3	0.990	TR	TR	TR	TR	Injector strip survey test *
024	5-11	2-1A	0.3	0.990	TR	TR	TR	TR	Injector strip survey test *
025	5-13	3-1A	0.3	0.990	TR	TR	TR	TR	Injector strip survey test *
026	5-13	3-1A	0.3	0.990	TR	TR	TR	TR	Injector strip survey test *
027	5-21	2-1A	3.7	0.990	937	641	5.81	2.638	Related program
028	5-21	2-1A	3.9	0.990	1415	971	6.50	4.038	Related program
029	5-21	2-1A	3.7	0.990	420	306	5.04	1.223	Related program
030	5-21	2-1A	4.1	ER	1909	1239	7.01	5.740	Nozzle throat eroded, related program
031	5-27	4-1A	0.4	0.990	1850	1364	9.71	8.123	Injector erosion
032	5-31	1-2A	0.4	0.990	1850	1614	7.78	6.859	Bomb test
033	6-6	2-1B	4.3	0.980	896	630	5.91	2.345	
034	6-6	2-1B	4.3	0.980	1377	974	6.43	3.947	
035	6-6	2-1B	4.0	0.980	430	325	5.69	1.340	
036	6-6	4-1A	4.3	0.980	1710	1189	6.38	WU	Coolant leak into combustion chamber
037	6-7	4-1A	4.2	ER	930	613	6.10	2.796	
038	6-7	4-1A	4.1	ER	500	313	5.31	0.854	
039	6-7	4-1A	4.2	ER	1240	764	6.15	3.537	
040	6-10	2-1C	4.2	ER	1040	643	2.15	1.232	
041	6-10	2-1C	3.9	ER	500	303	IF	IF	
042	6-10	2-1C	4.1	ER	1300	793	IF	IF	
043	6-10	2-1C	4.0	ER	1045	633	IF	IF	
044	6-13	2-1D	3.7	ER	510	314	6.03	1.402	
045	6-13	2-1D	4.3	ER	1025	653	IF	IF	
046	6-16	2-1D	4.3	0.980	446	334	5.79	1.394	
047	6-16	2-1D	4.4	0.980	955	680	6.07	2.753	
048	6-16	2-1D	4.3	0.980	953	665	5.94	2.749	
049	6-16	2-1D	4.3	0.990	920	658	5.80	2.653	
050	6-21	2-1E	4.2	0.955	425	326	5.38	1.304	

* Related Program

NOTE:

TR = transient data, no steady state
ER = nozzle throat eroded, throat area varied during test
WU = total flowrate unknown because of cooled water leak into chamber
IF = instrumentation failure, LOX flowrate unknown

TABLE B-1

(Continued)

Run No.	Test Date, 1966	Injector No.	Duration, seconds	Throat Area, sq in.	Thrust, pounds	Chamber Pressure, psia	Mixture Ratio, o/f	Total Weight Flowrate, lb/sec	Comments
051	6-21	2-1E	4.3	0.965	909	653	5.62	2.599	
052	6-21	2-1E	4.3	0.965	911	658	5.63	2.631	
053	6-22	2-1E	4.2	0.965	418	318	5.31	1.254	
054	6-22	2-1E	4.3	0.965	672	495	5.79	1.970	
055	6-22	2-1E	4.3	0.965	898	654	5.90	2.666	
056	6-23	2-1F	4.2	0.965	420	338	5.96	1.411	
057	6-23	2-1F	4.3	0.965	860	644	5.56	2.565	
058	6-23	2-1F	4.3	0.965	620	484	5.99	2.070	
059	6-24	2-1G	4.2	0.965	880	659	5.80	2.671	
060	6-24	2-1G	4.1	0.965	620	484	5.45	2.176	
061	6-24	4-1B	4.2	0.965	620	483	5.41	2.192	
062	6-24	4-1B	4.3	0.965	405	334	5.46	1.562	
063	6-30	4-1B	4.1	0.965	620	485	5.57	2.000	Injector strip-to-land separation, buzzing induced by strip-to-land separation
064	6-30	4-1B	4.0	0.965	740	564	6.94	2.368	
065	6-30	4-1B	4.1	0.965	635	494	5.89	2.076	
066	6-30	4-1B	4.2	0.965	685	515	6.39	2.214	
067	7-1	4-1B	4.2	0.965	670	513	4.27	2.130	
068	7-1	2-1G	3.7	0.965	650	510	3.87	1.956	
069	7-1	2-1G	3.7	0.965	625	503	3.84	1.945	
070	7-1	2-1G	3.8	0.965	650	514	3.92	1.932	
071	7-1	2-1G	3.8	0.965	675	544	4.76	2.156	
072	7-5	1-3A	4.0	0.950	745	549	6.84	2.270	
073	7-5	1-3A	4.3	0.950	1062	779	5.70	3.096	
074	7-5	1-3A	4.3	0.950	1057	773	5.15	2.942	
075	7-6	1-3A	NM	NM	NM	NM	NM	NM	Nozzle throat eroded
076	7-8	1-3B	4.4	0.950	870	634	5.64	2.522	
077	7-8	1-3B	4.4	0.950	886	647	5.88	2.622	
078	7-8	1-3B	4.4	0.950	846	621	5.59	2.488	
079	7-12	1-3B	14.3	0.940	1079	779	6.11	3.094	
080	7-12	1-3B	14.3	0.940	1061	766	6.21	3.055	
081	7-13	3-2A	0.4	OP	1900	1514	7.63	6.614	Uncooled hardware
082	7-15	3-2A	12.7	0.940	1111	805	6.52	3.172	
083	7-18	1-3B	1.2	0.940	360	274	4.61	1.120[a]	Gas tapoff
084	7-18	1-3B	0.8	0.940	369	285	5.96	1.419[a]	Gas tapoff
085	7-18	1-3B	1.4	0.940	400	304	6.16	1.437[a]	Gas tapoff

NOTE:

NM = no data
OP = orifice plate nozzle eroded
a = flowrate includes gas tapoff flow

TABLE B-1
(Continued)

Run No.	Test Date, 1966	Injector No.	Duration, seconds	Throat Area, sq in.	Thrust, pounds	Chamber Pressure, psia	Mixture Ratio, o/f	Total Weight Flowrate, lb/sec	Comments
086	7-18	1-3B	1.4	0.940	572	429	5.11	1.815[a]	Gas tapoff
087	7-18	1-3B	1.2	0.940	849	608	5.67	2.515[a]	
088	7-21	1-3B	1.3	0.940	410	317	5.87	1.373[a]	
089	7-21	1-3B	1.3	0.940	830	609	5.32	2.489[a]	
090	7-22	1-3B	1.5	0.940	547	412	5.43	1.685[a]	
091	7-22	1-3B	1.7	0.940	505	387	5.20	1.574[a]	
092	7-22	1-3B	1.8	0.940	679	506	5.63	2.104[a]	
093	7-27	1-3B	1.3	0.940	964	695	5.72	2.777[a]	
094	7-27	1-3B	1.4	0.940	929	678	4.96	2.774[a]	
095	7-27	1-3B	1.3	0.950	957	688	6.52	2.916[a]	
096	7-27	1-3B	1.4	0.950	934	668	5.74	2.818[a]	
097	7-29	1-3B	1.8	0.880	866	705	5.10	2.593[a]	
098	7-29	1-3B	1.8	0.880	856	698	4.52	2.565[a]	
099	7-29	1-3B	1.9	0.880	892	709	6.26	2.765[a]	
100	8-2	1-3B	ND	ND	ND	ND	ND	ND	
101	8-2	1-3B	3.4	0.950	992	720	5.28[d]	WU	Coolant leak into combustion chamber
102	8-2	1-3B	3.5	0.950	1385	1004	4.94[d]	WU	Coolant leak into combustion chamber
103	8-2	1-3B	3.5	0.950	1617	1169	5.16[d]	WU	Coolant leak into combustion chamber
104	8-3	1-3B	3.6	ER	1902	1364	5.81[d]	4.684	Nozzle throat eroded
105	8-5	1-3B	3.3	0.950	2105	1491	6.89[d]	6.001[b]	
106	8-5	3-2A	3.2	0.950	2130	1505	7.07[d]	6.152[b]	
107	8-9	4-1B	3.3	0.950	2151	1504	8.05[d]	6.454[b]	
108	8-9	4-1B	3.7	0.950	1022	741	6.19[d]	3.062[b]	
109	8-9	5-1A	4.4	0.950	527	385	5.74[d]	1.696[b]	Related program
110	8-9	5-1A	0.8	0.950	2176	1491	6.87[d]	6.135[b]	Related program
111	8-12	3-2A	4.9	0.970	390	284	4.55[d]	1.289[b]	
112	8-12	3-2A	4.8	0.970	406	304	5.54[d]	1.236	
113	8-12	3-2A	4.6	0.970	1378	969	6.08[d]	3.902[b]	
114	8-12	3-2A	3.4	0.970	1340	946	6.11[d]	3.766[b]	
115	8-12	3-2A	3.4	ER	2303	1562	8.13[d]	6.762[b]	Nozzle throat eroded
116	8-17	2-2A	ND	ND	ND	ND	ND	ND	Ignitor malfunction
117	8-19	3-2A	3.9	0.925	860	639[c]	5.12[d]	2.593[b]	
118	8-19	3-2A	3.9	0.925	874	650	6.93[d]	2.811[b]	
119	8-19	3-2A	4.5	0.925	411	324	3.90[d]	1.263[b]	
120	8-19	3-2A	4.5	0.925	398	317	4.03[d]	1.211[b]	

Film-cooled tests

NOTE:

a = flowrate includes gas tapoff flow
b = flowrate includes film-coolant flow
c = indicated instrumentation error
d = mixture ratio based on injector flowrates
ND = no data
WU = total flowrate unknown because of cooled water leak into chamber
ER = nozzle throat eroded, throat area varied during test

TABLE B-1

(Continued)

Run No.	Test Date, 1966	Injector No.	Duration, seconds	Throat Area, sq in.	Thrust, pounds	Chamber Pressure, psia	Mixture Ratio, o/f	Total Weight Flowrate, lb/sec	Comments
121	8-23	3-2B	3.5	0.925	887	666	5.24[d]	2.526[b]	
122	8-23	3-2B	2.9	0.925	1012	1049	5.72[d]	3.973[b]	
123	8-24	4-2A	3.9	0.925	838	633	5.12[d]	2.329[b]	
124	8-24	4-2A	3.8	0.925	810	614	4.68[d]	2.214[b]	
125	8-24	4-2A	2.7	0.925	1354	1005	5.39[d]	3.692[b]	
126	8-24	4-2A	2.0	0.925	1782	1320	5.16[d]	4.887[b]	Film cooled
127	8-24	4-2A	2.6	0.925	2032	1492	6.35[d]	5.671[b]	Sequence malfunction
128	8-26	4-2A	ND	0.925	ND	ND	ND	ND	
129	8-26	4-2A	1.7	0.935	1231	992	5.39[d]	3.426	
130	8-26	3-2B	1.7	0.935	1020	762	5.88[d]	2.999	
133	8-31	4-2A	2.2	0.925	401	326	4.53	1.305	
134	8-31	4-2A	2.5	0.925	411	330	4.60	1.330	
135	8-31	4-2A	1.8	0.925	470	333	6.41	1.379	
136	8-31	4-2A	2.4	0.925	1261	969	4.97	3.579	
137	8-31	4-2A	2.6	0.925	1264	988	6.59	3.791	
138	9-1	4-2B	1.7	0.925	460	324	5.43	1.370	
139	9-1	4-2B	1.6	0.925	1239	956	5.23	3.635	
140	9-6	4-2C	1.9	0.925	490	334	5.52	1.382	
141	9-6	4-2D	2.0	0.925	372	319	4.89	1.228	
142	9-6	4-2E	1.6	0.925	373	315	4.45	1.145	
143	9-6	4-2E	ND	0.925	ND	ND	ND	ND	
144	9-6	4-2F	1.8	0.925	448	326	5.69	1.397	
169	9-26	4-2G	1.5	0.925	442	324	4.14	1.164	
170	9-26	4-2G	1.5	0.925	413	341	5.45	1.254	Gas tapoff
171	9-26	4-2G	1.3	0.925	461	374	6.21	1.561	
172	9-26	4-2G	1.3	0.925	813	665	5.39	2.226	
173	9-26	4-2G	1.2	0.925	1100	871	6.79	3.046	
174	9-26	4-2G	1.3	0.925	487	397	6.84	1.448	
175	9-28	4-2G	1.3	0.925	377	316	5.27	1.182	
176	9-28	4-2G	2.3	0.925	377	316	5.07	1.090	
177	9-28	4-2G	2.3	0.925	378	316	5.07	1.097	
178	9-28	4-2G	2.4	0.925	390	321	5.35	1.170	
179	9-28	4-2G	2.4	0.925	385	315	6.27	1.300	
180	9-28	4-2G	2.4	0.925	2005	1581	5.90	5.509	
181	9-30	4-2G	0.7	0.925	1377	1088	5.95	3.437	

NOTE:

b = flowrate includes film-coolant flow
d = mixture ratio based on injector flowrates
ND = no data

TABLE B-1
(Concluded)

Run No.	Test Date, 1966	Injector No.	Duration, seconds	Throat Area, sq in.	Thrust, pounds	Chamber Pressure, psia	Mixture Ratio, o/f	Total Weight Flowrate, lb/sec	Comments
182	9-30	4-2G	1.0	0.925	1657	1308	6.69	4.037	Gas tapoff
183	9-30	4-2G	1.0	0.925	1802	1416	4.40	4.693	
184	10-3	4-2G	1.5	0.925	402	335	7.29	1.018	
185	10-3	4-2G	2.2	0.925	390	339	6.36	0.949	
192	10-18	6-1A	ND	ND	ND	ND	ND	ND	Facility malfunction
193	10-18	6-1A	ND	ND	ND	ND	ND	ND	
194	10-18	6-1A	ND	ND	ND	ND	ND	ND	
195	10-20	6-1A	3.6	0.970	444	347	4.74	1.350	
196	10-20	6-1A	3.8	0.970	444	344	4.58	1.318	
197	10-20	6-1A	3.9	0.970	1316	930	4.58[d]	3.231	Film cooled
198	10-24	6-1A	4.2	0.970	2208	1548	6.04[d]	6.151[b]	
199	10-24	6-1A	4.2	0.970	1341	959	5.64[d]	3.858[b]	
200	10-26	6-1B	1.4	0.930	371	292	4.05	1.200	Gas tapoff
201	10-26	6-1C	1.6	0.980	397	299	4.28	1.243	
202	10-26	6-1D	1.5	0.930	366	288	4.13	1.212	
203	10-26	6-1D	1.6	0.980	1235	868	5.94	3.849	
204	10-26	6-1D	1.6	0.980	1876	1285	7.00	5.963	

NOTE:

b = flowrate includes film-coolant flow
d = mixture ratio based on injector flowrates
ND = no data

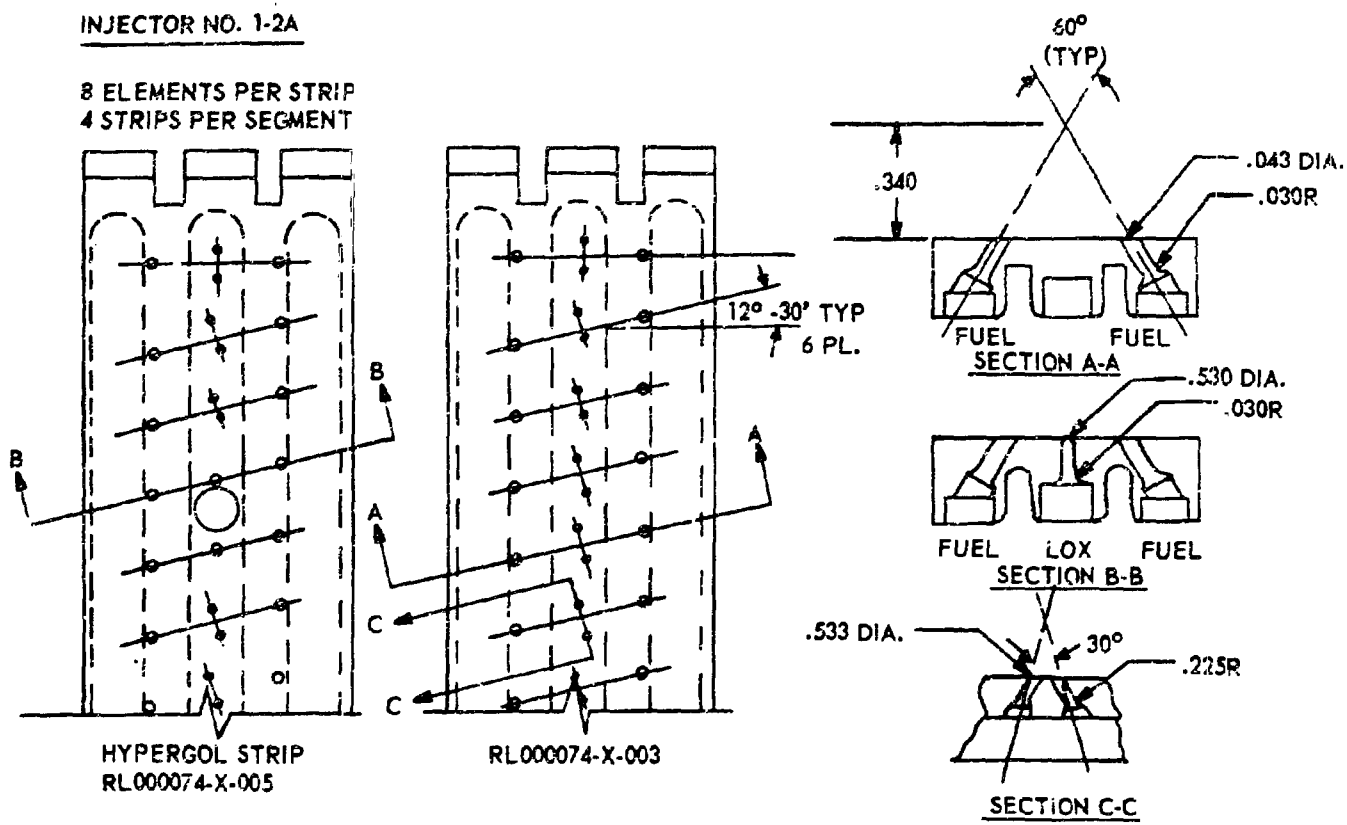

Figure B-1. Injector Orifice Pattern Designs

INJECTOR NOS. 1-3A TO 1-3B

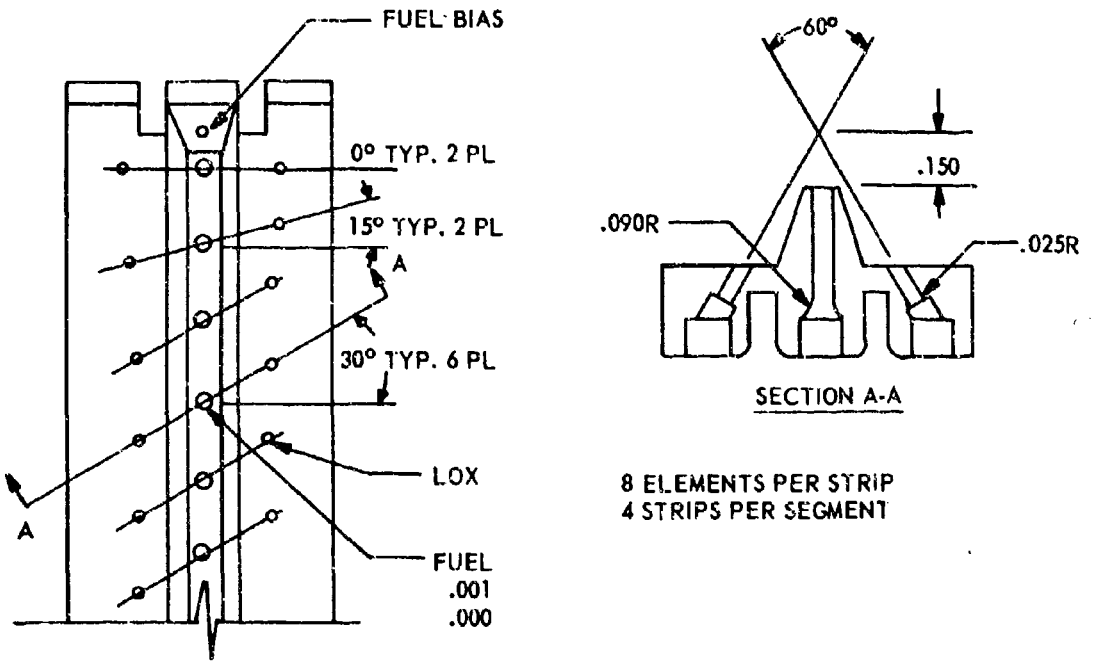

DASH NUMBER	MODIFICATION
-3B	ADDED 8 EACH 0.031-INCH-DIAMETER FUEL BIAS ORIFICES AT STRIP ENDS

Figure B-1. (Continued)

INJECTOR NOS. 2-1A TO 2-1G

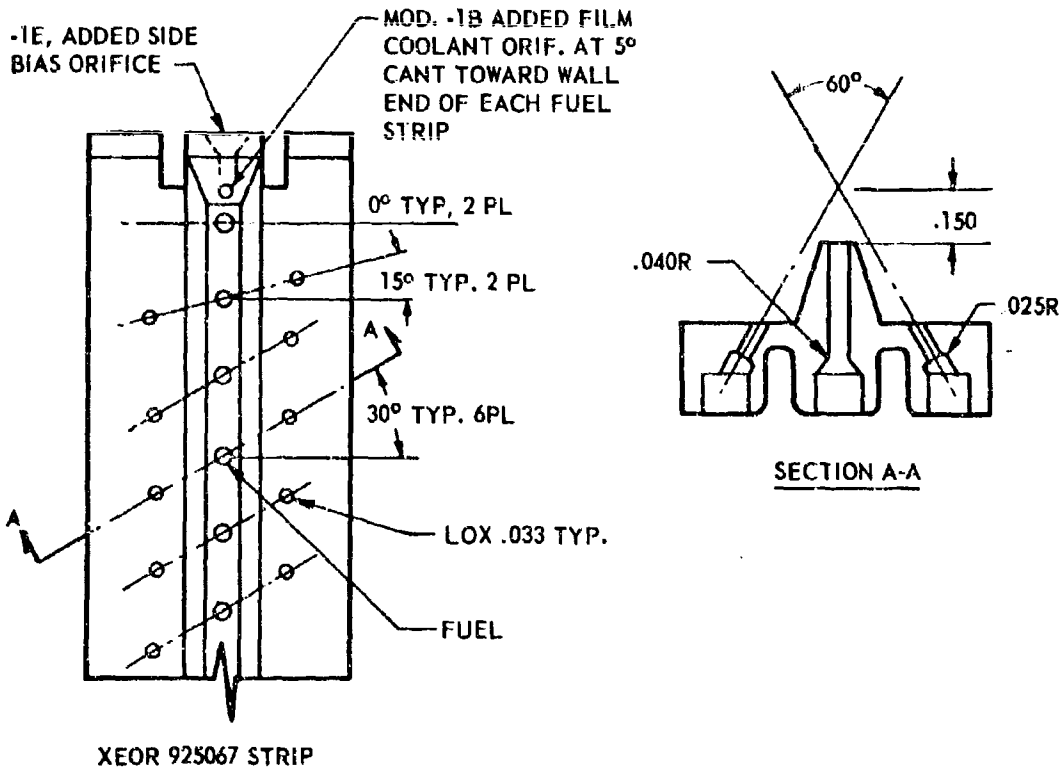

DASH NUMBER	MODIFICATION
-1B	ENLARGED FUEL ORIFICE TO 0.066-INCH DIAMETER, ADDED 0.031-INCH DIAMETER FUEL BIAS
-1C	ENLARGED FUEL BIAS TO 0.042 DIAMETER
-1D	ENLARGED FUEL ORIFICES TO 0.070 DIAMETER
-1E	PLUGGED FUEL BIAS AT FUEL STRIP ENDS, ADDED SIDE BIAS ORIFICES
-1F	PLUGGED SIDE BIAS ORIFICES
-1G	DRILLED FUEL STRIP END ORIFICE FROM 0.070-INCH DIAMETER TO .0995-INCH DIAMETER

Figure B-1 (Continued)

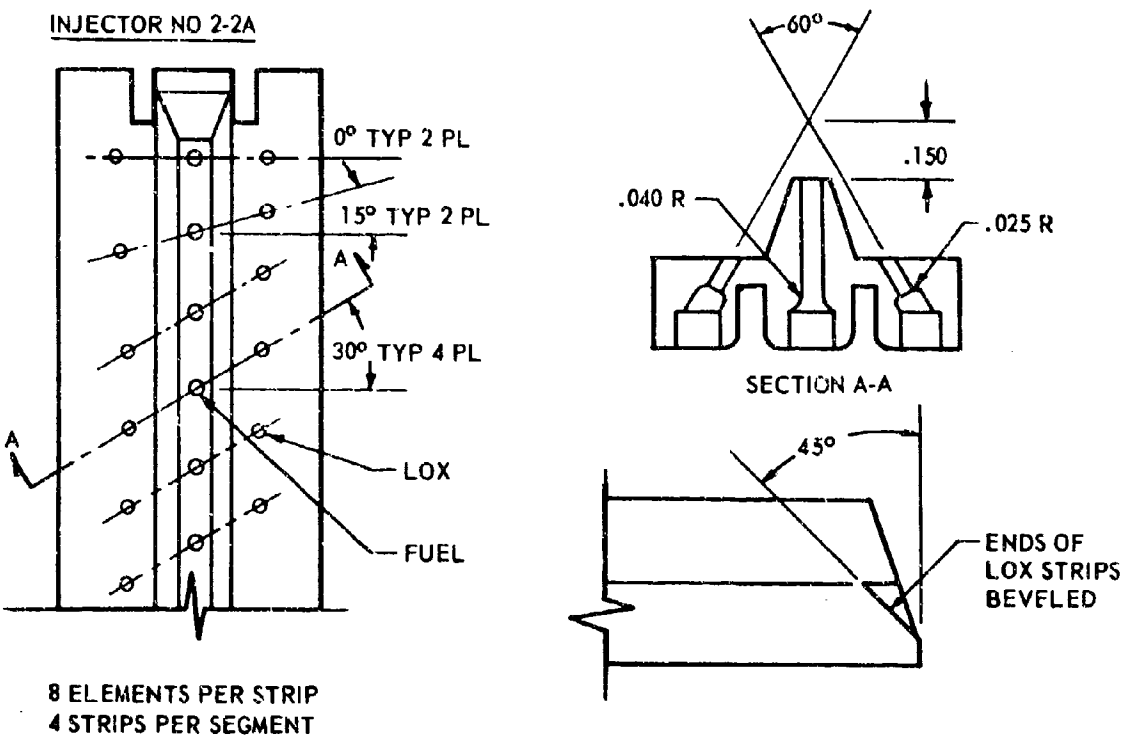

NO MODIFICATIONS

Figure B-1 (Continued)

INJECTOR NOS. 3-2A TO 3/2B

STRIP - RL000090
ASSY - RL000023-X-031

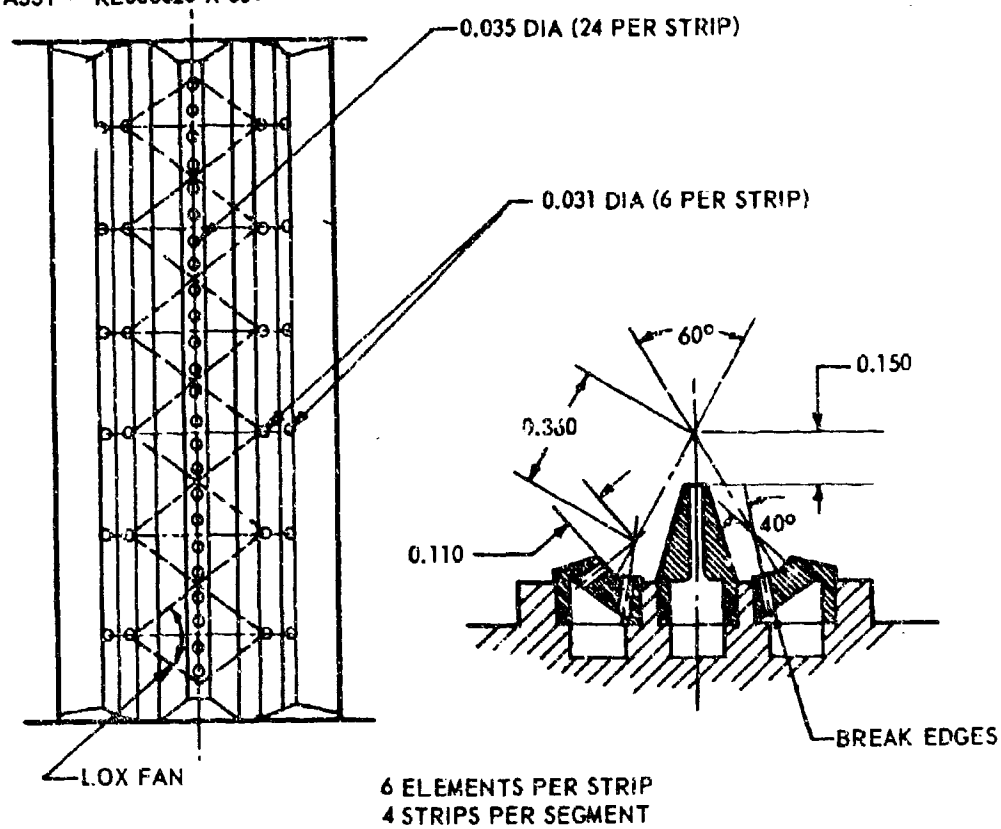

DASH NUMBER	MODIFICATION
-2B	ENLARGED OUTER TWO FUEL ORIFICES ON EACH STRIP TO 0.0465-INCH DIAMETER; ENLARGED CORE FUEL ORIFICES TO 0.040-INCH DIAMETER

Figure B-1. (Continued)

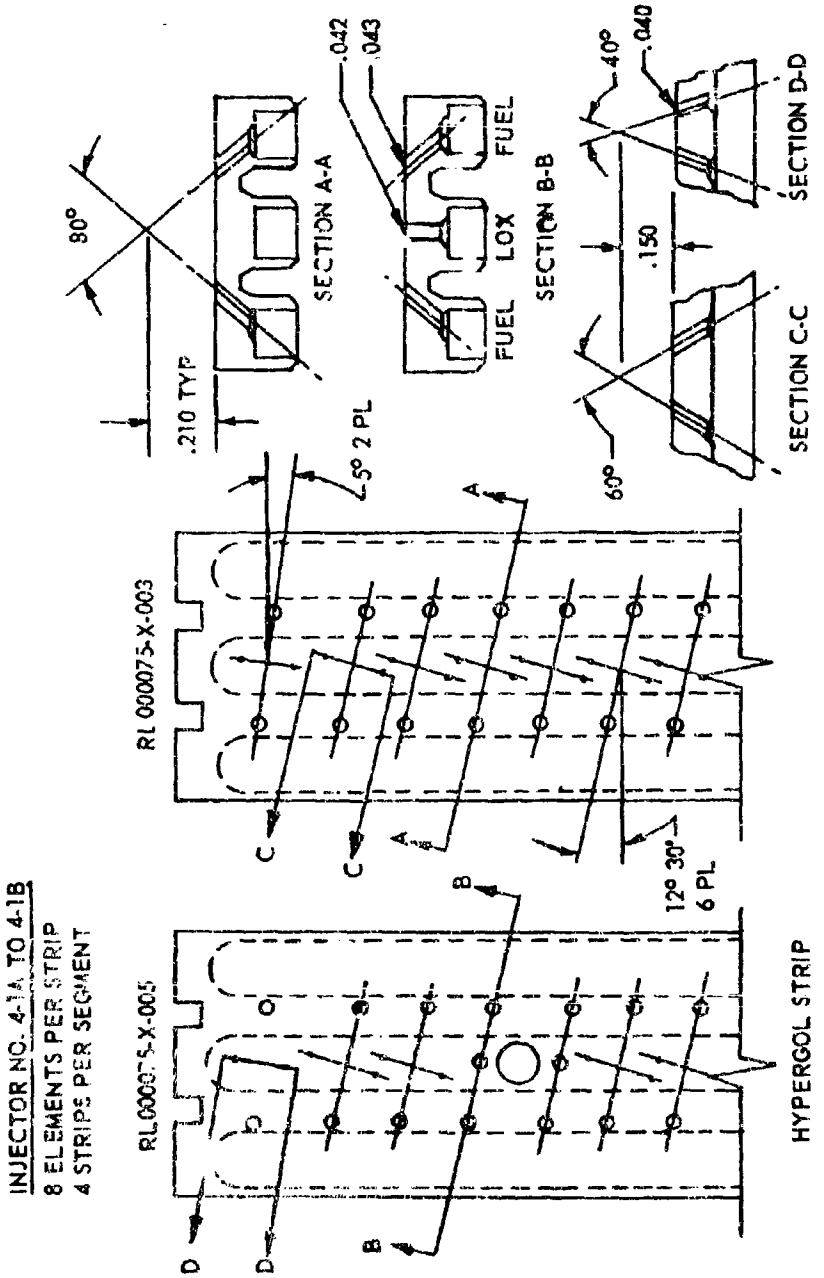

DASH NUMBER	MODIFICATIONS
-1B	ENLARGED MAIN FUEL ORIFICE FROM 0.043-INCH DIAMETER TO 0.0483-INCH DIAMETER

Figure B-1. (Continued)

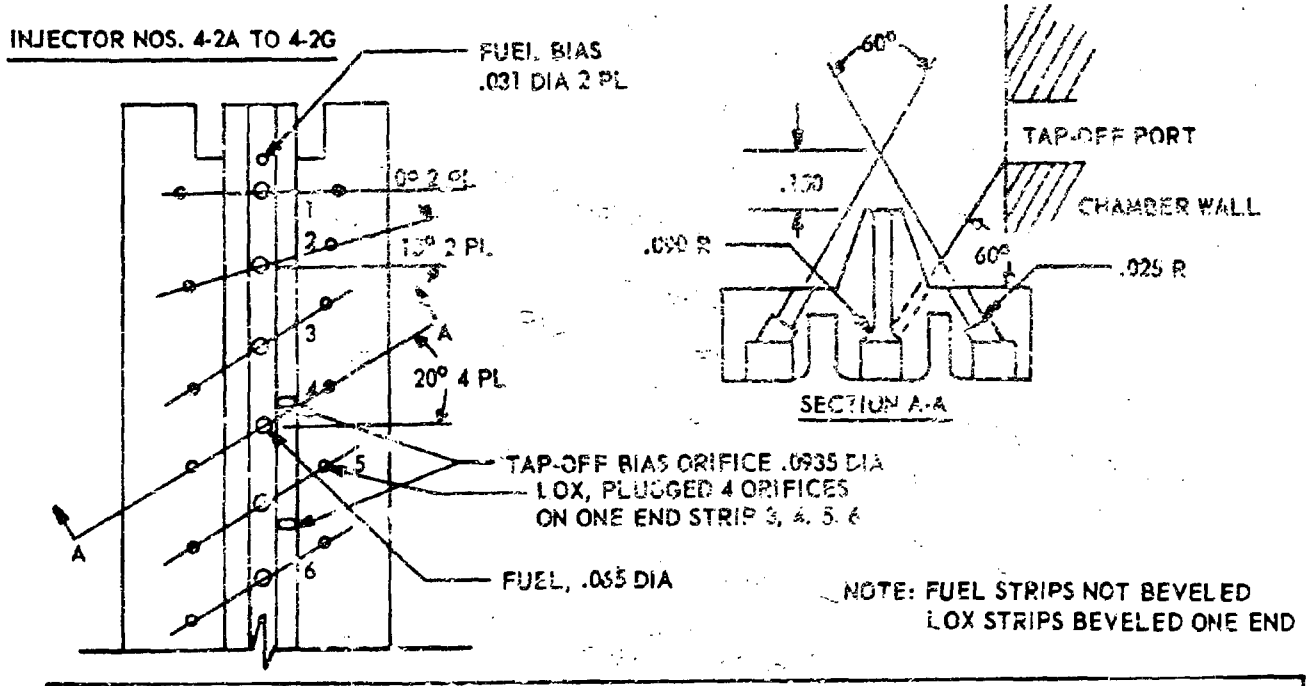

DASH NUMBER	MODIFICATIONS
-2B	ADDED TWO EACH 0.032-INCH DIAMETER TAPOFF BIAS ORIFICES AT BASE OF FUEL STRIP
-2C	ENLARGED TAPOFF BIAS ORIFICES TO 0.067-INCH DIAMETER
-2D	ENLARGED TAPOFF BIAS ORIFICES TO 0.076-INCH DIAMETER
-2E	ENLARGED TAPOFF BIAS ORIFICES TO 0.089-INCH DIAMETER
-2F	ENLARGED FOUR CORE FUEL ORIFICES AT TAPOFF AREA TO 0.0435-INCH DIAMETER
-2G	PLUGGED FOUR LOX ORIFICES, ADDED TWO 0.0935-INCH DIAMETER FUEL TAPOFF BIAS ORIFICE

Figure B-1. (Continued)

ROCKETDYNE • A DIVISION OF NORTH AMERICAN AVIATION, INC.

INJECTOR NOS. 6-1A TO 6-1D

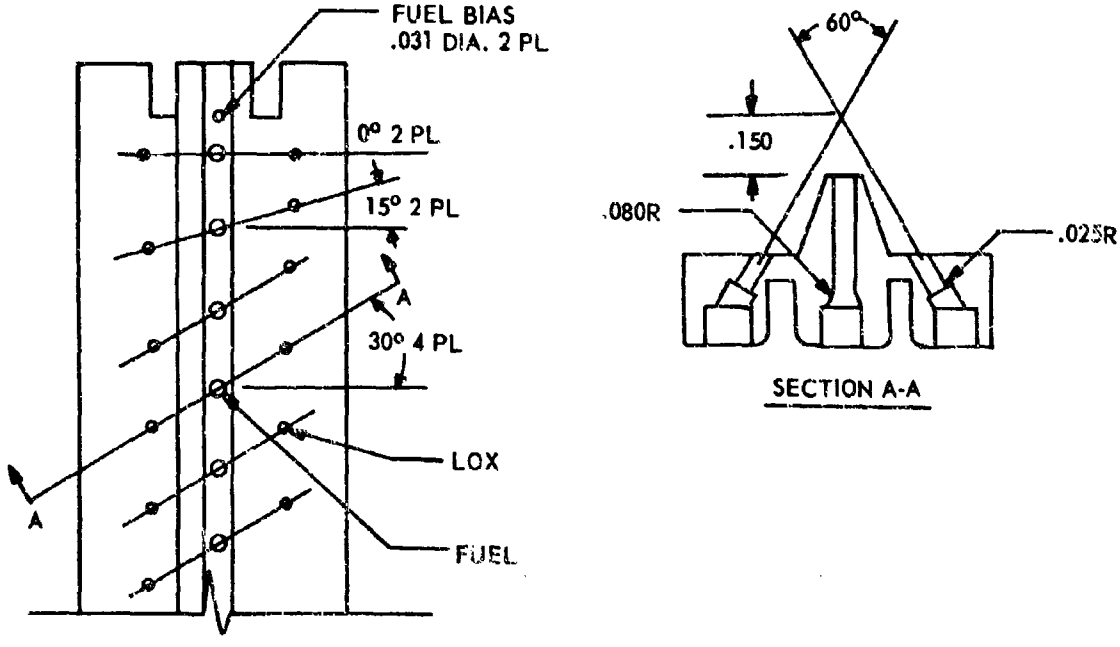

DASH NUMBER	MODIFICATION
-1B	PLUGGED THREE LOX ORIFICES AT TAPOFF LOCATION
-1C	ADDED TWO 0.070-INCH-DIAMETER TAPOFF BIAS ORIFICES
-1D	ENLARGED TAPOFF BIAS TO 0.0935-INCH-DIAMETER

Figure B-1. (Concluded)

UNCLASSIFIED

Security Classification

DOCUMENT CONTROL DATA - R&D

(Security classification of title, body of abstract and indexing annotation must be entered when the overall report is classified)

1. ORIGINATING ACTIVITY (Corporate author) Rocketdyne, a Division of North American Aviation Inc. 6633 Canoga Avenue, Canoga Park, California	2a. REPORT SECURITY CLASSIFICATION CONFIDENTIAL 2b. GROUP 4

3. REPORT TITLE

ADVANCED CRYOGENIC ROCKET ENGINE PROGRAM, AEROSPIKE NOZZLE CONCEPT

4. DESCRIPTIVE NOTES (Type of report and inclusive dates)

Fourth Quarterly Progress Report, 1 December 1966 to 28 February 1967

5. AUTHOR(S) (Last name, first name, initial)

Rocketdyne Engineering

6. REPORT DATE 31 March 1967	7a. TOTAL NO. OF PAGES 172 & xiii	7b. NO. OF REFS 5
8a. CONTRACT OR GRANT NO. AF04(611)-11399 b. PROJECT NO. c. d.	9a. ORIGINATOR'S REPORT NUMBER(S) R-6537-4 9b. OTHER REPORT NO(S) (Any other numbers that may be assigned this report) AFRPL-TR-67-91	

10. AVAILABILITY/LIMITATION NOTICES

N/A

11. SUPPLEMENTARY NOTES N/A	12. SPONSORING MILITARY ACTIVITY Air Force Rocket Propulsion Laboratory Edwards Air Force Base, California

13. ABSTRACT

(U) Program status and technical results obtained at the end of the report period are described for the Advanced Development Program, Aerospike. This program includes analysis and preliminary design of an advanced rocket engine using an Aerospike nozzle and experimental evaluation of critical technology related to the Aerospike concept. Component and system features, physical arrangements, and design parameters and details have been established for an optimum demonstrator engine. Studies of application of a flight engine to certain vehicles are completed. Experimental injector performance investigations on a segment chamber and experimental cooling investigations on segment chambers and material studies are completed. Fabrication of full-scale, cooled thrust chambers for performance demonstrations is under way. Fabrication of segments for structural and cooling evaluations is also in progress.

DD FORM 1 JAN 64 1473

UNCLASSIFIED

Security Classification

14. KEY WORDS	LINK A		LINK B		LINK C	
	ROLE	WT	ROLE	WT	ROLE	WT
Task I, Design and Analysis Module Design Applications Study Task 2, Fabrication and Test 2.5K Segment Injector Performance Investigation Thrust Chamber Cooling Investigations Thrust Chamber Nozzle Demonstration Segment Structural Evaluation						

INSTRUCTIONS

1. **ORIGINATING ACTIVITY:** Enter the name and address of the contractor, subcontractor, grantee, Department of Defense activity or other organization *(corporate author)* issuing the report.

2a. **REPORT SECURITY CLASSIFICATION:** Enter the overall security classification of the report. Indicate whether "Restricted Data" is included. Marking is to be in accordance with appropriate security regulations.

2b. **GROUP:** Automatic downgrading is specified in DoD Directive 5200.10 and Armed Forces Industrial Manual. Enter the group number. Also, when applicable, show that optional markings have been used for Group 3 and Group 4 as authorized.

3. **REPORT TITLE:** Enter the complete report title in all capital letters. Titles in all cases should be unclassified. If a meaningful title cannot be selected without classification, show title classification in all capitals in parenthesis immediately following the title.

4. **DESCRIPTIVE NOTES:** If appropriate, enter the type of report, e.g., interim, progress, summary, annual, or final. Give the inclusive dates when a specific reporting period is covered.

5. **AUTHOR(S):** Enter the name(s) of author(s) as shown on or in the report. Enter last name, first name, middle initial. If military, show rank and branch of service. The name of the principal author is an absolute minimum requirement.

6. **REPORT DATE:** Enter the date of the report as day, month, year; or month, year. If more than one date appears on the report, use date of publication.

7a. **TOTAL NUMBER OF PAGES:** The total page count should follow normal pagination procedures, i.e., enter the number of pages containing information.

7b. **NUMBER OF REFERENCES:** Enter the total number of references cited in the report.

8a. **CONTRACT OR GRANT NUMBER:** If appropriate, enter the applicable number of the contract or grant under which the report was written.

8b, 8c, & 8d. **PROJECT NUMBER:** Enter the appropriate military department identification, such as project number, subproject number, system numbers, task number, etc.

9a. **ORIGINATOR'S REPORT NUMBER(S):** Enter the official report number by which the document will be identified and controlled by the originating activity. This number must be unique to this report.

9b. **OTHER REPORT NUMBER(S):** If the report has been assigned any other report numbers *(either by the originator or by the sponsor)*, also enter this number(s).

10. **AVAILABILITY/LIMITATION NOTICES:** Enter any limitations on further dissemination of the report, other than those imposed by security classification, using standard statements such as:

(1) "Qualified requesters may obtain copies of this report from DDC."

(2) "Foreign announcement and dissemination of this report by DDC is not authorized."

(3) "U. S. Government agencies may obtain copies of this report directly from DDC. Other qualified DDC users shall request through _____."

(4) "U. S. military agencies may obtain copies of this report directly from DDC. Other qualified users shall request through _____."

(5) "All distribution of this report is controlled. Qualified DDC users shall request through _____."

If the report has been furnished to the Office of Technical Services, Department of Commerce, for sale to the public, indicate this fact and enter the price, if known.

11. **SUPPLEMENTARY NOTES:** Use for additional explanatory notes.

12. **SPONSORING MILITARY ACTIVITY:** Enter the name of the departmental project office or laboratory sponsoring *(paying for)* the research and development. Include address.

13. **ABSTRACT:** Enter an abstract giving a brief and factual summary of the document indicative of the report, even though it may also appear elsewhere in the body of the technical report. If additional space is required, a continuation sheet shall be attached.

It is highly desirable that the abstract of classified reports be unclassified. Each paragraph of the abstract shall end with an indication of the military security classification of the information in the paragraph, represented as *(TS)*, *(S)*, *(C)*, or *(U)*.

There is no limitation on the length of the abstract. However, the suggested length is from 150 to 225 words.

14. **KEY WORDS:** Key words are technically meaningful terms or short phrases that characterize a report and may be used as index entries for cataloging the report. Key words must be selected so that no security classification is required. Identifiers, such as equipment model designation, trade name, military project code name, geographic location, may be used as key words but will be followed by an indication of technical context. The assignment of links, rules, and weights is optional.